

POLITECNICO DI TORINO

MASTER's Degree in Sustainable Architecture



MASTER's Degree Thesis

**Scripting Architecture: Orienting Early
Design Choices via Optimisation**

Supervisors

Prof. GIACOMO CHIESA

Candidate

ZIYAN ZHUO

12 2023

Summary

This paper provides a comprehensive exploration of how parametric design, simulation, and optimization methodologies intertwine, showcasing their effectiveness in architectural design across various geographical contexts.

Specifically, firstly, We found a way to design an imagined box office with parametric skill, then build it within a 3D software environment. Secondly, we managed to evaluate it in 3 perspectives, which are economical assessment, energy usage intensity and comfort measurement. Thirdly, we applied a genetic algorithm on it to get the optimized results, and repeat the experiment under different climate conditions. Lastly, we collect the result, visualize it and analyse it.

We published the result and the workflow on Internet, in order to get feedback. Rethinking the defects in the experiment, I gained the experience and a polished idea on this philosophy while writing the thesis.

Acknowledgements

已乘蓝鹤去，过川蜀昆仑
扶摇三千仞，披霞万里云
身展鸿鹄志，闭日嗅蔷薇
问云何处往，遥遥阿尔卑

to
My beloved and those support me

Table of Contents

List of Tables	IX
List of Figures	XI
Acronyms	XIV
1 Introduction	1
1.1 Primer: <i>firmitas, utilitas, and venustas</i>	1
1.2 Goals: <i>Comfort, Efficiency, Economicity</i>	2
1.3 Climate change	2
1.3.1 Public awareness	2
1.3.2 The earth is warming, the mankind is delaying	3
1.3.3 Call for the change	3
1.3.4 EU Incentives for Change	5
1.4 Human-Body-Oriented Design	6
1.5 Short-Term Expenses vs. Long-Term Profit	7
1.6 Inspirations from Computer Science	7
1.6.1 Parametric platform as an intermediate	7
1.6.2 Philosophy of Algorithms	9
1.6.3 Translating the design mission to coding	9
1.6.4 Skipping from "Knowing How" to "Getting It Done"	10
1.7 From dark knowledge to grokking	11
2 Study of the Art	12
2.1 EP parametric and optimization interfaces	12
2.1.1 EnergyPlus platform	12
2.1.2 Interfaces of EnergyPlus	13
2.1.3 A prevailing interface of EnergyPlus: OpenStudio	14
2.1.4 DesignBuilder	15
2.1.5 conclusion for the platforms	16
2.2 Grasshopper	17

2.3	Related works	17
2.3.1	Galapagos	17
2.3.2	Octopus and its practice	18
2.3.3	NSGA-II and Wallacei in architecture	21
3	Methodology for simulations	23
3.1	Approach for Energy simulation	23
3.1.1	Math of thermal transmittance	24
3.2	Approach for lighting simulation	24
3.3	Approach for economical analysis	26
3.4	Approach for comfort metrics	29
3.4.1	Thermal comfort	30
3.4.2	Predicted Mean Vote	30
3.4.3	Adaptive comfort	31
3.4.4	Comfort visualization	33
3.5	GAin arhitecture design and NSGA-II	35
3.5.1	Features and analogy of GA	36
3.5.2	Mathematical process of Simulated Binary Crossover	37
3.5.3	NSGA-II	38
4	Methodology for Designing examined box	41
4.1	Design Object: "Hardware" and "Software"	41
4.2	Proposal for Retrofitting: Static Design	42
4.2.1	Opaque Envelope	42
4.2.2	Transparent Envelope	43
4.2.3	Shading Device	45
4.3	Proposal for Retrofitting: Operative Design	46
4.3.1	Brief Introduction & Classification of Operative Design	46
4.3.2	HVAC System	47
4.3.3	Controlled Natural Ventilation	47
4.3.4	Dimmer Control	49
5	Workflow	50
5.1	Introduction for generating process	50
5.1.1	Step I: Preset	50
5.1.2	Step II: Database	51
5.1.3	Step III: BIM Setting	52
5.1.4	Step IV: Operational Setting	53
5.1.5	Step V: Run the Simulation	54
5.1.6	Step VI: Repeat by the GA	55
5.1.7	After experiment: Visualisation	55

5.2	Boundary Conditions	57
5.2.1	Local climate	57
5.2.2	Context	60
5.3	Model building	61
5.3.1	HB Opaque Material	62
5.3.2	HB Weekly Schedule	64
5.3.3	HB Face	65
5.3.4	HB Room	66
5.4	Energy simulation	68
5.4.1	Weather file	68
5.4.2	Analysis period	68
5.4.3	HB All-Air HVAC	68
5.4.4	HB Ventilation Control	70
5.4.5	HB Export to OSM	72
5.5	Lighting simulation	74
5.5.1	HB Sensor Grid	75
5.5.2	HB Annual Daylight	76
5.5.3	Daylight estimation	77
5.6	Economical simulation	77
5.6.1	NPV calculator	78
5.7	Comfort simulation	78
5.7.1	LB PMV Comfort	79
5.8	Optimization	81
5.8.1	Wallacei X	81
5.8.2	Wallacei section	83
5.9	Visualization	85
5.9.1	Objective Space	85
5.9.2	The Matrix	89
5.9.3	Pareto front mark	90
5.9.4	Selection criteria	91
6	Application	93
6.1	Test for the effectiveness of the optimization	93
6.1.1	General symmetric mapping	93
6.1.2	Convergence	93
6.1.3	Non-Fungible solutions	95
6.1.4	Effectiveness of the CNV	96
6.2	Oslo	99
6.2.1	Climate	99
6.2.2	Chromosome matrix display	101
6.2.3	Genotype analysis	102

6.2.4	Phenotypes Analysis	102
6.2.5	Strategy	103
6.2.6	Selection from Human	104
6.3	Kiev	105
6.3.1	Climate	105
6.3.2	Chromosome matrix display	107
6.3.3	Genotype Analysis	107
6.3.4	Phenotypes Analysis	109
6.3.5	Strategy	109
6.3.6	Selection from Human	110
6.4	Rome	111
6.4.1	Climate	111
6.4.2	Chromosome matrix display	113
6.4.3	Genotype Analysis	114
6.4.4	Phenotype Analysis	114
6.5	Palermo	116
6.5.1	Climate	116
6.5.2	Chromosome matrix display	119
6.5.3	Genotype Analysis	120
6.5.4	Phenotype Analysis	120
6.6	Geneva	122
6.6.1	Climate	122
6.6.2	Analysis of Genotype and Phenotype	124
6.7	Torino	126
6.7.1	Climate	126
6.7.2	Chromosome matrix display	128
6.7.3	Analysis of Torino Genotype and Phenotype	129
6.8	Canton	131
6.8.1	Climate	131
6.9	Hong Kong	133
6.9.1	Climate	133
7	Conclusion	135
7.1	Improvements can be adapted	135
7.1.1	Improvement in settings	135
7.1.2	Improvement in design	136
7.1.3	Improvement in the visualization	136
7.2	Evaluation of the method	136
7.2.1	Comparison of the similar climates	136
7.2.2	Same Method Behaves Differently in Different Climates	137
7.3	Experience gained from the Results	137

7.3.1	Before vs after: Controlled natural ventilation	138
7.3.2	Typical strategies for EUI	138
7.4	As real cases	138
A	Algorithm	140
B	Result matrix	145
B.1	Torino	146
B.2	Geneva	148
B.3	Oslo	150
B.4	Kiev	151
B.5	Roma	152
B.6	Palermo	154
	Bibliography	156

List of Tables

3.1 Utilisation factor to search	25
4.1 Insulation price	43
4.2 Construction of roof	43
4.3 Construction of wall	44
4.4 Construction of floor	44
4.5 Glazing types of the window	45
5.1 Köppen classification scheme symbols	58
5.2 Cities selected and classification	59
6.1 Oslo.Gen.99	101
6.2 Oslo.Gen.00	101
6.3 Kiev.Gen.99	107
6.4 Kiev.Gen.00	108
6.5 Roma.Gen.99	113
6.6 Roma.Gen.00	113
6.7 Palermo.Gen.99	119
6.8 Palermo.Gen.00	119
6.9 Torino.Gen.99	128
6.10 Torino.Gen.00	128
B.1 Torino.Gen.50	146
B.2 Torino.Gen.96	146
B.3 Torino.Gen.97	147
B.4 Torino.Gen.98	147
B.5 Geneva.Gen.50	148
B.6 Geneva.Gen.96	148
B.7 Geneva.Gen.97	149
B.8 Geneva.Gen.98	149
B.9 Oslo.Gen.97	150
B.10 Oslo.Gen.98	150

B.11 Kiev.Gen.97	151
B.12 Kiev.Gen.98	151
B.13 Roma.Gen.50	152
B.14 Roma.Gen.96	152
B.15 Roma.Gen.97	153
B.16 Roma.Gen.98	153
B.17 Palermo.Gen.50	154
B.18 Palermo.Gen.96	154
B.19 Palermo.Gen.97	155
B.20 Palermo.Gen.98	155

List of Figures

3.1	Neutral temperatures for buildings in FR mode against prevailing mean outdoor temperature	32
3.2	Comfort model based on EN-16798-1 2019	34
3.3	Comfort chart for Geneva - after	35
3.4	Psychrometric Chart of Torino Optimized	36
3.5	Heat loss Chart of Torino Optimized	39
3.6	Distribution of SBX	40
5.1	General GH Canvas	50
5.2	GH section A	51
5.3	GH section B	52
5.4	GH section C	53
5.5	GH section D	54
5.6	GH section E	56
5.7	GH section F	57
5.8	Asian selected cities	59
5.9	European selected cities	60
5.10	Example of context	61
5.11	HB Opaque Material in application	63
5.12	HB Weekly Schedule	64
5.13	HB Room	67
5.14	HB component classification	68
5.15	HB HVAC	69
5.16	HB Ventilation Control	70
5.17	HB Export to OSM	73
5.18	ALS grid to receive the daylight	75
5.19	HB Annual Daylight	76
5.20	Illuminance calculator	77
5.21	Wallacei X Component	82
5.22	Sections of Wallacei X	83

5.23	Clusters using Hierarchical of the Pareto fronts in the optimization of Torino	85
5.24	Clusters using K-means of the Pareto fronts in the optimization of Torino	86
5.25	Objective space in the Wallacei interface of the Pareto fronts in the optimization of Torino	86
5.26	OS presenting in RH Axonometric	87
5.27	Objective space presenting in RH from front	88
5.28	chromosome matrix introduction	89
6.1	The variation of mean values	94
6.2	The variation of standard deviation	94
6.3	The distribution of standard deviation	95
6.4	Modified gen.99 CNV Comparison	96
6.5	Performance of the system without CNV	98
6.6	Performance of the system with CNV	98
6.7	Ratio of CNV	98
6.8	Oslo: the comfort metric of PMV	99
6.9	Oslo: wind rose	100
6.10	Oslo: original KPI	100
6.11	Kiev: the comfort metric of PMV	105
6.12	Kiev: wind rose	106
6.13	Kiev: original KPI	106
6.14	Roma: the comfort metric of PMV	111
6.15	Roma: wind rose	112
6.16	Roma: original KPI	112
6.17	Palermo: the comfort metric of PMV	116
6.18	Palermo: wind rose	117
6.19	Palermo: original KPI	117
6.20	Geneva: the comfort metric of PMV	122
6.21	Geneva: wind rose	123
6.22	Geneva: original KPI	123
6.23	Torino: the comfort metric of PMV	126
6.24	Torino: wind rose	127
6.25	Torino: original KPI	127
6.26	Canton: the comfort metric of PMV	131
6.27	Canton: wind rose	132
6.28	Canton: original KPI	132
6.29	Hong Kong: the comfort metric of PMV	133
6.30	Hong Kong: wind rose	134
6.31	Hong Kong: original KPI	134

A.1	Chord Graphic of matching tournament	141
A.2	The whole process flow of NSGA2	142
A.3	General GH canvas, part 1/2	143
A.4	General GH canvas, part 2/2	144

Acronyms

AI	Artificial Intelligence
ASHRAE	American Society of Heating Refrigerating Air-Conditioning Engineers
ALS	Ambient Light Sensors
ASE	Annual Sunlight Exposure
BESOS	Building and Energy Simulation, Optimization and Surrogate Modeling
BIM	Building information modeling
BTO	Building Technologies Office
CAD	Computer-aided design
cDA	continuous Daylight Autonomy
CEN	Comité Européen de Normalisation; European Committee for Standardization
CNV	Controlled Natural Ventilation
CO ₂	Carbon dioxide
DA	Daylight autonomy
DEPC	Dynamic Energy Performance Certification
DGP	Daylight Glare Probability
DOE	U.S. Department of Energy
DNA	Deoxyribonucleic Acid
ECM	Energy Conservation Measures
E-DYCE	Energy-flexible DYnamic building Certification
EI	Energy Intensity
EP	EnergyPlus
EPB	Energy Performance of Building
EPBD	Energy Performance of Building Directive
EPC	Energy Performance Certificates
EPW	EnergyPlus Weather

EU	European Union
EUI	Energy Use Intensity
FR	Free Running (mode)
GA	Genetic algorithm
Gen.	Generation index (Used in the optimized result matrix)
GH	Grasshopper
GHG	Green house gas
GUI	Graphical user interface
HB	Honeybee
HVAC	Heating, ventilating and air conditioner
HypE	Hypervolume Estimation algorithm
ICT	Information and Communications Technology
IDD	Input Data Dictionary
IDF	Intermediate Data File
Indiv.	Individual index (Used in the optimized result matrix)
IEA-EBC	International Energy Agency Energy in Buildings and Communities Programme
IT	Information Technology
KPI	Key Performance Indicator
LB	Ladybug
LBT	Ladybug Tool
LCC	Life Cycle Costing
LEUI	Lighting Energy Use Intensity
Low-E	Low Emissivity (glass)
NDC	Nationally Determined Contribution
NSGA-II	Non-dominated sorting genetic algorithm II
OS	OpenStudio
OSM	OpenStudio Model

PAT	Parametric Analysis Tool
PCM	Phase Change Materials
PET	Physiological Equivalent Temperature
PMV	Predicted Mean Vote
POLITO	Politecnico di Torino
PREDYCE	Python semi-Realtime Energy Dynamics and Climate Evaluation
PPD	Predicted Percent of Dissatisfied
PVAV	Packaged Variable Air Volume
RGB	Red, Green, Blue color model
RH	Rhinoceros v7 (software)
RH	Relative Humidity
SBX	Simulated Binary Crossover
SD	Standard Deviation
sDA	Spatial Daylight Autonomy
SDK	Software Development Kit
SET	Standard Effective Temperature
SPEA-II	Strength Pareto Evolutionary Algorithm II
TEUI	Thermal Energy Use Intensity
UN	United Nation
UNFCCC	United Nations Framework Convention on Climate Change
UNESCO	United Nations Educational, Scientific and Cultural Organization
UCTI	Universal Thermal Climate Index
U-value	thermal transmittance (reciprocal of R-value)
VC	Ventilation Cooling
WWR	Window-to-Wall Ratio

Chapter 1

Introduction

1.1 Primer: *firmitas, utilitas, and venustas*

Multiple Goals in Design

*Design is a dance with chains.*¹

Good architectural design isn't just about pursuing the independent goals of solidity, comfort, and delight that Vitruvius [1] spoke of; it's about skillfully balancing and integrating them into a unified whole. Architectural design is akin to a dance with shackles, where designers must navigate a balance among diverse demands to create a breathtaking amalgamation. On this stage, architects aren't merely problem solvers but creative catchers, seamlessly blending functionality, structural integrity, and aesthetic appeal. For instance, a building can achieve not only strength and safety through ingenious structural design but also use these structural elements to craft compelling artistic expressions. Exceptional architectural design doesn't merely meet each individual objective but finds resonance between beauty and utility within this balanced synthesis, resulting in architectural masterpieces that transcend individual aims. Thus, in the theater of architectural design, the elements of solidity, comfort, and delight aren't isolated; they are amalgamated into a harmonious whole through the ingenuity and creativity of the designer.

¹*Dancing in Chains*, According to Friedrich Nietzsche in 1880s, artists impose restrictions on themselves to encourage creativity and even have a way of “making things difficult” – imposing new constraints on themselves within which they have to dance.

1.2 Goals: *Comfort, Efficiency, Economicity*

In contemporary sustainable design, this notion remains relevant, much like E. Vignani's mention [2, p.46] that visual comfort often conflicts with thermal comfort. Our task is to optimize multiple objectives through algorithms. Drawing inspiration from Vitruvius, we have established the following goals: Comoditas, Efficientia, Economicitas (Comfort, Efficiency, Economicity). These objectives encompass nearly all the requirements of modern office buildings. In other words, if these three indicators perform well, the evaluated office space will indeed be considered superior. Moreover, these three goals are designed to be as independent of each other as possible. It's preferable not to optimize DA (Daylight autonomy) while simultaneously optimizing Useful Daylight Illuminance, to avoid wasting computational resources and the risk of redundant optimization efforts.

And the other practical reasons why we've chosen these objectives are presented in the following paragraphs.

1.3 Climate change

1.3.1 Public awareness

In recent decades, there has been a widespread acknowledgment of climate change, compelling the urgency for extensive renovation to become a matter of public concern. According to a survey conducted by Eurobarometer in 2021, 93% of EU citizens identified climate change as the most pressing global issue [3]. Presently, a noticeable trend has emerged, especially among the youth, in taking to the streets to demand concrete actions to curtail global warming, with passionate declarations of affection for Earth [3]. The Swedish activist Greta Thunberg, renowned for founding the climate strike movement known as Fridays For Future (FFF) in 2018, has played a pivotal role in shaping attitudes toward climate change. The movement's advocacy for action has garnered widespread support among students worldwide, rallying for the protection of their future.

While environmental activism has recently gained substantial traction, primarily leveraging the power of social media, its origins trace back to the early 1970s when climate change began surfacing as a critical political concern. The pivotal moment came in 1972 with the UN Conference on the Human Environment (UNCHE) held in Stockholm, Sweden. This conference marked the first major attempt to address environmental issues globally, with participating nations concurring on the imperative for coordinated, global-scale efforts to address climate change [3].

1.3.2 The earth is warming, the mankind is delaying

Subsequently, numerous conferences have convened on this matter [3], yet the issue has often been deferred, leaving it for future generations to tackle [3, 4]. Consequently, the climate crisis has historically been perceived as "a distant danger, a scenario that we can address tomorrow" [5]. Governments have delayed prioritizing its resolution while addressing short-term predicaments such as financial and economic concerns [3]. However, humanity is now facing the consequences of these decisions. According to NASA/GISS data [6], global temperatures have risen by 1.01°C between 1880 and 2021, with 2020 recorded as the hottest year since the 19th century. Earth's temperature is escalating at an alarming pace, concurrent with a surge in atmospheric CO₂ levels. Heatwaves have become more frequent, raising temperatures and humidity levels, notably in urbanized regions (for instance, the highest temperature recorded in Europe was 48.8°C in Syracuse, Sicily, in August 2021). Shrinking Arctic sea ice has accelerated the rise in ocean levels, posing a threat of floods to coastal cities. Moreover, the thawing of permafrost could release trapped CO₂ and methane, further intensifying greenhouse gas levels in the atmosphere [7]. Droughts and wildfires have ravaged entire regions such as California and Australia, while vast areas of the Amazon Rainforest are incinerated annually, jeopardizing wildlife. Human-induced climate alterations are precipitating environmental disruptions that disproportionately affect vulnerable populations and ecosystems, yielding significant implications not only for nature but also for human health and well-being. Consequently, the issue has transcended mere environmental and economic concerns, evolving into an imminent social challenge, and the window of opportunity for action is rapidly closing [3, 8].

1.3.3 Call for the change

Therefore, climate issues have ascended to the forefront of the international political agenda. The 21st Conference of the Parties (COP21) held in Paris in 2015 marked a significant acceleration in efforts. In December of the same year, the 196 participating parties reached a milestone by delineating shared objectives and endorsing the Paris Agreement. This landmark accord represents the "first-ever universal, legally binding global climate change" treaty [9]. The Agreement introduced a dual-sided strategy aimed at combating global warming through adaptation and mitigation policies.

Adaptation involves reducing societal vulnerability to expected climate change impacts, enhancing resilience to adverse conditions. Mitigation aims at "holding the increase in global average temperature to well below 2°C above pre-industrial levels and pursuing efforts to limit the temperature increase to 1.5°C," recognizing that this would significantly alleviate the risks and impacts of climate change [10]. To curtail global warming, substantial reductions in GHG (Green house gas) emissions

are imperative, striving towards a zero-emission scenario.

To align with the treaty's stipulations, each country is obliged to outline and communicate its NDC (Nationally Determined Contribution) every five years to the UNFCCC (United Nations Framework Convention on Climate Change) secretariat, outlining the objectives it intends to achieve [10, art.4 para.2]. For instance, the initial NDC of the European Union committed to reducing GHG emissions by 40% by 2030 compared to 1990 levels. Subsequently, in December 2020, the EU updated its NDC, setting a more ambitious target of reducing emissions by at least 55% by 2030 [5], thereby progressing towards decarbonization and climate neutrality.

One of the most impactful sectors contributing to emissions is power generation and heat production, which accounted for nearly 39% of global CO₂ emissions in 2020 and escalated to 46% in 2021 [11, 12]. The COVID-19 pandemic in 2020 led to reduced energy demand and a consequent drastic decline in CO₂ emissions. This presented governments with an opportunity to prioritize green recovery, reconstructing a global economy that invests in low-carbon technologies, mitigating global warming, and aligning with the Paris Agreement's objectives. As highlighted by Rosen and Forster [5], a robust green economic recovery could potentially halve the rate of warming in the forthcoming decades, aiding in keeping the temperature increase below the 1.5°C goal.

However, as the world began recovering from the health crisis, it became evident that a sustainable restoration was not being pursued. CO₂ emissions, particularly those stemming from coal combustion, surged once again, reaching 36.3 billion tons in 2021, the highest level ever recorded in history [12]. According to the European Commission [13], 40% of EU energy consumption and 36% of energy-related GHG emissions in 2021 were attributed to buildings, primarily due to inefficient existing building stock, of which 75% lacks energy efficiency. Inadequate efficiency adversely affects both the environment and human quality of life. Higher energy consumption leads to elevated bills, burdening household budgets and exacerbating energy poverty. Furthermore, inefficient buildings fail to provide adequate indoor comfort and sanitary conditions in residential and workspaces, contributing to health issues and reduced productivity [14]. In light of this evidence, a pressing need arises for a revolutionary transformation within the construction sector, not merely in construction practices but also in the conceptualization of buildings from their earliest design stages. The aim is to curtail resource exploitation, diminish pollution, address social inequalities, and enhance present and future health and quality of life within a sustainable development framework [4, 15].

1.3.4 EU Incentives for Change

Climate action has emerged as a paramount concern in the European landscape. In pursuit of achieving climate neutrality by 2050, the legislative framework addressing this concern remains in constant evolution, alongside the establishment of various funding programs. Reports, such as [14], estimate that the EU (European Union) dedicates approximately 40% of global investments toward enhancing building energy efficiency annually. Notably, progress has been made in enhancing energy performance, significantly reducing new buildings' energy consumption by half compared to similar structures two decades ago [14]. However, the primary challenge persists within the existing building stock, where the rate of retrofitting falls short of the necessary level to meet European decarbonization and reduced consumption objectives [14, 16]. This limitation stems partly from the unattractiveness of renovation processes to investors due to their perceived high costs, time-intensive nature, and limited short-term cost-effectiveness.

In a bid to stimulate building retrofit initiatives, certain EU countries have introduced tax reliefs. For instance, Italy has introduced, among other existing fiscal facilitations, the "Superbonus 110%" initiative [7]. This initiative allows contributors to deduct 110% of intervention costs for energy efficiency enhancements, structural consolidations, and renewable installations. Despite its commendable intentions, the potential of the Superbonus 110% remains underutilized. According to a report by Legambiente [15], this economic incentive tends to benefit affluent users more than vulnerable families, whereas addressing energy poverty and facilitating widespread building renovations should be the primary focus. Enhancing fund management and programming remains imperative to fully capitalize on such initiatives.

Another challenge lies in persisting barriers and misinformation, particularly among end-users. The lack of a clear framework hampers the understanding, measurement, and monetization of the actual benefits arising from energy savings [14]. To invigorate building refurbishment efforts and promote energy efficiency policies, investments, and savings, the EU primarily relies on its pivotal legislative instrument—the EPBD (Energy Performance of Building Directive). Initially published in 2002 (Directive 2002/91/EC), subsequently recast in 2010 (Directive 2010/31/EU), and further revised in 2018 (Directive 2018/844/EU), a new revision for 2022 has been proposed as part of the “Fit for 55” package [17]. This proposed revision aims to update objectives and enhance the existing regulatory framework. It envisages introducing mandatory minimum energy performance standards (MEPS) and strengthening obligations to provide EPC (Energy Performance Certificates), establishing common criteria for performance classes [18]. To complement the EPBD, the EPB (Energy Performance of Building) standards set by CEN [19] evaluates the overall energy performance of both new and existing (i.e., renovated) buildings using a comprehensive approach considering multiple facets.

Aligned with this strategy, the EU's funding program, Horizon 2020 [10], issued a call for tenders titled "Building a Low-carbon, Climate Resilient Future" (H2020-LC-SC3-2018-2019-2020) under the H2020 SC3 Societal Challenge – Secure, Clean, and Efficient Energy. Of particular interest is the LC-SC3-EE-5-2018-2019-2020 topic, focusing on the "Next-generation of Energy Performance Assessment and Certification" [16]. This call encourages participants to present innovative assessment and certification systems compliant with EPBD and EPB standards to harmonize evaluation methodologies and enhance the application of EPCs. Providing a standardized framework renders assessments and certifications more reliable, comparable at the EU level, and user-friendly, potentially overcoming the aforementioned barriers.

Answering the calling, we also regard the energy performance as a valuable pursuit, so the **energy performance** is selected to be one of the objectives.

1.4 Human-Body-Oriented Design

Alvar Aalto, known for his architectural prowess, exhibited a profound understanding of humanistic design principles, particularly attuned to the exigencies of extreme climates prevalent in his native Finland. His architectural oeuvre stands as a testament to a sensitive approach, seamlessly intertwining human emotions and environmental consciousness within the built environment.

A UNESCO World Heritage Centre report lauds Alvar Aalto's works for their distinctive capacity to encapsulate human emotions within architectural forms, citing his unique ability to translate feelings and senses into tangible architectural expressions [20]. Notably, Aalto's architectural repertoire is acknowledged as an integral component of international modernism, underscoring the universal resonance and significance of his designs on a global scale [20].

Moreover, scholarly investigations, such as the research paper titled "Atmospheres of space: the development of Alvar Aalto's free-flow section as a climate device," delve into the symbiotic relationship between Aalto's designs and the Finnish climate. This exploration illuminates how Aalto ingeniously harnessed natural light and ventilation, leveraging these elements to craft indoor environments that harmonize with the climatic demands, ensuring comfort even amidst extreme weather conditions [21].

Generally, following the step of Aalto, we decided to set up a objective considering the humanistic design principles, i.e. the **comfort** is chosen as one of the goals.

1.5 Short-Term Expenses vs. Long-Term Profit

Facilitating society's transition towards sustainability poses a pivotal challenge, where economic advantage emerges as a key determinant. While policy directives and environmental advocacy play supportive roles in propelling societal changes, effecting substantial transformation hinges significantly on economic leverage. To seek substantive change, a blueprint can be drawn from Elon Musk's methodology in implementing sustainable transformation. His approach emphasizes the pivotal role of economic advantage, harnessing economic viability as a prime driver for societal evolution. Musk's application of the first principles theory suggests that solely relying on policy directives and environmental rhetoric might not induce fundamental societal shifts in the short term. Conversely, providing economic advantage can stimulate individuals to proactively initiate changes based on self-interest. In this case, the first principle is to replacing all the carbon calculation or GHG emission with the simple value, the **cost**.

Fortuitously, the issue of energy performance fundamentally relates to economics. Over extended comparative periods, superior energy performance theoretically establishes an advantage. In essence, superior energy performance aligns with our goals over prolonged periods. Thus, clarification of the study's duration can substantiate this assertion.

For instance, Tesla's 'Master Plan Part 3' released in 2023 elucidates the company's objective: achieving a sustainable global energy economy through end-use electrification and sustainable electricity generation and storage. This plan delineates a trajectory toward this objective, supported by detailed calculations and assumptions. The ultimate goal is to expedite the global shift to sustainable energy without environmental compromise. [3, 22, 23]

The ultimate goal is also the goal for our sustainable architecture, so we can set up an objective of **Cost**, imitating after the Tesla Masterplan.

1.6 Inspirations from Computer Science

1.6.1 Parametric platform as an intermediate

Horizon 2020-funded projects are pivotal in catalyzing profound innovations in performance evaluation and sustainable strategies. Acknowledging the advent of a new digital era, these initiatives leverage the widespread accessibility of ICT (Information and Communications Technology), IT (Information Technology), and the ubiquitous availability of computers, driving a monumental technological revolution across diverse domains [24, 25, 26, 27, 28, 29, 30]. The conventional dichotomy between the digital and physical realms is dissipating, giving way to a

dynamic, continuous interplay and amalgamation between these two realities [24, 30].

Establishing smart-sensor² grids within the built environment facilitates the control of physical spaces through digitization, enabling the influence of virtual models based on real-time data [24]. Sensors collect vast amounts of real-time data, which computers can efficiently manage and sift through, a task beyond human capabilities without simplification [12]. Precision in small-data accuracy logic is abandoned, acknowledging that single-measurement precision from sensors cannot be guaranteed. Instead, an abundance of data aids in comprehending phenomena and forecasting trends [24].

The applications of these extensive datasets are diverse. They can enhance the definition of a new generation of building performance assessment, as proposed in the H2020 LC-SC3-EE-5 call [16], thereby elevating the quality and reliability of performance and indoor comfort certification. For instance, the H2020-funded project E-DYCE (Energy-flexible DYnamic building Certification) introduces DEPC (Dynamic Energy Performance Certification) as an evolution of conventional EPCs, aligning them closer to actual building operational conditions [26].

Monitoring data offers insights into actual energy consumption in buildings, facilitating informed energy consumption planning [27]. These insights are channeled into advanced control systems aimed at improving building intelligence, fostering healthier and more comfortable indoor environments, reducing energy consumption, carbon footprint, and optimizing the utilization of renewable energy resources.

For the effective implementation of these technologies on a larger scale, simpler, interactive, and cost-effective solutions must be developed. Projects like the EU-funded PRELUDE (H2020 LC-EEB-07-2020 call) endeavor in this direction [27, 28, 29].

Moreover, the advent of big data has implications for the design process and modeling, necessitating the modernization of designer's role and methodologies. Architects, who initially embraced digital tools in the 1990s, now face a reluctance to adopt the new paradigm brought forth by the ICT revolution, potentially jeopardizing their relevance [24, 31]. Carpo suggests that design professionals often believe their expertise, rooted in traditional knowledge, cannot be replaced by machines [25, p. 161] However, in an era of proliferating information and evolving requirements demanding new management models, the conventional conception of an architect is challenged. Geymonat contends that specialization must be reinterpreted and transcended to achieve overall quality and sustainability in

²E.g. ALS (Ambient Light Sensors) of the lighting data

projects.

In this contemporary landscape, designers evolve from solitary entities into active participants contributing sectoral knowledge to a holistic, interdisciplinary design process [25]. Collaboration and transparency are key elements, necessitating designers to articulate and share project information and strategies, facilitated by tools like BIM (Building information modeling) software. The form and performance of buildings must reflect this multidisciplinary approach [32].

1.6.2 Philosophy of Algorithms

At the methodological level, there exists a profound connection between the concepts of computational algorithms and the non-aesthetic indicators within architectural design. Both control theory principles and evolutionary algorithms are centered around the optimization and control of systems, striving to achieve optimal outcomes under specific conditions. In architectural design, these non-aesthetic indicators involve energy utilization, environmental impact, cost-effectiveness, among others, aligning with the optimization goals pursued by computational algorithms.

Contemporary architectural design trends emphasize energy efficiency, environmental consciousness, and sustainability. This pursuit necessitates considerations of multiple variables such as material selection, structural design, thermal analysis, among others, where the optimal combination of these variables directly impacts a building's energy efficiency and overall performance. The application of computational algorithms provides an effective means to navigate through vast design spaces, searching for optimal solutions that meet diverse non-aesthetic criteria.

Optimization algorithms e.g. evolutionary ones simulate natural evolution processes or search for the best solutions, aiding designers in swiftly identifying designs that satisfy various conditions and constraints. This aligns with common optimization objectives in architecture design, such as minimizing energy consumption while maintaining structural stability or significantly reducing environmental impact.

Therefore, at the methodological level, computational algorithms and the non-aesthetic indicators in architectural design both aim to achieve optimal outcomes through optimization. Utilizing data analysis and simulation, they strive to identify optimal solutions to meet multifaceted design requirements.

1.6.3 Translating the design mission to coding

In line with the conversion of design elements into quantifiable variables, aspects that require optimization in the design process are all inherently quantifiable, such as insulation thickness and WWR (Window-to-Wall Ratio). These variables have been structured into forms amenable to computational algorithms, thereby serving as the optimized elements within the design process.

Regarding the methodologies and considerations, a crucial aspect emerges in the selection of quantifiable, objective, and measurable fitness values. Parameters like insulation thickness and WWR stand as direct and effective optimization targets, aiding algorithms in the pursuit of optimal solutions. Simultaneously, for subjective metrics such as the 'Percentage of people dissatisfied,' referencing conclusions derived from statistical experiments like PMV (Predicted Mean Vote) or adaptive comfort criteria proves instrumental. This approach allows the inclusion of subjective elements within the algorithmic framework through objective, quantifiable proxies.

This approach to translating design problems into algorithmic ones hinges on the transformation of qualitative design goals into quantitative fitness criteria. Quantifiable design elements are utilized as objective optimization targets, while subjective metrics are addressed through statistical or empirical conclusions, effectively guiding the algorithmic optimization process. In essence, this framework facilitates the incorporation of both objective and subjective considerations within the algorithmic design optimization paradigm.

1.6.4 Skipping from "Knowing How" to "Getting It Done"

The design profession has historically centered on shaping reality and giving form to human-inhabited environments. The advent of computational tools, like CAD (Computer-aided design) software in the early 1990s, initially served as replacements for traditional paper-based drawing methods among architects [24, 32, 33]. These digital instruments, notably, facilitated the handling of complex shapes, enabling architects to explore previously elusive mathematical elements, such as splines and free-form curves [25].

In its infancy, digital architecture primarily fixated on creating visually striking objects with high aesthetic value and spatial intricacy, often pursuing modernity. This architectural trend, exemplified by the emergence of "blob architecture," gave rise to isolated streamlined structures lauded as mere landmarks and symbols of innovation, featuring almost naturalistic, yet contextually detached, forms that lacked justifiable reasoning [4]. However, such an approach is deemed inadequate in the context of developing a more sustainable construction sector. Contemporary architecture seeks inspiration from nature not solely in form but also in functionality [4], aiming to mimic nature's adaptability to diverse environmental conditions.

A paradigm shift is underway – from "Form must be made" to "Form must be found." This shift in design philosophy aligns with a performance-driven approach, wherein form originates from fulfilling a set of requirements, marrying technical choices with functional necessities [34]. The "requirement-driven approach," known as the "metodo esigenziale-prestazionale" developed in Italy between the '60s and '70s, finds contemporary application as performance-driven or performative design

[34, 35, 36].

Traditionally, designers explored a limited number of design solutions due to cognitive limitations in managing complexity and vast amounts of data [37, 38]. However, leveraging parametric and algorithmic approaches integrated within the workflow allows architects to explore and compare numerous design alternatives at the preliminary phase [24, 37, 33]. These approaches, such as evolutionary algorithms like GA (Genetic algorithm), are increasingly utilized in form-finding and form-optimization within environmental design [39, 40].

By integrating performance simulation directly into the design process, architects can manipulate specific parameters, generating design solutions evaluated against performance metrics. This enables a comprehensive exploration of design alternatives, considering building quality, functional efficiency, and environmental impact, thus surpassing the constraints of traditional design methodologies [24, 37, 33]. The shift from mere form-making to form-finding, coupled with the infusion of machine learning's dark knowledge, stands to redefine the essence of architectural design and practice.

Our research is increasingly supported by computer science, with algorithms providing inspiration.

1.7 From dark knowledge to grokking

In this evolution, theAI (Artificial Intelligence) on some complex mission performance better than human being, appearing with "intelligence". And we call it "to grok³". In the meanwhile, the concept of "dark knowledge" in machine learning becomes relevant. Dark knowledge represents the opaque decision-making process of artificial intelligence, often imperceptible to humans [41]. As machine learning becomes increasingly powerful, human theories might no longer be essential, with neural networks directly yielding results more expediently. This dynamic aligns with the performative design methodology, where performance evaluation guides the design process from its inception. Employing performance evaluation in early design stages enables architects to assess whether conceptual ideas align with expectations and lead to the iterative refinement of solutions meeting a set of sometimes conflicting objectives.

³Grokking is a slang term that means to understand something intuitively or empathetically. It was coined by Robert A. Heinlein in his book "Stranger in a Strange Land". In the context of machine learning, Grokking refers to a specific learning process where a model suddenly transitions from memorizing training data to being able to process and understand unseen data after prolonged training.

Chapter 2

Study of the Art

This chapter serves as a platform to explore the foundational background and the sources of inspiration for this study. The proposed GH (Grasshopper) tool represents a parametric and optimizing GUI (Graphical user interface) designed for the EnergyPlus analysis engine. It distinguishes itself among a plethora of existing tools with similar functionality. The chapter dedicates its efforts to scrutinizing the commonalities and distinctions between these tools and the proposed GH interface. Moreover, it presents a concise literature review concerning analysis and optimization experiences related to HB (Honeybee) and LBT (Ladybug Tool). Detailed exploration of other specific facets of the state of the art will unfold in subsequent chapters.

Then, we discuss about the anglo-saxon influence in project management in Italy, which indicates that the life cycle concept is rising. And LCC (Life Cycle Costing) method is also developing.

Lastly, the core process of the NSGA-II (Non-dominated sorting genetic algorithm II)[42, 43, 44] is briefly introduced, indicating it has a good ability in studying. In the end the related works in the similar realm are presented.

2.1 EP parametric and optimization interfaces

2.1.1 EnergyPlus platform

EP (EnergyPlus) is an influential open-source, cross-platform whole-building simulation software, originally developed by the U.S. Department of Energy's BTO (Building Technologies Office) in 1997 [45]. It ranks as one of the most extensively utilized tools for executing performance-oriented energy analyses and conducting optimization processes. EP employs the IDF (Intermediate Data File) file format, a

text-based repository housing all the requisite building data for energy simulations. Each IDF is composed of an array of meticulously ordered string fields, all aligning with an associated IDD (Input Data Dictionary) file linked to a specific EP release. The IDD provides an exhaustive catalog of all conceivable EP objects, along with a specification of the data requirements for each object [46], elucidating the protocol for EP in interpreting an IDF file. Notably, EP lacks a GUI, rendering it a challenging platform to navigate, especially for non-experts. This limitation has led to the creation of various tools designed to offer interfaces for EP, facilitating parametric energy simulations and optimization processes. Parametric interfaces can be categorized into scripting-based and GUI-based approaches.

2.1.2 Interfaces of EnergyPlus

One notable example of a scripting-based interface is BESOS (Building and Energy Simulation, Optimization and Surrogate Modeling). Launched in July 2019, BESOS stands as a cloud-based, open-source platform rooted in Python code and Jupiter Notebooks, striving to establish a unified interface for traditional modeling tools while harnessing novel optimization and machine learning techniques [47, p. 5]. BESOS is structured as an ensemble of modules, enabling parametric building energy simulations through EP via Eppy¹ or EnergyHub, and executing multi-objective optimizations through the use of evolutionary algorithms via the Platypus library [48]. BESOS Platform provides a robust avenue for conducting extensive energy analyses, yet it necessitates a certain level of proficiency in coding and familiarity with file formats from the user's end.

Conversely, graphical interfaces, such as that offered by jEPlus² [49], have traditionally been recognized for their user-friendliness, requiring fewer programming skills. jEPlus is an open-source project originally introduced in 2009, implemented in Java. It provides a parametric GUI for EP, empowering users to define design parameters, edit models, manage simulation runs, and collect results [49]. When paired with an evolutionary algorithm, jEPlus excels in efficiently undertaking building design optimizations, encompassing both single-objective and multi-objective paradigms [50]. Nevertheless, similar to script-based tools, a fundamental understanding of the "EP modeling process and the text input files" is a prerequisite for jEPlus users [49].

¹Eppy is a scripting language written in Python for IDF files and other EP output files. More on Eppy at <https://pypi.org/project/eppy/>

²jEPlus – An parametric tool for EnergyPlus and TRNSYS

More accessible than jEPlus is the PREDYCE (Python semi-Realtime Energy Dynamics and Climate Evaluation) tool, which is a Python library developed by researchers at POLITO as part of the EU-funded project E-DYCE (Energy-flexible DYnamic building Certification) [51]. This tool offers a user-friendly interface that allows users to launch (parametric) simulations and select from a range of pre-built actions [52]. Importantly, it doesn't necessitate any prior knowledge of Python and generates highly graphical outputs. PREDYCE comprises three primary, independent modules (an IDF editor, Key Performance Indicators calculator, and runner), as well as additional modules (e.g., EPW compiler) that can be combined to create task-oriented scripts known as "scenarios" [51]. The KPI (Key Performance Indicator) encompass various aspects, such as thermal comfort, indoor air quality, and ventilative cooling. This tool is primarily designed for free-running building simulations and optimization.

However, unlike typical GUIs, it stands out due to its ability to seamlessly integrate with 3D modeling software, notably RH-GH. This feature transforms PREDYCE into a highly graphical interface for EP and other analysis engines, including Radiance and Daysim. This integration allows users to conduct daylight simulations, encompassing all aspects of comfort when optimizing building design. Furthermore, PREDYCE offers an intuitive interface with pre-configured Python code, sparing users the need for programming expertise and manual handling of input and output files. These files are automatically edited, read, and translated into numerical values or visual outputs, such as bar charts and annual hourly charts, thereby streamlining the simulation process.

2.1.3 A prevailing interface of EnergyPlus: OpenStudio

OS (OpenStudio) [53] is a widely used graphical interface for EP. It operates as a user-friendly SDK (Software Development Kit) and seamlessly integrates with the SketchUp 3D modeling software. A key feature of OS is the use of "OS Measures," which are sets of programmatic instructions designed to modify energy models, known as OSM (OpenStudio Model)[54]. For further details, additional references can be found in the *OpenStudio Measure Writer's Reference Guide*[55]. These measures facilitate the implementation of ECM (Energy Conservation Measures) and allow for the creation of building models in a parametric fashion.

This approach, often referred to as "procedural modeling," shares similarities with GH-HB, as both methodologies involve linking various components to construct detailed building models. OS further supports parametric analysis through the OS PAT (Parametric Analysis Tool). PAT systematically applies combinations

of OS (OpenStudio) Measures to the OSM, generating and comparing multiple design alternatives to assess their energy performance [56, p.322 323]. In OS's PAT, users have the choice of specifying measure values. These values can be manually defined, which may be time-consuming, or they can be automatically selected from a predefined range using optimization algorithms. This automated approach facilitates the exploration of broader solution sets [57].

Notably, PAT closely aligns with the tool presented in this paper, both offering graphical parametric interfaces to EP and supporting multi-objective optimizations. Furthermore, PAT can perform daylight analysis through the Radiance engine. However, it's important to highlight that PAT's algorithmic optimizations require cloud-based processing, such as Amazon cloud or dedicated servers, due to their complexity. While this approach reduces simulation time, it can be challenging to obtain and manage detailed results, as they are typically large files that need to be downloaded from the server immediately after the simulation, with the risk of data loss if the server is shut down [57].

In contrast, the presented tool employs the Wallacei plug-in[58, 59], which can be run locally. While this may lead to longer simulation times, it offers the advantage of periodically saving optimization results during the simulation and storing them within the GH document. This feature allows for easier analysis of the obtained data, as solutions can be directly reinstated into the GH environment.

2.1.4 DesignBuilder: a parallel tool in addition to EP

DesignBuilder [60] is a widely embraced and versatile tool used by architects and engineers. It provides a robust environment for creating diverse building geometries, including complex designs. Notably, DesignBuilder offers seamless interoperability, allowing the import of 3D models created using other BIM/CAD tools. The DesignBuilder seamlessly integrates various analysis tools, such as EP and Radiance, providing a holistic view of building performance. Parametric analysis allows for the generation of design curve outputs by adjusting up to two variables [61], facilitating quick assessments of design decisions and solution comparisons [60]. DesignBuilder employs a genetic algorithm for optimization, searching for the optimal combination of selected design variables to maximize or minimize specific KPIs [62]. While supporting multi-objective optimization, it is limited to two objectives. In contrast, the presented tool, with the Octopus plug-in, can simultaneously consider a minimum of two and theoretically an unlimited number of objectives [63].

2.1.5 Conclusion and their weakness

Both OS and DesignBuilder are widely used tools in the field of building performance analysis. OS offers a powerful graphical interface for EP and enables parametric modeling and analysis. However, it requires cloud-based deployment, limiting its accessibility for local processing. Mentioned in §2.1.4, DesignBuilder is favored for its versatility and interoperability, allowing the import of 3D models from other BIM/CAD tools. Nevertheless, its optimization capabilities are limited to two objectives, which can be restrictive in scenarios that require the consideration of multiple performance goals. Understanding these limitations is crucial when choosing the right tool for a specific project, as they may impact the efficiency and comprehensiveness of building performance analysis. To address the limitations posed by cloud-based deployment and the restriction of optimization objectives, a solution lies in finding a platform that enables local execution of EP simulations while offering the flexibility to deploy advanced algorithms, like NSGA-II.

In the field of building energy simulation, Octopus, powered by the SPEA-II (Strength Pareto Evolutionary Algorithm II), has made significant strides (see §2.3.2). Looking at the entire parametric design domain, a new tool has emerged, Wallacei. Unlike Octopus, which incorporates various machine learning components, Wallacei is solely focused on genetic algorithm optimization. It boasts superior visualization capabilities and provides enhanced interactivity for form generation.

Octopus has gained an early advantage in academic research and enjoys widespread popularity. As a result, Wallacei has introduced a specific feature to read and visualize Octopus' outcomes. However, their core algorithmic engines differ, with Octopus using SPEA-II and Wallacei relying on NSGA-II[59]. Starting from 2020-2021, Wallacei has been increasingly involved in urban design activities, such as urban planning in Barcelona and applications in BIG architecture firm projects[64].

Nevertheless, this integration primarily occurs in design activities. In the realm of academic architectural studies, the NSGA-II hasn't been thoroughly explored yet. The study has shown that SPEA-II and NSGA-II are considered highly similar algorithms with comparable performance[43]. The former produces better optimization results, while the latter can save nearly half of the simulation time. A summary article highlights that in scenarios with an extensive range of objectives, SPEA-II demonstrates an advantage. However, NSGA-II excels in providing a broader genotype diversity in the final optimized results, making it more inclined to offer a more diverse gene pool as an outcome[65]. And also it produces lots of studies in architecture, see §2.3.3.

2.2 GH linking with EnergyPlus

When considering a platform for conducting comprehensive building performance analysis, GH emerges as a promising choice. Operating within the RH-GH environment, this powerful tool extends its capabilities through various plug-ins. Alongside renowned solutions like Ladybug Legacy and Honeybee, GH supports other plug-ins that establish a seamless link with EP, Radiance, and Daysim simulation engines, enabling the execution of parametric performance analyses. One such example is ClimateStudio [66], a fully parametric software developed by Solemma LLC [67]. This advanced tool specializes in daylighting, electric lighting, and conceptual thermal simulations, making it a valuable addition to the GH ecosystem. ClimateStudio is renowned for its user-friendliness and comprehensibility, much like HB and LB, allowing architects and engineers to efficiently perform energy and daylight analyses. Moreover, it offers a range of optimization capabilities, making it a versatile platform for fine-tuning building designs. GH, in conjunction with these plug-ins, not only streamlines the analysis process but also empowers users to explore design alternatives and assess performance parameters with greater accuracy and flexibility. This comprehensive environment encourages creative solutions and efficient problem-solving in the field of building design and performance optimization.

Repeatedly, to underline, by linking to the EP, Radiance, our GH is empowered to simulate the EUI (Energy Use Intensity) and DA.

2.3 Related works

The tool developed in this study aligns with a broader framework of research endeavors that integrate parametric modeling with building performance assessment while harnessing the power of GAs to facilitate fully-automated design optimizations. The mechanics of the algorithm is introduced in §3.5. To provide valuable context for this work, we have conducted a comprehensive review of prior studies within this domain. Our focus has been on investigations where the integration of HB and LB plug-ins for GH is complemented by GH optimization add-ons, including Galapagos, Octopus, and Wallacei.

2.3.1 Galapagos

Galapagos, a straightforward GH plug-in, has historically served as a valuable resource for single-objective optimizations. It leverages an evolutionary algorithm but focuses on addressing a single objective at a time. However, the intricate

interplay between optimization objectives, such as daylight performance and energy efficiency, has underscored the need for more advanced multi-objective optimization tools within the GH environment. Notably, Octopus has emerged as a prominent solution to address this challenge.

2.3.2 Octopus and its practice

This transition to multi-objective optimization is well exemplified in the work of Qingsong and Fukud[68]. In their research, a simple office building in Beijing was analyzed to identify the optimal window configurations on each of the four cardinal directions. The objective was to maximize useful daylight illuminance (percentage of time illuminance exceeds 300 lx on the analysis plane) while minimizing total TEUI. Galapagos was employed, with separate processes for daylight and energy optimization. Intriguingly, the optimal window dimensions for daylight and energy goals were found to be distinct. This underscores the limitations of single-objective optimization tools and the additional burden they place on designers to interpret results and strike a balance between often conflicting objectives. Multi-objective optimization, as exemplified by the Octopus tool, provides a compelling solution to the intricate relationship between daylighting and energy performance, as demonstrated by Toutou et al.[69]. In their study, Spatial Daylight Illumination (SDI) and EUI were the focal points of optimization, considering a set of seven variables encompassing factors like south window-to-wall ratio, window material, wall construction, shading angle and dimensions. This investigation yielded a critical insight: optimal design solutions, when viewed from the perspectives of daylighting and energy, often do not align. This divergence in design objectives is further substantiated in Fang's PhD thesis[70]. Fang undertook a two-fold optimization process, utilizing the Galapagos plug-in for single-objective optimization. The first optimization sought to maximize Useful Daylight Illuminance (UDLI), while the second aimed to minimize EUI. Subsequently, an Octopus multi-objective optimization process was employed to identify trade-off solutions that optimize both objectives. Notably, this workflow was applied across varying U.S. climatic conditions, highlighting its versatility and adaptability. Conducting these optimizations under different climatic conditions not only validates the robustness of the established workflow but also underscores its applicability in diverse contexts, as corroborated by previous studies[71, 72].

The utilization of the Octopus plug-in to address conflicting design objectives is well-documented in a range of studies[73, 74, 75]. Zhang and Ji , for instance, engaged in multi-objective optimization that simultaneously aimed to minimize

cooling energy consumption while maximizing DA and wind speed[73]. This optimization process involved varying WWR on the four facades of the building under investigation. Another notable example is presented in the work of Zhang A. et al.[74], who optimized various design parameters for a school building in China. Their objectives centered on maximizing Useful Daylight Illuminance (UDLI) within a range of 100-2000 lx while concurrently reducing heating and lighting energy requirements and minimizing summer discomfort. The optimization process considered variables such as building orientation, space depth, WWR of different facades, glazing materials, and shading types. Pilechiha et al. [75] introduced an innovative approach to assess the "Quality of View" in office buildings while maintaining a balance with energy performance and daylighting. Their study focused on optimizing window location and dimensions through the Octopus plugin, employing design goals encompassing sDA (Spatial Daylight Autonomy), ASE (Annual Sunlight Exposure), EUI, and Quality of View (QV). Multi-objective optimization techniques are frequently employed to identify shading configurations that not only enhance occupants' comfort but also optimize energy consumption. A noteworthy example is the work of Bahdad et al.[76], who harnessed the power of Octopus to determine the optimal design for light-shelves. Their objective was to strike a balance between minimizing EUI, maximizing Useful Daylight Illuminance (UDLI), and minimizing DGP (Daylight Glare Probability). This use of Octopus for enhancing occupants' comfort and energy efficiency can be observed in various other studies as well[77, 78]. These investigations highlight the versatility of the Octopus tool in addressing a wide range of design objectives and performance parameters, making it a valuable asset for researchers and designers seeking to create sustainable and occupant-centric built environments.

The study by Bakmohammadi and Noorzai[79] delves into the complex realm of design optimization, extending beyond the objectives of previous research. In their investigation, a multitude of objectives is considered, encompassing occupants' thermal and visual comfort, as well as energy consumption.

Five distinct goal parameters guide the optimization process:

- Useful Daylight Illuminance between 100 and 2000 lx(UDLI100-2000)
- DA (Daylight autonomy)
- TEUI (Thermal Energy Use Intensity)
- LEUI (Lighting Energy Use Intensity)
- Occupants' thermal comfort

The integration of an adaptive thermal comfort model, even in conditioned spaces, is indicative of the research's depth. EP (EnergyPlus) analysis outputs are utilized to calculate TEUI and LEUI values, providing a comprehensive perspective. Furthermore, the study acknowledges the importance of glare mitigation by

introducing DGP as a critical measure. This aspect is incorporated into the evaluation process after the optimization phase, allowing for the selection of the final optimal solution.

Multi-objective optimization extends its applicability to find harmonious trade-off solutions between occupants' comfort, energy consumption, and additional variables. Notably, studies such as Sun et al.[80] introduce the minimization of envelope cost as one of the optimization objectives. In a similar vein, research by Manni et al.[81] explores multi-objective optimization with the aim of balancing comfort and energy efficiency with environmental considerations.

A comprehensive review of relevant literature reveals that Octopus optimization has predominantly been applied to fully conditioned buildings. In these scenarios, energy use intensity (total EUI or thermal and lighting separately) is typically included among the optimization objectives, aiming for their reduction. Surprisingly, this method has rarely been utilized to discover optimal design configurations for free-running buildings. In contrast, the proposed tool expands the horizons of optimization by considering thermal and visual comfort metrics without the involvement of mechanical systems. The primary objective is to minimize discomfort by harnessing the inherent potential of the building's design itself. Only in a subsequent phase, the approach introduces HVAC (Heating, ventilating and air conditioner) and lighting systems into the optimization process, suggesting control schedules to eradicate discomfort while concurrently reducing energy consumption. Consistent with findings from reviewed papers, the developed workflow optimizes a diverse array of variables, encompassing various design aspects. These include window positioning and configuration, insulation, shadings, and natural ventilation, all directed toward enhancing both visual and thermal comfort. As observed in examples from [70, 71, 72], the tool's adaptability is rigorously tested across various real climate conditions, confirming its robustness and versatility in diverse real-world scenarios.

Manni and Nicolini's insights, as highlighted in [82], shed light on a critical yet often overlooked aspect of research. Few studies incorporate climate change effects into their multi-objective optimizations, despite the potential for future climatic conditions to render current optimal design solutions obsolete. To address this significant concern, the developed tool is subjected to rigorous testing under various European climates, ensuring its adaptability to diverse environmental conditions. Furthermore, the tool's resilience is put to the test by examining its performance under simulated 2050 weather conditions.

Eleonora Vignani[2] delves further into her research to explore the conditions of the year 2050. She conducted two algorithmic experiments with a focus on comfort,

optimizing for visual aspects (max DA, max UDLI, min ASE) and thermal sensation (Max percent of time comfortable). The genes to be optimized include Orientation, four orientations of WWR, Insulation thickness, % of glazed area operable for natural ventilation, and shading devices angle.

She selected ten European cities and estimated their 2050 weather conditions based on the report for scenarios-1[83]. Subsequently, using the algorithm, she conducted optimization under both current and future climate conditions for each city. Following this, her second experiment applied the algorithm to two specific building renovation projects in the Piemonte region. Her research is extensive in both temporal and spatial scales, highlighting the robustness of GA.

This not only underscores the significance of practicing Scripting Architecture in the design approach but also emphasizes the need for forward-thinking regarding the raw input data in research. In the design development process, sustainability, climate change, and optimization algorithms can be considered simultaneously. When exploring the future, climate reports, in addition to algorithms, require significant attention.

2.3.3 NSGA-II and Wallacei in architecture

S. Chaturvedi et al.[84] propose a multi-objective optimization framework that integrates BIM with NSGA-II to optimize building envelope parameters for energy efficiency and thermal comfort. The paper utilizes DesignBuilder software to simulate the energy performance and thermal comfort of a sample office building in Tehran, Iran. Four building envelope parameters are considered: WWR, window orientation, glazing type, and shading device. The method is to define two objective functions: minimizing the annual total energy consumption (ATEC) and maximizing the percentage of occupied hours within the thermal comfort range (POHC). NSGA-II is applied to generate a set of optimal solutions (Pareto front³) for the two objectives. The outcomes can be summarized as the Pareto front and the optimal values of the building envelope parameters for different scenarios. The paper analyzes the trade-off between the two objectives and the sensitivity of the results to variations in the parameters. It is found that WWR and window orientation have the most significant impact on the energy performance and thermal comfort of the building. Furthermore, the paper compares the results with the conventional design method and demonstrates that the proposed framework can achieve better energy savings and higher thermal comfort levels.

³The introduction and definition of Pareto front can be seen in §5.9.4

Yang et al.[85] emphasize the significance of energy-efficient building design for environmental sustainability, addressing the challenges in balancing conflicting parameters. They highlight the use of GA to optimize urban building designs. The limitations of existing simulation models are discussed, leading to the development of ENVLOAD for assessing building envelope energy performance. The study integrated NSGA-II with a building envelope energy estimation model (BEM) to create a multiobjective optimal BEM decision support system (MOPBEM) for designing green building envelopes. The developed BEM was derived from the ENVLOAD, and the MOPBEM was validated in a real building design case.

Designing green buildings involves multiple parameters like insulation, window area, climate, and orientation, making it a complex task. Subjective approaches often fall short, necessitating optimization. The paper integrate NSGA-II with an energy performance model to achieve:

- minimizing ENVCOST - the envelope construction cost
- minimizing ENVLOAD - the building energy demand
- maximizing WOPR - the façade window opening rate

The optimizing objectives are really similar to ours. But they focus more on the envelope. In summary, Yang et al. underscore the importance of energy-efficient building design, address challenges, and introduce an optimization model to achieve optimal green building envelopes.

Similar to Yang's study. Wang et al.[86], conducted an optimization experiment on an architectural model, illustrating the relationship between traditional GA (Genetic algorithm) and quantum evolution generation (QGA). According to the comparison, it can be found that compared with the genetic algorithm, when the quantum genetic algorithm is used to deal with the optimization problem of building energy saving, the ENVCOST will be lower by selecting the appropriate material type and reasonably allocating the area occupied by each part (windows, walls and glass curtain wall) under the condition of ENVLOAD; the rate of convergence is faster; the total window area is larger by 13.8%, which means that the natural ventilation is better; glass curtain wall ratio increased by 14%, which means that indoor lighting is better; the generation number to achieve convergence is reduced by 50%, which means the convergence is faster. And compared with original design, the total cost reduces by 35.3%.

The article addresses uncertainties and the algorithm's robustness, acknowledging that results vary with input parameter changes. Nevertheless, it asserts the algorithm's applicability to building designs in tropical and subtropical regions, providing a valuable contribution to the field.

Chapter 3

Methodology for simulations

In the examination, we conduct 4 calculations, whose methodologies will be presented in the referring section:

- Energy Use Intensity in §3.1
- Lighting in §3.2
- Costing in §3.3
- Comfort metric §3.4

in order to get the 3 **fitness values**.

And 1 **optimization**. in §3.5

The EUI, comfort metric and the optimization are conducted under the complete and mature programs, i.e. EP and OS[53, 87]; LBT[88]; Wallacei_X[58].

The lighting simulation we operate with HB Radiance and also our arithmetic is combinedeqs. (3.4) to (3.7). The economic simulation is calculated fully under our arithmeticeqs. (3.8) to (3.11). This chapter is aiming at introducing these.

3.1 Approach for Energy simulation

The main body of the exam is to do the EI (Energy Intensity) simulation. Because it is difficult to do the EI simulation with a large amount of input parameters. We spend many steps, those introduced in §4, to complete and attune the parameters. So, the approach is congruent with the main work flow, and will be introduced in §5. But there's a lighting part that relates to the EI we can present here.

3.1.1 Math of thermal transmittance

However, the basic formula to describe the thermal transmittance[89] is not difficult and can be written as follow:

$$U = \frac{1}{R_t} \quad (3.1)$$

$$R_t = R_{si} + \sum_{i=1}^n R_i + R_{se} \quad (3.2)$$

$$R = \frac{D}{\lambda} \quad (3.3)$$

where:

U = Thermal Transmittance ($\text{W}/\text{m}^2 \cdot \text{K}$)

R_t = Total Thermal Resistance of the element ($\text{m}^2 \cdot \text{K}/\text{W}$)

R_{si} = Interior Surface Thermal Resistance (according to climatic zone)

R_{se} = Exterior Surface Thermal Resistance (according to climatic zone)

R_i = Thermal Resistance of i-th layer

D = Material Thickness (m)

λ = Thermal Conductivity of the Material ($\text{W}/\text{K} \cdot \text{m}$)

This only consider one-dimensional situation, in reality, the heat transfers 3-dimensionally. So we use the simulation program to help.

In the formula, we can see 2 main factors effect on U -value the thermal transmittance, i.e. λ and D . Those are the main role we consider for the insulation. And we further study it in §4.2. And also because of this, D the thickness is one of the **objective** for optimization.

3.2 Approach for lighting simulation

Lumen Method Calculations:

This method[90, p. 4] uses the utilisation factor tables created from photometric measurement of each luminaire. Firstly, the Room Index (K) of the space must be calculated, which is the relationship and measure of the proportions of the room:

$$K = \frac{W \cdot L}{(W + L) \cdot H_m} \quad (3.4)$$

where:

K = length of room

W = width of room

H_m = height of luminaire above working plane

With the room index and reflectances we can search for the utilisation factor in the table[90, p. 6].

Reflect.			Room Index								
C	W	F	0.75	1.0	1.25	1.5	2.0	2.5	3.0	4.0	5.0
70	50	20	N/A	66	72	76	81	85	87	90	92
70	30	20	N/A	60	66	71	77	81	84	87	90
70	10	20	N/A	56	62	67	73	78	81	85	88
50	50	20	N/A	64	70	73	79	82	84	87	89
50	30	20	N/A	59	65	69	75	78	81	84	86
50	10	20	N/A	56	61	66	72	76	78	82	85
30	50	20	N/A	63	68	71	76	79	81	83	85
30	30	20	N/A	58	64	68	73	76	78	82	83
30	10	20	N/A	55	61	65	70	74	76	80	82
0	0	0	N/A	53	58	62	67	71	73	76	78
BZ			1	2	2	2	2	3	3	3	3

Table 3.1: Utilisation factor to search

The first 3 columns are the reflectances, the rest on the right are the room index in first row. The last row are the BZ-class level, and where:

$Reflect.$ = Reflectance

C = Ceiling reflectances

W = Wall reflectances

F = Floor reflectances

BZ = British zonal classification[91]

The result is used in conjunction with room reflectance values to obtain a specific utilisation factor for the surface illuminated from the tables. This can then be used as part of the calculation to determine the average illuminance level, using the following formula:

$$E = \frac{F \cdot n \cdot N \cdot F_M \cdot F_U}{A} \quad (3.5)$$

where:

- E = average luminance
- F = initial lamp lumens
- n = number of lamps in each luminaire
- N = number of luminaires
- F_M = maintenance factor
- F_U = utilisation factor
- A = area

The maintenance factor is a multiple of factors and is determined as follows:

$$F_M = F_{LLM} \cdot F_{LS} \cdot F_{LM} \cdot F_{RSM} \quad (3.6)$$

where:

- F_M = maintenance factor
- F_{LLM} = lamp lumen maintenance factor - the reduction in lumen output after specific burning hours
- F_{LS} = lamp survival factor - the percentage of lamp failures after specific burning hours
- F_{LM} = luminaire maintenance factor - the reduction in light output due to dirt deposition on or in the luminaire
- F_{RSM} = room surface maintenance factor - the reduction in reflectance due to dirt deposition in the room surfaces

From now on, the quantity of lumen we need to produce in the light source is clear. We just need to convert it into energy usage.

$$LEUI = \eta^{-1} \cdot Lumen \quad (3.7)$$

where the η symbolizes efficacy, which is assumed to [92] 100 lumen per watt. With it we can finally calculate the EUI.

3.3 Approach for economical analysis

We can know the methodology of evaluating a building or a project from theoretically to practically from the book[93], which also gives us how the methodology has been developed.

The LCC approach advances the principles of "technical and economic" assessment of design/technology alternatives in case of works in the construction field. It is based on a research line developed in the United States in the 1960s and 1970s, which spread to other countries[93, p. 79]. To encourage the development of this

methodology, several factors must act together, like the cultural context in which it operates, its full maturity on the level of legislation, the support of the owners and the awareness of its limitations by using cost of construction as understood in the traditional sense (see [94]). LCC allows one to determine the total cost of the project considering its entire life cycle[93, p. 80]. The total cost could include its planning, design ,use, management, maintenance, disposal, the residual value must be included, considering it as possible income (see [95, sections 3.1.4 and 4.4.7]).

In order to calculate the **cost** as the fitness values, we need to dive into the formula, and realize it in the GH platform. With LCC method we can evaluate the project value in a future period. And the formula is as followed:

$$LCC = \sum_{t=0}^N \frac{C_o + C_m}{(1+r)^t} \pm V_r \left(\frac{1}{(1+r)^N} \right) \quad (3.8)$$

where:

- LCC = Life Cycle Cost
- C_i = investment costs
- C_o = operational costs
- C_m = maintenance costs
- t = the year when the cost is incurred
- N = the number of years of the entire period considered for the analysis
- r = discounted rate
- V_r = residual value of the asset, materials or components

A diversity of "evolutions" of the mathematical models are presented, all of which come from the basic formula (see [95, 96, 97]). It can be generalized into mathematical model by distinguishing between continuous cost and the discontinuous ones. And including costs for the substitution of building components or refurbishing of the envelopes, etc.

the formula can be written:

$$NPV = c_0 + \sum_i^n \sum_{t=0}^T c_{it}(1+r_{it})^{-t} + \sum_j \sum_{t=0}^T c_{jt}(1+r_{jt})^{-t} - d(1+r_d)^{-T} \quad (3.9)$$

where:

NPV = Net Present Value

c_0 = the *procurement cost* at 0 moment in time

c_{it} = the annual cost of a period t support of the function i

c_{jt} = the cost at a moment t in time which refers the discontinuous costs j

r_{it} = discount rates applicable to support respectively the i function

r_{jt} = discount rates applicable to support respectively the j function

d = value of the asset to be disposed minus disposal costs

r_d = discounted rate applicable to the disposal of asset in period from 0 to T

However, we don't need to actually calculate the NPV for all the components, because our aim is the cost. In other words, we just need to calculate all the cost parts. That is, to calculate the initial cost and add up all the NPV for the future costs. Notably, LCC are generally difficult to evaluate because they are significantly variable in terms of the discount and inflation rate, durability of the materials the number of substitutions needed and maintenance cycles during the useful life of the building (in this case expressed in the form of replacement and maintenance costs). Obviously, the actual estimation of the Global Cost depends on the availability of all the data necessary of each project/technology alternative, using methods such as the "stratigraphy" of costs. In our study this weakness is scaled up, as the financial state and material market diverse, and also the costs of labor vary. But at least, within the EU it's comparable. And also the methodology is universally adopted which can be applied in different environments, once we've input the value with higher accuracy, more assured result we can obtain. Lastly, using a same price database makes our result numbers in a similar scale. In a single study that benefits in the comparability and legibility.

This method can be extended into a deeper financial realm with a more cohesive GA. E.g. I can set leverage rate as a genotype, so the investment strategy would be optimized. More financial calculation can be brought in this mechanics. The matter is the balance whether the study is leaned more to the economy side or the energy simulation side. And also considered a bad legibility for too many financial numbers. I just keep a basic formula in the method, preserving it as simple as clear.

Considering only for the cost, formula turns into a direct way, only to calculate the Global Cost:

$$C_G(\tau) = C_I + \sum_j \left[\sum_{i=1}^{\tau} (C_{a,i}(j) \cdot R_d(i)) - V_{f,\tau}(j) \right] \quad (3.10)$$

$$R_d = \frac{1}{(1 + R_r)^p} \quad (3.11)$$

where:

- $C_G(\tau)$ = the Global Cost, referred to in the initial year τ_0
- C_I = initial investment cost
- $C_{a,i}(j)$ = the annual cost at year i, for the j component (including running costs and the periodic or replacement costs)
- $R_d(i)$ = the discount rate at the year i
- $V_{f,\tau}(j)$ = the final value of the j component at the end of the calculation period (referred to the initial year τ_0)
- R_d = discount factor
- R_r = real discount rates
- p = the reference period

And in eqs. (3.8) to (3.11), we can refer to [98] for the market interest rate in real time. The bank rate fluctuates violently in 2023. But at the moment we began the experiment, this rate is 3.25%, which is solidified in the to all the simulations and stay fixed to the end.

3.4 Approach for comfort metrics

Comfort, fundamental to human physical and mental well-being, stands as a primary gauge within the built environment[99]. Given that individuals spend approximately 85% of their lifetimes indoors[100], the microclimate indoors becomes a pivotal concern in architectural design, profoundly impacting occupants' wellness, health, mood, productivity, work performance, and energy utilization. Indoor comfort, an amalgamation of thermal, visual, and acoustic elements, is subject to the influence of diverse environmental factors including temperature, humidity, lighting, and air quality. The model delineated in this study revolves around predicting occupants' thermal and visual comfort by evaluating multiple parameters signifying individual satisfaction and adherence to regulatory benchmarks.

Initially, our primary focus was on investigating thermal comfort, particularly emphasizing the study of winter thermal comfort within the zone by conducting the EPenergy simulation. Although our attention does extend to both thermal comfort and visual comfort, our primary emphasis remains directed towards understanding and enhancing winter thermal comfort. Design strategies that optimize one might inadvertently affect the other. For instance, a reduction in WWR could ostensibly enhance the building envelope's thermal performance. Paradoxically, this reduction may curtail daylight ingress, leading to escalated energy usage for artificial lighting. Conversely, elevating WWR could augment visual comfort while potentially increasing heat transfer through transparent surfaces, potentially culminating in excessive thermal dissipation or overheating, thereby amplifying energy requirements for heating/cooling systems.

This intertwined relationship underscores the indivisibility of control over thermal

and visual comfort. Consequently, both facets are incorporated into consideration to provide a more comprehensive depiction of indoor comfort dynamics.

3.4.1 Thermal comfort

The ASHRAE (American Society of Heating Refrigerating Air-Conditioning Engineers) Standard-55[101] defines thermal comfort as "that condition of mind that expresses satisfaction with the thermal environment and is assessed by subjective evaluation." Hence, the perception of thermal comfort is highly individualistic, influenced by various personal factors like age, physical attributes, habitual tendencies, and acclimatization to specific climates. Essentially, these comfort-determining parameters may elicit different responses and sensations among individuals. However, established scientific methodologies enable the estimation of user satisfaction or dissatisfaction within a given environment. Two prevalent comfort models exist in literature: static (or steady-state) and adaptive[102].

The former, often referred to as the rational or heat balance model[103], was developed by P.O. Fanger in the early 1970s[104]. This approach is widely employed in both national and international standards (e.g., ISO-7730:2005 [105]) for evaluating indoor comfort. According to Fanger's model, thermal sensation emerges from the "difference between the internal heat production and the heat loss to the actual environment for a person maintained at the comfort values for skin temperature and sweat production at the current activity level" [104]. Thermal comfort is influenced by six variables, four of which are environmental (air temperature, mean radiant temperature, relative humidity, and airspeed), while the other two are physiological (clothing insulation and activity level or metabolic rate).

The collective impact of these variables on comfort is commonly assessed through the PMV index and the PPD (Predicted Percent of Dissatisfied). PMV is derived from a complex mathematical equation formulated based on controlled climate chamber experiments under stable conditions and regulated environmental (e.g., temperature, humidity, etc.) and physical variables (e.g., clothing).

3.4.2 Predicted Mean Vote

It represents the average mean vote on thermal sensation of a group of people in a given environment. Mean vote can be associated with a seven-point scale that ranges from -3 (very cold) to +3 (very hot); 0 represents thermal neutrality. PPD, instead, is a statistical index that expresses the percentage of people in that same environment who are not satisfied with the indoor thermal conditions. ISO 7730 regulation suggests that PPD should be kept around 10%, which corresponds to a PMV between -0.5 and +0.5.

The static comfort model, as previously delineated, finds its application primarily

within fully conditioned buildings where a controlled and stable indoor climate is rigorously upheld, relatively detached from the considerably variable outdoor conditions. Conversely, in naturally ventilated buildings where indoor temperatures continuously fluctuate in response to outdoor variations, Fanger's method proves unsuitable, potentially introducing inaccuracies in evaluating occupants' thermal perception. De Dear et al. revealed substantial disparities between computed PMV values and actual comfort ratings in naturally ventilated structures, assembling the ASHRAE RP-884 thermal comfort database¹ [106, 107]. Fundamentally, such contexts exhibit a tendency for the PMV index to overestimate occupants' dissatisfaction, particularly in warmer conditions[103]. This discrepancy may be attributed to occupants of naturally ventilated buildings under diverse climatic settings accepting a broader spectrum of comfort temperatures than presupposed by the heat balance model – as detailed in, for example, [108]. Furthermore, occupants play an active role, adapting to dynamic thermal conditions by modifying clothing or adjusting openings when temperatures are less conducive. The adaptability of occupants underscores that maintaining indoor environments at uniform temperatures stipulated by standards can result in superfluous energy consumption and, paradoxically, discomfort (such as overheating during winter or excessive coldness in summer due to air conditioning). Even in buildings with advanced HVAC systems, discontentment with thermal environments remains prevalent [103].

To address the limitations of the PMV method in free-running buildings, adaptive comfort models emerged, founded upon extensive field studies conducted in authentic settings. These investigations yielded a significant finding that the comfort (or neutral) temperature demonstrates a robust correlation with the prevailing outdoor mean temperature, as illustrated in fig. 3.1. Specifically, the neutral temperature aligns with the indoor operative temperature, itself subject to fluctuations mirroring changes in the mean outdoor air temperature.

3.4.3 Adaptive comfort

Adaptive comfort principles have integrated into various national and international regulations, including the American ASHRAE Standard-55[101] and the EuropeanCEN Standard EN 15251[111], subsequently succeeded by EN 16798-1:2019[112]. Notably, the latter standard specifies that the "adaptive method only applies for occupants engaged in sedentary activities without stringent clothing regulations, where occupants primarily regulate thermal conditions by manipulating building envelope elements (e.g., windows, ventilation flaps, roof lights)" ([111,

¹RP-884 project represents a quality-controlled database built up assembling 21,000 samples from thermal comfort field studies in 160 buildings, both naturally ventilated and with HVAC systems, across different climate regions all over the world.

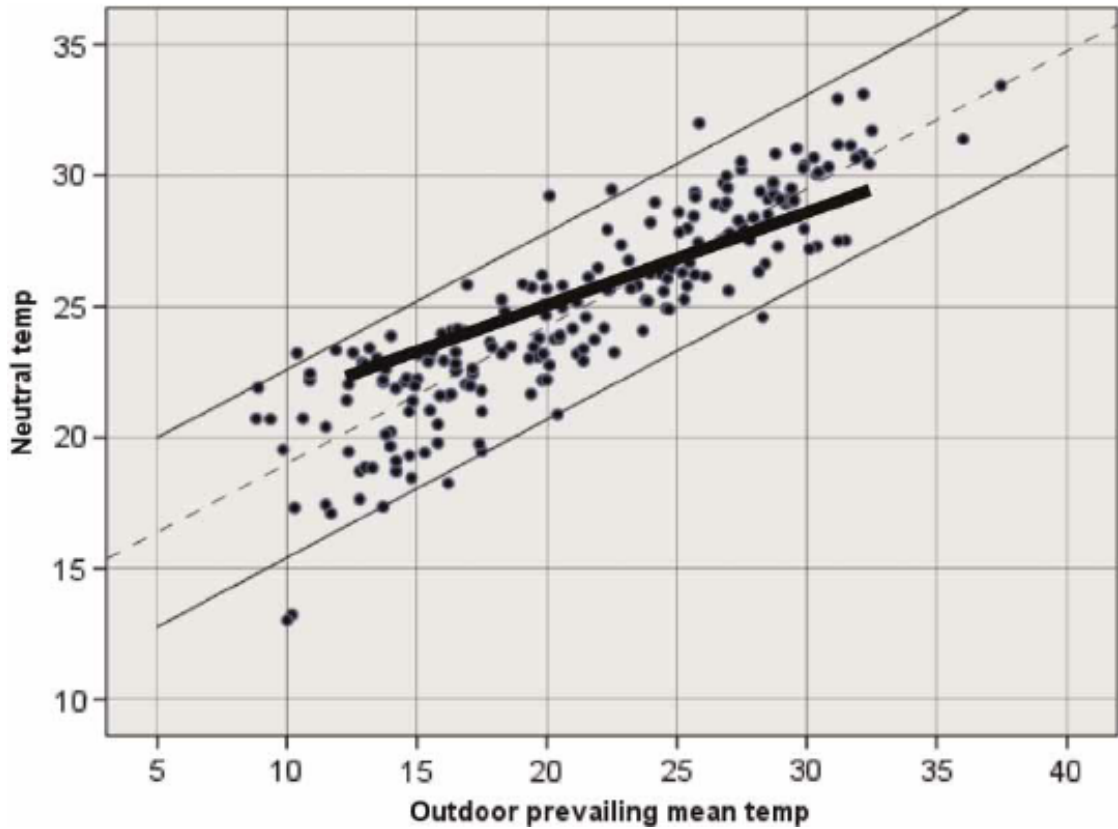


Figure 3.1: Neutral temperatures for buildings in FR mode against the prevailing mean outdoor temperature. Optimal comfort temperatures calculated from EN 15251 (single thick line) are shown for comparison though the outdoor temperature here is expressed in terms of prevailing mean temperature rather than the running mean so the comparison is only indicative. Source: Humphreys et al. (2010).

[109, 110]

p.19]). Therefore, the adaptive comfort model does not encompass considerations for clothing insulation, metabolic rate, or RH (Relative Humidity), despite the extensive investigations into RH's influence on thermal comfort perception.

Although RH's significance in comfort perception has been extensively explored, studies by Nicol[113] and De Dear[114] suggest its impact is generally minor and insufficient to significantly affect comfort. Givoni (2011) underscores the predominantly psychological nature of humidity's effect in a personal communication ([103, p.58]), with climatic adaptation playing a substantial role in its perception. However, in naturally conditioned buildings, outdoor RH profoundly influences internal humidity and, being beyond occupants' direct control, is anticipated to affect their thermal sensation, as evident in Vellei et al.[102]. This research for

the first time indicates that incorporating RH into the adaptive model causes a shift in the comfort range, indicating higher comfort temperatures and steeper gradients than predicted by the ASHRAE standard. Notably, elevated RH levels (>60%) exhibit a pronounced impact, resulting in lower comfort temperatures and a narrower acceptability range[102].

Here, we derive the RH value post EUI simulation using the *HB Read Room Comfort Result* component. Considering Torino as an example, we observe that during less than 9.7% of all the hours, the RH exceeds 60%. Given that our simulations do not encompass cities with excessively high humidity, we can reasonably assert the accuracy of the majority of the comfort metric predictions.

The LB AdaptiveComfortCalculator component assesses the adaptive comfort of the zone during the occupancy period. Given the European context of this research, preference is given to the standard EN 15251 (now EN 16798-1) over the ASHRAE standard for evaluation. A notable divergence lies in the database used to establish the adaptive standard:CEN regulations draw from the European SCATs project database, aggregating comfort data recorded over the same period across five European countries, employing standardized instruments and methodologies[103]. Standards EN 15251 and EN 16798 delineate buildings based on their conditioning system (mechanical or natural) and delineate three categories (I, II, III). The tested building aligns with Category II, designated for "normal levels of expectation and suitable for new constructions and renovations"[111]. For Category II, upper and lower limits of comfort temperatures are derived using formulas 1 and 2 [112]. These limits are applicable only when the running mean outdoor temperature falls within the range of 10°C to 30°C - as depicted in fig. 3.2.

$$\text{upper limit} : \theta_o = 0.33 \theta_{rm} + 18.8 + 3 \quad (3.12)$$

$$\text{lower limit} : \theta_o = 0.33 \theta_{rm} + 18.8 - 4 \quad (3.13)$$

Optimal operative temperature is defined by formula eq. (3.14)

$$\theta_c = 0.33 \theta_{rm} + 18.8 \quad (3.14)$$

where:

θ_o = indoor operative temperature [°C]

θ_{rm} = running mean outdoor temperature [°C]

θ_c = optimal operative temperature [°C]

3.4.4 Comfort visualization

The PMV component assesses the comfort of the defined environmental conditions for occupants, determining the PMV. PMV, a scale ranging from cold (-3) to hot

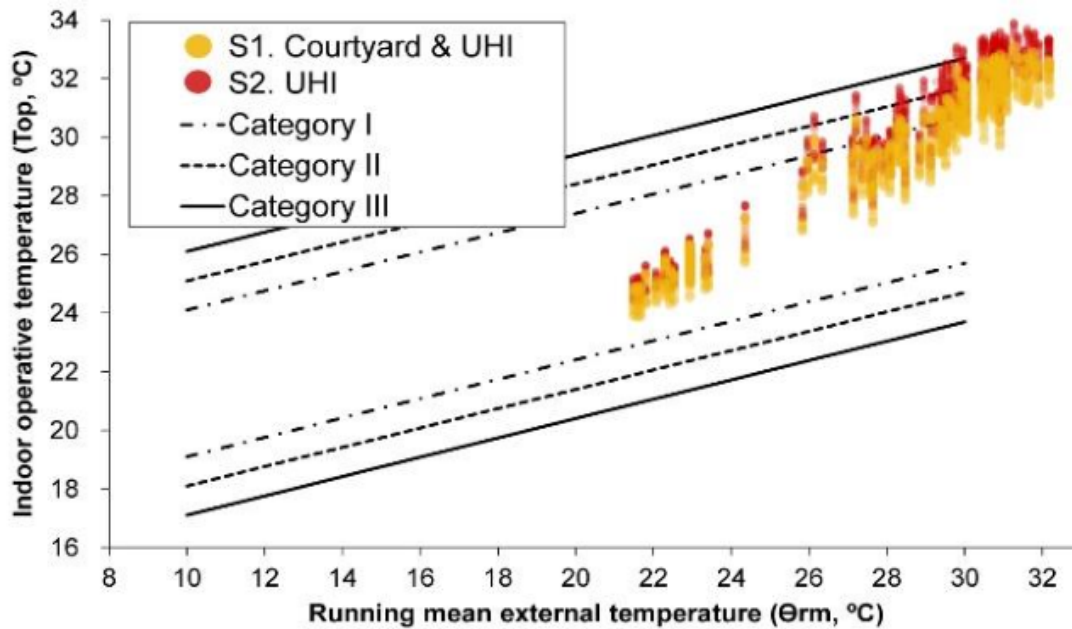


Figure 3.2: Comfort temperatures ranges for free-running building categories I, II and III as a function of the exponentially-weighted running mean of the outdoor temperature. Upper and lower limits define design values for indoor temperature during summer and winter seasons. Source: EN 16798-1

[109, 110]

(+3), was utilized in comfort evaluations by P.O. Fanger. Each integer value within the scale represents distinct comfort levels:

- 3 - Cold
- 2 - Cool
- 1 - Slightly Cool
- 0 - Neutral
- +1 - Slightly Warm
- +2 - Warm
- +3 - Hot

Each numerical value corresponds to an hour within the analysis period.

The developed GH script facilitates the creation of high-quality visualizations in the RH scene, aiding in a comprehensive interpretation of the outcomes. For instance, displaying the percentage of time spent in comfortable, hot, or cold conditions can be achieved by presenting colored meshes on an annual graph using the *LB Hourly Plot* component. An illustrative example of this chart is depicted in fig. 3.3. It give us a intuitive scan of the annual indoor thermal environment,

which indicates us the need for pursuing the maximum comfort. It's a great tool for us to quickly obtain the global cognition for the environment.

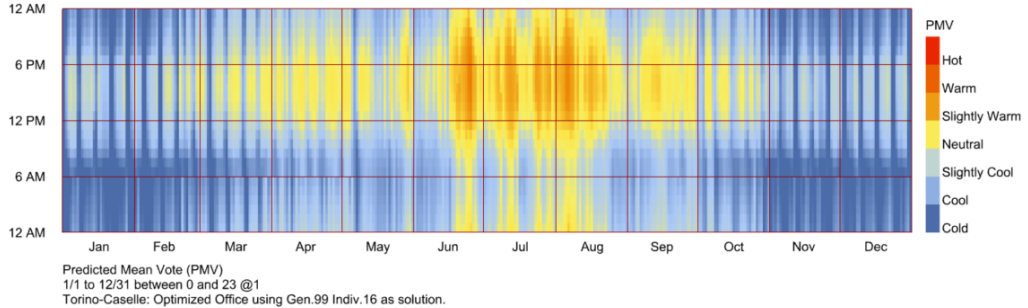


Figure 3.3: 3D chart generated with LB. It displays the percent of time comfortable, hot and cold that resulted from the simulation of the optimized solution for Geneva. Note that the "global cognition" is being of redundancy. Our **fitness value** is aiming at the comfort in the winter day during working hours. That's a range within 6 am. to 18 pm.

Another valuable output is the *LB Psychrometric Chart* and *LB PMV Polygon*. This chart visualizes the duration, within the considered occupancy period, during which temperatures fall between the upper and lower limits of the comfortable range for specific input conditions. Unlike fig. 3.3 which indicates the indoor condition distribution among the day time, fig. 3.4 show the condition of RH, describing how long the distance from the status to the comfort zone. Although depicted as colored meshes similar to those in fig. 3.3, the variables are different, hours are represented on the chart. The colored 'pixels' situated below the lower comfort limit indicate periods when occupants might feel cold, while those above the upper limit depict times when occupants might experience heat discomfort.

Lastly, we can analyse the human being. Rather than on the surface of building, this time we can analyse the thermal transmittance that take place of the human body, with the help of *LB Hourly Plot*. In fig. 3.5, we can know that in Torino the heat is taken away mainly by radiation and convection. And we can know when this happens.

3.5 GAin arhitecture design and NSGA-II

Genetic algorithm is a stochastic optimization method developed based on the principles of natural selection and the simulation of biological evolution. It was

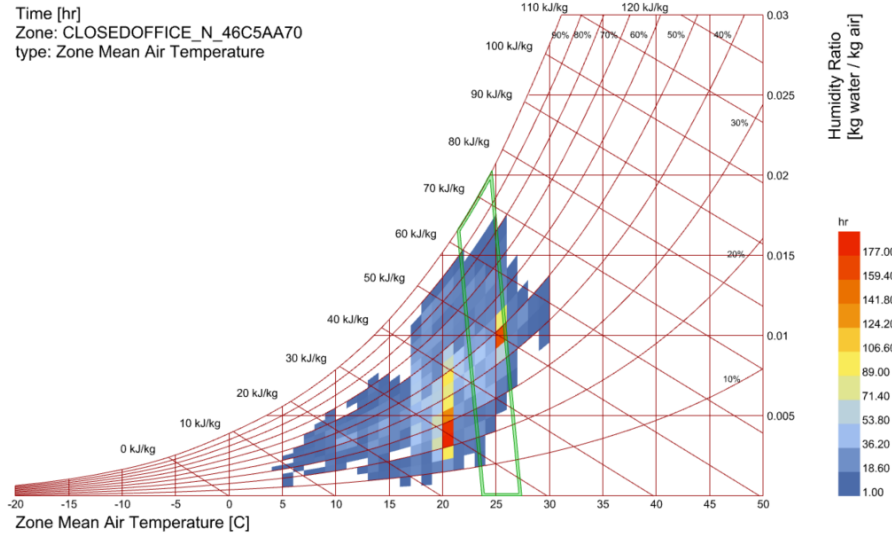


Figure 3.4: Psychrometric Chart of Torino Optimized with solution of Gen.99 Indiv.01

created by Professor Holland and his students at the University of Michigan in 1975[44].

Being as an "evolutionary algorithm", GA itself has evolved into a group of diversity. A comprehensive analysis[115] of recent advances in GA, which discusses the challenges and future research directions in the area of genetic operators, fitness function, and hybrid algorithms. The article also suggests some possible ways to improve the performance and efficiency of GAs.

3.5.1 Features and analogy of GA

- **Genetic Representation:** The genetic composition of a dog is symbolically represented as a chromosome, with each gene corresponding to distinct phenotypic traits. For example, individual genes may represent traits such as coat color, fur length, and activity level.
- **Crossover:** The selected parental dogs engage in gene crossover, where genetic material from both the mother and father contributes to the genetic composition of the offspring. For instance, a resulting offspring may inherit the light coat color gene from the mother and the long fur trait gene from the father.

- **Mutation:** During the reproductive process, genetic mutations may spontaneously occur, inducing slight alterations in specific traits. For example, a minor mutation may affect the activity level gene, resulting in a new generation of dogs exhibiting increased activity.
- **Selection:** The fitness of each dog is rigorously evaluated, taking into consideration traits such as coat color, fur length, and activity level. Dogs exhibiting higher fitness levels are chosen as parental candidates for the process of reproduction.
- Across successive generations of selection, crossover, and mutation, the optimization of specific traits within the dog breed is systematically achieved. Dogs with superior fitness levels are retained, while less favorable traits gradually diminish. Ultimately, a dog breed characterized by light coat color, longer fur, and heightened activity levels is selectively bred to align with the breeding objectives. **Genetic Representation** and **Crossover** the core of the whole algorithm, which take place in every solution generating. So I introduce it following in §3.5.2.

In this analogy, the genetic algorithm's core mechanism emulates the evolutionary process found in nature. It continuously refines candidate solutions through genetic operations, facilitating the attainment of a more suitable, optimal, or near-optimal solution.

3.5.2 Mathematical process of Simulated Binary Crossover

SBX (Simulated Binary Crossover) is a crossover operator used in GA for real-valued optimization problems. SBX is an extension of the binary crossover operator used in binary-coded GAs. The SBX operator simulates the single-point crossover operator of binary-coded GAs by using a probability density function to generate offspring solutions. The SBX operator is able to overcome the Hamming cliff, precision, and fixed mapping problems that are associated with binary-coded GAs[115].

As discussed in §3.5.1, the core process is run under the SBX method. The complete algorithm refers to [42]. And core process *Simulated Binary Crossover* is introduced in [116], which I've summarize in to following features:

- The gene values of offspring maintain an equal distance from the mean gene value of their parents.
- Each chromosome position has an identical probability of being chosen as a crossover point.
- Lower-bit crossovers result in minor alterations in gene values.
- Offspring tend to be in close proximity to their parental genotypes.
- SBX utilizes a probability density function that simulates the single-point crossover found in binary-coded GA.

Giving the parental value an additional Gaussian distribution, then there's the new one. It can be understood as 2 Gaussian distribution stacked together fig. 3.6.

These features are instrumental in preserving genetic diversity by ensuring that offspring values remain at an appropriate distance from one another. This prevents the dilution of filial values to an average level, which is beneficial for the subsequent selection phase, enabling an effective selection process.

With this key characteristic, many variants are created. They can be categorized by *Fitness assignment*, *Diversity mechanism*, *Elitism*, etc. [65, 118] Among them SPEA-II and NSGA-II are competitive[43].

3.5.3 Non-dominated Sorting Genetic Algorithm II

NSGA-II is a multi-objective optimization algorithm used to solve optimization problems with multiple objective functions. The algorithm was proposed by Kalyanmoy Deb and others in 2002[44]. It is a variant of GA designed to address multi-objective optimization problems where multiple conflicting objectives exist.

The core idea of NSGA-II is to maintain a set of non-dominated solutions by partitioning the candidate solutions into different non-dominated levels or fronts. These solutions are not dominated by other solutions. It then performs operations based on non-dominated sorting and crowding distance to maintain a set of high-quality solutions that are balanced across various objectives.

The algorithm flow of NSGA-II includes the following key steps:

1. **Population Initialization:** Create an initial population of candidate solutions.
2. **Non-dominated Sorting:** Rank the solutions in the population through non-dominated sorting, dividing them into different front levels.
3. **Crowding Distance Computation:** Calculate the crowding distance for each solution to measure the distribution density of solutions.
4. **Elite Selection:** Select solutions from the front levels to ensure that the next generation's population contains high-quality solutions.
5. **Crossover and Mutation:** Apply crossover and mutation operations to the selected solutions, generating the next generation.
6. Repeat the above steps: Repeatedly execute the above steps until a stopping condition is met.

NSGA-II has become one of the widely used algorithms for solving multi-objective optimization problems[115]. It finds a set of Pareto-optimal solutions, allowing decision-makers to make trade-offs and selections among different objectives by maintaining diversity and balance in the solutions. This is exactly what we need for our project.

Methodology for simulations

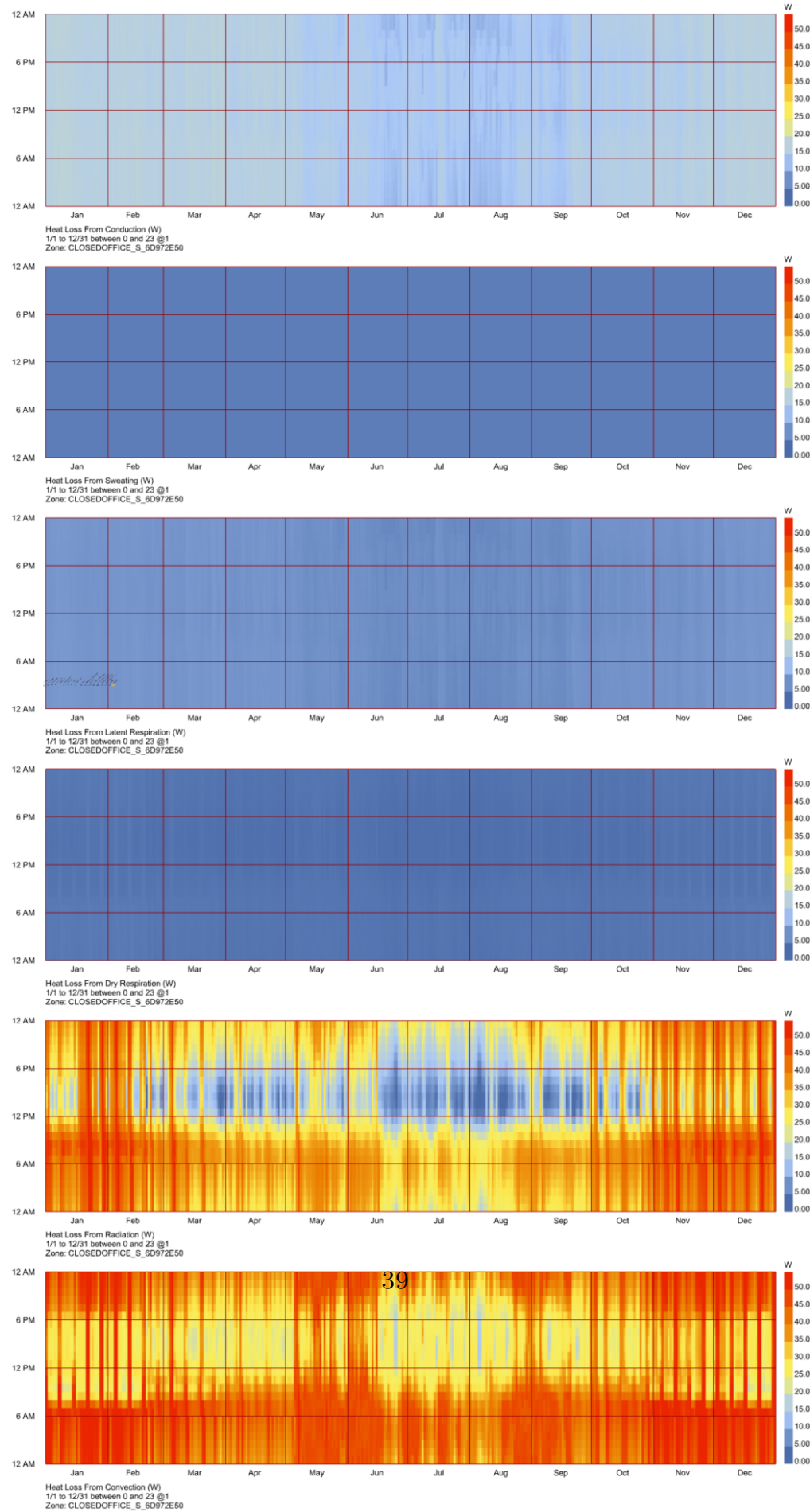


Figure 3.5: Heat loss Chart of Torino Optimized with solution of Gen.99 Indiv.01

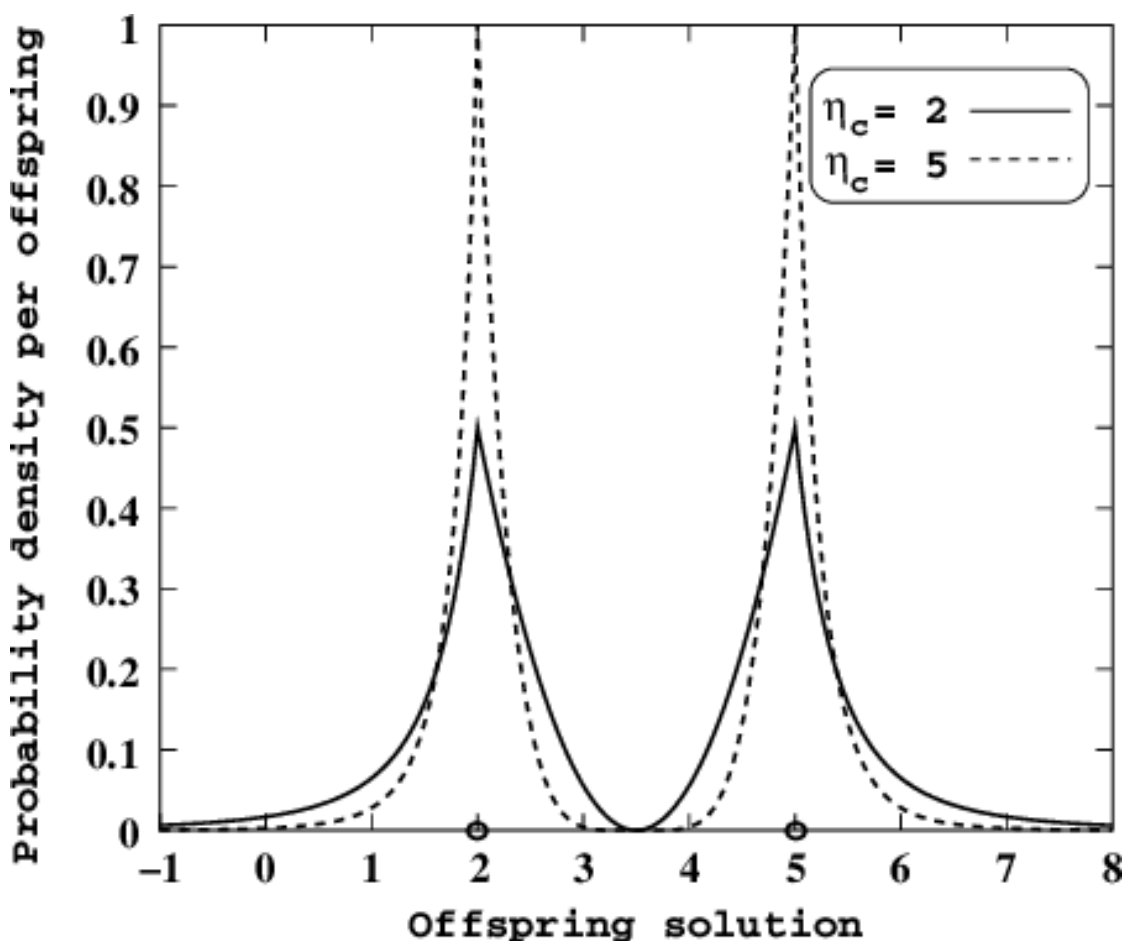


Figure 3.6: Distribution of SBX, note that there's 0 possibility in the mean value [117]

Chapter 4

Methodology for Designing examined box

4.1 Design Object: "Hardware" and "Software"

The concepts of *bionics* or *biologically inspired engineering* involve drawing inspiration from nature's wealth of experience. Rather than merely imitating the physical forms of creatures, we aim to extract the underlying philosophy. Our planet, through billions of years of evolution, has offered us a multitude of life forms. These life forms are not just organisms; they also represent solutions that can adapt to their environments. In the animal kingdom, natural forms shape not only physical structures but also behavior.

Buildings, too, need to exhibit behavior and adapt to increasingly severe extreme weather conditions. They cannot rely on fixed operational templates; instead, they should be capable of adaptation and evolution.

Our goal is to optimize both the physical form and the operational behavior of buildings, similar to designing "hardware" and "software." What makes a machine powerful? It's the combination of both hardware and software. What makes a species competitive? It's the interplay of body and behavior. In the context of building design, what makes a building efficient? It's the synergy between equipment and operation.

To enhance efficiency, we intend to design both the building's physical form and its operational program. These components are categorized as **static** design and **operative** design. Conventionally, in our pursuit of exceptional indoor environments, we have relied on passive and dynamic design methods, distinguished primarily by their energy consumption. However, this time, we adopt the analogy of "Hardware and Software." This approach involves classifying the design into two different categories: **Static** and **Operative**. The primary distinction lies in

whether the designed functionalities can be controlled or turned off.

4.2 Proposal for Retrofitting: Static Design

Static design plays a fundamental role in sustainable architecture, and this time we approach it with a biological analogy.

Imagine your room as a living organism, akin to a playful dog. Just as a dog's fury coat provides protection, the shading elements in a room serve a similar purpose. Thoughtful planning and the use of appropriate shading materials keep the room cool in summer and warm in winter, much like a dog's fur.

Now, consider the room's outer layer as its skin. A healthy dog with smooth skin efficiently regulates its body temperature. Similarly, an excellent room envelope design optimizes energy exchange between the interior and exterior, ensuring a stable indoor temperature and reducing energy waste.

Our mission is to make the room self-sufficient, reducing its reliance on external resources. By incorporating shading elements (akin to fur) and designing an efficient room envelope (akin to skin), we ensure year-round comfort while reducing dependency on conventional energy sources. This approach promotes environmental friendliness and sustainability.

In this case, we focus on two main elements of passive design: the opaque and transparent envelope, which are basic components in modern architecture.

4.2.1 Opaque Envelope

When designing the opaque envelope, several aspects require attention:

- **Insulation:** Adding high-quality insulation to the walls, roof, and floors minimizes heat transfer, enhancing interior comfort and reducing the need for heating and cooling.
- **Thermal Mass:** Incorporating materials with high thermal mass, such as concrete or stone, in the opaque facade can absorb and store heat during the day and release it at night, contributing to temperature stability.
- **Airtightness:** Ensuring airtight construction prevents air leakage.
- **Thermal Bridge Mitigation:** Addressing thermal bridges in the building envelope helps eliminate localized areas of increased heat transfer.
- **PCM (Phase Change Materials):** The introduction of PCMs into the opaque facade can store and release energy during phase transitions, contributing to temperature regulation.

We focus on insulation and thermal mass, as they are the most common methods. Airtightness and thermal bridge mitigation are highly related to the construction method, with limited impact on the entire room. PCMs represent an exciting future direction due to their ability to influence both temperature and transparency, making them crucial for light and form considerations.

Our idea is to add a new insulation layer to the existing wall, allowing the original wall volume to serve as a thermal mass. This approach is universally applicable to modern buildings, with facade strength being the primary concern. However, our insulation panels are relatively lightweight, and any retrofitting proposals must account for their load-bearing capacity.

Table 4.1: Insulation price

	Wall	Roof	Floor
	180	180	200

The unit of the numbers are euro per cubic meter.

INSULATION - ROOF	Opaque Materials		Roughness	Thickness [cm]	Conductivity [W/(m.K)]	Density [kg/m^3]	Specific heat [J/kg-K]	Attributes of Opaque Mat.	Price [€/m^3]
	Layer	New							
		Polyurethane	MediumRough	Variable to optimz.	0.022	32.0	1590		180
	1	Metal Roof Surface	Smooth	0.08	45.2	7824	499.7	Thermal absorptance	0.9
	2	NoMass, Typical Insulation-R2	MediumSmooth	-	2.11*	-	-	Solar absorptance	0.7
	3	Roof Membrane	VeryRough	0.95	0.16	1121	1456	Visible absorptance	0.7
<i>From top to down</i>									
* is R-value (m^2-K/W)									
Shared for all									
Existing									

Table 4.2: Construction of roof

Pricing I assume that a simple attachment method can be used for the panels, which applies to all selected proposals. I use an assumed cost of 2000 euros to represent this attachment method. Since our construction method remains constant, our goal is to investigate the optimal thickness of the insulation. In other words, thickness is the only variable for opaque design. And the thickness affects the final price for the insulation. The database here is built by referring to the real-time suppliers' website. With their product tabular[119], we choose *Knauf*, and we also consider the general retrofitting case in Italy [120]. And we simplify the price into integer values. See §4.2.1.

4.2.2 Transparent Envelope

When designing the transparent envelope, we consider several aspects:

INSULATION - WALL	Opaque Materials		Roughness	Thickness [cm]	Conductivity [W/(m.K)]	Desnsity [kg/m^2]	Specific heat [J/kg-K]	Attributes of Opaque Mat.	Price [€/m^3]
	Layer								
New-A	PlasterFinishing	MediumRough	0.2	0.04	2275.0	950			180
New-B	PSE-G-EPS	MediumRough	Variable to optimz.	0.8	15.0	1470			Removed
1	TIN Stucco	Smooth	2.5	0.69	1858	836			
2	BIN CONCRETE HW RefBdg	Rough	20.3	1.31	2240	836	Thermal absorptance 0.9		
3	NoMass Typical Insulation-R4	MediumSmooth	-	0.7*	-	-	Solar absorptance 0.7		
4	1/2N Gypsum	Smooth	0.95	0.16	785	829	Visible absorptance 0.7		
<i>From exterior to interior</i>									
* is R-value [m^2-K/W]									

Table 4.3: Construction of wall

INSULATION - FLOOR	Opaque Materials		Roughness	Thickness [cm]	Conductivity [W/(m.K)]	Desnsity [kg/m^2]	Specific heat [J/kg-K]	Attributes of Opaque Mat.	Price [€/m^3]
	Layer								
New-A	Finishing	MediumRough	0.2	0.04	2275.0	950			
New-B	Polyurethane	MediumRough	Variable to optimz.	0.022	32.0	1590	Thermal absorpt 0.9		200
1	Normalweight Concrete Floor	MediumRough	2.5	2.3	2322	831	Solar absorptan 0.7		
<i>From exterior to interior</i>									
* is R-value [m^2-K/W]									

Table 4.4: Construction of floor

- **Low-E Coatings.**¹
- **Double or Triple Glazing.**
- **Solar Control Films.**
- **Operable Windows.**

To facilitate this, I have designed six types of glazing using the acg configurator website. These types vary in cost and U-value, with three being double glazing and three being triple glazing. The choice of window frame remains consistent, based on sistema secco's products.

Glazing systems are complex and difficult to parameterize due to their highly compact nature. A linear function cannot easily describe the performance and input parameters of a window system. To address this, I have categorized the glazing types based on their U-values, assigning them serial numbers from 0 to 5, where higher numbers correspond to higher U-values.

In practice, the algorithm requires a wider domain than the range from 0 to 5, so a division trick² is applied to accommodate this. As the integer increases, the U-value output steps up non-smoothly, reflecting the challenge in customizing window systems.

Pricing The cost of window systems, representing both the glazing and framework, is a complex issue. The supply chain involves multiple links, with each affecting the

¹Applying Low-E (Low Emissivity (glass)) coatings to glazing reduces heat transfer and helps control solar heat gain.

²the real variable is defined in 0 – 50, then divided integrally by 10, so the outcome seems a variable from 0 to 5.

WINDOW SYSTEM	GLAZING TYPE		Thickness [mm]	U - value [W/(m^2.K)]	Price[€/m^2]
	Index in Matrix	Light Transmittance [%]			
0 Double_Base	0 Double_Base	81	27	2.6	250
	1 Double_Pro	44	25	2.6	300
	2 Double_SilverFlex	17	29.4	1	350
	3 Triple_Standard	50	33	0.9	400
	4 Triple_Pro	23	28	0.8	450
	5 Triple_Kryton	56	32	0.5	600
	FRAME	Width[mm]	Conductance[W/(m^2.K)]	Price[€/m^2]	
	SeccoSistema_DS2	45	10.7	250	

Table 4.5: Glazing types of the window

final price. Installation costs also vary based on factors such as the environment, height from the ground, and the type of external wall.

However, I have obtained reference costs from several sources, providing a reasonably persuasive range. Similar to the approach used for U-values, I manually assigned costs to each type, following the principle that higher cost correlates with better performance. The costs fall within the range of 250 to 600 euros per square meter.

In summary, I have created an idealized supplier that offers a variety of products at a constant price, following the principle of "higher cost for lower U-value." While this simplification methodology sacrifices some authenticity, it retains the core logic of the experiment. It's important to note that in actual projects, real suppliers can provide product data, allowing for the immediate application of the same logic to obtain optimized results.

4.2.3 Shading Device

The shading device, in contrast to the fur and skin of the building, is not equally fundamental. In this context, we utilize fixed louver shading. This approach is practical and aligns with our research goals. Our objective is to strike a balance between multiple goals, and we anticipate scenarios where trade-offs exist. Fixed louvers enable us to explore such trade-offs effectively.

While dynamic devices could be used, their fixed cost makes it a single-goal problem. For fixed louvers, we can focus on the quantity of louvers, which directly affects the cost. By varying the number of louvers, we can adjust the shading coverage from top to bottom. The challenge is to determine the required shading area and its associated cost. The use of *division trick*³ helps address this issue.

³the real variable is defined in 0 – 50, then divided integrally by 5, so the outcome seems a variable from 0 to 9.

In addition to louvers, I have included an enclosed extrusion border shading with a depth of 0.2 meters.

Pricing The pricing for shading devices follows a straightforward rule: the more louvers, the higher the cost. Although this section has its weaknesses, it has a relatively minor impact on the simulation. Additionally, shading devices are typically more cost-effective. If a designer has a budget of 1000 euros to complete the envelope, they would likely allocate around 900 euros for windows and 100 euros for shading, if required. I assumed that the basic framework for each shading system costs 20 euros, and the louvers are priced at 2 euros per meter.

4.3 Proposal for Retrofitting: Operative Design

4.3.1 Brief Introduction & Classification of Operative Design

The operative elements are those capable of automatically changing their functioning condition and can be subdivided into two classes: high power and low power. The former, like HVAC systems, consume a significant amount of power when operating, while the latter, such as CNV, requires minimal power for opening and closing windows. The high power elements are usually integrated with control systems, while the low power elements are typically static components with added controls, such as manual windows with openers.

The realm of lighting occupies an interesting position, serving as an intermediate term between the two. In this project, we also develop a more intelligent lighting system.

Drawing parallels with the analogy of a dog's primary and smaller muscles, we can think of:

- High-Energy Operative Design is akin to a dog needing vigorous physical activity, such as running or playing. In architecture, this involves using HVAC systems, much like a dog regulates heat through panting and sweating, actively to adjust temperature and ventilation.
- Low-Energy Operative Design is comparable to controlling the dog's state to keep it calm or alert. In architecture, this involves intelligent control systems that adjust indoor temperature and lighting through natural ventilation and daylight. Just as a dog's fur can raise to regulate its temperature, building shading devices can automatically adjust to keep the interior cool.

The goal of operative design is to ensure optimal thermal conditions indoors, much like ensuring the comfort and state of a small dog. Through intelligent control

systems, natural ventilation, and shading devices, we can maintain comfort, reduce energy consumption, and provide occupants with a pleasant living environment.

4.3.2 HVAC System

To simulate the HVAC system, I have chosen the All-air HVAC, which can condition and deliver the necessary volume of air. Specifically, I selected PVAV with a gas boiler reheat. This choice allows for comparisons between different weather zones, making it a reasonable selection, even though I don't necessarily transfer the system among different regions.

I have maintained other parameters as default settings, representing various conditions. Due to constraints from HB, I didn't explore this aspect in depth. However, for those interested in optimizing the HVAC system itself, the Ironbug component series from LBT can be used to obtain more detailed results.

Pricing The energy consumption cost electricity power, which finally cost currency as well. The price is assumed to 95 euro per kWh[121], which's accessed in the summer of 2023. Notably, due to not only the political issue, the energy price is fluctuating at the time. However, since we use the same price for all the cities, this factor just affects on the absolute value of the cost FV, it doesn't make difference in the relative ranking of each solution. „„„„

4.3.3 Controlled Natural Ventilation

Natural ventilation, also recognized as comfort-ventilation[122], stands as a fundamental passive cooling strategy employed to ameliorate occupant comfort during periods of perceived indoor warmth. An established tool for assessing the potential of climate-driven ventilation is available—namely, the VC (Ventilation Cooling) potential tool, developed within the framework of the IEA-EBC (International Energy Agency Energy in Buildings and Communities Programme) Annex 62 project[123, 124, 125]. This tool, structured on an Excel platform, serves as a valuable resource for early-design stage comparisons, evaluating the efficacy of diverse low-energy cooling systems across varied climatic conditions and building attributes, facilitating informed decision-making processes.

The VC tool, leveraging hourly climate data, computes the need for cooling in a single-zone model and identifies the most appropriate ventilative strategy for each hour throughout the year. In contrast, the proposed tool within this study allows for the simulation of various common types of natural ventilation (such as window-based, chimney/cowl, or fan-driven natural ventilation) through the dedicated HB component. Additionally, it discerns the specific hours during the year necessitating cooling. Moreover, an energy model constructed with EP, akin to the one employed

in this study, boasts greater precision compared to the VC tool, which employs certain simplifications in its computations. These simplifications might lead to potential overestimations or underestimations of the efficacy of ventilative cooling, particularly during the summer months[125].

For the simulation, the choice is directed towards daytime natural ventilation via windows. The design allows for cross-ventilation, assuming simultaneous opening of windows on opposing walls to create a pressure gradient, thereby augmenting the potential for ventilative cooling. Allowing outdoor air to enter the indoor environment, even when it is warmer than the average indoor temperature, induces a direct physiological cooling effect on occupants. Increased airspeeds, resulting from this airflow, elevate the upper limit of comfort by enhancing the rate of sweat evaporation[122].

The volume of air flowing and its velocity inside the space depend on the operable area of the glazed surfaces facilitating natural ventilation. In this study, all zone windows are presumed fully operable in their height, with the operable area fraction ranging from 50% to 100%. This parameter remains subject to refinement through the optimization process. Additionally, the presence of fly screens introduces additional friction, thereby influencing airflow. Hence, HB accounts for this by considering a stack discharge coefficient, multiplied by the window area, which can vary from 0 (no stack ventilation) to 1, with a default coefficient assumed at 0.17.

However, recognizing that natural ventilation might not be suitable year-round, particularly during periods requiring heating, a specified temperature range for employing this passive strategy is delineated. The glazing operable area can only be opened when the outdoor temperature exceeds 12°C, and the indoor temperature is at least 25°C. This approach amplifies the efficacy of ventilative cooling, restricting its operation solely to periods when deemed necessary.

Implementing smart control systems for operable windows is essential for CNV. Key components include the window opener (*aprifinestra automatica*) or actuator (*attuatore*). When combined with a control system, this creates the "behavior" of the window, allowing control over when natural ventilation is activated. This is analogous to controlling a dog's mouth, facilitating heat dissipation through natural air exchange.

Within the simulation, there is a specific component for controlling natural ventilation, with a key parameter known as delta temperature. This value is typically positive, ensuring ventilation only occurs when the outdoor temperature is cooler than the indoor temperature. Negative values indicate how much hotter the outdoor temperature can be compared to the indoor temperature before ventilation ceases.

And as it is an office building the fraction ratio of operable is set to 0.15.

Pricing A set of the actuator *apri finestra* with a motor and chain is 60 euro[126]. We need 2 to control a window, but if the WWR is lower than 25% maybe 1 is sufficient. And totally we have 6 windows, so 720 euro is added into the cost. The running energy cost is ignored.

4.3.4 Dimmer Control

Compliance with lighting norms is essential, with a requirement of 500 lux on the analyzed surface in office spaces. The working plane, typically situated at 0.8 meters from the ground, should receive adequate illumination. However, in practice, most ALS (Ambient Light Sensors) are installed on the ceiling. To achieve direct calculation based on the first principle, I place a ALS grid on the desk plane to measure illuminance.

For lighting compensation, if daylight is insufficient to meet the 500 lux requirement, artificial lighting is activated. The shortfall in illuminance is measured, and radiance values from the artificial light source are determined. Energy consumption is calculated by considering the luminous efficacy. The calculation takes into account the maintenance factor and utilization factor, reflecting light diffusion and reflection within the room.

In summary, if daylight falls short of 500 lux, the difference is factored into the formula, providing the energy consumption for the given period. When daylight can work autonomously, artificial lighting is solely provided for the corridor at 100 lux.

The "zero-sum" situation is evident in this context. For windows, thermal performance and DA represent a trade-off. Both factors contribute to energy consumption. The WWR is another key consideration. Balancing these factors while considering costs is a complex multi-objective problem. Demanding high thermal performance often results in reduced DA due to greater closure or opacity. Achieving the perfect window is challenging, as it must block UV light while maintaining high visible light transmittance. Balancing energy consumption, DA, and cost is a complex optimization challenge, where the algorithm plays a crucial role.

Chapter 5

Workflow

5.1 Introduction for generating process

In this section, we provide an overview of the simulation process. Prior to commencing the simulation, all necessary software and programs are prepared. The simulation process unfolds in the following sequential steps. To realize it, a GH programme is built up. A general canvas (see fig. 5.1) is presented here, which is sub-divided into 6 parts. All the 6 parts are presented below. The roman numbers refer to which following step is conducted within this red block. For deeper information, please turn to the relative sub-part of the canvas.

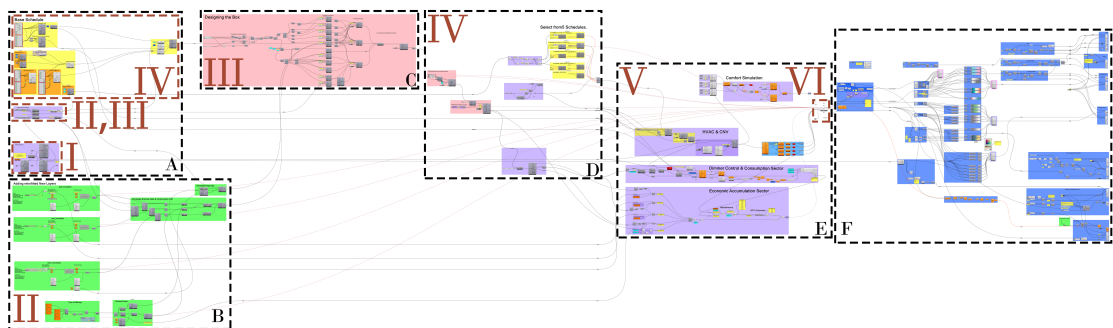


Figure 5.1: General GH Canvas¹

5.1.1 Step I: Preset

In this initial step, the climate data, formatted as .epw files, are defined, and contextual surroundings are imported as geometries in RH.

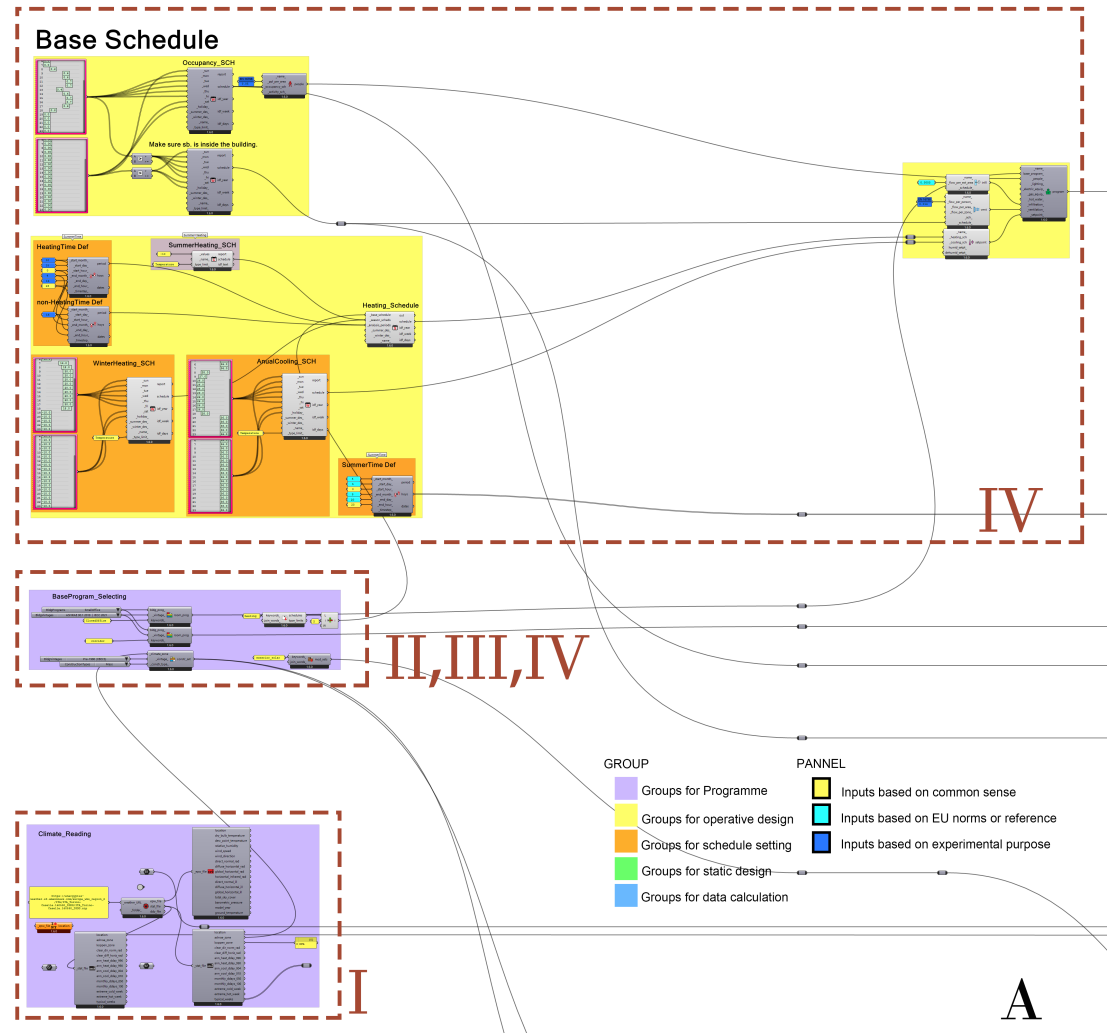


Figure 5.2: GH section A

5.1.2 Step II: Database

This step involves designing new constructions added to the existing ones. Using the *HB_Opaque Material* and *HB_Opaque Construction* components, new layers are incorporated. Material properties are derived from the Design Builder database and the Matweb[127]. Cost and price data, as explained in §§4.1 to 4.3, are associated with each material and imported into GH. Presented in fig. 5.3, 3 insulation and window construction set are completed, which are:

- Insulation of Wall

- Insulation of Roof
- Insulation of Floor (control group)
- Glazing of Window
- Framework of Window

The unchanged parts stay as the vintages are. Also the prices are here input into the program.

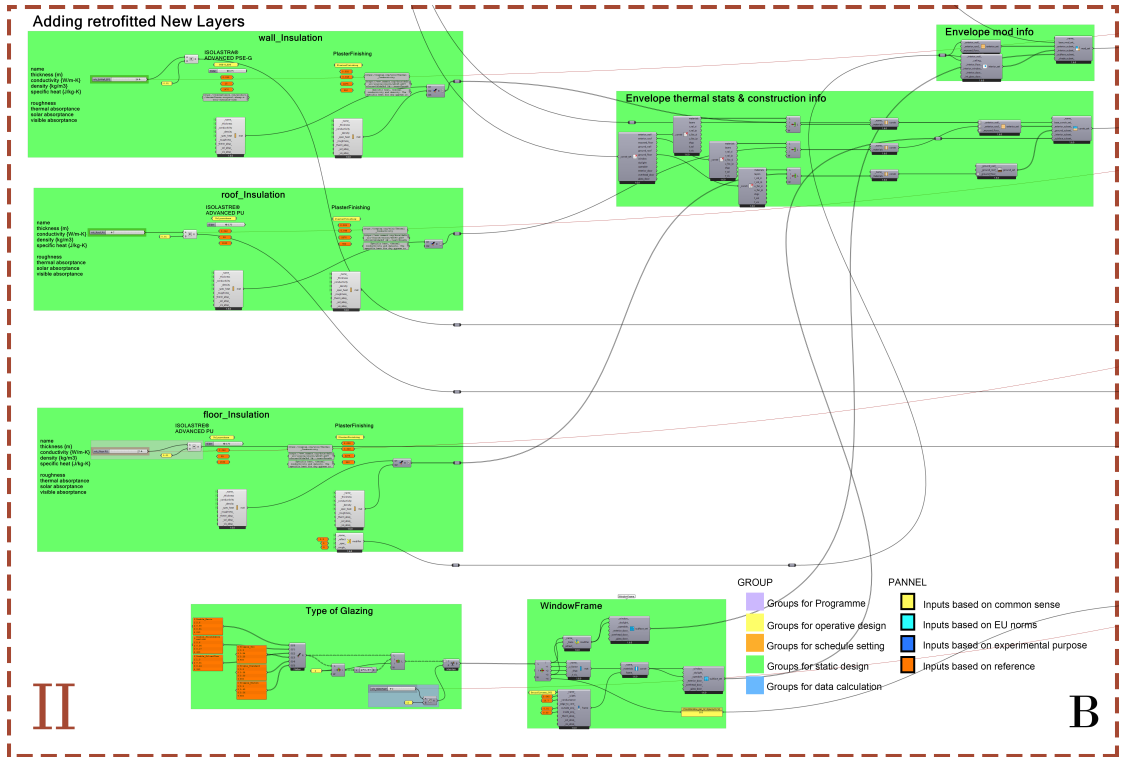


Figure 5.3: GH section B

5.1.3 Step III: BIM Setting

This stage encompasses BIM, wherein the model contains both geometric and non-geometric data, defining horizontal faces into office or corridor, also doing the vertical ones into external or internal walls (see fig. 5.4). This is achieved through the use of the *HB Face component*. Subsequently, the *HB Room* is created, with attention to using the *HB Solve Adjacency* component for interior face matching, resulting in an information-rich model.

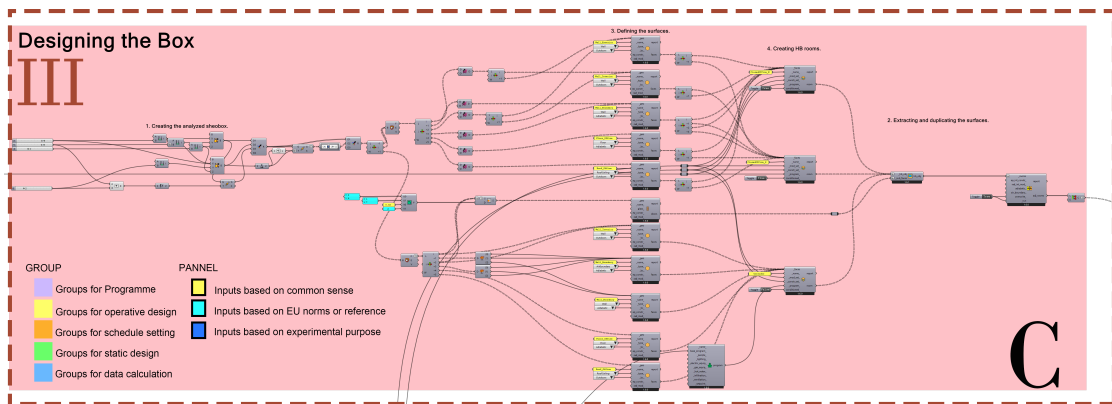


Figure 5.4: GH section C

5.1.4 Step IV: Operational Setting

Beyond the typical BIM, schedules for CNV and HVAC systems, as discussed in the operative design, are established. This includes:

- **Occupancy schedule:** This schedule indicates the occupancy ratio inside the room relative to its capacity, influencing other schedules. For unoccupied hours, the schedule is set to 0, with variations during working hours. (see fig. 5.2 Base schedule)
- **Set-points:** Set-points for heating and cooling are adjusted based on occupancy. For unoccupied hours, they are set to maximum tolerance levels. (see fig. 5.2 Heating and Cooling schedule)
- **Lighting schedule:** Based on occupancy schedule, lighting is set to 0 lux during unoccupied hours and operates in a smart mode when occupancy is greater than 0. (see fig. 5.2 sb. inside)
- **Ventilation control:** Based on occupancy schedule, it's applied on top of delta set-point. That's temperature differential in Celsius between indoor and outdoor below which ventilation is shut off. This should usually be a positive number so that ventilation only occurs when the outdoors is cooler than the indoors. Negative numbers indicate how much hotter the outdoors can be than the indoors before ventilation is stopped. This number is one of the **Genomes**. (see fig. 5.5)
- **HVAC system type:** PVAV_Boiler is selected, since I want a HVAC system that fit to majority for the buildings, so a PVAV HVAC system benefits that. (see fig. 5.6 HVAC part)

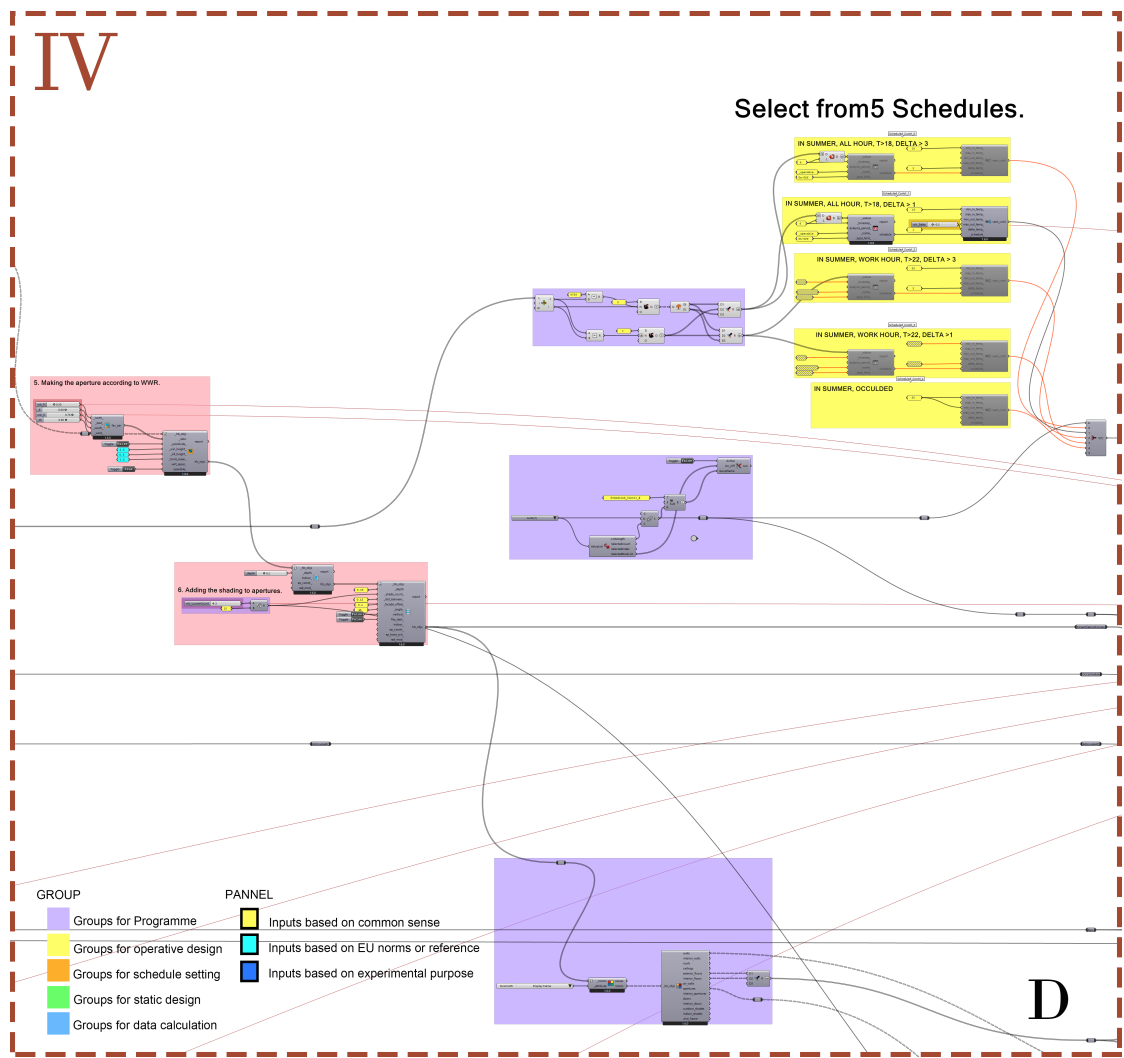


Figure 5.5: GH section D

5.1.5 Step V: Run the Simulation

Once the model from Step II is combined with the schedule from Step III, the *HB_Model* is developed, allowing for the execution of simulations. 4 simulation programs are conducted (see fig. 5.6), including:

- **EUI simulation:** Using *HB Model to OSM* to start, operating on EP. And read the result by *HB Read Room Energy Result*. This process needs a *toggle* to activate.
- **Comfort assessment:** Run after the EUI simulation. Using *HB Read Room*

Comfort Result to get the data, with an analysis period prepared, insert these inputs into *LB PMV Comfort*, then output the PPD. This process needs a *toggle* to activate.

- **daylighting analysis:** Firstly, extract all the faces to be evaluated. Secondly, use *LB Generate Point Grid*, *LB Generate Point Grid*, *LB Generate Point Grid* applied to the HB Model. Parallelly, use *HB Wea From EPW* to set the weather. Thirdly, run the *HB Annual Daylight* and use *HB Annual Results to Data* to get the data of natural light. Lastly, use the mathematical method presented in §3.2, eqs. (3.4) to (3.7) to calculate the consumption. This process needs a *toggle* to activate to transfer to Radiance.
- **economic accumulation:** Practice it with the mathematical method presented in §3.3, eqs. (3.8) to (3.11). Unit price times quantity. To get total prices for all the sections, here're the initial cost:
 - Price of Wall
 - Price of Roof
 - Price of Floor
 - Price of Window
 - Price of Louver
 - Price of Labor

Here're the annual cost:

- Total HVAC consumption
- Lighting consumption

Add them together, then input into the NPV calculator that I've invented, so that we can evaluate how much is the net present cost. This process is activated **automatically**, it doesn't need to transfer to EP or Radiance.

5.1.6 Step VI: Repeat by the GA

To iterate through the simulation process, the Wallacei_X component is employed to automate parameter adjustments. It facilitates the generation of parameters for subsequent simulations, ensuring the process repeats automatically until reaching a specified generation count. This is presented in the VI block in fig. 5.6.

5.1.7 After experiment: Visualisation

This step processes after all the GA generations are done. Presented in fig. 5.7, it can be sub-divided into 4 steps:

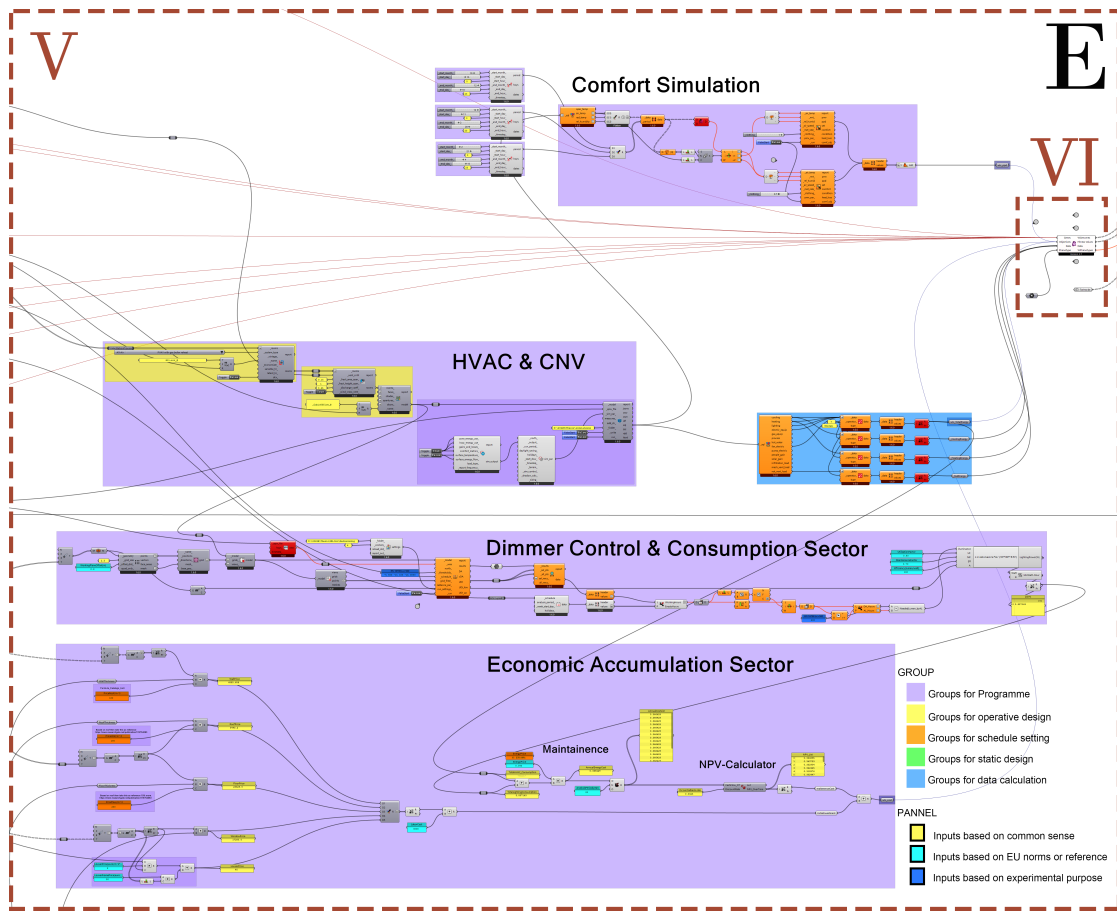


Figure 5.6: GH section E

- **Decoding and extracting the data:** The data is stored in the *Wallacei X* component. Before all, we can use a *tree branch* or *split tree* to extract to analysed generation. For the *WGenomes* and the *WPhenotypes*, we shall apply a decoding component to translate them.
- **From numbers to colors:** Firstly, use *bounds* to get the boundary of the numbers. Then, use a *Gradient* with limits connecting to the bounds, translate the numbers in to RGB colors.
- **Generating the chromosome matrix:** Use *series* and *mesh plane* to create the display matrix. And also print all the title bars.
- **Coloring the matrix:** Use a human plug-in[128], *Custom Preview with Materials* with 2 matching diffuse color and geometry data tree. It can render the colored mesh on screen.

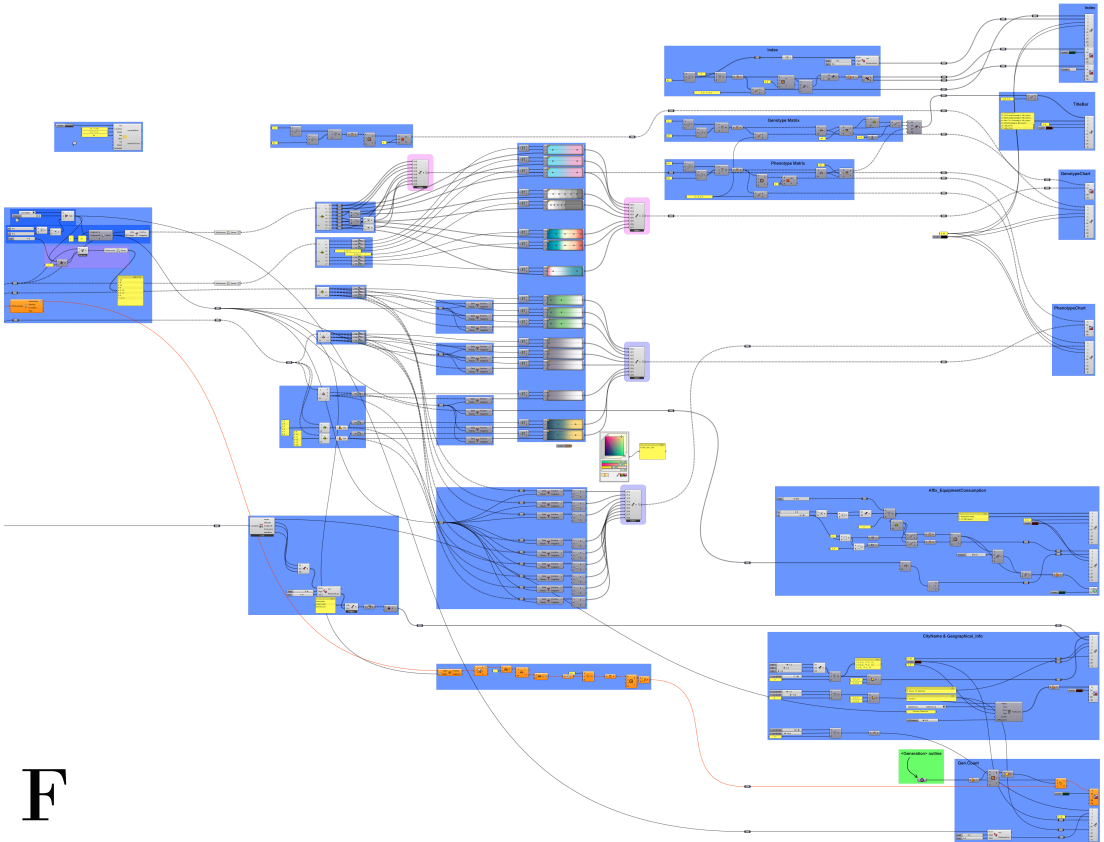


Figure 5.7: GH section F

5.2 Boundary Conditions

This section outlines the key assumptions considered for the experiment, including boundary conditions i.e. context and orientation.

5.2.1 Local climate

Weather data is imported into the GH environment using LB with *LB Import EPW (EnergyPlus Weather)* files. EPW files are text files containing hourly information on temperature, relative humidity, wind speed and direction, solar radiation, illuminance, and pressure for a specific location. In the first eight lines of each EPW file, additional information is provided, including location coordinates, design conditions, typical/extreme periods, ground temperatures, holidays/daylight savings, data periods, and comments[129].

The proposed method is implemented by considering ten representative locations across Italy and worldwide(see table 5.2), each characterized by distinct climatic conditions. These locations include Palermo, Rome, and Turin in Italy, as well as Geneva in Switzerland, Oslo in Norway, and Kiev in Ukraine among European countriesfig. 5.9. Additionally, there are Canton, Hong Kong, Tientsin in China, Busan in Korea, and Kyoto in Japan, representing Asian regionsfig. 5.8. The weather data is obtained from meteorological ground stations near these cities.

To obtain the weather data, EPWMap website is visited[130].

1st	2nd	3rd
(A) Tropical	(f) Rainforest (m) Monsoon (w) Savanna, dry winter (s) Savanna, dry summer	
(B) Dry	(w) Arid Desert (s) Semi-Arid or steppe	(h) Hot (k) Cold
(C) Temperate	(w) Dry winter (f) No dry season (s) Dry summer	(a) Hot summer (b) Warm summer (c) Cold summer
(D) Continental	(w) Dry winter (f) No dry season (s) Dry summer	(a) Hot summer (b) Warm summer (c) Cold summer (d) Very cold winter
(E) Polar		(T) Tundra (F) Ice cap

Table 5.1: Köppen classification scheme symbols
[131, 132, 133]

The Köppen climate classification scheme categorizes the types with 3 letters (see table 5.1). The first letter divides climates into five main climate groups: *A* (tropical), *B* (arid), *C* (temperate), *D* (continental), and *E* (polar)[12]. The second letter indicates the seasonal precipitation type, while the third letter indicates the level of heat[133]. Summers are defined as the 6-month period that is warmer either from April–September and/or October–March, while winter is the 6-month period that is coole[131].

CLIMATIC ZONE	LOCATION		DESCRIPTION	CLASSIFICATION	
	CITY	Köppen		ASHERAЕ	DESCRIPTION
European city	Oslo	Dfb	Continental, No dry season, Warm summer	7A	Humid Continental (Cool Summer)
	Kiev			6A	Humid Continental (Warm Summer/Cool Summer)
	Geneva	Cfa	Temperate, No dry season, Hot summer	4A	Humid Subtropical/Humid Continental (Warm Summer)
	Torino				
	Roma			3A	Humid Subtropical (Warm Summer)
	Palermo	Cfa	Dry, Semi-arid, Cold		
	Tientsin			5A	Humid Continental (Warm Summer)
	Busan			4A	Humid Subtropical/Humid Continental (Warm Summer)
	Kyoto		Temperate, No dry season, Hot summer		
	Canton				
	Hongkong			2A	Humid Subtropical (Warm Summer)

Table 5.2: Cities selected and classification



Figure 5.8: Asian selected cities



Figure 5.9: European selected cities

5.2.2 Context

Context geometries are initially modeled in RH and subsequently imported into GH as Breps or Meshes (see fig. 5.10). These geometries are then integrated into the GH environment using the *HB Shade* plugin.

The study assumes that the analyzed office space is situated within an urban setting. To simulate the surrounding urban context, a series of adjacent buildings are generated as solid blocks. §5.2.2 illustrates this random generation of neighboring buildings. It's important to note that the context remains consistent across all selected locations.

Furthermore, a ground surface is created directly within GH as a HB surface. This addition enhances the accuracy of daylight calculations within the simulation.

The overall performance of the building is assessed by evaluating two key aspects

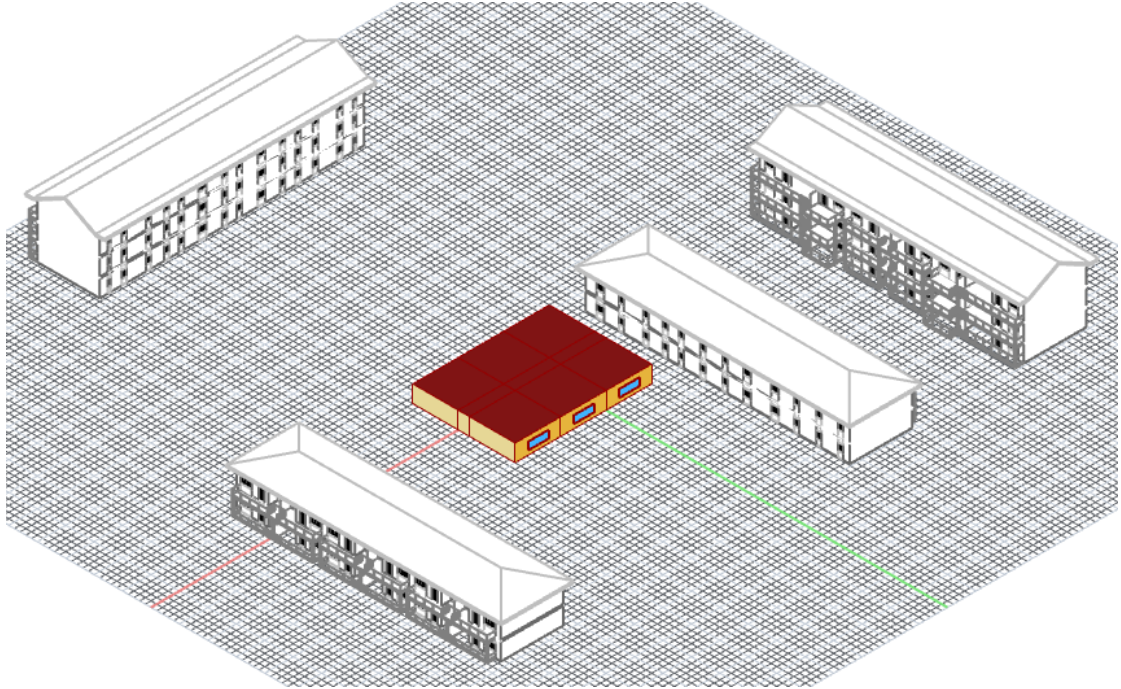


Figure 5.10: Example of context

that significantly influence indoor comfort and efficiency: energy usage and daylight availability. Two concurrent and detailed dynamic simulations are executed using the HB plug-in (v1.6.0) and the LBT (v1.6.26), serving as interfaces with EP, Radiance, and Daysim simulation engines. These components are integrated within a single pollination[134] package for seamless coordination. It's worth noting that, for this phase of the research, the thermal zone operates in a free-running mode. This paragraph provides information about the software programs employed, the configuration of simulation parameters, and the formats of the output files generated. The definitions presented in this paragraph are primarily sourced from the descriptions of inputs and outputs of the HB components.

5.3 Model building

The overall performance of the building is assessed by evaluating two key aspects that significantly influence indoor comfort and efficiency: energy usage and daylight availability. Two concurrent and detailed dynamic simulations are executed using the Honeybee plug-in (v1.6.0) and the LBT (v1.6.26), serving as interfaces with EP, Radiance, and Daysim simulation engines. These components are integrated within a single pollination[134] package for seamless coordination. It's worth noting

that, for this phase of the research, the thermal zone operates in a free-running mode. This paragraph provides information about the software programs employed, the configuration of simulation parameters, and the formats of the output files generated. The definitions presented in this paragraph are primarily sourced from the descriptions of inputs and outputs of the HB components.

Model are conducted using EP (v22.2.0) in conjunction with OpenStudio (v3.5.1). OS serves as the bridge connecting the three-dimensional parametric model created in RH and GH (RH-GH) with the simulation engine.

The workflow involves utilizing the HB component *HB Export To OSM* to export the developed HB zone into an OSM file. This OSM file is then translated into an IDF format and subsequently run through EP. The *HB Export To OSM* component requires a set of inputs, which include simulation parameters, and generates various output files in different formats as part of the analysis process. The key component in modeling part are as followed.

Note that many the 4 simulations are entwined, they're processing parallelly. And some inputs are the source for plural simulations. If it is related to Energy simulation, it'll be introduced into this section.

5.3.1 HB Opaque Material

Create a standard opaque material, which can be insert the information of material into the program. The data transfer flow is:

the source → *HB Opaque Material* → *HB Opaque Construction* → *HB Exterior Construction Subset* → *HB Construction Set* → *HB Room* And also this:

the source → *HB Opaque Modifier* → *HB Exterior Modifier Subset* → *HB Modifier Set* → *HB Room*

Then form the *HB Room*, the model is applied with this modified material. Note that the construction data is basically from thermology which is for the EPsimulation; and the modifier data is from optics which is for the Radiance simulation. But both data is combined within the *HB Room*, so in the following process the program can directly read the construction (see §5.4.5) and modifier (see §5.5.2) data from *HB object*.

For the source, we can use a *TT toolbox* to read a excel document. However, here in the figure for the integrity we use display the number on the GH canvas(see fig. 5.11).

Inputs Parameters:

- _name_ (Generic Data): Text to set the name for the material and to be incorporated into a unique material identifier.

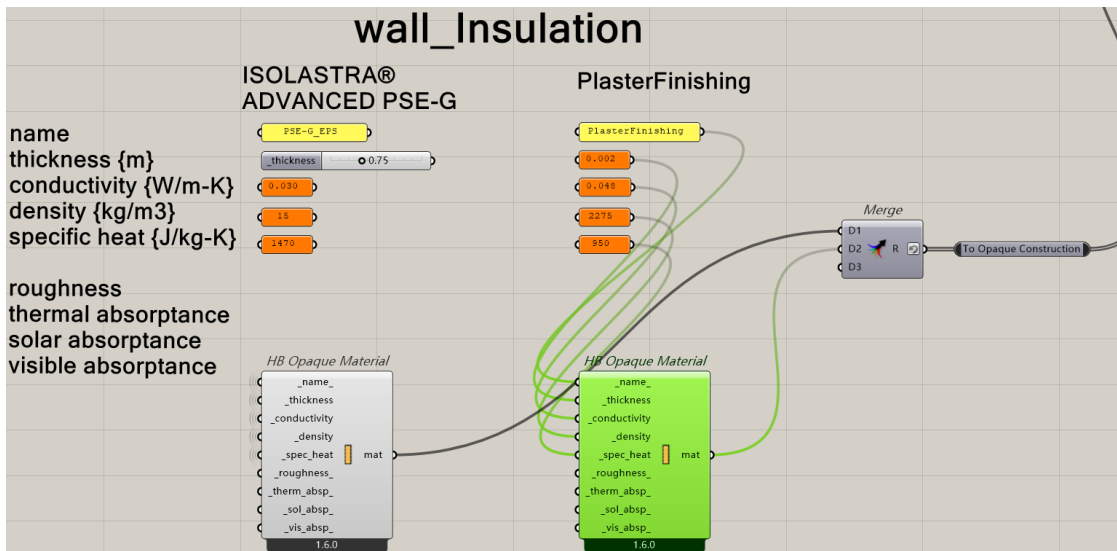


Figure 5.11: HB Opaque Material in application

- `_thickness` (Generic Data): Number for the thickness of the material layer [m].
- `_conductivity` (Generic Data): Number for the thermal conductivity of the material [W/m-K].
- `_density` (Generic Data): Number for the density of the material [kg/m3].
- `_spec_heat` (Generic Data): Number for the specific heat of the material [J/kg-K].
- `_roughness_` (Generic Data): Text describing the relative roughness of the material. Must be one of the following: 'VeryRough', 'Rough', 'MediumRough', 'MediumSmooth', 'Smooth', 'VerySmooth' (Default: 'MediumRough').
- `_therm_absp_` (Generic Data): A number between 0 and 1 for the fraction of incident long wavelength radiation that is absorbed by the material (Default: 0.9).
- `_sol_absp_` (Generic Data): A number between 0 and 1 for the fraction of incident solar radiation absorbed by the material (Default: 0.7).
- `_vis_absp_` (Generic Data): A number between 0 and 1 for the fraction of incident visible wavelength radiation absorbed by the material. Default value is the same as the `_sol_absp_`.

Output Parameters:

- `mat` (Generic Data): A standard opaque material that can be assigned to a HB Opaque construction.

5.3.2 HB Weekly Schedule

This is the most commonly used component to create a schedule (see fig. 5.12). This is the most representative one, also the *HB Constant Schedule*, *HB Seasonal Schedule* are being used in the program. The schedules support 2 simulations in the end, the energy performance and the lighting one. The first data flow transfer: *HB Weekly Schedule* → *HB Ventilation*, *HB Setpoint* and *HB People* → *HB Program Type* → *HB Room* from here the setting is applied to theHB model. The second data flow transfer:

HB Weekly Schedule → *HB Annual Daylight* Which directly inserted into the daylight simulation.

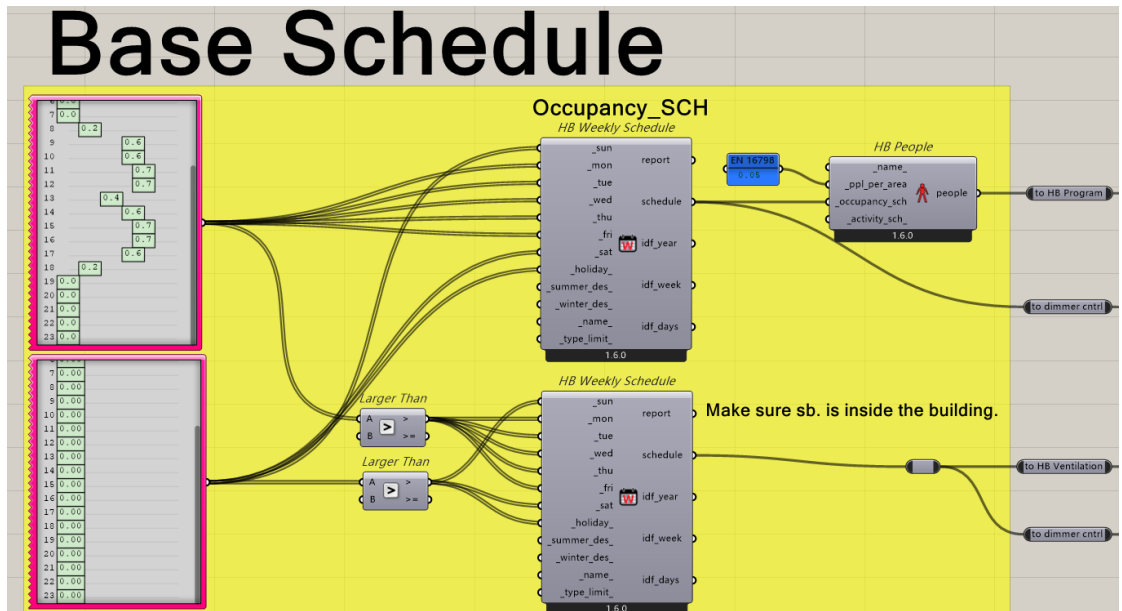


Figure 5.12: HB Weekly Schedule

The inputs of this component are straightforward. Only the limit type should be paid attention to, which is a text string from the identifier of the ScheduleTypeLimit to be looked up in the schedule type limit library. This can also be a custom ScheduleTypeLimit object from the "HB Type Limit" component. The input here will be used to validate schedule values against upper/lower limits and assign units to the schedule values. Default: "Fractional" for values that range continuously between 0 and 1. Choose from the following built-in options:

- Fractional
- On-Off
- Temperature

- Activity Level
- Power
- Humidity
- Angle
- Delta Temperature
- Control Level

Output Parameters:

- `schedule` (Generic Data): A ScheduleRuleset object that can be assigned to a Room, a Load object, or a ProgramType object.
- `idf_year` (Generic Data): Text string for the EnergyPlus ScheduleYear that will ultimately be written into the IDF for simulation. This can also be used to add the schedule to the schedule library that is loaded up upon the start of HB by copying this text into the honeybee/library/schedules/user_library.idf file along with the other idf text outputs.
- `idf_week` (Generic Data): Similar to the `idf_year`.
- `idf_days` (Generic Data): Similar to the `idf_year`

5.3.3 HB Face

This is for us to define the interface where the thermal transmittance happen, with which the HB Room can be enclosed. From architectural aspect, it defines the floor, roof and wall. See 5.13

Input Parameters:

- `_geo` (Generic Data): RH Brep or Mesh geometry.
- `_name_` (Generic Data): Text to set the name for the Face and to be incorporated into a unique Face identifier. If the name is not provided, a random name will be assigned.
- `_type_` (Generic Data): Text for the face type. The face type will be used to set the material and construction for the surface if they are not assigned through the inputs below. The default is automatically set based on the normal direction of the Face (up being RoofCeiling, down being Floor, and vertically-oriented being Wall). Choose from the following:
 - Wall

- RoofCeiling
 - Floor
 - AirBoundary
- `_bc_` (Generic Data): Text for the boundary condition of the face. The boundary condition is also used to assign default materials and constructions, as well as the nature of heat exchange across the face in energy simulation. Default is Outdoors unless all vertices of the geometry lie below the XY plane, in which case it will be set to Ground. Choose from the following:
 - Outdoors
 - Ground
 - Adiabatic
 - `ep_constr_` (Generic Data): Optional text for the Face's energy construction to be looked up in the construction library. This can also be a custom OpaqueConstruction object. If no energy construction is input here, the face type and boundary condition will be used to assign a default.
 - `rad_mod_` (Generic Data): Optional text for the Face's radiance modifier to be looked up in the modifier library. This can also be a custom modifier object. If no radiance modifier is input here, the face type and boundary condition will be used to assign a default.

Output Parameters:

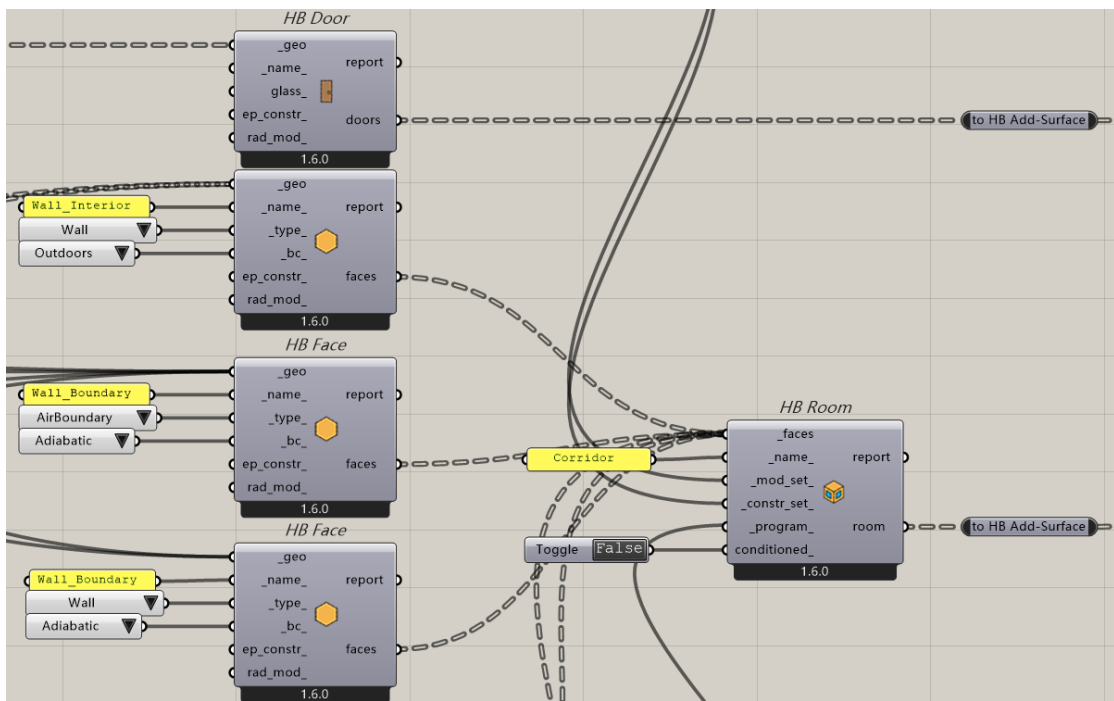
- `faces` (Generic Data): HB surface. Use this surface directly for daylight simulation or to create a HB zone for Energy analysis.

5.3.4 HB Room

Create HB Room from HB Faces. Note that each Room is mapped to a single zone in EP/OS and should always be a closed volume to ensure correct volumetric calculations and avoid light leaks in Radiance simulations. To define a room (see fig. 5.13), we need information applied to the model, which come from 3 aspects:

- **Geometrical data:** comes from the *HB face*, see §5.3.3
- **Physical data:** comes from the *HB Construction Set* and similarly the *HB Modifier Set*, see §5.3.1
- **Operative data:** comes from the *HB Program Type*, see §5.3.2.

So that the HB Room is built up, which is the unitary object to put in to the energy performance study (see §5.4). We can read the result for each room, distinguishing them by the name. So it's the core in the modeling part and worth diving into its i/o.

**Figure 5.13:** HB Room**Input Parameters:**

- _faces (Generic Data): A list of HB Faces to be joined together into a Room.
- _name_ (Generic Data): Text of Room identifier.
- _mod_set_ (Generic Data): Just as the below.
- _constr_set_ (Generic Data): Text for the construction set of the Room, which is used to assign all default energy constructions needed to create an energy model. Text should refer to a ConstructionSet within the library, such as that output from the "HB List Construction Sets" component. This can also be a custom ConstructionSet object. If nothing is input here, the Room will have a generic construction set that is not sensitive to the Room's climate or building energy code.
- _program_ (Generic Data): Text for the program of the Room (to be looked up in the ProgramType library) such as that output from the "HB List Programs" component. This can also be a custom ProgramType object. If no program is input here, the Room will have a generic office program. Note that ProgramTypes effectively map to OS space types upon export to OS.

- _conditioned_ (Generic Data): Boolean to note whether the Room has a heating and cooling system.

Output Parameters:

- **room** (Generic Data): HB room. These can be used directly in energy and radiance simulations.

5.4 Energy simulation

HB creates, runs, and visualizes daylight simulations using Radiance and energy models using OS and EP[135]. So here in this section, we mainly introduce the core of HB Energy. As we can see in fig. 5.14, the HB energy components are put into 9 categories. We can see *0::Basic Properties* in fig. 5.2, also the Opaque Material (in §5.3.1) can represent *1::Construction*, while the weekly schedule (in §5.3.2) making example for *2::Schedules*, and *HB People* in fig. 5.12 symbolizing the *3::Loads*. In this section, we focus on *4::HVAC* and *5::Simulation*, taking *HB All-Air HVAC*, *HB Model to OSM* as examples.



Figure 5.14: HB component classification

5.4.1 Weather file

an EPW file imported to GH via *LB Import EPW*.

5.4.2 Analysis period

an optional analysis period can be set using the corresponding LB component. In this case, no analysis period is specified, so that simulation is run for the entire year. But the for the setpoint, the cooling and heating are restricted to the half year.

5.4.3 HB All-Air HVAC

Apply an All-Air template HVAC to a list of HB Rooms. All-air systems provide both ventilation and satisfaction of heating + cooling demand with the same stream

of warm/cool air. They often grant tight control over zone humidity. However, because such systems often involve the cooling of air only to reheat it again, they are often more energy-intensive than systems that separate ventilation from meeting thermal loads. The context and detail is presented in fig. 5.15

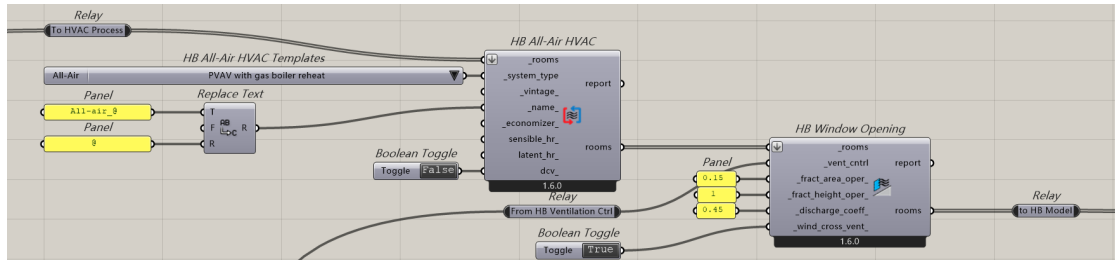


Figure 5.15: HB HVAC

Input Parameters:

- `_rooms` (Generic Data): HB Rooms to which the input template HVAC will be assigned. This can also be a HB Model for which all conditioned Rooms will be assigned the HVAC system.
- `_system_type` (Generic Data): Text for the specific type of all-air system and equipment. The "HB All-Air HVAC Templates" component has a full list of the supported all-air system templates.
- `_vintage_` (Generic Data): Text for the vintage of the template system. This will be used to set efficiencies for various pieces of equipment within the system. The "HB Building Vintages" component has a full list of supported HVAC vintages. (Default: ASHRAE_2019).
- `_name_` (Generic Data): Text of HVAC identifier.
- `_economizer_` (Generic Data): Text to indicate the type of air-side economizer used on the HVAC system. Economizers will mix in a greater amount of outdoor air to cool the zone (rather than running the cooling system) when the zone needs cooling and the outdoor air is cooler than the zone. Choose from the options below. (Default: NoEconomizer).
 - NoEconomizer
 - DifferentialDryBulb
 - DifferentialEnthalpy
 - DifferentialDryBulbAndEnthalpy

- FixedDryBulb
- FixedEnthalpy
- ElectronicEnthalpy
- **sensible_hr_** (Generic Data): A number between 0 and 1 for the effectiveness of sensible heat recovery within the system. Typical values range from 0.5 for simple glycol loops to 0.81 for enthalpy wheels (the latter tends to be fairly expensive for air-based systems). (Default: 0).
- **latent_hr_** (Generic Data): A number between 0 and 1 for the effectiveness of latent heat recovery within the system. Typical values are 0 for all types of heat recovery except enthalpy wheels, which can have values as high as 0.76. (Default: 0).
- **dcv_** (Generic Data): Boolean to note whether demand-controlled ventilation should be used on the system, which will vary the amount of ventilation air according to the occupancy schedule of the zone. (Default: False).

Output Parameters:

- **report** (Generic Data): Reports, errors, warnings, etc.
- **rooms** (Generic Data): The input Rooms with an all-air HVAC system applied.

5.4.4 HB Ventilation Control

Create a Ventilation Control object to dictate the temperature setpoints and schedule for ventilative cooling (e.g., opening windows). Note that all the default setpoints of this object are set to always perform ventilative cooling, allowing individual decisions on which setpoints are relevant to a given ventilation strategy. Here's the data transfer:

Base schedule or input schedule → *HB Ventilation Control* with its settings → *HB Window Opening* → *HB Model* → *HB Export to OSM* then the OS receives the data, also see in fig. 5.16.

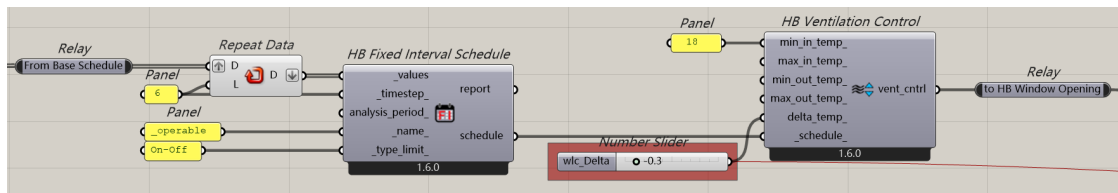


Figure 5.16: HB Ventilation Control

Input Parameters:

- **min_in_temp_(Generic Data)**: A number between -100 and 100 for the minimum indoor temperature at which to ventilate in Celsius. Typically, this variable is used to initiate ventilation with values around room temperature above which the windows will open (e.g., 22°C). (Default: -100°C).
- **max_in_temp_(Generic Data)**: A number between -100 and 100 for the maximum indoor temperature at which to ventilate in Celsius. This can be used to set a maximum temperature at which point ventilation is stopped and a cooling system is turned on. (Default: 100°C).
- **min_out_temp_(Generic Data)**: A number between -100 and 100 for the minimum outdoor temperature at which to ventilate in Celsius. This can be used to ensure ventilative cooling doesn't happen during the winter even if the Room is above the min_in_temp. (Default: -100°C).
- **max_out_temp_(Generic Data)**: A number between -100 and 100 for the maximum outdoor temperature at which to ventilate in Celsius. This can be used to set a limit for when it is considered too hot outside for ventilative cooling. (Default: 100°C).
- **delta_temp_(Generic Data)**: A number between -100 and 100 for the temperature differential in Celsius between indoor and outdoor below which ventilation is shut off. This should usually be a positive number so that ventilation only occurs when the outdoors is cooler than the indoors. Negative numbers indicate how much hotter the outdoors can be than the indoors before ventilation is stopped. (Default: -100°C).
- **_schedule_(Generic Data)**: An optional schedule for the ventilation over the course of the year. This can also be the name of a schedule to be looked up in the standards library. Note that this is applied on top of any setpoints. The type of this schedule should be On/Off, and values should be either 0 (no possibility of ventilation) or 1 (ventilation possible). (Default: "Always On").

Output Parameters:

vent_cntrl_(Generic Data): HBZones with their airflow modified.

The math logic of this component can be translate in to the formula, for every specific moment j , there are:

$$\Delta_T(j) = T_i(j) - T_o(j) \quad (5.1)$$

$$D(j) = \begin{cases} 1, & \text{if } \Delta_T(j) > \Delta_t \\ 0, & \text{otherwise} \end{cases} \quad (5.2)$$

$$I(j) = \begin{cases} 1, & \text{if } T_i(j) \in [\min_in_temp, \max_in_temp] \\ 0, & \text{otherwise} \end{cases} \quad (5.3)$$

$$O(j) = \begin{cases} 1, & \text{if } T_o(j) \in [\min_out_temp, \max_out_temp] \\ 0, & \text{otherwise} \end{cases} \quad (5.4)$$

where:

$\Delta_T(j)$ = the temperature difference at moment j

Δ_t = the component input "delta_temp"

$T_i(j)$ = the indoor temperature at moment j

$T_o(j)$ = the outdoor temperature at moment j

$D(j)$ = the differential condition at moment j

$I(j)$ = the indoor condition at moment j

$O(j)$ = the outdoor condition at moment j

Note: \min_in_temp , \max_in_temp , \min_out_temp , \max_out_temp are from the component's input.

And also with the \mathbf{S} , the schedule condition defined by the input with the same name. E.g. there are 8760 hours of the year, conventionally, we define a schedule with 8760 boolean numbers. Then for every specific moment j , there is $\mathbf{S}(j)$. Based on these boolean numbers, we apply the *HB Ventilation Control* calculation. From $\mathbf{S}(j)$, the new schedule can be written as:

$$VT_{ctrl}(j) = S(j) \cdot D(j) \cdot I(j) \cdot O(j) \quad (5.5)$$

Notice that, the Δ_t i.e. the input parameter *delta_temp*, is one of the **Genomes** to be optimized. It subsequently effects on the $D(j)$, and then effects the natural ventilation control, which eventually plays a role in the summer simulation.

5.4.5 HB Export to OSM

Write a HB Model to an OSM file, which can then be translated to an IDF file and run through EP. As we can see, it often run along with *HB Simulation Output*, *HB Simulation Parameter* in fig. 5.17. This is the core component, it transfer to the OS per se. In addition, some commonly used setups is packaged into *HB Simulation Output*, *HB Simulation Parameter*. On the other hand, the deeper interation with EPshould employ the input of *add_str_*, which is the as the command line interface work as EPitself.

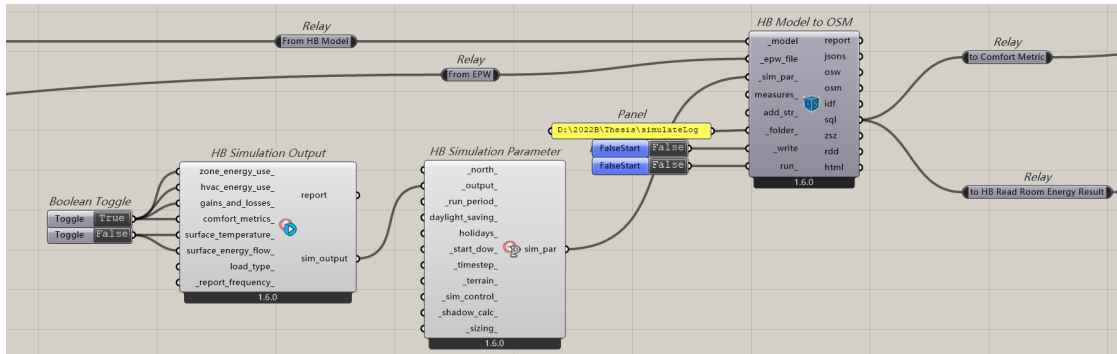


Figure 5.17: HB Export to OSM

Input Parameters:

- `_model_` (Generic Data): A HB model object possessing all geometry and corresponding energy simulation properties.
- `_epw_file_` (Generic Data): Path to an .epw file on this computer as a text string.
- `_sim_par_` (Generic Data): A HB Energy SimulationParameter object that describes all of the settings for the simulation. If None, some default simulation parameters will automatically be used.
- `measures_` (Generic Data): An optional list of measures to apply to the OS model upon export. Use the "HB Load Measure" component to load a measure into GH and assign input arguments. Measures can be downloaded from the NREL Building Components Library (BCL) at `_add_str_` (Generic Data): THIS OPTION IS JUST FOR ADVANCED USERS OF ENERGYPLUS. You can input additional text strings here that you would like written into the IDF. The input here should be complete EP objects as a single string following the IDF format. This input can be used to write objects into the IDF that are not currently supported by HB.
- `_folder_` (Generic Data): An optional folder on this computer, into which the IDF and result files will be written.
- `_write_` (Generic Data): Set to "True" to write out the HB JSONs (containing the HB Model and Simulation Parameters) and write the OS Workflow (.osw) file with instructions for executing the simulation.
- `_run_` (Generic Data): Set to "True" to translate the HB JSONs to an OSM (.osm) and EnergyPlus Input Data File (.idf) and then simulate the .idf in EP.

This will ensure that all result files appear in their respective outputs from this component. This input can also be the integer "2," which will only translate the HB JSONs to an osm and IDF format without running the model through EP. It can also be the integer "3," which will run the whole translation and simulation silently (without any batch windows).

Output Parameters:

- `report_(Text)`: Check here to see a report of the EP run.
- `jsons_(Generic Data)`: The file paths to the HB JSON files that describe the Model and Simulation Parameter. These will be translated to an OSM.
- `osw_(Generic Data)`: File path to the OS Workflow JSON on this machine. This workflow is executed using the OS command line interface (CLI) and it includes measures to translate the HB model JSON as well as any other connected measures.
- `osm_(Generic Data)`: The file path to the OSM that has been generated on this computer.
- `idf_(Generic Data)`: The file path of the EnergyPlus IDF that has been generated on this computer.
- `sql_(Generic Data)`: The file path of the SQL result file that has been generated on this computer. This will be None unless `run_` is set to True.
- `zsz_(Generic Data)`: Path to a .csv file containing detailed zone load information recorded over the course of the design days. This will be None unless `run_` is set to True.
- `rdd_(Generic Data)`: The file path of the Result Data Dictionary (.rdd) file that is generated after running the file through EP. This file contains all possible outputs that can be requested from the EnergyPlus model. Use the "HB Read Result Dictionary" component to see what outputs can be requested.
- `html_(Generic Data)`: The HTML file path containing all requested Summary Reports.

5.5 Lighting simulation

Annual daylight simulations are conducted employing the Radiance (v5.4a) engine, a freely available, highly accurate ray-tracing software system developed by the DOE (U.S. Department of Energy) with collaborative support from the Swiss Federal

Government [136]. Radiance is extensively utilized by engineers and architects to anticipate and visualize daylighting distribution and assess visual comfort during the initial stages of the design process. The process involves exporting the zone to a RAD file, a text-based format that translates HB geometries and materials into the primary input file for Radiance. Key inputs and outputs relevant to this HB component are comprehensively discussed below.

In this section 3 missions are presented: ALS installation; Daylight simulation; Artificial lighting estimation. Each of the a key component is introduced.

5.5.1 HB Sensor Grid

To build a ALS grid, it's better to keep the consistency of the whole workflow. So, we apply it to theHB model. Firstly, it's needed to deconstruct theHB object (which is created in §5.3) via *HB Visualize by Type*, which help us to extract all the horizontal faces. Secondly, based on these faces a grid is created via *LB Generate Grid Point*. Lastly, we can use these points and faces to build up the ALS grid via *HB Sensor Grid*.

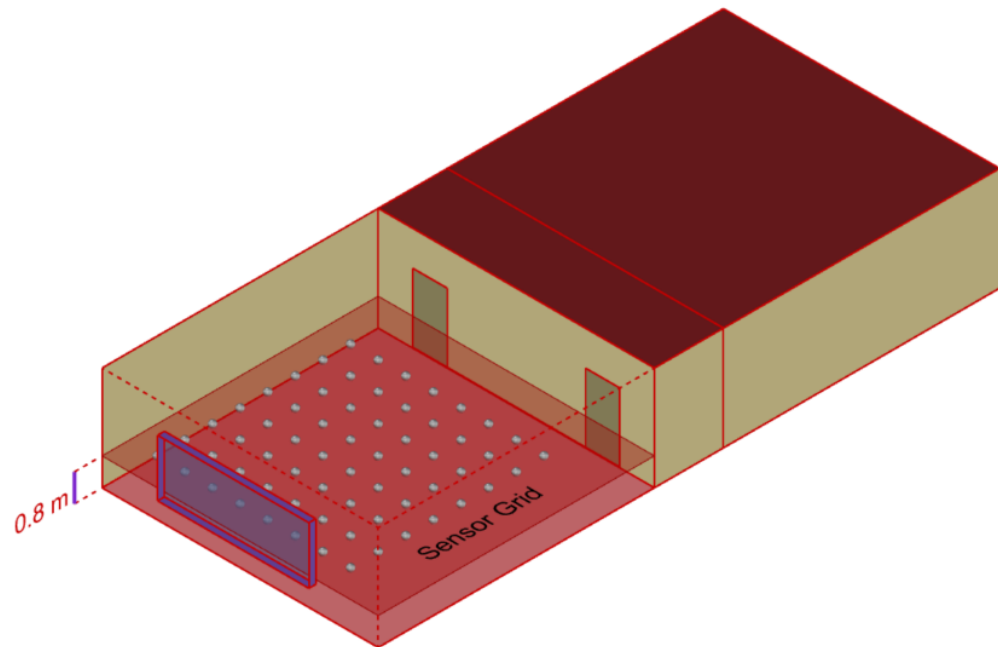


Figure 5.18: ALS grid to receive the daylight

5.5.2 HB Annual Daylight

In the fig. 5.19, we can see *HB Object*, *Analysis Recipe* are connected to the component. This is the setting for the Radiance simulation engine. Nevertheless, before in-plugged to the component, the weather file should be translated via *HB Wea From EPW*. Here's the data transfer:

Geometrical data is borrow from *HB Object*(see §5.3) via *HB Visualize by Type* → *LB Generate Point Grid* → *HB Sensor Grid* → *HB Assign Grids and Views* → *HB Get Grids and Views* → *HB Annual Daylight* → *HB Annual Results to Data* → a data extractor(see §5.5.3) → the illuminance calculator(see fig. 5.20) → converted to electric consumption → finally goes to the economic simulation sector.

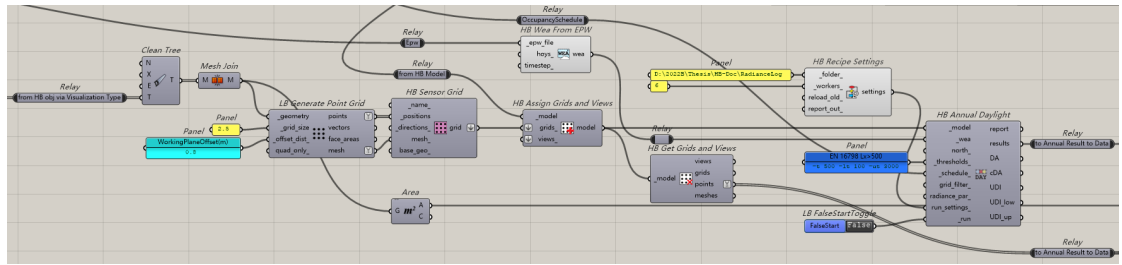


Figure 5.19: HB Annual Daylight

HB Object

TheHB object (which is created in §5.3) is also needed, for its apertures information.

Analysis recipe

Radiance boasts diverse simulation capabilities, prompting HB to offer various analysis recipes for this input field. Among these options are daylight factor simulations, grid-based or image-based lighting analyses, and annual daylight simulations. For the scope of this research, the focus lies on the latter. Hence, the 'annualDaylightSimulation' recipe is constructed, utilizing the EPW file and creating a test points grid and mesh aligned with the zone's floor area.

- **Number of CPUs:** Determine the desired number of CPUs for conducting the studies.
- **File name and working directory:** Define a project name and designate a directory for storing result files. Avoid using spaces in the directory name, similar to energy simulation constraints.

Daylight simulation is then initiated by setting the `writeRad` and `runRad` fields to `True`. It's important to note that Radiance requires more time (often several minutes) compared to EP to execute the analysis.

5.5.3 Daylight estimation

Firstly, we filter the annual data, to extract the daylight data during the working hours. We use the occupancy schedule as the filter (see §5.3.2 and fig. 5.2) via *dispatch*. Then we employ the *dispatch* again, to extract all the hour within the working period the daylight is insufficient to 500 lux.

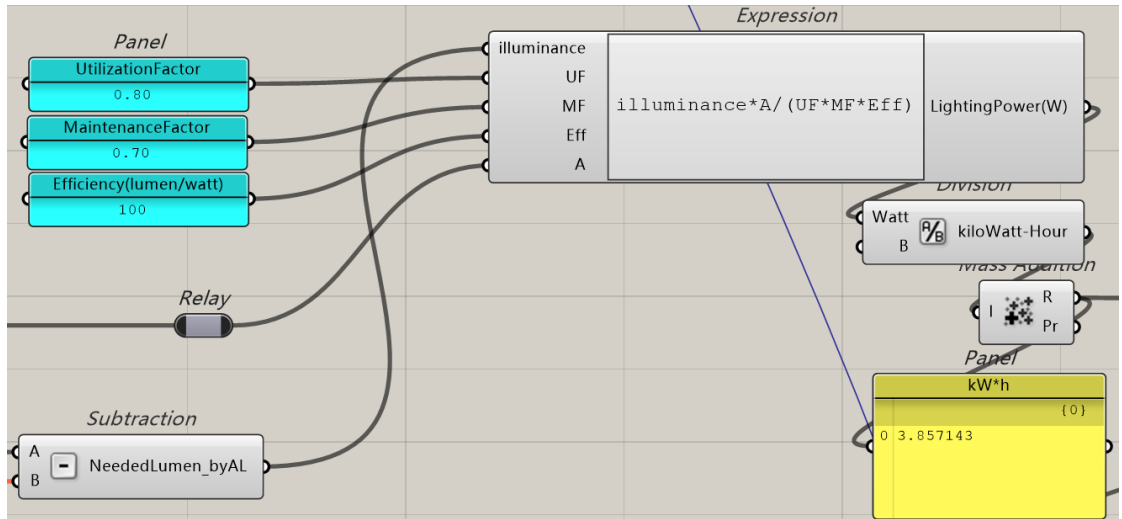


Figure 5.20: Illuminance calculator

Daylight simulation is then run by setting to `True` the `run` fields. Radiance usually takes up a longer time (several minutes) with respect to EP, but it can be shortened by minimizing the grid numbers. However, the setting of Radiance is much more flexible and robust than the EP. Unlike EPall the faces should be well defined, if aHB model is only for radiance simulation, the geometry arrangement is less strict. Building a *HB Modifier* is easier than *HB Opaque Construction* as well. This is an example of so-called "hard for mankind, but easy for machine" issue.

5.6 Economical simulation

As we introduced, there're 2 kinds of costs: the initial cost and the annual cost. The initial cost refers to §4.2, while the annual cost referring to §4.3 and §5.1.4.

Before the NPV is calculated, the 2 kinds of cost should be all prepared. And then the annual cost will be processes the NPV calculation. Lastly, the outcome will add up with the initial cost. The result is the final value, which is the **fitness value**, the goal of optimization.

5.6.1 NPV calculator

The approach is based on the formula in eqs. (3.10) and (3.11). The pseudocode is on 78:

Algorithm 1 NPV Calculator

```
1: procedure NPVL(CashFlow_OverTime, DiscountRate, NPV_OverTime)
2:   NPV_OT ← an empty list
3:   for  $i \leftarrow 0$  to length of CashFlow_OverTime – 1 do
4:     period ←  $i + 1$ 
5:      $D_n \leftarrow (1 + \text{DiscountRate})^{\text{period}}$ 
6:     NPV_S ← CashFlow_OverTime[i]/ $D_n$ 
7:     NPV_OT.add(NPV_S)
8:   end for
9:   NPV_OverTime ← NPV_OT
10: end procedure
```

5.7 Comfort simulation

It is suggested in the notation of the component, that different comfort assessment is used for different scenarios. Conventionally, it follow the type of the space being assessed. Mainly there're 4 comfort metric can be selected:

- **PMV comfort:** mainly for the indoor space conditioned.
- **Adaptive comfort:** mainly for the indoor space without AC.
- **UCTI comfort:** can be used for the outdoor space.
- **PET Comfort:** estimating core body temperature and whether a given set of conditions is likely to induce hypothermia or hyperthermia in a specific individual.

Obviously, to analyse an indoor office, we choose PMV comfort as the method. In addition, we already consider the indoor - outdoor temperature in eq. (5.1). So here using the PMV can minimized the cross interference.

5.7.1 LB PMV Comfort

The methodology is introduced in §3.4.2. The `_air_temp`, `_rel_humid`, `_mrt_` are gained from the *HB Read Room Comfort Result* after the simulation *HB Export to OSM* is done. and the `_air_speed_` is set to $0.014\text{m}^3/\text{s}$.². And it's discussed in §4.3.3.

Input Parameters:

- `_air_temp` (Generic Data): Data Collection or individual value for air temperature in C.
- `_mrt_` (Generic Data): Data Collection or individual value of mean radiant temperature (MRT) in C. Default is the same as the `air_temp`.
- `_rel_humid` (Generic Data): Data Collection or individual value for relative humidity in %. Note that percent values are between 0 and 100.
- `_air_speed_` (Generic Data): Data Collection or individual value for air speed in m/s. Default is a very low speed of 0.1 m/s, typical of room air speeds induced by HVAC systems.
- `_met_rate_` (Generic Data): Data Collection or individual value of metabolic rate in met. Default is set to 1.1 met for seated, typing. Typical values include:
 - 1 met = Metabolic rate of a resting seated person
 - 1.2 met = Metabolic rate of a standing person
 - 2.4 met = Metabolic rate of a person walking at 1 m/s (2 mph)
- `_clothing_` (Generic Data): Data Collection or individual value of clothing insulation in clo. Default is set to 0.7 clo for long sleeve shirt and pants. Typical values include:
 - 1 clo = Three-piece suit
 - 0.5 clo = Shorts + T-shirt
 - 0 clo = No clothing
- `pmv_par_` (Generic Data): Optional comfort parameters from the "LB PMV Comfort Parameters" component to specify the criteria under which conditions are considered acceptable/comfortable. Default assumes a PPD threshold of 10% and no absolute humidity constraints.

²It should be pointed out that an air speed over 0.8 m/s could cause discomfort in office places, as it tends to move office papers from the desks[112]

- `_run` (Generic Data): Set to True to run the component.

Output Parameters:

- `report` (Text): Reports, errors, warnings, etc.
- `pmv` (Generic Data): Predicted Mean Vote. PMV is a seven-point scale from cold (-3) to hot (+3) that was used in comfort surveys of P.O. Fanger. Each integer value of the scale indicates:
 - -3 = Cold
 - -2 = Cool
 - -1 = Slightly Cool
 - 0 = Neutral
 - +1 = Slightly Warm
 - +2 = Warm
 - +3 = Hot
- `ppd` (Generic Data): Predicted Percent of Dissatisfied. Indicates the percent of people who would have a PMV beyond acceptable thresholds (typically <-0.5 and >+0.5). Best achievable PPD is 5% and most standards aim for PPD below 10%.
- `set` (Generic Data): SET (Standard Effective Temperature) in Celsius, describing what the given input conditions "feel like" in relation to a standard environment.
- `comfort` (Generic Data): Integers noting whether the input conditions are acceptable according to the assigned `comfort_parameter`. Values are:
 - 0 = uncomfortable
 - 1 = comfortable
- `condition` (Generic Data): Integers noting the thermal status of a subject according to the assigned `comfort_parameter`. Values are:
 - -2 = too dry (but thermally neutral)
 - -1 = cold
 - 0 = neutral
 - +1 = hot
 - +2 = too humid (but thermally neutral)
- `heat_loss` (Generic Data): A list of 6 terms for heat loss from the human energy balance calculation underlying PMV. Values are in W. Terms are

ordered as follows: Conduction, Sweating, Latent Respiration, Dry Respiration, Radiation, Convection.

- comf_obj (Generic Data): A Python object containing all inputs and results of the analysis. Can be used in components like the "Comfort Statistics" component to obtain further information.

5.8 Optimization

The optimization aims to identify optimal configurations among a defined set of parametric, independent design variables that ensure satisfactory levels of occupants' thermal and visual comfort without mechanical conditioning. This iterative process facilitates the exploration of a broad spectrum of potential design solutions, shedding light on both optimal and sub-optimal choices in construction and their impact on overall building performance. Given the multifaceted and often conflicting nature of factors influencing cost or EUI performance, addressing this as a multi-objective complex problem necessitates the utilization of Octopus, a Genetic Algorithm (GA)-based evolutionary simulator.

Octopus, employing the SPEA-II combined with the HypE algorithm, enables the concurrent optimization of multiple parameters [137]. Its maturity appeals to many researchers to run their optimization on it.

Wallacei is catching up with Octopus these days. Using NSGA-II as the core, it benefits the researcher especially on the result analytic and expression. On the other hand, it also performs effectively in the optimization process. The search for optimal solutions encompasses balancing various objectives simultaneously. Thus, the most favorable solutions are those capable of reconciling the optimality of all considered objectives. This section delves into the theoretical foundation governing Wallacei's operations, detailing the chosen simulation parameters and objectives, and outlining the criteria for identifying optimal solutions.

5.8.1 Wallacei X

The Wallacei solver component, depicted in §5.8.1 here aside, is utilized for optimization tasks. We can find the introduction and tutorials of it in [138]. Genetic information should be connected to the Genes field, while the Objectives field gathers the objectives of the simulation (fitness), with a minimum of two objectives.

³If we name the gene or phenotype beginning with "wlc_" then the component can automatically select all the sliders and objectives via rightclick or Gene Pool and Slider Shuffler component.

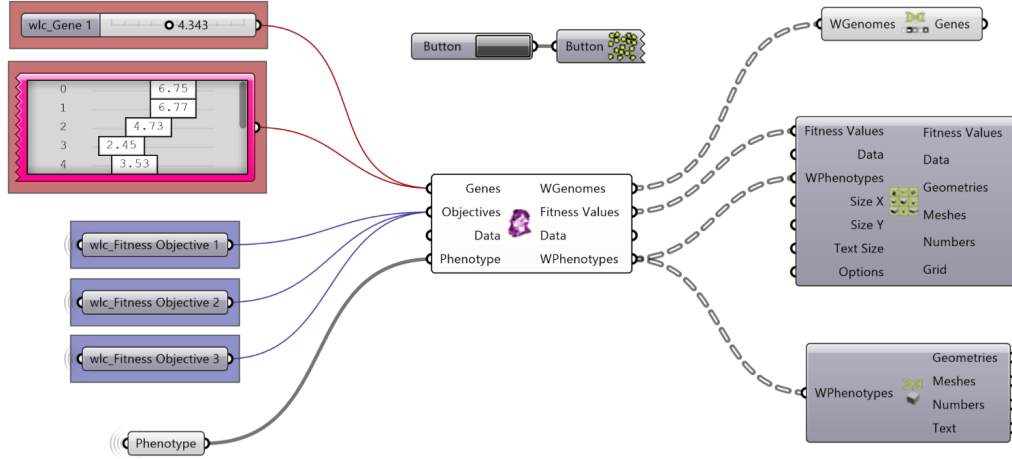


Figure 5.21: Wallacei X Component³

Both numerical and text parameters, representing the values and names of the objectives, can be input here. It is advisable to organize these elements into two separate lists: one for numerical values and the other for objective names. Optionally, a 3D mesh can be linked to Wallacei, defining the phenotype (P) and allowing visual assessment of the solutions [61]. Variations of the phenotype are compiled into a tree and outputted by the Wallacei component (Ps). In this particular case, no mesh is included to prevent overloading the simulation. Here provides a list of the variables and objectives considered for the analysis developed.

Eight parameters are chosen to construct the genome:

- Thickness of Insulation for Walls
- Thickness of Insulation for Roof
- Thickness of Insulation for Floor
- Glazing Type
- Louvers Count
- Window-to-Wall Ratio for South Facade (WWR_S)
- Window-to-Wall Ratio for North Facade (WWR_N)
- Delta Temperature

The fitness values:

- PPD (Predicted Percent of Dissatisfied)
- EUI (Energy Use Intensity)
- Cost

5.8.2 Wallacei section

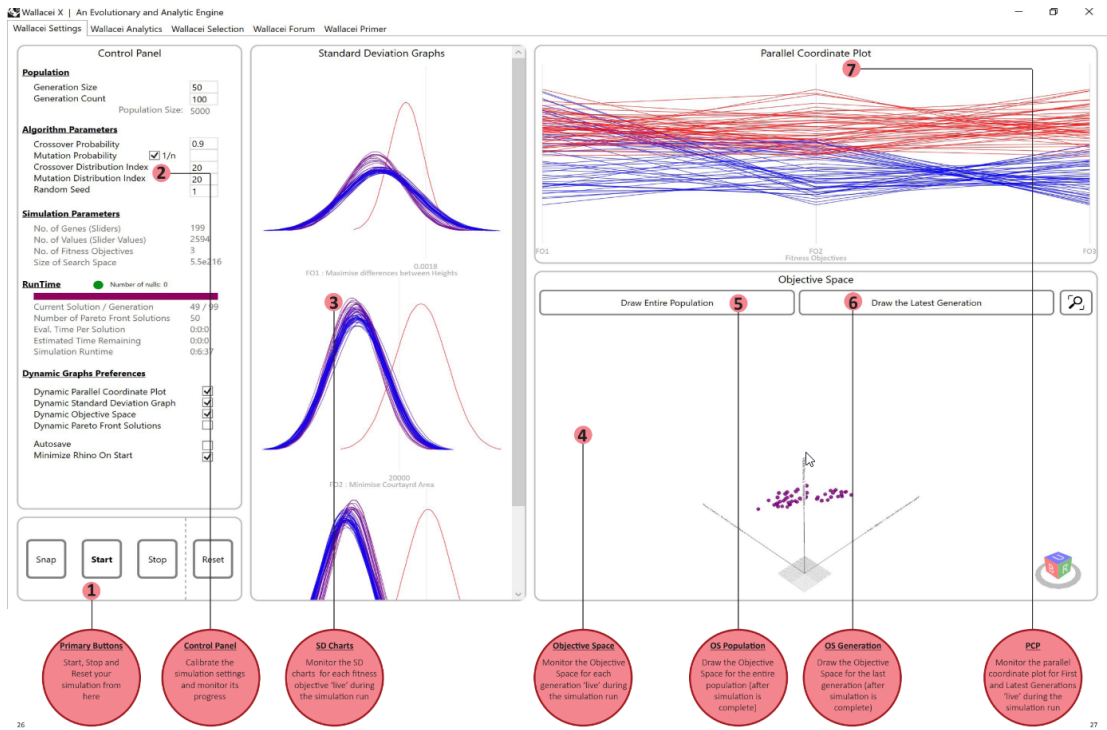


Figure 5.22: Sections of Wallacei X

In the fig. 5.22

- **Primary Buttons:**

- **Snap:** Takes a screen-shot of your screen and saves it to the desktop. It is recommended you maximise the user interface window before taking a screen shot for best results.
- **Start:** Clears any existing data in the solver and starts a new simulation. When the simulation finishes, a popup window is displayed informing the user that the simulation is complete.
- **Stop:** Stops the simulation. When clicked, a popup window is displayed informing the user that the simulation has been aborted.
- **Reset:** Clears any data stored in the solver and resets the simulation settings to the default values.

- **Control Panel:**

- **Population:** Set the generation size (how many individuals per generation) and generation count (how many generations in the simulation) for your simulation.
- **Algorithm Parameters:**
 - * **Crossover Probability (0.0 to 1.0):** Percentage of solutions in the generation that will reproduce for the next generation.
 - * **Mutation Probability (0.0 to 1.0):** Percentage of mutations taking place in the generation.
 - * **Crossover and Mutation Distribution Index (0 to 100):** A large distribution index value gives a higher probability for creating offspring near parent solutions and a small distribution index value allows distant solutions to be selected as children solutions.
- **Dynamic Graphs Preferences:**
 - * Toggle to allow Wallacei to draw different graphs live as the simulation is running.
- **Autosave:**
 - * If Toggled, Wallacei will autosave the GH definition at the end of each generation evolved in the simulation.
- **SD Charts:**
 - * Dynamically draws the Standard Deviation chart for each fitness objective independently.
- **Objective Space:**
 - * Dynamically draws the objective space for each generation in the simulation, representing up to 6 dimensions.
- **Objective Space - Draw entire population/Latest Generation:**
 - * Once the simulation is complete, this button becomes enabled allowing the user to display the objective space for all solutions or the last generation in the population.
- **Parallel Coordinate Plot:**
 - * Dynamically draws the parallel coordinate plot for the simulation, reducing simulation runtime by drawing for the first and latest generation.

The Wallacei X is a strong component, not only the optimization can be conducted on it, also it can function as a observer to the data, using its analytic function. In figs. 5.23 and 5.24 we can see the Pareto fronts' distribution in the Wallacei interface. Nevertheless, such these graphics can be generated outside the

Wallacei interface, just using the Wallacei analytic component set. So that, the graphic is created in the format of GH geometry, which benefit us of the interaction of other RH functionality. We can see more examples in §5.9.

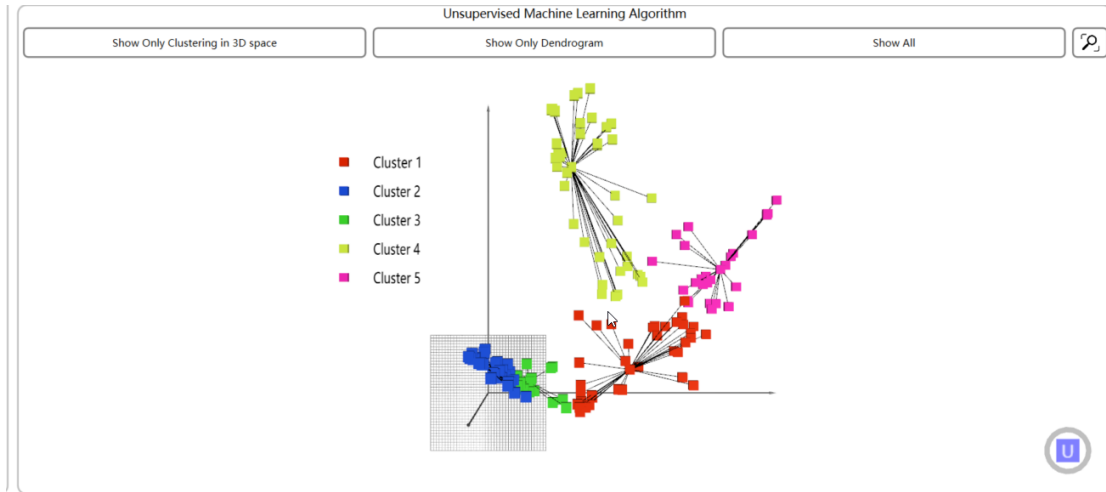


Figure 5.23: Clusters using Hierarchical (complete linkage) of the Pareto fronts in the optimization of Torino. Cluster 2 and 3 show that many solutions are urged to crowd into the low cost field. It's a very common strategy we can detect in nearly every city's optimization.⁴

5.9 Visualization

To visualize the data is to analyse it. And before analysing the result data, we'd better to arrange them and visualized them. In this section, we visualized the data into graphic and matrix, as it's done, some heretical patterns and survival strategies reveal.

5.9.1 Objective Space

In fig. 5.25, all the solution are placed in a 3 dimensional space, and all the Pareto fronts are marked. However, all the points are stacked together.

So in order to have a better view of the objective space, we developed a process to export the objective space via *Wallacei Analytics_Objective Space*. Note that

⁴This strategy we name it "cheap is the key", see the example in §6.2.5

⁵This figure indicated the heritage relationship of the referring solutions. Here it presents the heritage linkage of all the Pareto front. And we can complete bloodline in ??.

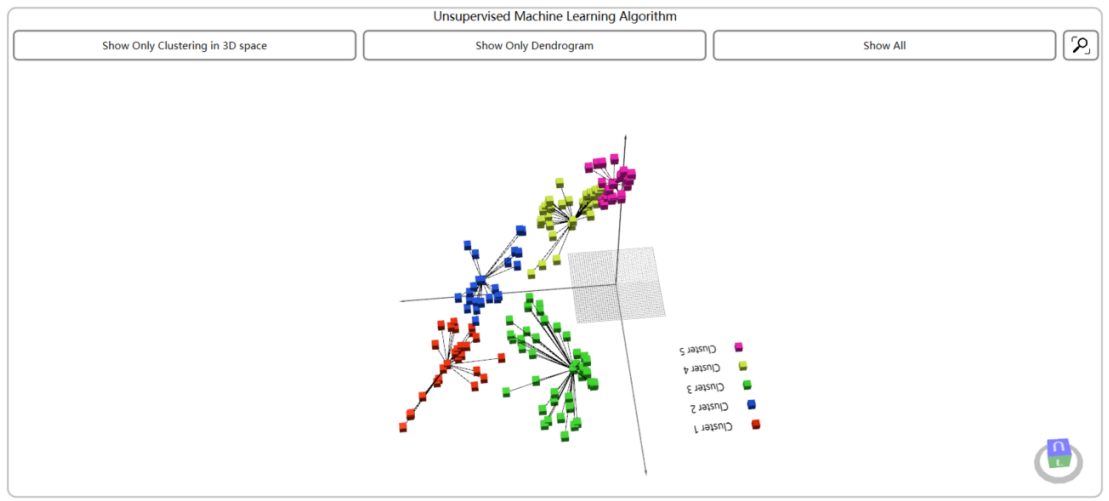


Figure 5.24: Clusters using K-means of the Pareto fronts in the optimization of Torino. In the figure cluster 2 and 3 are the preferred solution. We can also see that in the low cost field(close to Z-axis) those solution share a distinctive bloodline, and the sharing a worse diversity.⁵

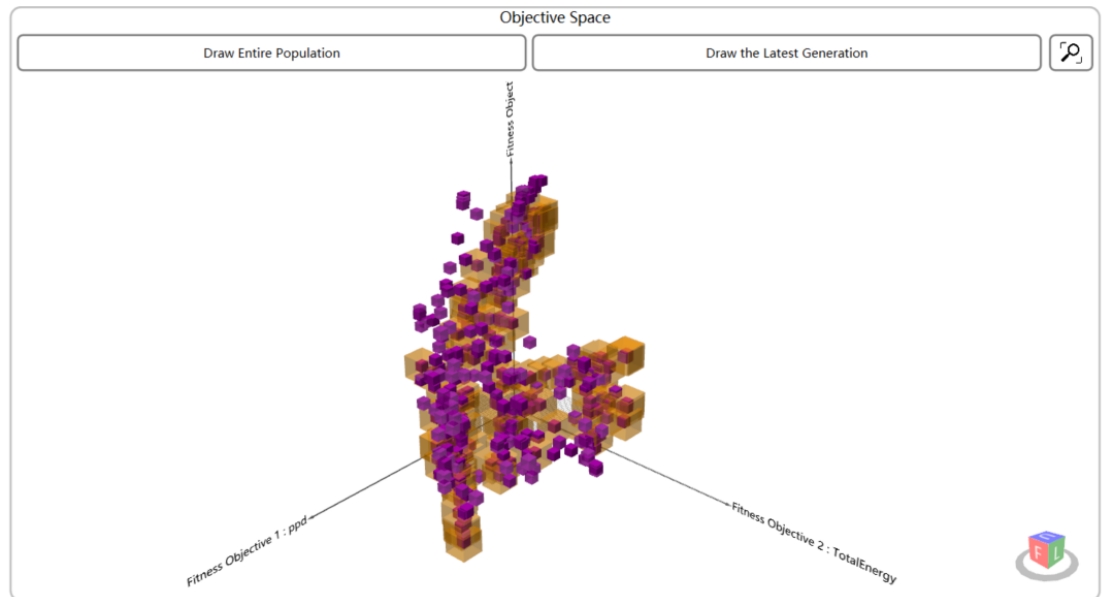


Figure 5.25: Objective space in the Wallacei interface of the Pareto fronts in the optimization of Torino

this component can also generate the graphic with the fitness value from Octopus, and because of that, before inputting the fitness value an additional step should be

applied, i.e. *Wallacei Analytics_Extract Octopus Text Files* for the Octopus data, and *Wallacei Analytics_Order FVs From WallaceiX* for the wallacei data.

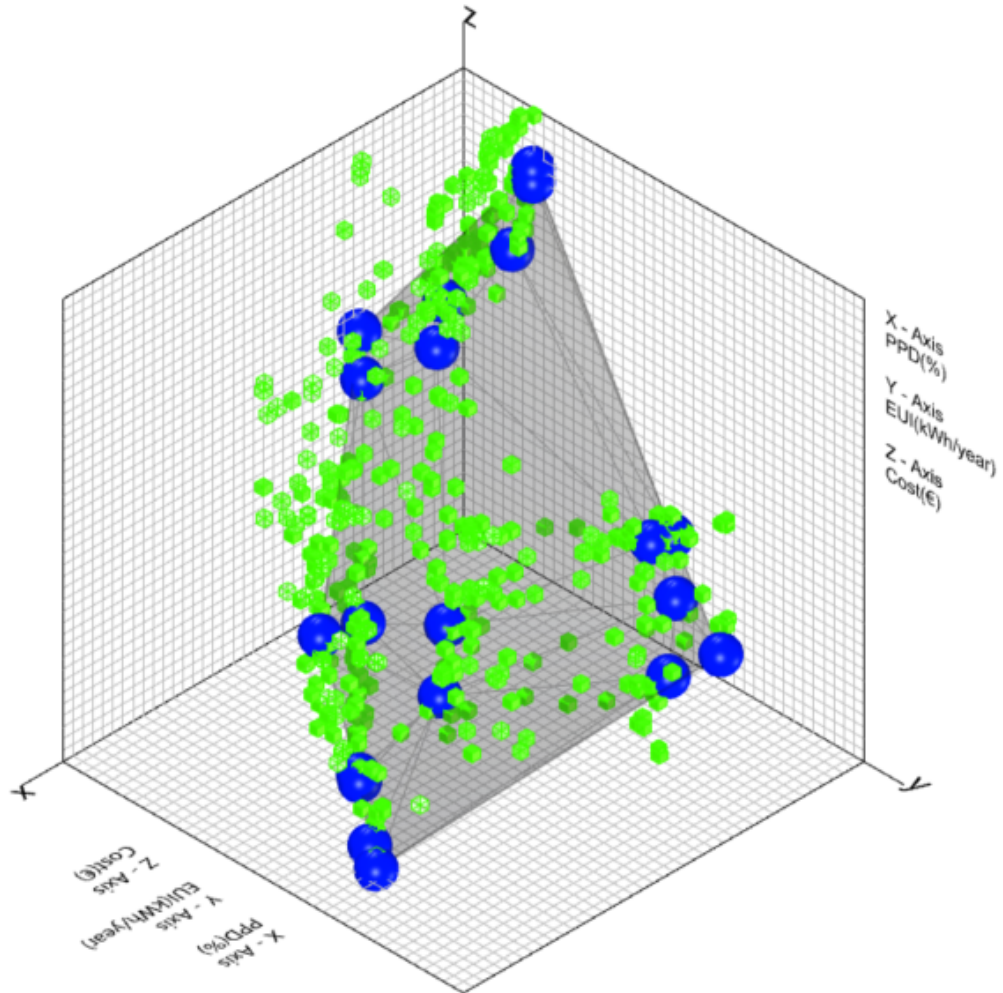


Figure 5.26: Axonometric objective space presenting in RH of all the solution in the optimization of Torino. The Delaunay mesh are created from Gen.99. The blue balls the selected solutions from Gen.99

Exported to the GH environment, the perspective and the scale can be adjusted and calculated parametrically. In the optimization of Torino, in fact, only 440 unique solutions are generated. Meaning that up to 1500 solutions are the exact copies of the 440, sharing exactly the same genotypes. This is because for these fitness value, these genes are really competitive that survive to the end, all the solutions are just permutations and combinations from the same gene pool, and

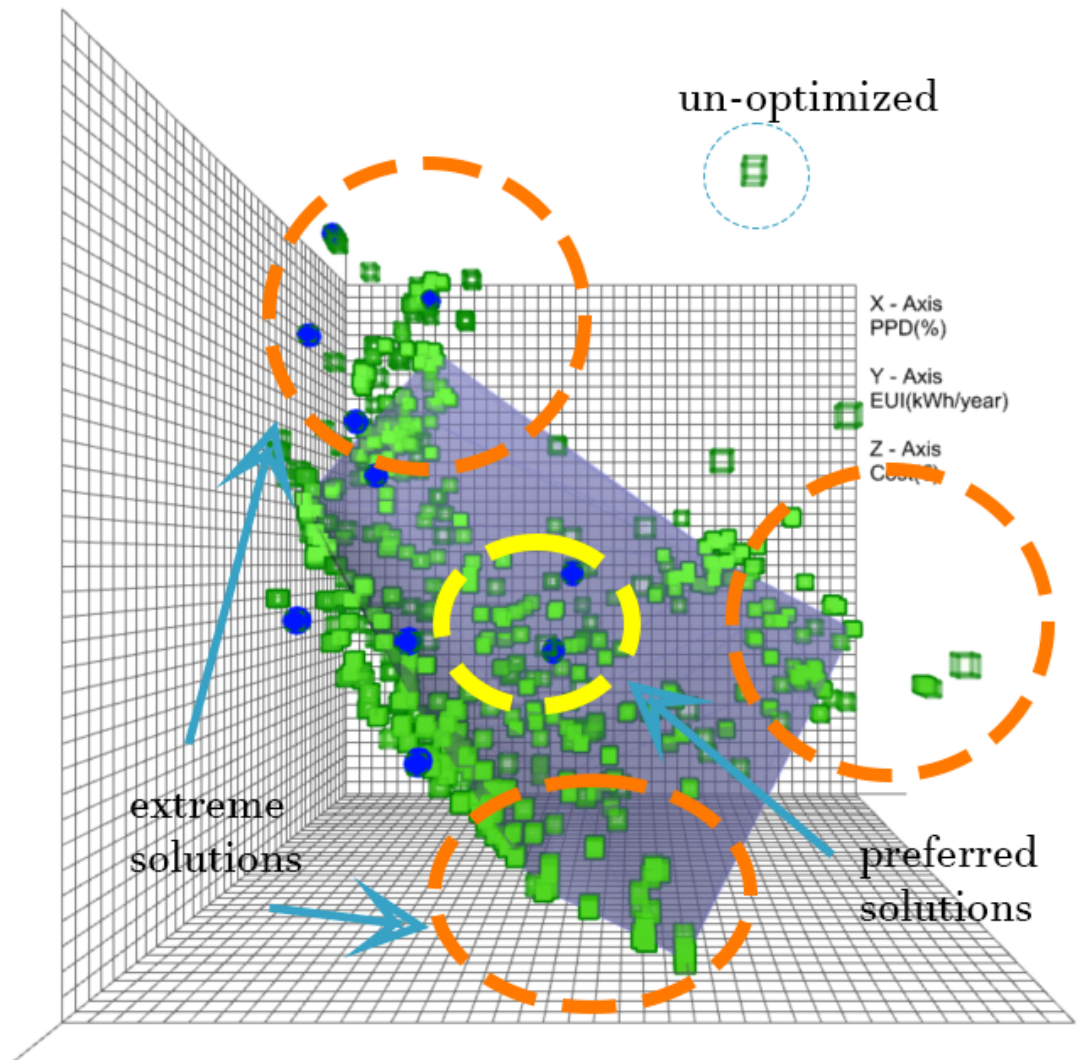


Figure 5.27: Front objective space presenting in RH of all the solution in the optimization of Torino. The greener the graphic is colored the denser the solutions are crowded in space.

the same combination just shows up across generations, where the **Crowding distance computation** (introduced in §3.5.3) isn't functioning expectedly. This is a shortage of our method, a small generation size limit the crowding distance computation performance, also over simplifying the Delaunay mesh in fig. 5.26. However, our method ensure the convergence become effective fully. Generally speaking, our method focus on quality rather than diversity over all the solutions.

5.9.2 The Matrix

The method to create the matrix is introduced §5.1.7. In this section, the content of the matrix will be in-lighted.

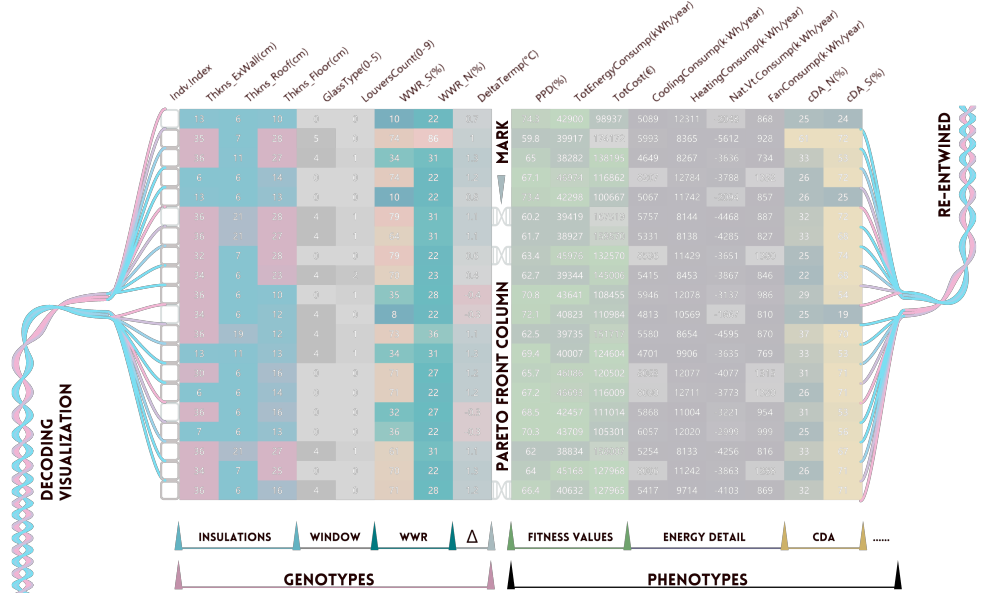


Figure 5.28: chromosome matrix introduction. The content of the matrix are the data displayed from Torino Optimization, generation 50.

The idea of the method to present the chromosome of fig. 5.28, comes from process of decoding and re-entwined of the DNA molecular and in-lighted by the *Genomic Visualization*(Wallacei component)⁶. The matrix is divided into 2 parts, where the left one is the field of genotypes, and the right is the field of phenotypes. The genotype, also known as, genomes are all the parameters that the program used to produce the digital model, and it's read via *Decode Genome*(Wallacei component). So far it's modelling after the *Genomic Visualization* method. And we add more information to it in the following process.

The first field on the right, is the the displaying of the phenotypes, which are the performances of the digital model. Among them, the key performances are **Fitness values** which are colored into green tones. Additionally, the darker color indicates this datum is closer to the optimal, while the paler one indicates worse

⁶The method is adaptive. Both the display color and scale can be modified. However, the objects to displayed are limited. Individuals of all the generations are exported in the same time. And it's hard for us to observe the variation generation by generation.

performances.

In second field on the right, the grey colors are the groups of EUI. They're the subdivided usage numbers inside the *TotEnergyConsumption*, showing more details from the energy consuming conditions. Similarly, the darker color indicates this datum is closer to the optimal and vice versa. All the values here and the equipment, lighting consumption, consist the *TotEnergyConsumption*⁷.

The third field on the right are two columns of cDA (continuous Daylight Autonomy). Obviously, the cDA are mainly influenced by the WWR of each directions. In some specific color range, a mirroring projection is observed.

Lastly, it's important to notice that the digital models can be measured in many ways. In addition to the **Fitness values**, there are hundreds of performances can be quantified. The phenotype matrix here is to present the key performance indicators, which help us to understand and compare the solutions.

5.9.3 Pareto front mark

Also in the fig. 5.28,between the 2 matrix there is a empty column for the Pareto front marks. If the *gene-like mark* is put in the middle of a row, it means its representing individual is one of the Pareto front solutions. Notice that, only the firstly appeared combination of the genes is the Pareto front, will be mark with the icon. Even though the upcoming genotypes might have the same combination due to the genetic mechanism, they won't be marked. So that means each mark represents a single unique isolated Pareto front. As mentioned in §5.9.1, 440 unique solutions are provided where 146 of them are Pareto fronts.

Having completed the visualization process, the human can scan quickly the matrix to obtain the general understanding of the individuals. Then the human designers can select some solutions as the references in the early design stage. If more time is available, an analysis process can be conduct in order to know how the strategy wins out to the end.

"From designing to choosing" that is our ultimate goal. Among so many solutions provided in the late generations. How do we select? The Pareto front is one of the criterion. And it's a rational criteria.

⁷Conventionally, this value consider the lighting as well. Since the LEUI is calculated aside, here the consumption is double added. But the lighting simulation of HB room isn't optimized, which mean it stays a constant value, making no harm to the final results of the optimization

5.9.4 Selection criteria

Primary selection

Upon completion of the optimization process, solutions are compared to identify the optimal configuration of genes that best meets the objectives. In multi-objective optimization, a good set of solutions typically clusters near or aligns along the approximated Pareto front generated by the software. Named after Vilfredo Pareto, who first used this concept in his studies at the turn of the 19th and 20th centuries, Pareto front (or Pareto set) is described as "the set of non-dominated solutions, where each objective is considered as equally good" [139]. It is represented by a geometric entity that could be either bidimensional or three-dimensional, depending on the number of fitness values considered. Non-dominated solutions, also called Pareto optimal or Pareto efficient, are those individuals for which "an optimal trade-off between two or more contradicting objectives" is achieved, and no change in the genes can lead to an improvement in some of the objectives' results without degrading the others [140, p. 16]. In contrast, dominated solutions are named because there is always a solution that is better than them in terms of goals values. The Pareto front concept is really helpful, as it allows the designers to restrict their attention to the set of solutions that are really optimal, rather than analyze every individual in search of the best ones. Generally speaking, the first selection is based on the Pareto fronts.

Secondary selection

Not all Pareto-efficient solutions are deemed optimal for the design intent. So on top of the primary selection, the secondary ones are applied. As depicted in fig. 5.26, these solutions demonstrate a broad distribution in the 3D cubeview diagram, encompassing extremes in data. However, it is plausible that multiple optimal solutions exist within this context; the determination of the "best" one among them is the designer's prerogative. Optimal design solutions are often situated closer to the center of the graph, near the origin of the three Cartesian axes. fig. 5.27 reveals that within the circle of optimal solutions. Indeed, as highlighted in [137], "each of these solutions falls within the most desirable range of outcomes, but individually possesses its own advantages and disadvantages that would make it more or less favorable for further design development." The preferred design option (or options) sought by the designer is one that effectively balances all 3 objectives (PPD, EUI, Cost). Design configurations lying outside the circle of optimal solutions are not considered truly optimal because, while one or two objectives might be significantly optimized, others are adversely affected. For instance, the non-optimal solution

illustrated in fig. 5.27 exhibits commendable values in brightness and EUI, alongside a minimal cost value, yet at the expense of a compromised PPD.

Some of the criterion should be taken into consideration:

- **Balance:** Because the mechanics of the GA, The apex points of each fitness values would be always preserved for de-crowding computation. Yet, those solutions in apex, are too extreme in reality, being unpractical from the aspects of designers. So these solutions should be neglected by the secondary selection. In other words, balanced ones are preferred.
- **Sufficient daylight:** The GA will provide the extremely low WWR solutions, which are unacceptable in the office building. I.e. the larger windows are preferred.
- **High performance:** Since this research is technique-motivated, being encouraged by the EU commission, to obtain a sustainable performance is the goal. I.e. the better EUI performance solutions are preferred.

Chapter 6

Application

6.1 Test for the effectiveness of the optimization

6.1.1 General symmetric mapping

Although it's universally acknowledged that "machine makes no mistakes", we still want to test its accuracy. Overall the consistency of the inputs and outputs of the program need to be confirmed. Even though the model is very complicated not a input alone can judge an output, some relationships can be observed as the proof of the consistency, according to our common sense.

Here're some relation should be detected in the mapping.

- **WWR_N - cDA_N:** it should be positive correlation.
- **WWR_S - cDA_S:** it should be positive correlation.
- **Insulation Thickness - Heating Consumption:** it should be negative correlation.
- etc.

We've detected all these features in the matrix, so we can say, at least the optimization is conformed to our common sense.

6.1.2 Convergence

We have to make sure the results are already optimized enough. The algorithms operates in loop, so the exit condition needs to be considered, in case of a too early break-out. The optimized process can be detected from the variation of the results.

So in the beginning, we conducted a experiment with an iteration of 100, generation size of 20, in the environment of Torino. The result show in figs. 6.1 and 6.2.

Among them, we can confirm that the convergence is deeply completed. So these experiment settings are proved valid.



Figure 6.1: The variation of mean values



Figure 6.2: The variation of standard deviation

To evaluate the convergence, we have to analyze all the fitness values. In fig. 6.1, we can see the *TotEnergyConsump*, *Cost* shrinking quickly within 10 generations. While *PPD* converges slower, and get to the stable situation in around 20-30 generation.

On the other hand, in fig. 6.2 we can see SD varies in the process of iteration. The

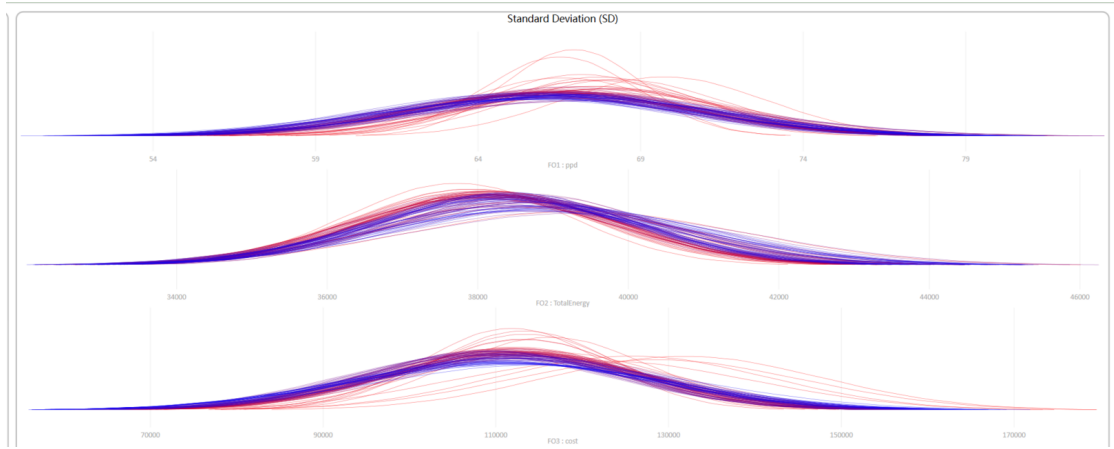


Figure 6.3: The distribution of standard deviation. It shows 0-9 generations in red color; and 50-99 generations in the gradient from red to blue. Among them we can observe the SD is growing wider, resulting in a richer range of genotypes.

SD doesn't vary significantly, specially the *PPD*. If a group of numbers, whose mean value and SD don't change a lot, we can predict the composition of these number are similar. And so do the genotypes, and we can say the evolution comes to an equilibrium. And in fig. 6.3, we can fell the pause of evolution. In general, 100 iterations are enough for optimizing the genes in our project.

6.1.3 Non-Fungible solutions

If all the solutions are fungible, the optimization become meaningless. Due to the de-crowding computation, usually the GA is keen on providing diverse solutions. However, if it constantly produce similar combinations, we can predict some mechanics are overwhelming the GA's de-crowding operation, which often indicates the object has a simple answer in math, e.g. use a rope to enclose as much area as it can, the answer is the more similar the surround shape to a circle, the larger area it can contain. We can answer this question, once it has an answer, it become meaningless for optimization. Only if the answer is hard or there's no a good-for-all answer, the multiple objects optimization algorithm makes sense.

On the other hand, the designers love to choose among diverse solution, which inspiring them with more perspectives.

The diversity of the genotypes can be easily detected by its being colored with different colors. Thankfully, we can observe that all the matrix are in kaleidoscope. So the diversity is no doubt.

6.1.4 Effectiveness of the CNV

We've conducted 2 times of the experiments, so that we could make comparisons among the controled variable. Specifically, during the second experiment, we have done 2 simulations on Torino, one is with *Smart CNV*, while other's without any operable windows. The windows are completely shut down during the summer, in order to test how effective the smart CNV system is. And by the comparison we can also measure the advance of the smart CNV system and test its performances under different climates.

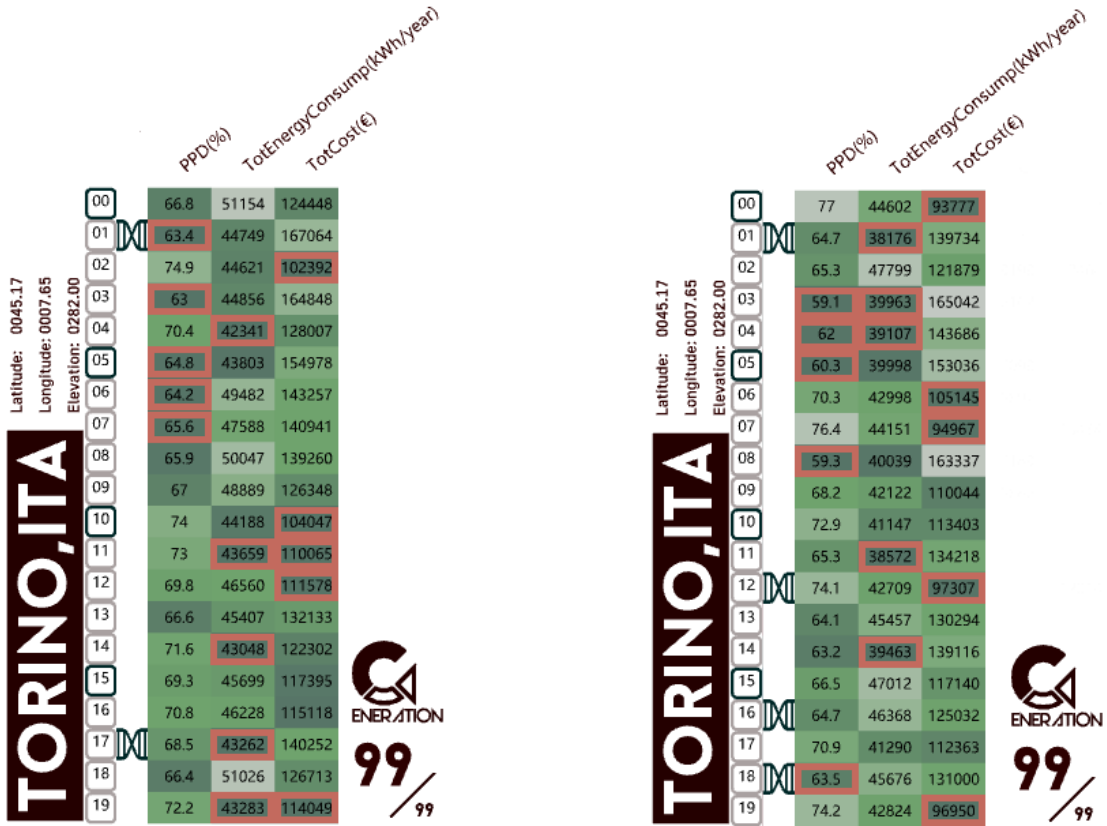


Figure 6.4: Red marks indicates the selected elite values from Gen.99 in Torino where the CNV is blocked on the left and activated on the right.

In analogy, in some cases of the second simulation, we dress the cute dogs with clothing, blocking the cutaneous respiration (breathing via skin), and then observe the direction of the evolution.

How to measure the effectiveness

The two groups of dogs are bread under controlled condition. And we will measure the final performance of each group. Obtained the final data, 6 KPIs are extracted to make comparison.

- General mean value of PPD
- General mean value of EUI
- General mean value of Cost
- Elite mean value of PPD
- Elite mean value of EUI
- Elite mean value of Cost

Mean value is selected as the key indicator as it represents the general performance of the final generation. However, due to the de-crowding mechanism inside the NSGA-II, the individual solution tends to go extreme in one specific performance while evolving. In this case, in order to estimate the top elites' performance, the high ranking solutions need to be measured. Hence, in each fitness value, (as in fig. 6.4) the top 5 solutions are extracted and summed up, which give the sense of the depth of the evolution trace.

Comparison by CNV

In figs. 6.5 and 6.6, EUI is in KWh, Cost is in Euro. CNV system globally benefits all the indicators. Also shown in fig. 6.7, CNV enhances the performances generally and also creates more diversity by benefiting the elites solutions. Furthermore, it actually present more pragmatic for designers. Since where without the CNV, in order to pursuit some Fitness Values, the solutions occur with extreme low WWR. Those solutions are impossible to go deeper otherwise it become a prison. When the CNV is introduced, the problem solved. Technically, it enhances the importance of the windows, so the solutions with larger WWR prevail. With a larger windows, the solutions look more like the human designs, helping to a better inspiration on designers.

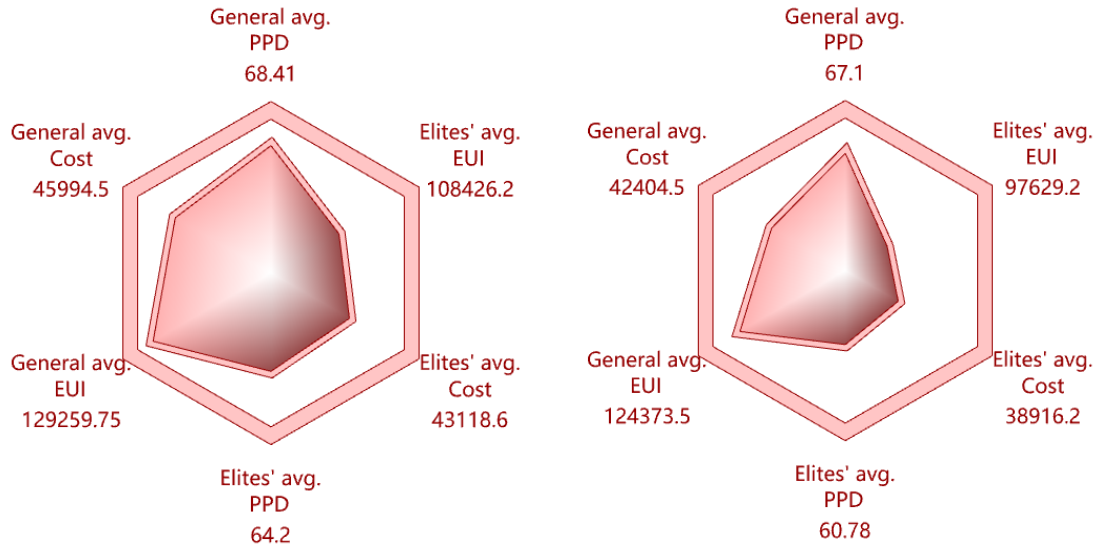


Figure 6.5: Performance of the system without CNV.

Figure 6.6: Performance of the system with CNV.

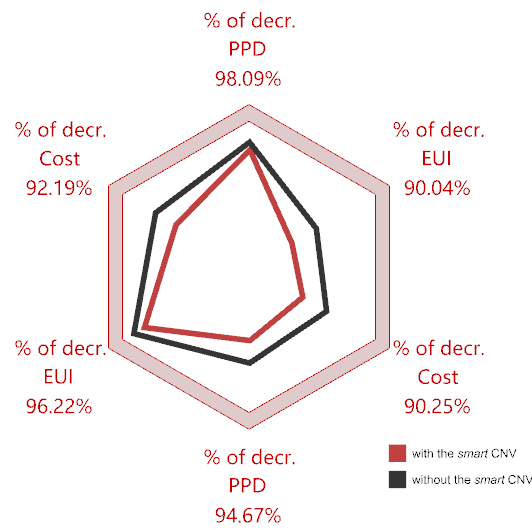


Figure 6.7: Ratio of decrement with the CNV system activated.

6.2 Oslo

A typical city around the North sea, a scenario for a cold European city. We choose it for its coldness. Also compare to §6.3 Kiev that also share the cold climate.

6.2.1 Climate

Latitude: 59°

Oslo, situated in the high-latitude region of Norway at approximately 59 degrees, experiences a climate influenced by both its high-latitude position and maritime conditions.

Classification: Dfb - Humid Continental Mild Summer, Wet All Year

According to the Köppen climate classification, Oslo's climate falls under the Dfb category (6A in ASHRAE), representing "Humid Continental Mild Summer, Wet All Year." The characteristics of high-latitude regions and the effects on sunlight play a significant role in Oslo's climate.

Basic climate graphics

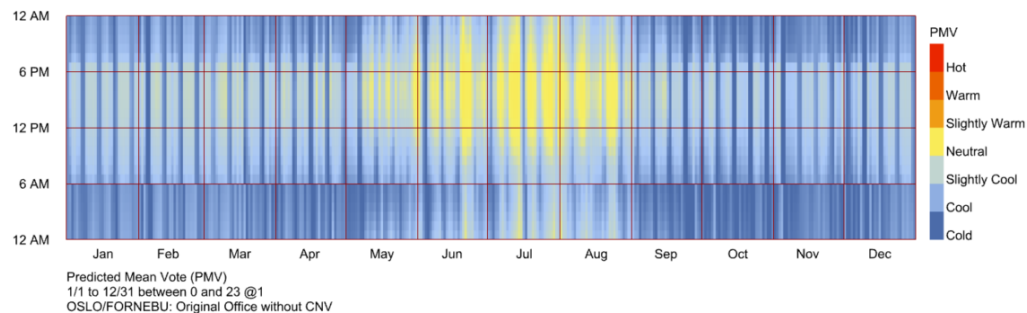


Figure 6.8: Oslo: the comfort metric of PMV.

General Description

In Oslo's climate, the high-latitude position results in substantial differences in daylight hours between summer and winter. During the summer, Oslo experiences longer daylight hours with higher solar elevations, leading to warmer temperatures ranging between 15-25 degrees Celsius. Additionally, due to its high-latitude

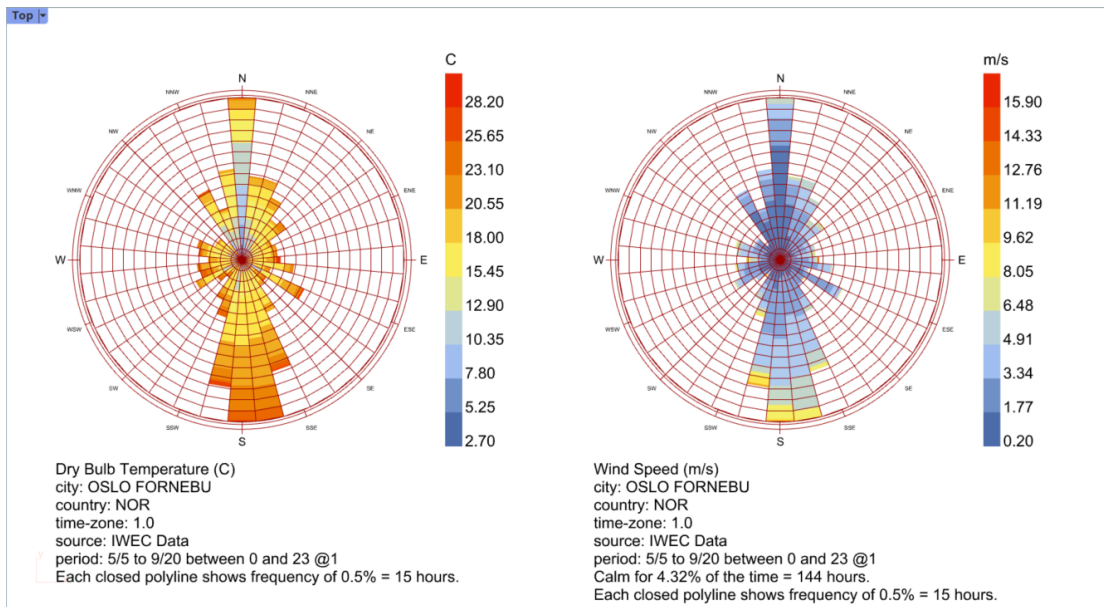


Figure 6.9: Oslo: wind rose

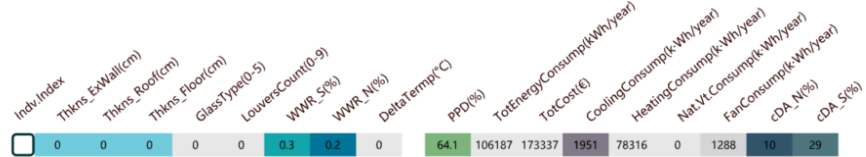


Figure 6.10: Oslo: original KPI

location, Oslo may also witness the phenomenon of "white nights" during the summer, where the sky remains bright even during nighttime. However, a strict room occupancy schedule, where lighting is activated only if someone is in the office, means that the "white night" doesn't benefit the DA. On the contrary, the high latitude makes the sunlight weaker, making DA harder to achieve.

6.2.2 Chromosome matrix display

	Indx	Thkns_ExWall(cm)	Thkns_Roof(cm)	Thkns_Floor(cm)	GlassType(0-5)	LouverCount(0-9)	WWR_S(%)	WWR_N(%)	DeltaTemp(C)	PPD(%)	TotEnergyConsump(kWh/year)	TotCost(E)	CoolingConsump(kWh/year)	HeatingConsump(kWh/year)	Nat.Vt.Consumer(kWh/year)	cDA(%)
OSLO,NOR	Latitude: 0059.9	Longitude: 0010.62	Elevation: 0017.00													
00	9	4	5	3	0	5	5	5	0	83.3	49447	100091	2389	21643	-2076	7
01	37	39	22	4	0	85	6	0	0.3	73.3	44668	177663	3431	15695	-6959	9
02	37	40	22	4	2	37	7	0	0	75.7	41805	155026	2329	14220	-4830	7
03	37	40	7	4	0	89	6	0.3	0.6	73.1	44921	167498	3522	15832	-7115	9
04	36	24	24	6	4	0	86	6	0	74.6	45502	153629	3428	16517	-6951	8
05	16	8	7	3	0	8	5	0	0.7	81.8	47230	104471	2348	19519	-2511	6
06	35	40	5	4	0	38	6	-0.7	0.6	75.6	42529	140667	2608	14594	-4690	9
07	24	13	5	3	0	5	6	0	0.6	80.2	45372	105396	2308	17748	-2414	8
08	24	25	6	3	0	7	6	0	0.6	78.4	43655	113762	2277	16100	-2743	8
09	10	26	5	3	0	5	5	0	0	79.4	44816	111046	2339	17164	-2287	6
10	14	7	5	3	0	5	5	0	0	82.2	47821	101441	2355	20090	-2173	6
11	9	7	5	3	0	5	5	0	0	82.6	48460	101052	2370	20698	-2121	6
12	32	25	5	4	0	46	5	0	0	76.3	43198	132365	2611	15250	-5205	7
13	24	39	6	3	0	7	6	0.6	0.6	77.4	42814	123484	2274	15279	-2776	7
14	36	39	6	5	0	13	6	0.5	0.5	76.6	42133	129844	2288	14593	-3374	9
15	36	39	5	3	0	13	6	0	0	77	42454	126711	2275	14923	-3282	9
16	31	39	6	5	0	73	6	0.5	0.5	73.9	43906	156764	3159	15279	-6498	8
17	8	6	5	3	0	5	5	0	0	83.1	49077	100884	2380	21289	-2089	6
18	33	25	6	4	0	7	6	0.6	0.6	77.9	43229	117177	2289	15668	-2809	9
19	36	25	5	4	0	11	6	0.6	0.6	77.7	43024	118551	2283	15474	-3202	8

Table 6.1: Oslo.Gen.99

	Indx	Thkns_ExWall(cm)	Thkns_Roof(cm)	Thkns_Floor(cm)	GlassType(0-5)	LouverCount(0-9)	WWR_S(%)	WWR_N(%)	DeltaTemp(C)	PPD(%)	TotEnergyConsump(kWh/year)	TotCost(E)	CoolingConsump(kWh/year)	HeatingConsump(kWh/year)	Nat.Vt.Consumer(kWh/year)	cDA(%)
OSLO,NOR	Latitude: 0059.9	Longitude: 0010.62	Elevation: 0017.00													
00	12	7	16	4	6	42	35	4.7	81.1	46727	129266	2427	18935	-2646	24	
01	7	27	4	1	3	89	63	2.9	87.4	60414	157761	2858	31811	-3893	57	
02	13	26	22	3	9	13	19	1.3	79.8	45062	134153	2231	17522	-2875	2	
03	33	9	24	1	8	80	52	3.3	85.5	54513	153749	2501	26455	-2600	29	
04	29	4	30	4	8	10	49	2.2	83.9	50259	142656	2335	22488	-2815	27	
05	13	40	22	2	4	62	63	1.8	80.6	46599	164333	2401	18823	-5108	54	
06	12	16	17	0	3	64	39	-0.1	84.8	53002	141739	2470	25005	-4642	41	
07	38	6	29	2	6	9	15	0.3	82.5	48180	130350	2286	20513	-2636	6	
08	6	15	18	1	9	79	73	0.3	86.8	57249	158653	2469	29158	-3523	37	
09	7	10	15	5	4	71	86	-0.3	80	47198	176164	2744	18995	-7922	61	
10	21	15	5	2	3	38	36	-1	81.4	47090	120873	2384	19325	-4227	38	
11	26	34	26	4	0	7	80	0.4	80.1	45698	162167	2331	18031	-4516	64	
12	35	21	11	0	1	37	45	1.2	80.9	50451	132205	3083	21795	-7618	53	
13	24	14	5	0	2	42	69	0.1	85.5	54356	133253	2446	26360	-4187	60	
14	8	34	30	1	9	60	78	3.2	86.1	55597	178625	2439	27585	-1935	42	
15	38	23	22	0	0	7	16	-0.6	80.2	45650	132036	2272	18056	-2765	22	
16	14	11	5	5	4	75	90	-0.3	79.4	46967	171839	2808	18694	-8131	61	
17	34	29	28	0	3	22	68	0.1	82.5	49984	154540	2517	22011	-6501	59	
18	6	28	20	1	0	53	26	0.3	83.8	51345	145266	2464	23393	-4753	36	
19	26	25	8	3	6	32	35	2.2	82.8	48646	138429	2307	20938	-2961	23	

Table 6.2: Oslo.Gen.00

6.2.3 Genotype analysis

Insulations

In Norway, thicker insulations are preferred. Roof and external wall insulations vary simultaneously, which is logical, as they serve a similar function of thermal isolation. Some floors stay around minimum values, which is a cost-effective strategy. However, some individuals use 22 cm of insulation, possibly for its thermal mass properties. In later generations, nearly half of the roof insulations reach the maximum of 39-40 cm, within the given range of 3-40 cm.

Glass Types

High-performance glass types are preferred.

Louvers Count

In Oslo's climate, louvers are unnecessary due to the lack of sunshine.

Window-Wall-Ratio

For the south facade, three strategies emerge: High ratio (70%-90%), covering 5 individuals out of 20; Medium ratio (35%-50%), covering 3 individuals; the rest are Low ratio (5%-15%). For the north facade, all the ratios are Low, with no exceptions.

Delta Temperature

Half of the individuals have a delta temperature of 0. Another 7 out of 20 have a delta temperature of 0.6, and 2 have a delta temperature of 0.3. One individual has a negative delta temperature of -0.7.

6.2.4 Phenotypes Analysis

Fitness Values

- **Energy Intensity:** The algorithm effectively optimizes the energy part, with values dropping significantly from about 60,000 to about 45,000 within 5 generations. For the following 95 generations, there is slight improvement.
- **Percentage of People Dissatisfied** Optimizing the PPD is more challenging, with values decreasing slowly. It takes 10 generations to reach 75%, and 20 generations to reach 73%, which is also the best value in the latest generation.

It's worth noting that Oslo's PPD is extremely high, indicating challenging weather conditions. Some solutions in the latest generations use thick insulation and consume over 17,000 kWh in heating, yet the PPD remains above 73%. This phenomenon is worth studying.

- **Cost:** In terms of cost, values range from 100,000 to 170,000 in the end game. This variation is reasonable, given that different prices lead to different combinations. The final cost is closely related to the south WWR, especially in Oslo, where the cost of glazing is much higher compared to opaque constructions. A larger south WWR also leads to higher consumption.

In terms of cost, values range from 100,000 to 170,000 in the end game. This variation is reasonable, given that different prices lead to different combinations. The final cost is closely related to the south WWR, especially in Oslo, where the cost of glazing is much higher compared to opaque constructions. A larger south WWR also leads to higher consumption.

Energy Performance

- **Cooling:** In Oslo, cooling is not a significant concern. However, there is an observable relation between cooling consumption and south WWR, ranging from 2,250 to 3,550 kWh.
- **Heating:** Heating is crucial in Oslo and constitutes over 80% of energy consumption. The value is inversely proportional to the thickness of insulation, ranging from 14,590 to 21,300 kWh.
- **Controlled Natural Ventilation:** With cooling being less necessary, the importance of natural also decreases.

Continuous Daylight Autonomy

Oslo's lack of sunlight results in all solutions performing poorly in this aspect, and they are quite homogeneous. There is little reference to draw from for our design.

6.2.5 Strategy

In the 99th generation, the solutions can be summarized into three strategies:

Cheap is the Key

This strategy sacrifices all other performance aspects to achieve the lowest cost. It may not be exciting for designers as it consistently chooses the cheapest solutions. Fortunately, it only occurs in 6 out of 20 of the population.

Open-Wide

With this strategy, the WWR on the south facade is high. It results in great PPD and considerably good energy consumption. It covers 4 out of 20 of the population. There is also an intermediate version named "Open-Up." It has a smaller WWR on the south facade, sacrificing PPD for better energy performance. "Open-Wide" and "Open-Up" together occupy 7 out of 20, offering an excellent option for designers looking to incorporate large windows.

Dimmy

This is a mainstream strategy, achieving a balance across all performance aspects. Although it wins the survival game in the simulation, it may not be popular among designers due to the darker interior conditions, which are rare in the 21st century. However, it can be a suitable choice for service rooms.

6.2.6 Selection from Human

I would recommend Generation 99, Individual 16 as my choice, which belongs to the "Open-Wide" strategy. In Oslo's climate, louvers are essentially useless. Setting the delta temperature to 0.5 is a good choice.

6.3 Kiev

6.3.1 Climate

Latitude: 50%

Kiev, located at approximately 50 degrees latitude, experiences a climate influenced by its moderate-latitude position and continental characteristics.

Classification: Dfb - Cool, Humid Continental (Warm Summer)

According to the Köppen climate classification, Kiev's climate falls under the Dfb category, representing "Cool, Humid Continental (Warm Summer)." The climate is characterized by marked seasonal variations.

Basic climate graphics

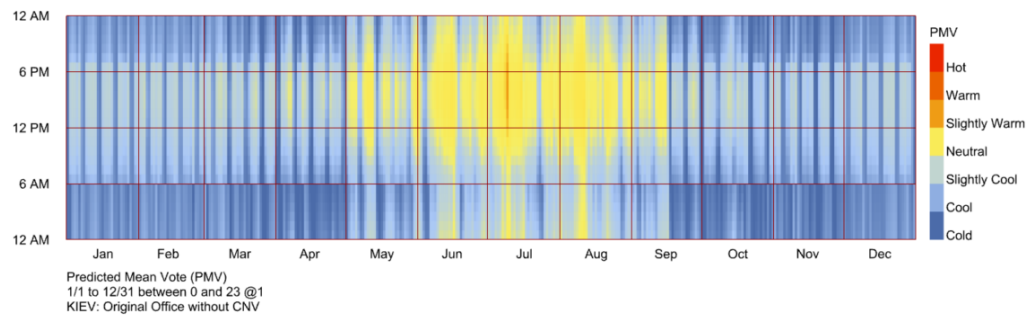


Figure 6.11: Kiev: the comfort metric of PMV.

General Description

In Kiev's climate, the moderate-latitude position results in distinct seasonal changes. Summers are characterized by warm temperatures, with daytime highs typically ranging between 25-30 degrees Celsius. The increased solar exposure due to the higher solar elevations during summer provides extended daylight hours for outdoor activities and showcases the city's historical and cultural attractions. Conversely, winters in Kiev are cold, with temperatures often dropping to -6 to -2 degrees Celsius. The city experiences shorter daylight hours and increased cloud cover during this season, contributing to a colder and darker atmosphere. Snowfall is common, transforming Kiev into a picturesque winter wonderland. Kiev's climate

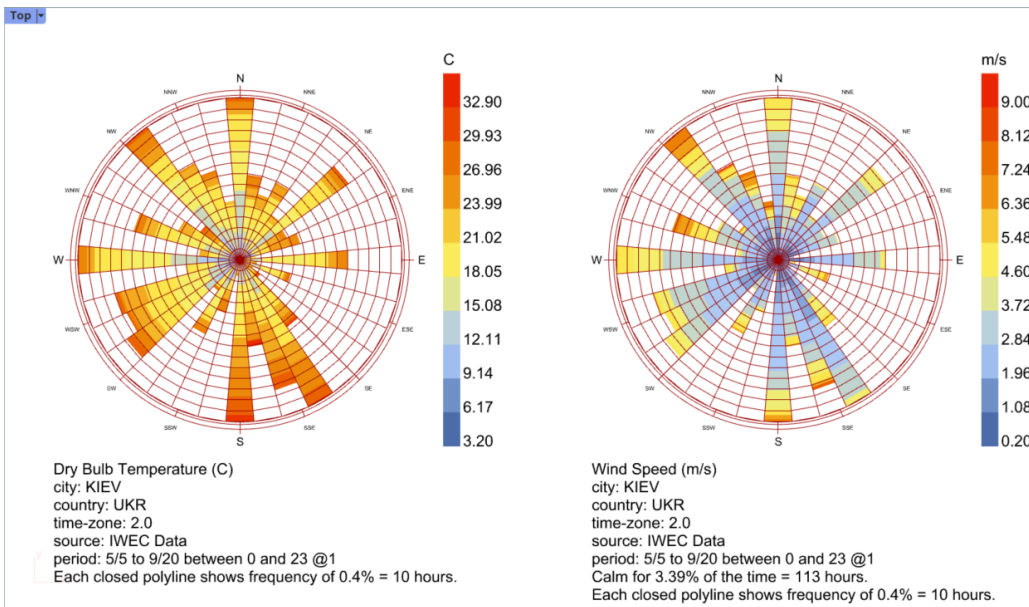


Figure 6.12: Kiev: wind rose

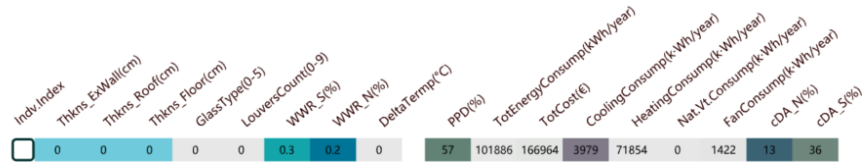


Figure 6.13: Kiev: original KPI

exhibits notable continental influences, with significant temperature fluctuations between summer and winter. This continental nature results in hot summers and cold winters. Additionally, the city's location on the Dnieper River, its proximity to the Black Sea, and the influence of the Mediterranean region contribute to the moderation of temperature extremes. This maritime influence helps keep Kiev milder during the winter months compared to other continental regions at a similar latitude.

6.3.2 Chromosome matrix display

	Indv_Index	Thkns_ExWall(cm)	Thkns_Roof(cm)	Thkns_Floor(cm)	GlassType(0-5)	LowersCount(-9)	WWR_Si(%)	WWR_N(%)	DeltaTemp(°C)	PPD(%)	TotEnergyConsump(kWh/year)	TotCost(€)	CoolingConsump(kWh/year)	HeatingConsump(kWh/year)	Nat.Vt.Consump(kWh/year)	cDA(%)
00	39	40	9	5	0	77	20	0.2	68.4	43794	167246	4434	13855	-6616	35	
01	17	27	9	0	0	86	6	-0.2	71.8	54332	141426	7315	20798	-6722	11	
02	20	4	4	2	0	8	6	2	81.6	49796	102241	3583	20739	-2219	10	
03	39	40	10	4	4	36	18	0.8	73.3	42253	149276	3117	13859	-4685	18	
04	39	39	6	5	4	86	18	0.6	69.8	43749	168342	4192	14089	-6255	18	
05	20	4	4	0	0	8	6	2	81.3	50239	102034	3815	20910	-2361	11	
06	19	27	9	5	0	86	18	0.8	69.3	45112	159638	4695	14846	-6799	32	
07	20	5	7	0	0	57.0	7	0.6	75.9	52503	116068	5716	20913	-5923	12	
08	20	31	7	5	0	61	14	0.6	70.8	43858	146978	4104	14299	-5726	25	
09	20	5	9	2	0	6	6	2	79.8	47997	104579	3661	18868	-1855	10	
10	20	31	6	0	0	86	14	0.6	71.7	53954	142207	7096	20676	-7972	26	
11	32	5	7	0	0	32	9	3	77.5	49625	110782	4569	19442	-4346	16	
12	22	5	11	0	0	53	7	0.6	74.8	50922	117134	5510	19605	-5731	12	
13	32	5	10	5	0	33	7	2	78.7	47669	122287	3766	18439	-4014	12	
14	20	5	11	0	0	61	9	0.6	74.5	51974	119541	5858	20225	-6385	16	
15	39	40	10	0	4	10	18	0.8	77.4	45148	134475	3181	16633	-3218	17	
16	20	5	11	2	0	8	6	2	79.2	47252	105740	3576	18236	-2114	10	
17	32	37	10	5	0	33	7	2	72.8	43315	141132	3756	14164	-3822	12	
18	22	28	9	0	0	53	6	0.6	72.4	49426	131156	5587	18042	-5537	11	
19	38	38	9	0	0	32	9	2	73.1	46172	134712	4502	16115	-4694	16	




Table 6.3: Kiev.Gen.99

6.3.3 Genotype Analysis

Insulations

The insulation of the roof differs from that of the exterior wall. Floors have a minimal insulation thickness. The thickness of the wall primarily falls into three ranges: 20, 30, and 38 cm, with no exceptions. Roof insulation thickness concentrates in three ranges: 40, 30, and 5 cm, with no exceptions. The thickness of the floor remains around 7 cm, indicating no need for thermal mass. It's worth noting that many solutions exhibit synchronicity between wall and roof insulation, either both at their highest or lowest levels.

Glass Types

Glass types are selected within the range of 0 to 5, reflecting diverse glazing choices. High-class glass significantly benefits energy performance.

	Indv.Index	Thkns_ExWall(cm)	Thkns_Roof(cm)	Thkns_Floor(cm)	GlassType(0-5)	LouversCount(0-9)	WWR_S(%)	WWR_N(%)	DeltaTemp(°C)	PPD(%)	TotEnergyConsump(kWh/year)	TotCost(€)	CoolingConsump(kWh/year)	HeatingConsump(kWh/year)	Nat.Vt.Consump(kWh/year)	cDAT(%)
00	12	7	16	4	6	42	35	4.7	78.4	46880	129328	3530	17946	-2765	29	
01	7	27	4	1	3	89	63	2.9	85	59943	156203	4457	29701	-3650	67	
02	13	26	22	3	9	13	19	1.3	78.1	45346	134475	3056	16965	-3073	2	
03	33	9	24	1	8	80	52	3.3	83.6	54518	153203	3709	25228	-2710	40	
04	29	4	30	4	8	10	49	2.2	82.1	50325	142678	3396	21468	-3317	36	
05	13	40	22	2	4	62	63	1.8	77.4	46414	163276	3462	17547	-5126	65	
06	12	16	17	0	3	64	39	-0.1	82.3	52604	140620	3635	23424	-4589	53	
07	38	6	29	2	6	9	15	0.3	80.9	48397	130574	3252	19743	-2759	7	
08	6	15	18	1	9	79	73	0.3	85	57236	158114	3694	27897	-3665	50	
09	7	10	15	5	4	71	86	-0.3	75.2	46527	174214	3991	17051	-7715	72	
10	21	15	5	2	3	38	36	-1	78.6	46741	119775	3310	18046	-4258	47	
11	26	34	26	4	0	7	80	0.4	77.4	45805	162238	3437	16981	-4535	75	
12	35	21	11	0	1	37	45	1.2	76.1	49492	130106	4513	19372	-7303	63	
13	24	14	5	0	2	42	69	0.1	84.5	56482	135188	3778	27070	-4382	71	
14	8	34	30	1	9	60	78	3.2	84.6	55843	178341	3619	26625	-2241	52	
15	38	23	22	0	0	7	16	-0.6	78.5	46228	132542	3293	17564	-2451	29	
16	14	11	5	5	4	75	90	-0.3	74.4	46264	169700	4080	16690	-7946	72	
17	34	29	28	0	3	22	68	0.1	78.8	49375	153029	3745	20141	-6606	69	
18	6	28	20	1	0	53	26	0.3	81.1	50869	144184	3588	21778	-4675	45	
19	26	25	8	3	6	32	35	2.2	80.9	48658	137993	3276	19962	-3495	32	

Table 6.4: Kiev.Gen.00

Louvers Count

The louvers' count varies between 0 and a few 4. Louvers with a count of 4 are present in only 2 out of 20 solutions, and they are typically associated with higher-cost luxury solutions.

Window-Wall-Ratio

The window-wall ratio for the south facade varies from 6% to 86%. The values exhibit significant variability and tend to cluster around 85%, 55%, 35%, and 10%. The window-wall ratio for the north facade ranges from 6% to 20% and falls into two main distribution ranges, with some solutions having high ratios around 18% and others with low ratios around 7%. No synchronicity is observed between the two window-wall ratios, and they vary independently.

Delta Temperature

Delta temperature values range from -0.2°C to 3°C. Notably, 10 out of 20 solutions have a delta temperature of approximately 0.6°C, while 8 out of 20 have values around 2°C. One solution features a negative delta temperature of -0.2°C, and

another has a delta temperature of 0.2°C. Solutions with a delta temperature of around 2°C tend to have lower window-wall ratios.

6.3.4 Phenotypes Analysis

Fitness Values

- **PPD (Predicted Percent of Dissatisfied):** PPD varies from 68% to 82%. The optimal PPD is achieved with large south-facing windows, high-class glazing, and thick insulation. However, increasing the window-to-wall ratio to 77% reduces PPD by 5%. Sunlight is crucial, and maximizing it during winter leads to better PPD.
- **Energy Consumption:** Energy consumption ranges from 42,000 to 55,000 kWh. Solutions achieving lower energy consumption values (e.g., 42,250 kWh) often employ louvers and maintain a 36% window-to-wall ratio for the south facade.
- **Cost:** Costs range from 102,000 to 170,000 euros. Economic solutions frequently involve trade-offs between PPD and energy performance. Solutions balancing the two prioritize maximizing the benefits of sunlight while managing costs. These balance-oriented solutions avoid prison-like room conditions.

Energy Performance

- **Cooling:** In Kiev, cooling consumption varies from 3,100 to 7,100 kWh. Large windows with low-class glazing result in higher cooling consumption, while small windows or high-class glazing lead to lower consumption.
- **Heating:** Heating is crucial in Kiev and constitutes over 80% of energy consumption. The value is inversely proportional to the thickness of insulation, ranging from 14,590 to 21,300 kWh.
- **Controlled Natural Ventilation:** With reduced cooling needs, the importance of natural ventilation also decreases.

Continuous Daylight Autonomy

Kiev's limited sunlight leads to consistently poor solutions, with little room for improvement.

6.3.5 Strategy

In the 99th generation, solutions fall into three main strategies:

Cost-Oriented Strategy

This strategy prioritizes cost savings but may not inspire designers as it consistently chooses the cheapest solutions.

Winter-Oriented Strategy

Characterized by large window-to-wall ratios, thick insulations, and high-class glazing, this strategy aims to maximize warmth in winter while maintaining low heating consumption.

Energy-Oriented Strategy

Solutions following this strategy exhibit superior performance in both cooling and heating. Notably, louvers play a significant role in reducing cooling consumption.

Balance Strategy

This strategy strikes a balance across all performance aspects, focusing on priorities such as wall insulation, glazing class, louvers, and window-to-wall ratios, while keeping costs in check.

6.3.6 Selection from Human

Given the high heating demand during winter and abundant sunlight, maximizing the use of winter sunlight is key. The optimal choice is a PPD-oriented strategy. Solutions within this strategy feature large south-facing windows and the highest class of glazing to ensure the best PPD during winter.

6.4 Rome

A distinctive city in the southern part of Europe, representing a Mediterranean climate. It is selected for its mild temperatures, offering a contrast to the colder climates of cities like Oslo and Kiev.

6.4.1 Climate

Latitude: 41°

Rome, located at approximately 41 degrees latitude, enjoys a Mediterranean climate characterized by mild, wet winters and hot, dry summers.

Classification: Cfa

According to the Köppen climate classification, Rome's climate falls under the Cfa category (3A inASHRAE), representing "Temperate, No dry season, Hot summer." The city experiences long, hot summers and mild, wet winters.

Basic climate graphics

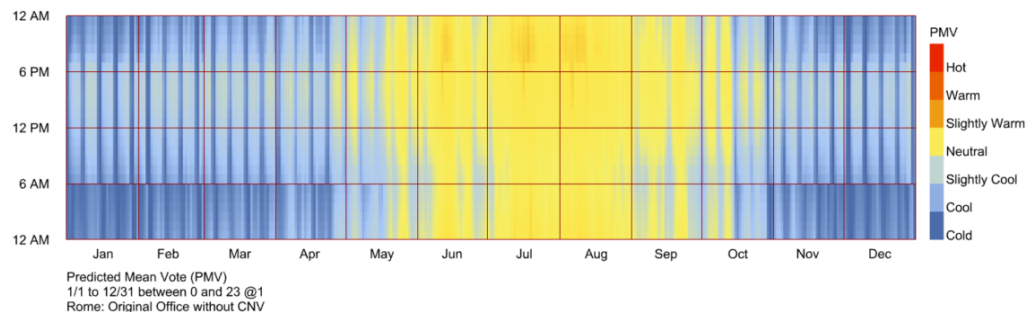


Figure 6.14: Roma: the comfort metric of PMV.

General Description

Rome's climate is marked by its proximity to the Mediterranean Sea, influencing its weather patterns. The city enjoys a Mediterranean climate, with mild temperatures, ample sunlight, and moderate rainfall. The Mediterranean Sea acts as a thermal regulator, moderating temperature extremes and contributing to the overall pleasant weather.

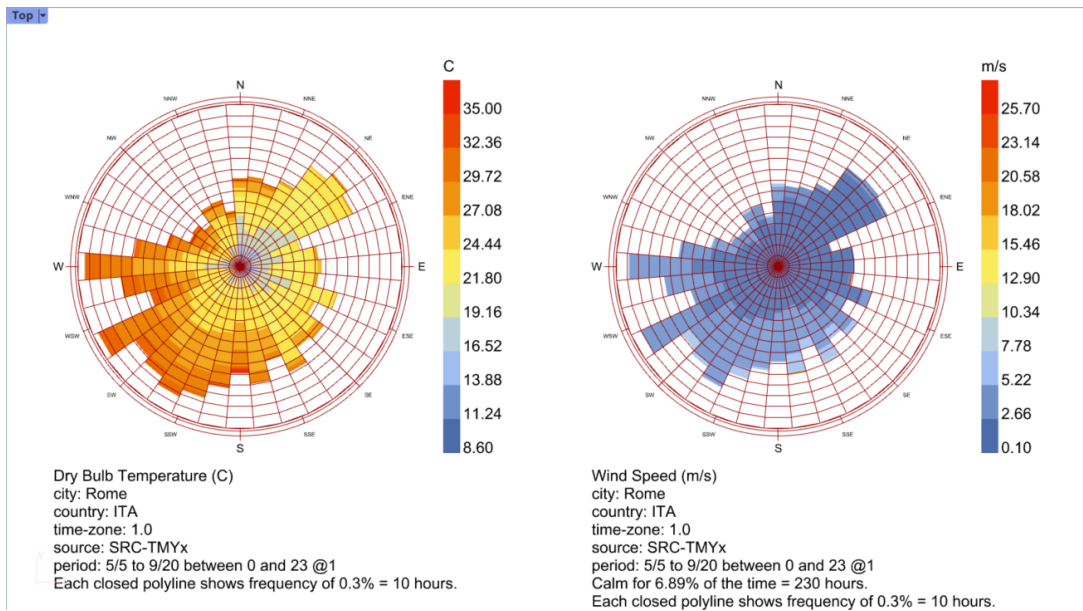


Figure 6.15: Roma: wind rose

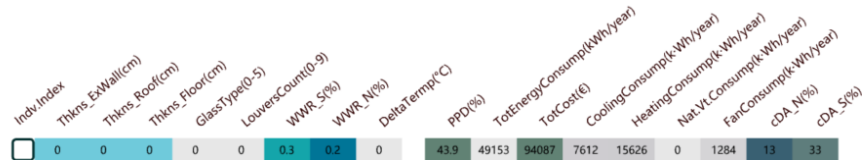


Figure 6.16: Roma: original KPI

In this climate, heating needs are generally low due to mild winter temperatures, rarely dropping below 10 degrees Celsius. Summers, on the other hand, can be hot, with temperatures ranging from 25-35 degrees Celsius. The demand for cooling systems is notable during the summer months, making effective cooling strategies an essential consideration in building design.

6.4.2 Chromosome matrix display

Indx-Index	Thkns_EWall(cm)	Thkns_Roof(cm)	Thkns_Floor(cm)	GlassType(0-5)	LouversCount(0-9)	WWR_S(%)	WWR_N(%)	DeltaTemp(C)	PPD(%)	TotEnergyConsump(kWh/year)	TotCost(E)	CoolingConsump(kWh/year)	HeatingConsump(kWh/year)	Nat_Vt_Consump(kWh/year)	FanConsump(kWh/year)	cDA_N(%)	cDA_S(%)	EquipConsump (k-Wh/year)
00	8	3	3	0	0	33	15	-0.9	47.4	39265	87123	8912	4675	-865	1047	17	56	14789
01	7	3	3	4	4	46	42	0.3	52.6	37060	115233	7020	4567	-3310	842	33	54	
02	8	3	3	0	0	90	17	-0.1	40.1	44216	103574	13431	4383	-1806	1772	20	78	
03	7	3	3	1	0	32	19	1.4	59.2	38543	87842	6921	6130	-2123	861	22	55	
04	7	11	3	4	0	90	90	-0.7	38.4	38830	161179	9789	3268	-3657	1142	65	79	
05	7	3	3	4	3	37	35	0.3	53.9	37293	108235	7029	4786	-2905	847	30	51	
06	6	3	3	0	0	66	15	-0.2	41.1	41837	95895	11477	4325	-1630	1404	17	72	
07	11	3	3	5	0	64	89	0.3	42.8	37812	141897	8652	3516	-4430	1012	65	72	
08	12	3	3	5	0	81	90	0.3	39.6	38373	150513	9328	3325	-4600	1088	65	77	
09	14	3	3	0	0	41	22	-0.4	44.8	39681	90553	9452	4486	-1770	1111	25	61	
10	13	4	3	0	0	55	22	0	42.1	40786	95050	10540	4346	-2201	1261	25	69	
11	7	11	3	4	0	89	90	-0.7	38.5	38787	160684	9746	3273	-3655	1136	65	78	
12	12	11	6	4	0	55	88	-0.7	44.9	37667	146311	8391	3664	-3416	981	65	69	
13	8	4	3	4	0	89	17	-0.1	40.8	38884	127465	9362	3803	-2556	1086	19	78	
14	7	3	3	1	0	42	18	1.4	57.9	38535	89830	7123	5988	-2248	882	20	62	
15	12	3	3	0	0	81	18	0.1	40.3	43290	101550	12678	4353	-2089	1628	20	77	
16	12	9	6	4	0	55	25	0.2	46.9	37600	120112	7935	4105	-2900	929	28	68	
17	4	3	3	0	0	81	14	-0.1	40.4	43366	100292	12733	4371	-1617	1630	16	77	
18	7	3	3	4	4	88	18	0.2	44.1	38146	126859	8503	4023	-2847	989	12	71	
19	7	3	3	4	0	47	15	-0.4	51.6	37935	96281	7661	4729	-1692	914	17	65	

C
ENERATION
99 / **99**

Table 6.5: Roma.Gen.99

Indx-Index	Thkns_EWall(cm)	Thkns_Roof(cm)	Thkns_Floor(cm)	GlassType(0-5)	LouversCount(0-9)	WWR_S(%)	WWR_N(%)	DeltaTemp(C)	PPD(%)	TotEnergyConsump(kWh/year)	TotCost(E)	CoolingConsump(kWh/year)	HeatingConsump(kWh/year)	Nat_Vt_Consump(kWh/year)	FanConsump(kWh/year)	cDA_N(%)	cDA_S(%)	EquipConsump (k-Wh/year)
00	12	7	16	4	6	42	35	4.7	58.5	39065	118246	7590	5899	-893	945	21	42	14789
01	7	27	4	1	3	89	63	2.9	58.2	40792	129282	8419	6677	-1681	1065	51	74	
02	13	26	22	3	9	13	19	1.3	62.5	39424	126244	6796	7132	-1292	865	3	3	
03	33	9	24	1	8	80	52	3.3	62.2	40217	133207	7449	7183	-1426	954	27	57	
04	29	4	30	4	8	10	49	2.2	62.2	39567	127784	6983	7066	-1771	887	25	2	
05	13	40	22	2	4	62	63	1.8	55.3	37849	150924	7166	5173	-3457	878	48	63	
06	12	16	17	0	3	64	39	-0.1	58.6	38951	121396	7192	6233	-2471	895	34	66	
07	38	6	29	2	6	9	15	0.3	62.9	40016	118944	7111	7363	-505	911	6	2	
08	6	15	18	1	9	79	73	0.3	63.4	39705	133408	6659	7557	-3123	857	36	54	
09	7	10	15	5	4	71	86	-0.3	45.4	37528	161232	8197	3736	-3991	964	57	67	
10	21	15	5	2	3	38	36	-1	57.7	37753	107164	6731	5569	-1800	821	31	52	
11	26	34	26	4	0	7	80	0.4	60.5	39505	153320	7434	6507	-2076	932	62	17	
12	35	21	11	0	1	37	45	1.2	47.3	39770	116417	9184	4854	-3288	1101	44	57	
13	24	14	5	0	2	42	69	0.1	61.3	39415	111511	6911	6997	-2728	875	56	57	
14	8	34	30	1	9	60	78	3.2	65.2	40639	157124	6931	8175	-1518	901	39	44	
15	38	23	22	0	0	7	16	-0.6	62.9	40261	124373	7308	7387	53	934	18	18	
16	14	11	5	5	4	75	90	-0.3	44.5	37633	157410	8364	3657	-4071	981	58	68	
17	34	29	28	0	3	22	68	0.1	56.6	39795	139974	8113	6045	-2644	1006	53	33	
18	6	28	20	1	0	53	26	0.3	57.1	38650	127154	7280	5842	-2324	898	29	68	
19	26	25	8	3	6	32	35	2.2	60.8	38006	123199	6255	6339	-2622	781	21	32	

C
ENERATION
00 / **99**

Table 6.6: Roma.Gen.00

6.4.3 Genotype Analysis

Insulations In Roma, insulation thickness for external walls ranges from 4 to 14 cm, with an average of approximately 8 cm. Roof insulation varies between 3 and 11 cm, averaging around 4.5 cm. Floor insulation is consistently at 3 cm.

Generally speaking all kinds of the insulations stay in the lowest value, no exceptions. We can see within the original 15 generations, the thicker insulations significantly decreases. After the 15 generation, the insulation stays in this "lowest state". Although this can be explained by its hot climate, however, compared to §6.5, and the other 2 hotter climtes §§6.8 and 6.9 this is unique, and it worth a further research.

Glass Types Roma's glass types varies. From type 0 to type 5 are all selected in specific solution. Not a dominating type is discovered.

Louvers Count Louvers count varies from 0 to 4. The majority of individuals have a louvers count of 0, and there is a smaller cluster around 4.

Window-Wall-Ratio

- *WWR south:* The Window-Wall-Ratio on the south facade varies across individuals, ranging from 32% to 90%. The distribution reveals three clusters, with the majority falling into Low ratio (32%-41%), followed by Medium ratio (46%-55%), and a smaller group in High ratio (81%-90%).
- *WWR nouth:* For the north facade, WWR values show a wider distribution. The clusters are more evenly spread, with individuals in Low ratio (14%-22%), Medium ratio (35%-42%), and High ratio (88%-90%).

To summarize, WWR are preferred in a large ratio in Roma. Compared to §6.5, which the WWR are also extremely high, the large ratio are preferred among the typical Mediterranean climate. While comparing to the hotter climate §§6.8 and 6.9, a middle ratio (around 35%) are preferred.

Delta Temperature The distribution of delta temperatures shows a diverse range, with values ranging from -0.9 to 1.4°C.

6.4.4 Phenotype Analysis

Fitness Values

- **Energy Intensity:** The algorithm optimizes the EUI while making it diversely, the beginning generations are more concentrated. But the absolute value decreases just by 1000 kWh, from the first to last. In the end, it ranges from 37000 to 44000 kWh.
- **Percentage of People Dissatisfied:** Optimizing PPD effectively drops. PPD values range from 38.4% to 59.2%.
- **Cost:** In terms of cost, values range from 87,123 to 161,179 in the end game. This variation is reasonable, given that different prices lead to different combinations. The final cost is closely related to the south WWR, especially in Roma, where the cost of glazing is much higher compared to opaque constructions. A larger south WWR also leads to higher consumption.

Energy Performance

- **Cooling:** In Roma, cooling is not a significant concern, with consumption ranging from 7,020 to 13,431 kWh, correlating with the glass type since all the WWR are significantly high.
- **Heating:** Heating is crucial in Roma, constituting a significant portion of energy consumption. Values are inversely proportional to insulation thickness, ranging from 3,268 to 6,130 kWh.
- **Controlled Natural Ventilation:** With reduced cooling needs, the importance of natural ventilation also decreases.
- **Fan:** Fan, namely, mechanical ventilation, is highly correlated to the cooling, they vary simultaneously.

Continuous Daylight Autonomy

- **cDA South:** On the south facade, cDA values are distributed around 55%, 65%, and 75%. The average cDA for the south facade is approximately 63.7%. Certainly, it's highly correlated to WWR_North, and even with a lowest WWR_S (32%), the cDA is 56% considerably good.
- **cDA North:** Roma's ample sunlight results in homogeneous solutions for cDA on the north facade, with values distributed around 17%, 30%, and 65%. And certainly, it's highly correlated to WWR_North.

This consolidated analysis provides a comprehensive overview of both genotype and phenotype aspects in Roma. If you have further instructions or adjustments, feel free to let me know!

6.5 Palermo

A distinctive city surrounded by the Mediterranean Sea, presenting a scenario for a temperate European city with hot summers. We selected Palermo for its temperate climate, contrasting with the cold climate of §6.2 Oslo and similar to §6.4 Rome.

6.5.1 Climate

Latitude: 38°

Palermo, located in the lower-latitude region of Italy at approximately 38 degrees, encounters a climate shaped by its moderate latitude and Mediterranean surroundings.

Classification: Cfa - Temperate, No Dry Season, Hot Summer

In accordance with the Köppen climate classification, Palermo falls into the Cfa category (3A in ASHRAE), signifying "Temperate, No Dry Season, Hot Summer." The impact of its latitude and the Mediterranean environment contributes significantly to Palermo's climate.

Basic climate graphics

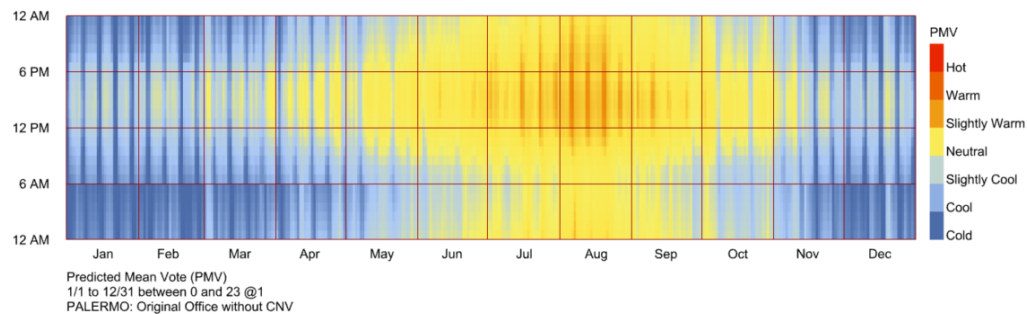


Figure 6.17: Palermo: the comfort metric of PMV.

General Description

In Palermo's unique climate, characterized by its island identity and proximity to the Mediterranean, the city showcases a distinctive blend of influences. Surrounded by the azure waters of the Mediterranean Sea, Palermo benefits from the moderating

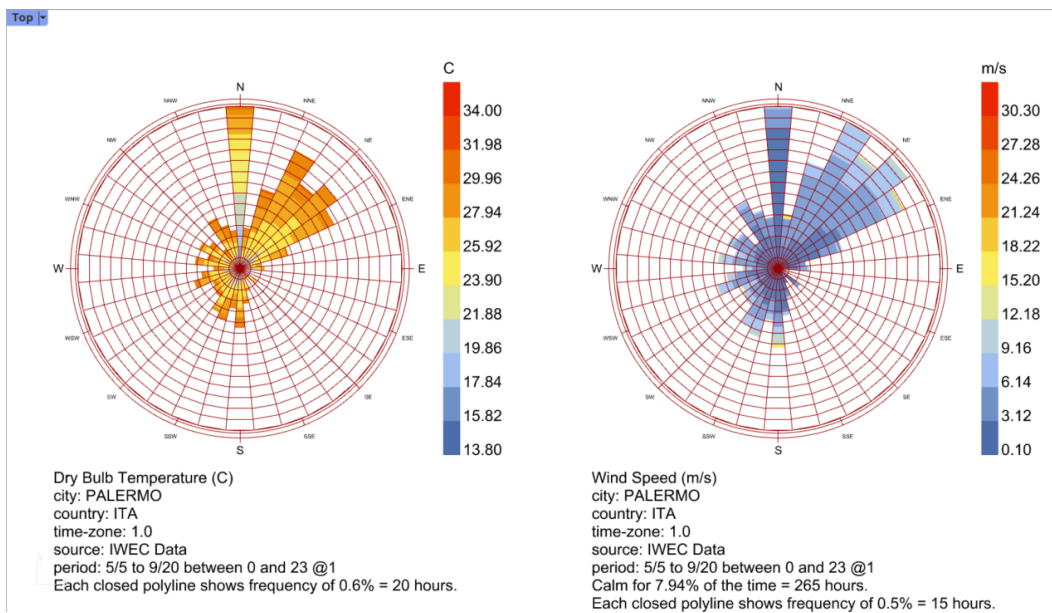


Figure 6.18: Palermo: wind rose

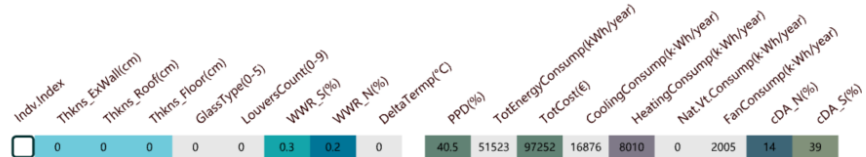


Figure 6.19: Palermo: original KPI

effect of the sea, leading to milder temperature fluctuations. Being an island city, Palermo experiences a certain climatic stability, with the Mediterranean Sea acting as a thermal regulator, providing warmth in winter and cooling breezes in summer. This island identity, coupled with its temperate climate, results in a harmonious balance conducive to comfortable living. The interplay between land and sea in Palermo's climate contributes to the city's vibrant energy. During the summer, the sea exerts a tempering influence, preventing extreme heat, while in winter, it retains warmth, preventing harsh cold. This delicate dance of nature not only defines Palermo's climate but also influences architectural and lifestyle choices, emphasizing the seamless integration of the city with its natural surroundings. Palermo's daylight characteristics, influenced by its latitude and maritime setting, contribute to a pleasant and well-lit environment. The extended daylight hours during summer, combined with the city's cultural and architectural richness, create

a unique ambiance. The Mediterranean allure enhances the DA, making it an inherent and advantageous feature for sustainable and energy-efficient building designs in Palermo.

6.5.2 Chromosome matrix display

	Indiv-Index	Thkns_EWall(cm)	Thkns_Roof(cm)	Thkns_Floor(cm)	GlassType(0-5)	LouversCount(0-9)	WWR_S(%)	WWR_N(%)	DeltaTemp(°C)	PPD(%)	TotalEnergyConsump(kWh/year)	TotalCost(€)	CoolingConsump(kWh/year)	HeatingConsump(kWh/year)	Nat.Vt.Consump(kWh/year)	zDA(%)
Latitude:	0038.17															
Longitude:	0013.1															
Elevation:	0034.00															
PALERMO,ITA	00	38	39	4	2	9	20	22	0.6	29.1	35512	123524	9337	652	332	6
	01	11	7	5	0	6	19	11	0.5	35.2	37282	89276	10282	1380	744	3
	02	12	4	3	0	0	8	9	-0.6	32.9	38570	83088	11626	1199	2451	17
	03	39	39	26	4	0	77	86	-0.7	15.6	41312	199483	15078	189	5854	84
	04	6	40	7	0	1	47	65	0.5	20	42378	130382	15818	390	661	81
	05	10	11	5	0	2	32	11	0.5	23.4	39011	94915	12636	563	913	16
	06	39	39	24	4	0	71	25	-0.9	16.6	39918	172909	13812	203	5636	47
	07	35	7	5	5	1	42	17	0.5	24.6	38169	114144	11865	565	633	31
	08	38	5	4	2	0	52	21	-0.9	26.8	38630	102288	12176	679	4902	40
	09	38	34	5	2	1	44	22	-0.4	23.6	36524	126319	10536	383	2037	40
	10	35	5	26	5	0	46	74	-0.4	17	38664	152674	12668	217	2596	83
	11	39	39	24	4	0	72	86	-0.9	15.6	41425	196039	15127	188	7771	84
	12	34	36	26	5	0	72	74	0.6	15.9	40165	189008	14029	196	173	83
	13	38	6	4	2	1	52	21	0.6	29.3	37814	107378	11287	825	364	38
	14	39	34	28	5	1	21	26	-0.4	22.4	36544	147696	10606	330	1927	46
	15	36	7	5	0	1	42	17	0.5	22.4	40806	100964	14303	509	990	30
	16	39	6	4	2	1	72	21	0.7	28.4	38504	113961	11939	794	284	37
	17	38	40	26	4	0	52	86	-0.9	16.5	39998	188820	13835	210	6848	84
	18	39	31	5	5	1	44	26	-0.4	18.3	37605	136499	11677	240	2264	46
	19	39	39	27	4	1	51	25	-0.9	17.5	38315	165173	12343	217	4765	45

Table 6.7: Palermo.Gen.99

	Indiv-Index	Thkns_EWall(cm)	Thkns_Roof(cm)	Thkns_Floor(cm)	GlassType(0-5)	LouversCount(0-9)	WWR_S(%)	WWR_N(%)	DeltaTemp(°C)	PPD(%)	TotalEnergyConsump(kWh/year)	TotalCost(€)	CoolingConsump(kWh/year)	HeatingConsump(kWh/year)	Nat.Vt.Consump(kWh/year)	zDA(%)
Latitude:	0038.17															
Longitude:	0013.1															
Elevation:	0034.00															
PALERMO,ITA	00	12	7	16	4	6	42	35	4.7	30	38562	117369	11856	897	-39	35
	01	7	27	4	1	3	89	63	2.9	34.8	41638	130074	13929	1660	-275	77
	02	13	26	22	3	9	13	19	1.3	30.2	36084	121596	9735	781	36	4
	03	33	9	24	1	8	80	52	3.3	33.5	39083	131394	11947	1314	-127	42
	04	29	4	30	4	8	10	49	2.2	34.8	37891	125469	10876	1326	-310	41
	05	13	40	22	2	4	62	63	1.8	24.5	38075	150975	11828	487	-273	73
	06	12	16	17	0	3	64	39	-0.1	29.2	38225	120042	11616	878	1774	56
	07	38	6	29	2	6	9	15	0.3	33.4	36943	114700	10179	1158	920	9
	08	6	15	18	1	9	79	73	0.3	34.3	38029	130873	10974	1363	779	56
	09	7	10	15	5	4	71	86	-0.3	19.9	39595	163796	13398	330	2511	81
	10	21	15	5	2	3	38	36	-1	25.8	37222	106299	11023	532	4892	51
	11	26	34	26	4	0	7	80	0.4	26.5	37127	150147	10940	524	486	83
	12	35	21	11	0	1	37	45	1.2	20.1	40640	117346	14259	392	-167	70
	13	24	14	5	0	2	42	69	0.1	31	37844	108808	11117	1038	1106	81
	14	8	34	30	1	9	60	78	3.2	36.6	38690	154134	11287	1637	-118	60
	15	38	23	22	0	0	7	16	-0.6	30	36498	119043	10133	765	2027	31
	16	14	11	5	5	4	75	90	-0.3	19.2	39819	159848	13626	305	2569	81
	17	34	29	28	0	3	22	68	0.1	23.3	38809	138508	12503	502	1167	78
	18	6	28	20	1	0	53	26	0.3	27.7	38059	126052	11570	761	937	49
	19	26	25	8	3	6	32	35	2.2	32.3	37176	121787	10516	1013	-280	34

Table 6.8: Palermo.Gen.00

6.5.3 Genotype Analysis

Insulations In Palermo, insulation thickness for external walls ranges from 6 to 39 cm, with an average of approximately 25.95 cm. Roof insulation varies between 4 and 40 cm, averaging around 20.85 cm. Floor insulation ranges from 3 to 27 cm, with an average of 12.55 cm.

Generally speaking, the thicknesses of insulations are extreme in Palermo, whether it's at the highest or at the lowest, not a intermediate group is detected all of the 3 insulations. And the exterior wall prefers more the thickest insulation(around 38cm), just 4 solutions are at around 10cm. The roof and floor are 50 to 50, half are at the thickest and the other lowest.

Glass Types Palermo's preference for glass types varies, with a significant number favoring type 5.

Louvers Count Louvers count varies from 0, 1, 2, 6, 9. The majority of individuals have a louvers count of 1, and there is a smaller cluster that's 6 and 9.

Window-Wall-Ratio

- **WWR South:** The Window-Wall-Ratio on the south facade varies across individuals, ranging from 8% to 90%. The distribution reveals three clusters, with the majority falling into Low ratio (8%-41%), followed by Medium ratio (44%-52%), and a smaller group in High ratio (72%-90%). On average, the WWR_S is approximately 50.75%.
- **WWR North:** For the north facade, WWR values show a wider distribution. The clusters are more evenly spread, with most of individuals in Low ratio (around 10%) and Medium ratio (around 26%), and 6 solutions are in High ratio (around 74%). The average WWR_N is approximately 32.7%.

Delta Temperature The distribution of delta temperatures shows a diverse range, with values ranging from -0.9 to 0.7°C. And the majority is in negative numbers, which is uncommon but like Roma.

6.5.4 Phenotype Analysis

Fitness Values

- **Energy Intensity:** The algorithm effectively optimizes the energy part, with values ranging from 36524 to 41425 kWh/year.

- **Percentage of People Dissatisfied:** PPD values range from 15.6% to 29.3%, with a cluster around 16.6%, 17%, and 18.3%.
- **Cost:** In terms of cost, values range from 83088 to 199483 € in the end game.

Energy Performance

- **Cooling:** In Palermo, cooling consumption ranges from 9337 to 15818 kWh/year, correlating with the glass type if the WWR is high just as Roma's §6.4.
- **Heating:** Heating is crucial in Palermo, constituting a significant portion of energy consumption. Values range from 189 to 1380 kWh/year, which just plays a small role.
- **Controlled Natural Ventilation:** This value shows that even the delta number is below 0, it can still bring out the heat from indoor via the operable windows.

Continuous Daylight Autonomy

- **cDA** The cDA values are distributed around 4%, 20%, and 76%. The average cDA for the south facade is approximately 46.6%.

This consolidated analysis provides a comprehensive overview of both genotype and phenotype aspects in Palermo. If you have further instructions or adjustments, feel free to let me know!

6.6 Geneva

A city nestled amidst the serene landscapes, Geneva is known for its picturesque surroundings and vibrant urban life.

6.6.1 Climate

Latitude: 46.2°

Geneva, situated at approximately 46.2 degrees latitude, features a Köppen classification of Cfa, indicating a temperate climate with no distinct dry season and hot summers. The ASHRAE classification designates it as a 4A Humid Subtropical/Humid Continental area with warm summers.

Classification: Cfa - Temperate, No Dry Season, Hot Summer

As per the Köppen climate classification, Geneva's climate falls under the Cfa category, characterized by temperate conditions, the absence of a distinct dry season, and hot summers. Furthermore, the ASHRAE classification categorizes it as a 4A Humid Subtropical/Humid Continental area with warm summers.

Basic climate graphics

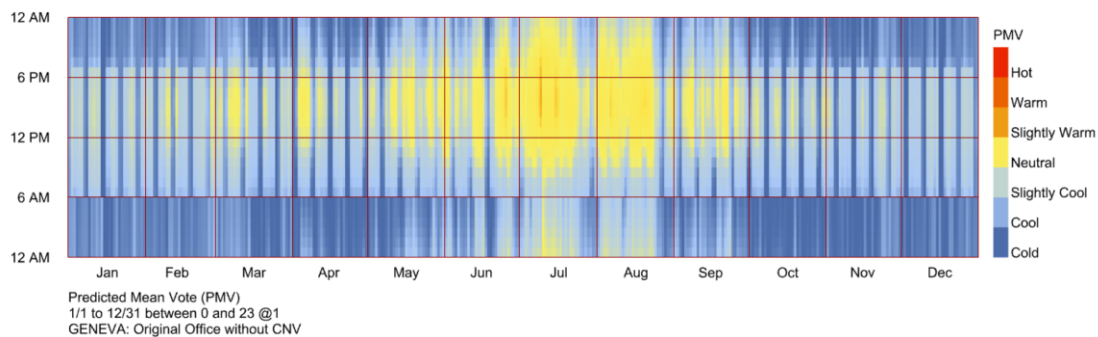


Figure 6.20: Geneva: the comfort metric of PMV.

General Description

Nestled near the majestic Alps, Geneva boasts a unique interplay between urban landscapes and the stunning Alpine range, shaping its climatic nuances. The

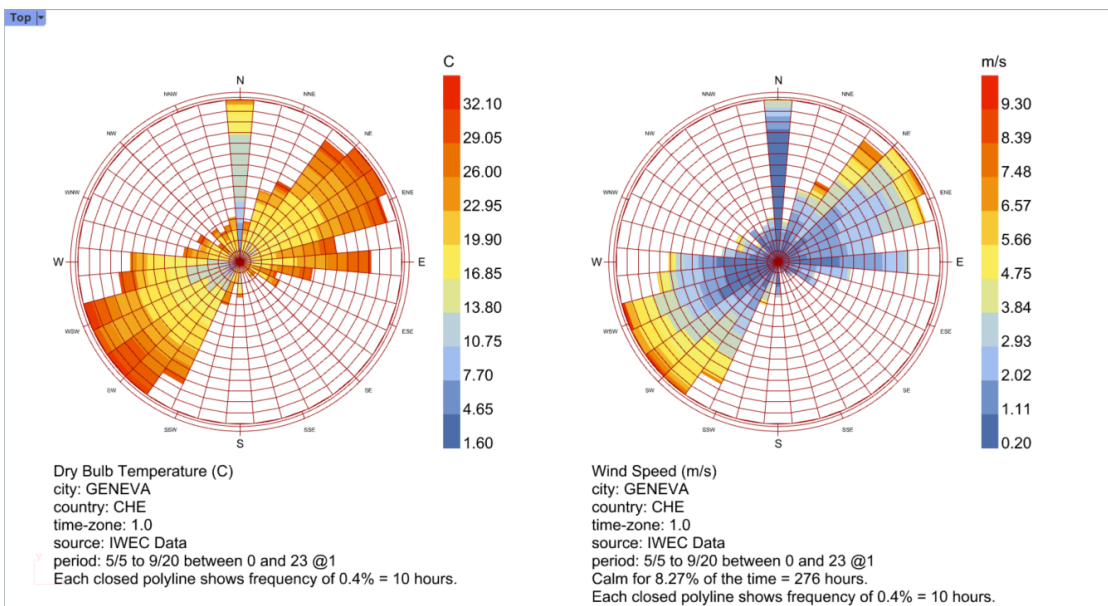


Figure 6.21: Geneva: wind rose

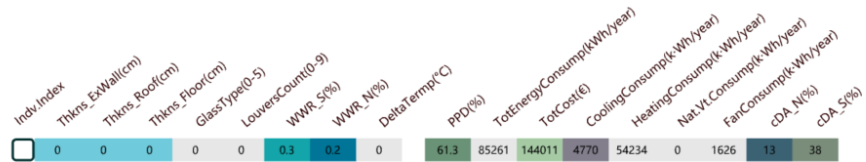


Figure 6.22: Geneva: original KPI

city experiences a temperate climate with distinct seasonal variations influenced significantly by the proximity to the Alps.

During the summer, Geneva enjoys a delightful blend of warm temperatures averaging between 25-30 degrees Celsius. The Alpine foothills contribute to a pleasant cooling effect, offering respite from the summer heat. However, the proximity to the mountains can occasionally lead to sudden weather changes, including thunderstorms, due to the orographic effect—the phenomenon where the mountains force moist air to rise, condense, and form precipitation.

As winter descends upon the region, Geneva encounters mild yet chilly weather, with temperatures often hovering around 0-5 degrees Celsius. The protective barrier offered by the Alps shields the city from harsher cold spells and biting winds, moderating the climate and ensuring a relatively milder winter compared to nearby regions.

The presence of the Alps plays a crucial role in shaping Geneva's microclimate, affecting wind patterns, precipitation, and temperature fluctuations. Additionally, the scenic backdrop of the snow-capped peaks contributes to Geneva's picturesque charm, attracting visitors and residents alike to embrace the beauty of this harmonious coexistence between city life and the stunning mountainous terrain.

6.6.2 Analysis of Genotype and Phenotype

Genotype Analysis

Insulations In Geneva, insulation thickness for external walls ranges from 16 to 39 cm, with an average of approximately 25.65 cm. Roof insulation varies between 16 and 39 cm, averaging around 27.3 cm. Floor insulation ranges from 3 to 29 cm, with an average of 6.05 cm.

Glass Types Geneva's preference for glass types varies, with a significant number favoring type 4 and 5.

Louvers Count Louvers count varies from 0 to 8. The majority of individuals have a louvers count of 0, and there is a smaller cluster around 0.5. On average, the louvers count is close to 0.3.

Window-Wall-Ratio

- *WWR South:* The Window-Wall-Ratio on the south facade varies across individuals, ranging from 9% to 81%. The distribution reveals three clusters, with the majority falling into Low ratio (9%-41%), followed by Medium ratio (56%-61%), and a smaller group in High ratio (60%-81%). On average, the WWR_S is approximately 44.95%.
- *WWR North:* For the north facade, WWR values show a wider distribution. The clusters are more varied, with individuals in Low ratio (5%-33%), Medium ratio (6%-33%), and High ratio (70%-70%). The average WWR_N is approximately 19.6%.

Delta Temperature The distribution of delta temperatures shows a diverse range, with values ranging from -1 to -0.2°C.

Phenotype Analysis

Fitness Values

- **Energy Intensity:** The algorithm shows EUI values ranging from 34929 to 42950 kWh/year.
- **Percentage of People Dissatisfied:** PPD values range from 54.8% to 68.8%, with a cluster around 57.5%, 58.5%, and 59.1%.
- **Cost:** In terms of cost, values range from 93767 to 178343 € in the end game.

Energy Performance

- **Cooling:** In Geneva, cooling consumption ranges from 2822 to 6375 kWh/year, correlating with the south WWR.
- **Heating:** Heating consumption values range from 6614 to 10639 kWh/year.
- **Controlled Natural Ventilation:** The natural ventilation consumption shows varying values across the dataset.

Continuous Daylight Autonomy

- **cDA South:** On the south facade, cDA values are distributed around 20%, 41%, and 70%. The average cDA for the south facade is approximately 49.65%.
- **cDA North:** Geneva exhibits more diversified cDA solutions for the north facade, with values distributed around 6%, 10%, and 33%. The average cDA for the north facade is approximately 19.65%.

This consolidated analysis provides a comprehensive overview of both genotype and phenotype aspects in Geneva. If you have further instructions or adjustments, feel free to let me know!

6.7 Torino

A typical city located in a scenario for a Mediterranean climate. We choose it for its warm temperate climate. Also compare to §6.2 Oslo that has a different climate.

6.7.1 Climate

Latitude: 45°

Torino, positioned near the 45th parallel, experiences a temperate climate influenced by its location and Mediterranean conditions.

Classification: Cfa - Temperate, No Dry Season, Hot Summer

According to the Köppen climate classification, Torino falls under the Cfa category (4A in ASHRAE), representing "Temperate, No Dry Season, Hot Summer." The Mediterranean climate characteristics significantly shape Torino's weather patterns.

Basic climate graphics

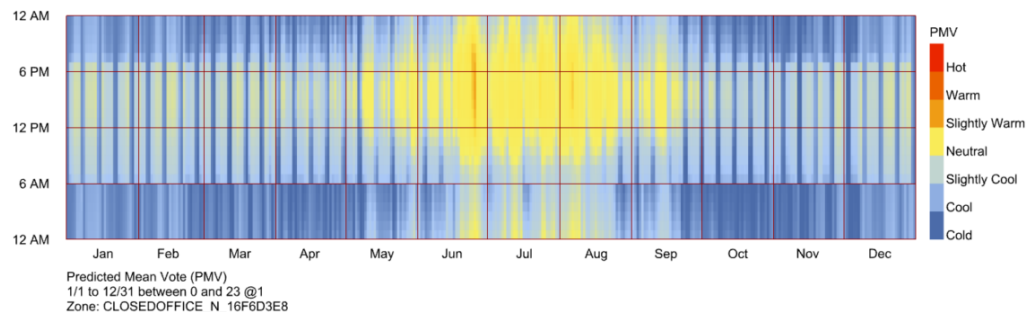


Figure 6.23: Torino: the comfort metric of PMV.

General Description

In Torino's Mediterranean climate, summers are characterized by hot temperatures averaging between 25-30 degrees Celsius. The absence of a dry season ensures relatively consistent precipitation throughout the year, fostering lush greenery and vibrant landscapes. Winters in Torino remain mild, with temperatures hovering around 0-5 degrees Celsius, influenced by the moderating effect of the Mediterranean Sea.

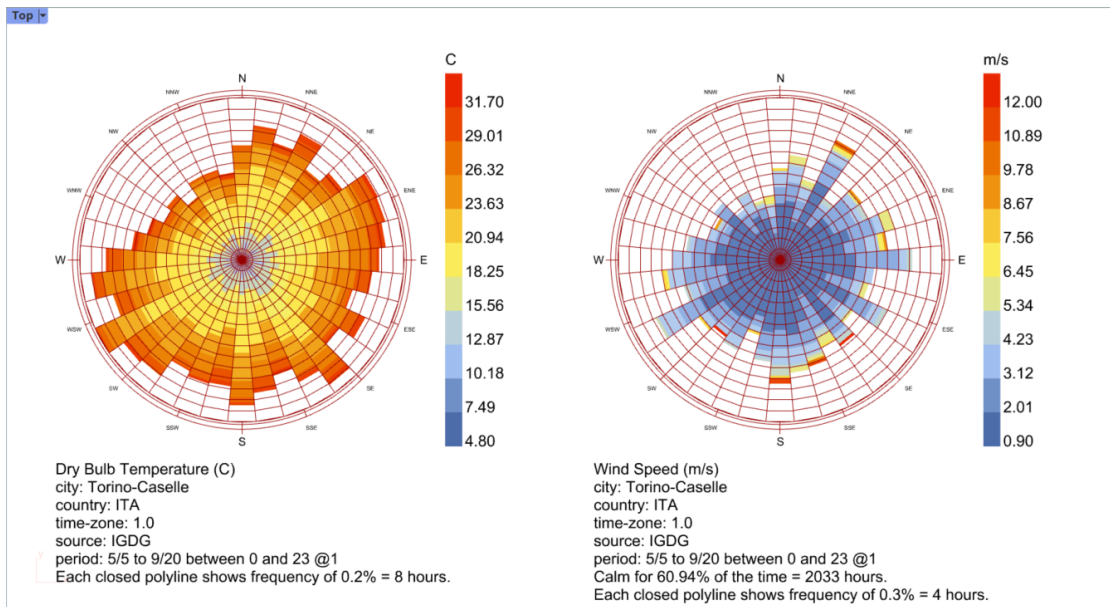


Figure 6.24: Torino: wind rose

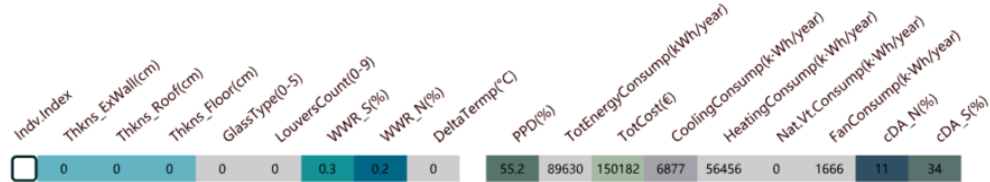


Figure 6.25: Torino: original KPI

The city's proximity to the Alps creates a unique microclimate, offering protection from extreme weather while also impacting local wind patterns. This interplay between the Mediterranean climate and the Alpine terrain enriches Torino's weather dynamics, contributing to its diverse and inviting atmosphere.

6.7.2 Chromosome matrix display

	Indiv-Index	Thkns_EWall(cm)	Thkns_Roof(cm)	Thkns_Floor(cm)	GlassType(0-5)	LouversCount(0-9)	WWR_S(%)	WWR_N(%)	DeltaTemp(C)	PPD(%)	TotEnergyConsump(kWh/year)	TotCost(E)	CoolingConsump(kWh/year)	HeatingConsump(kWh/year)	Nat_Vt_Consump(kWh/year)	FanConsump(kWh/year)	cDA_N(%)	cDA_S(%)	EquipConsump (k-Wh/year)
Latitude: 0045.17	00	12	5	4	0	0	8	14	0.6	0.2	77	44602	93777	5198	13858	-1354	914	17	21
Longitude: 0007.65	01	36	11	29	4	1	34	31	0.2	64.7	38176	139734	4649	8163	-3487	733	33	53	14789
Elevation: 0282.00	02	13	6	16	0	0	87	8	0.6	65.3	47799	121879	9198	12464	-2528	1505	9	75	
	03	39	11	27	4	0	89	35	0.2	59.1	39963	165042	6162	8224	-4561	946	39	75	
	04	36	7	26	5	0	61	23	0.3	62	39107	143686	5421	8213	-3750	842	27	68	
	05	34	7	26	5	0	83	20	-0.3	60.3	39998	153036	6098	8328	-3601	938	24	74	
	06	36	5	10	0	0	31	14	0.6	70.3	42998	105145	5897	11498	-2584	971	16	54	
	07	12	5	6	0	0	8	14	0.6	76.4	44151	94967	5180	13434	-1371	905	17	20	
	08	39	11	26	4	0	90	31	0.2	59.3	40059	163337	6189	8268	-4440	951	35	75	
	09	36	6	16	0	0	32	16	0.6	68.2	42122	110044	5886	10651	-2796	952	19	53	
	10	13	11	10	4	0	10	31	-0.3	72.9	41147	113403	4694	11032	-2188	790	35	25	
	11	38	11	27	4	0	32	20	0.4	65.3	38572	134218	4822	8355	-2926	764	23	54	
	12	15	5	10	0	0	10	13	-0.3	74.1	42709	97307	5179	12014	-1361	884	15	24	
	13	34	7	26	0	1	76	20	-0.3	64.1	45457	130294	8147	11368	-3109	1311	22	71	
	14	12	5	26	5	0	61	23	0.3	63.2	39463	139116	5404	8581	-3728	846	27	68	
	15	12	13	7	0	0	77	15	1.4	66.5	47012	117140	8461	12531	-3386	1388	18	73	
	16	31	10	17	0	0	77	9	-0.1	64.7	46368	125032	8604	11744	-2351	1388	10	73	
	17	36	13	17	0	0	12	9	-0.1	70.9	41290	112363	5308	10464	-1232	886	11	29	
	18	34	7	27	0	0	76	20	-0.3	63.5	45676	131000	8388	11309	-3112	1348	24	73	
	19	13	5	10	0	0	10	13	-0.3	74.2	42824	96950	5181	12125	-1356	887	15	24	

Table 6.9: Torino.Gen.99

	Indiv-Index	Thkns_EWall(cm)	Thkns_Roof(cm)	Thkns_Floor(cm)	GlassType(0-5)	LouversCount(0-9)	WWR_S(%)	WWR_N(%)	DeltaTemp(C)	PPD(%)	TotEnergyConsump(kWh/year)	TotCost(E)	CoolingConsump(kWh/year)	HeatingConsump(kWh/year)	Nat_Vt_Consump(kWh/year)	FanConsump(kWh/year)	cDA_N(%)	cDA_S(%)	EquipConsump (k-Wh/year)
Latitude: 0045.17	00	12	7	16	4	6	42	35	4.7	72.2	40704	120590	4589	10727	-2178	757	20	43	14789
Longitude: 0007.65	01	7	27	4	1	3	89	63	2.9	81	50445	140316	5668	19063	-2436	1082	48	71	
Elevation: 0282.00	02	13	26	22	3	9	13	19	1.3	72	40113	127289	4447	10277	-1720	758	2	2	
	03	33	9	24	1	8	80	52	3.3	78.4	44981	139972	4520	14995	-2322	834	25	54	
	04	29	4	30	4	8	10	49	2.2	78	44127	134143	4597	14067	-2320	832	23	2	
	05	13	40	22	2	4	62	63	1.8	70	39935	154202	4442	10123	-4029	739	46	60	
	06	12	16	17	0	3	64	39	-0.1	76.9	44097	128759	4518	14128	-3232	820	34	64	
	07	38	6	29	2	6	9	15	0.3	76.4	42939	123056	4637	12850	-1344	821	5	1	
	08	6	15	18	1	9	79	73	0.3	80.3	46202	142950	4108	16655	-3388	808	33	50	
	09	7	10	15	5	4	71	86	-0.3	68.1	41403	166973	5442	10439	-4924	891	54	63	
	10	21	15	5	2	3	38	36	-1	76.6	43375	115098	4558	13357	-2687	810	32	50	
	11	26	34	26	4	0	7	80	0.4	70.9	40548	154698	4833	10284	-2857	799	59	18	
	12	35	21	11	0	1	37	45	1.2	68.4	43192	121512	6109	11450	-4233	1001	44	55	
	13	24	14	5	0	2	42	69	0.1	80.4	47377	122682	4662	17186	-3166	897	53	55	
	14	8	34	30	1	9	60	78	3.2	79.6	45271	163857	4115	15738	-2315	786	35	41	
	15	38	23	22	0	0	7	16	-0.6	72.8	41149	125552	4854	10829	-968	834	19	17	
	16	14	11	5	4	75	90	-0.3	67	41216	162854	5548	10136	-5030	901	54	65		
	17	34	29	28	0	3	22	68	0.1	71.9	42912	144163	5336	12045	-3808	900	50	35	
	18	6	28	20	1	0	53	26	0.3	75.4	43217	133477	4620	13148	-3022	817	29	66	
	19	26	25	8	3	6	32	35	2.2	75.6	41624	128337	4009	12273	-3050	710	20	32	

Table 6.10: Torino.Gen.00

6.7.3 Analysis of Torino Genotype and Phenotype

Genotype Analysis

Insulations Torino shows diverse insulation thicknesses. External wall insulation ranges from 12 to 39 cm, with an average of approximately 24.8 cm. Roof insulation varies between 5 and 13 cm, with an average of 7.85 cm. Floor insulation ranges from 4 to 29 cm, with an average of 16.65 cm.

Glass Types There is a mix of glass types, with a notable presence of types 0, 4, and 5.

Louvers Count The majority of individuals have no louvers. Few have a louvers count of 1, contributing to a very low average count.

Window-Wall-Ratio

- **WWR South:** The Window-Wall-Ratio for the south facade shows diverse distributions, varying from 8% to 90%. There's a concentration in the Low ratio (8%-32%) and High ratio (61%-89%). On average, the WWR_S is approximately 49.15%.
- **WWR North:** The north facade's WWR varies widely, ranging from 8% to 35%. There's a mix of Low ratio (8%-23%) and Medium ratio (27%-39%). The average WWR_N is approximately 19.9%.

Delta Temperature The delta temperature ranges from -0.3°C to 1.4°C.

Phenotype Analysis

Fitness Values

- **Energy Intensity:** The algorithm shows energy intensity values ranging from 38176 to 47799 kWh/year.
- **Percentage of People Dissatisfied:** PPD values range from 59.1% to 77.4%, clustered mostly around 60%-65%.
- **Cost:** In terms of cost, values range from 93777 to 165042 € in the end game.

Energy Performance

- **Cooling:** Cooling consumption ranges from 4649 to 9198 kWh/year.
- **Heating:** Heating consumption values vary from 8163 to 13858 kWh/year.
- **Controlled Natural Ventilation:** The natural ventilation consumption shows diverse values across the dataset.

Continuous Daylight Autonomy

- **cDA South:** On the south facade, cDA values vary between 21% and 75%, with a considerable presence in the higher range. The average cDA for the south facade is approximately 59.45%.
- **cDA North:** For the north facade, cDA values vary from 9% to 39%, mostly concentrated around 15%-25%. The average cDA for the north facade is approximately 22.95%.

This consolidated analysis offers insights into the genotype and phenotype aspects in Torino. If you need further adjustments or more details, feel free to ask!

6.8 Canton

A typical city around the North Sea, representing a scenario for a warm humid subtropical city.

6.8.1 Climate

Latitude: 23.5°

Canton, situated at approximately 23.5 degrees latitude, experiences a temperate climate characterized by no dry season and hot summers.

Classification: Cfa - Temperate, No Dry Season, Hot Summer

According to the Köppen climate classification, Canton's climate falls under the Cfa category, representing "Temperate, No Dry Season, Hot Summer". Additionally, the ASHRAE classification designates it as a 2A Humid Subtropical area with warm summers.

Basic climate graphics

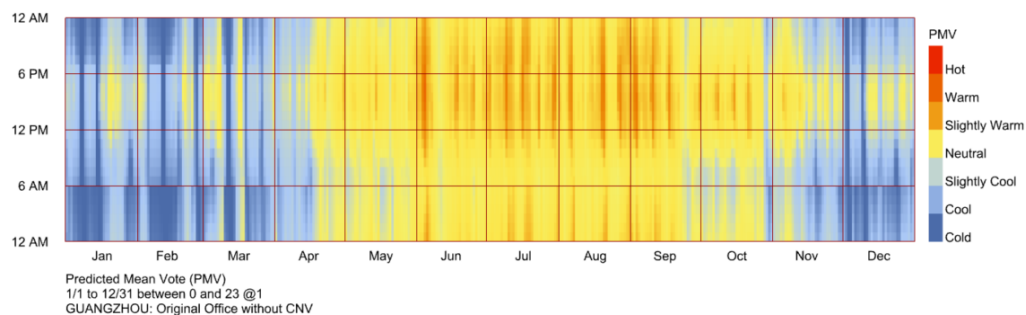


Figure 6.26: Canton: the comfort metric of PMV.

General Description

Canton's temperate climate, marked by hot summers and the absence of a distinct dry season, results in significant temperature fluctuations influenced by daylight hours. During summer, the city experiences prolonged daylight hours, contributing

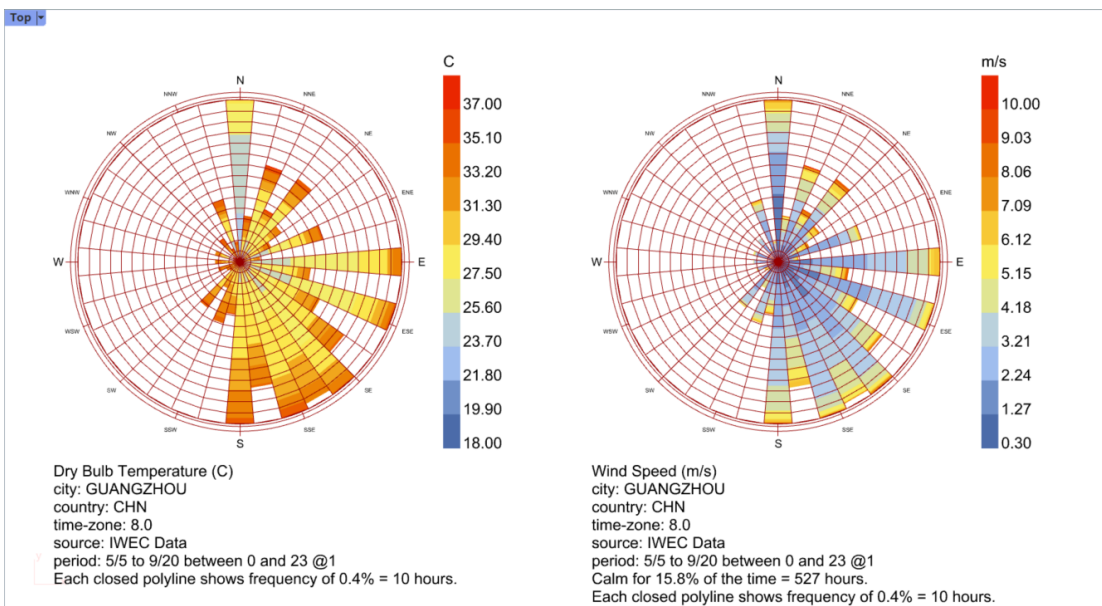


Figure 6.27: Canton: wind rose

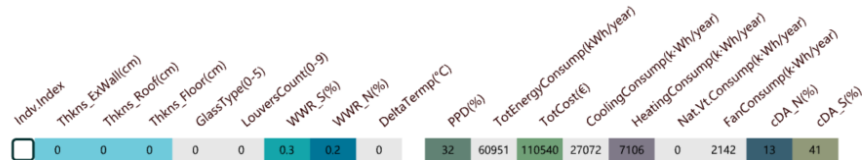


Figure 6.28: Canton: original KPI

to warmer temperatures ranging between 25–35 degrees Celsius. This climate characteristic creates an environment conducive to diverse vegetation and agricultural productivity.

Furthermore, Canton's high humidity levels during the summer months add to the perception of higher temperatures, impacting the overall thermal comfort of its inhabitants. The absence of a dry season presents challenges for certain outdoor activities, requiring adaptations to the prevalent climate conditions.

Additionally, daylight variations play a crucial role in energy consumption and building design considerations. Understanding the relationship between daylight availability and temperature variations is essential for optimizing energy efficiency and maintaining comfortable indoor environments.

6.9 Hong Kong

A prominent city known for its diverse culture and vibrant atmosphere, situated in a subtropical region.

6.9.1 Climate

Latitude: 22.3°

Hong Kong, positioned at approximately 22.3 degrees latitude, features a Cfa Köppen classification, characterized by a temperate climate with no distinct dry season and hot summers. ASHRAE classification designates it as a 2A Humid Subtropical area with warm summers.

Classification: Cfa - Temperate, No Dry Season, Hot Summer

According to the Köppen climate classification, Hong Kong's climate falls under the Cfa category, representing "Temperate, No Dry Season, Hot Summer". Additionally, the ASHRAE classification designates it as a 2A Humid Subtropical area with warm summers.

Basic climate graphics

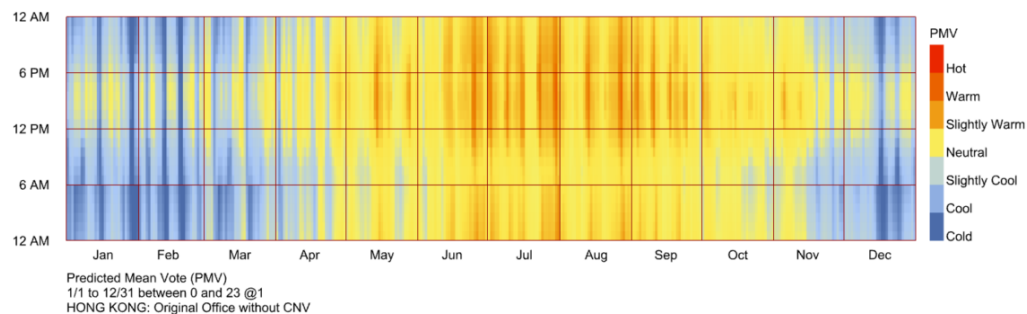


Figure 6.29: Hong Kong: the comfort metric of PMV.

General Description

Hong Kong's temperate climate features hot and humid summers with temperatures ranging between 28-35 degrees Celsius, along with mild winters averaging 15-20

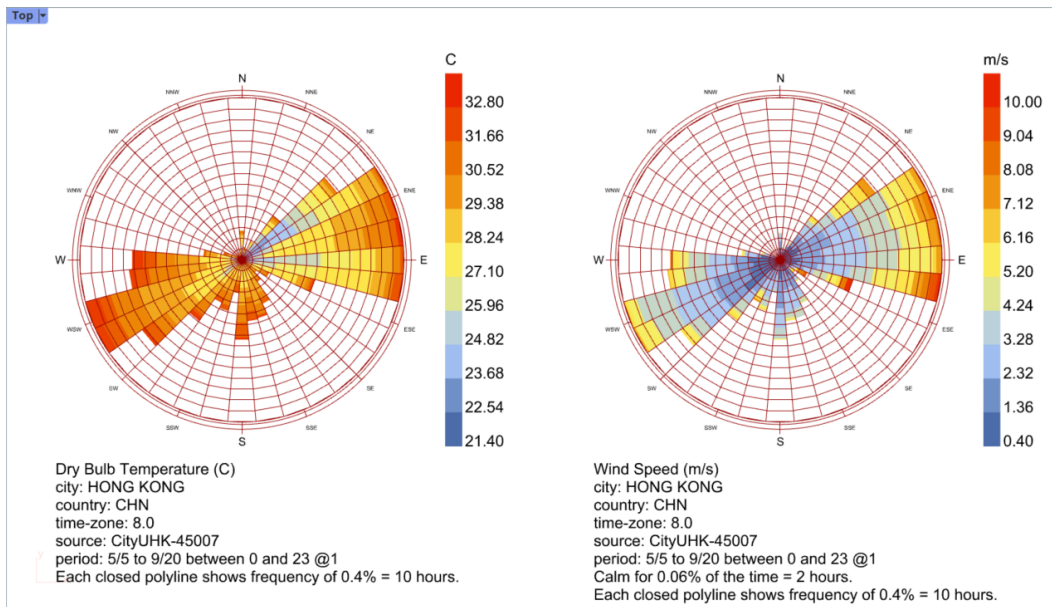


Figure 6.30: Hong Kong: wind rose

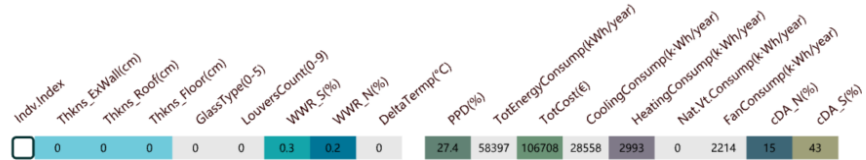


Figure 6.31: Hong Kong: original KPI

degrees Celsius. The absence of a distinct dry season and high humidity levels year-round present unique challenges and considerations for environmental management, energy utilization, and indoor comfort.

Chapter 7

Conclusion

The final section provides a conclusion, addressing the weakness and experience from the experiment.

7.1 Improvements can be adapted

Having done the experiment, we've gained more experience in the simulation. We have a deeper thinking of the experiment. Especially, some improvements can be made for a better performance.

7.1.1 Improvement in settings

GA setting

As mentioned in §5.9.1, now the GA de-crowding function is not completely unleashed. So a bigger generation size and shorter iteration can be made.

Also throughout the 2 whole months we were running the simulations, the program just unexpectedly broke out once. So its stability is confirmed. However, its capacity is still underestimated, 3 fitness value seem to be too simple.

Talking about more fitness values, average weighted method is not the best choice, based on the human logic. Giving some fitness value a priority, evaluating it more important than the others, it's more convinced way. However, this concept can't be easily applied in both Octopus or Wallacei.

7.1.2 Improvement in design

Firstly, our parametric generating method can be updated. In the current situation, the genes can be divided into 3 groups, i.e. **the opaque parameters, the transparent parameters, the schedule parameters**.

Comparing to the opaque parameters, the transparent parameters are more combined, e.g. the glazing type alone won't significantly affects the final performance. It works together with the WWR and others. In reality, these numbers may be packed up with more restriction.

And it's a weakness for our **schedule parameters**. As we only have 1 parameter in this group. Still being underestimated, the GA can deal with more. In the ideal condition, more set-points and the details of schedule should be introduced.

7.1.3 Improvement in the visualization

The Pareto front mark now provides insufficient information. As mentioned in §5.9.3, only the first appeared Pareto front individual will be marked. Which means in the end game, many repeated Pareto front individual is hard to distinguish. This should be updated into a new way. E.g. using 2 different marks, maybe one colored mark and one un-colored mark, symbolizing the first appeared or repeated appeared Pareto front independently.

7.2 Evaluation of the method

We assess the whole methodology here, to discover in which environment the method perform the best, which means it successfully find out some balance and advance combination of genotypes.

7.2.1 Comparison of the similar climates

As presented in §5.2, we selected the cities in purpose. That's to realize the comparisons. As Torino is playing the key character, so we have massive cities in the Cfa climate. And the others can also be compared in pairs. E.g.

- **Canton - Hongkong** are 2 cities closed to each others, the only difference is the distance from the ocean;
- **Oslo - Kiev** are all Dfb, but Kiev is in the middle of the continent while Oslo is facing Atlantic Ocean;
- **Kyoto - Busan** are all Cfa, the difference is the distance from the ocean;

- **Roma - Palermo** are all Cfa, the difference is the distance from the ocean;
- **Torino - Geneva** are all Cfa, and in the similar latitudes, the difference is Torino is on the southern foot of the Alps, while Geneva is on the north. So it's a chance to explore how a huge mountain affects the miditerraneo climate. But also Geneva is surrounded by the lake, while Torino is enclosed by the Alps.

Focusing on Torino, the optimized solutions are similar to those in Geneva, but the roof, louvers count, delta are different. So we can make a assumption that the solar light is stronger in Geneva with a stronger wind in summer. For Torino, it is harder to get heated up in winter; and in the summer, due to the calmness of the wind, once the heat is accumulated, it's also hard to disperse. This can be verify by fig. 6.24, to see the calm hours comparing to fig. 6.21.

It means the CNV works more effectively in Geneva. A more dedicated schedule should be considered in Torino, since it's lacking of the wind. For Torino, the passive design should think about more to the sun rather to the wind.

7.2.2 Same Method Behaves Differently in Different Climates

Comparing the result from Torino and from Oslo, we can discover that the 3-40 cm is suitable for Torino, but insufficient to the Oslo. Nevertheless, the program provides various WWR genes in other city, however in Oslo, the WWR_N are extremely monotonous. Maybe our design method is incapable to deal with the nordic weather.

7.3 Experience gained from the Results

An interesting phenomenon is observed, there're 4 cities evolve to have as less as the thickness of insulation. They're Roma, Busan, Kyoto and Tientsin¹. The end game matrix reveals that all the genes of thickness are in blues color, indicating them the monotonous lowest numbers.

This is very interesting that they're not from the same climate class. And the program work perfectly when it's applied on Geneva, Torino and Palermo, which are also from Cfa. Here I have a hypothesis, the program is robust, but it's specialized

¹Tientsin is slightly better where it has nearly a half of genes to have a 20 cm roof.

in the "hotter Cfa" or "inland Cfa". Once it's applied on the city that's cold enough and ashore, it suggests the monotonous lowest insulation.

7.3.1 Before vs after: Controlled natural ventilation

The CNV only works effectively in some cities. Thankfully, it works for Torino and Geneva reducing the summer load greatly, even though Torino is lacking of the winds. However, for those cities truely hot in summer, e.g. Canton, Hongkong or Roma. This system doesn't lighten the load.

7.3.2 Typical strategies for EUI

At least we can summarize some techniques to obtain a great performance in EUI. The program successfully works in Palermo, Geneva, Torino and Roma, where the EUI cover a large range and diverse genes are tested.

In Roma, Torino and Geneva, the key is to have a better glazing type. The matrix of these two reveal the column of glazing type and column of EUI are changing within the same pace.

In Palermo, the louvers count plays the important role but it's without the support from the transition solutions². In Geneva, the louvers work together with the glazing type.

7.4 As real cases

I've been living in Canton and Torino, so I use my personal experience to exam whether the selected solutions are created as the realistic design.

In Canton I selected Canton.Gen.99 indiv.12 as the reference.

My grandparents live in the 7th floor which is the top of the building. So I know the most concern of the top floor. During the afternoon and early evening, the envelope releases massive accumulated thermal. So on the roof top we need a lot of insulation, and also for the west facade. Since our program doesn't consider so detail as different construction for different orientations, I think the insulation Canton.Gen.99 indiv.12 passes the exam.

The transparent envelope is also outstanding for its protection from the sun.

²The louvers counts are either 9, 6 or 0. We don't know how the others perform

The delta is irrational, however comparing to the nearby solution, maybe it makes little difference.

In Torino I selected Torino.Gen.99.indiv.01 as the reference.

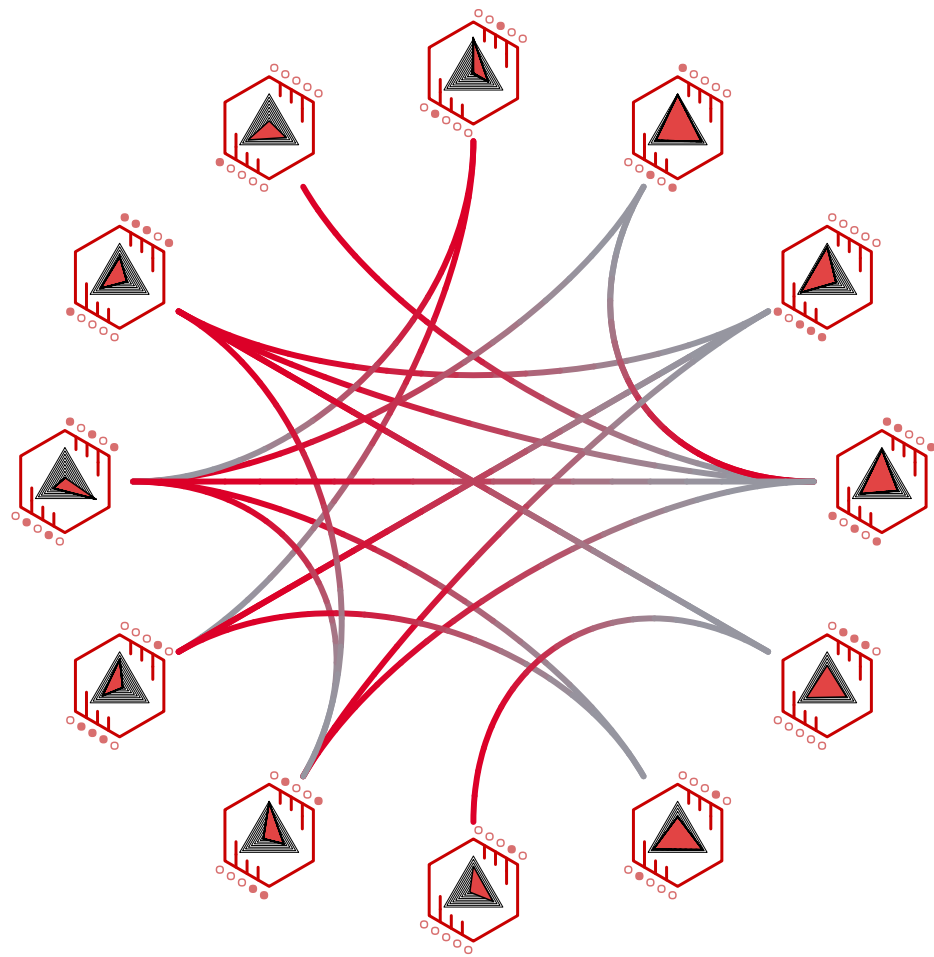
It seems everything is very rational to me, just as the building we can see on the Via Nizza. Especially, it has 2 equal WWR for 2 directions, accelerating the convection. So even the WWR is not half as the nearby solutions but the summer load reduction is as significant as the best.

Appendix A

Algorithm

In figs. A.1 and A.2 I introduce the logic of the algorithm. And in figs. A.3 and A.4 it's the general canvas. We can use it to navigate to the subsidiary sections which we can find in §5. Here present a clearer connections among the sections.

This fig. A.2 shows how the data are operated during the process, and which datum out of the data is selected out and being modified. When the iteration meets its limit, in this case is when "n" reaches 99 gen., the process terminates. So in the record, we can collect the genotypes and phenotypes of all gen.s.



TOURNAMENT FOR MATCHING

Figure A.1: 12 selected hexagons, which represent genotypes, involve in a tournament. The 10 dots around each hexagon represent 10 rounds of the competition. Each round, 4 genotypes are engaged, resulting into 2 winners and 2 losers. Each chord represent a individual gaming, the red end is connecting to the winner, while the grey end to the loser. Some of the pairs might be chosen for more than once. So one chord might contain the result of multiple gaming from different rounds. All the hexagons are placed clockwise according to their rankings, for the one at 12 o'clock overwhelms the other, while the one at 1 o'clock is the lowest ranked. So the chords' red end are always towards the larger figure, clockwise.

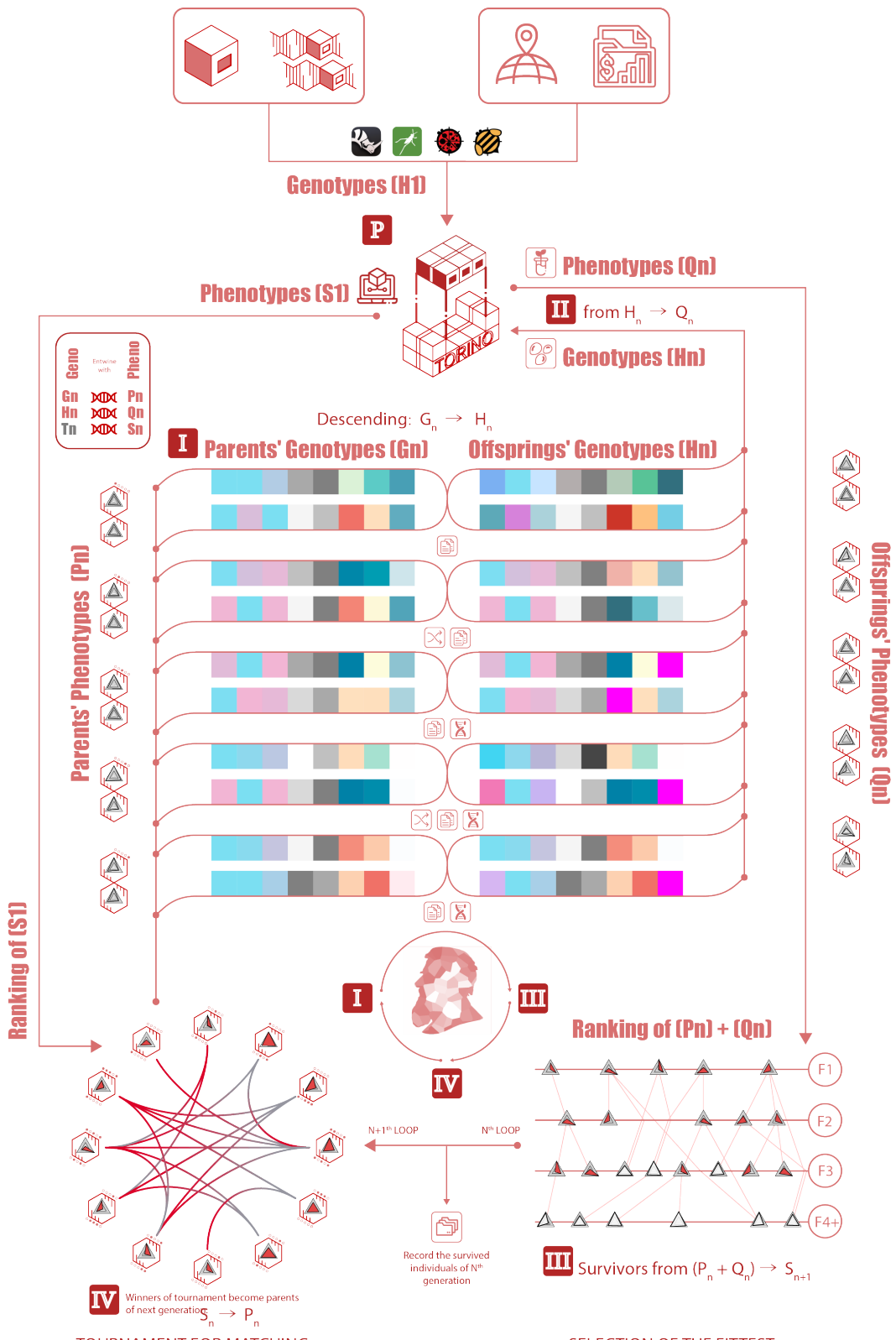


Figure A.2: The whole process flow of NSGA2

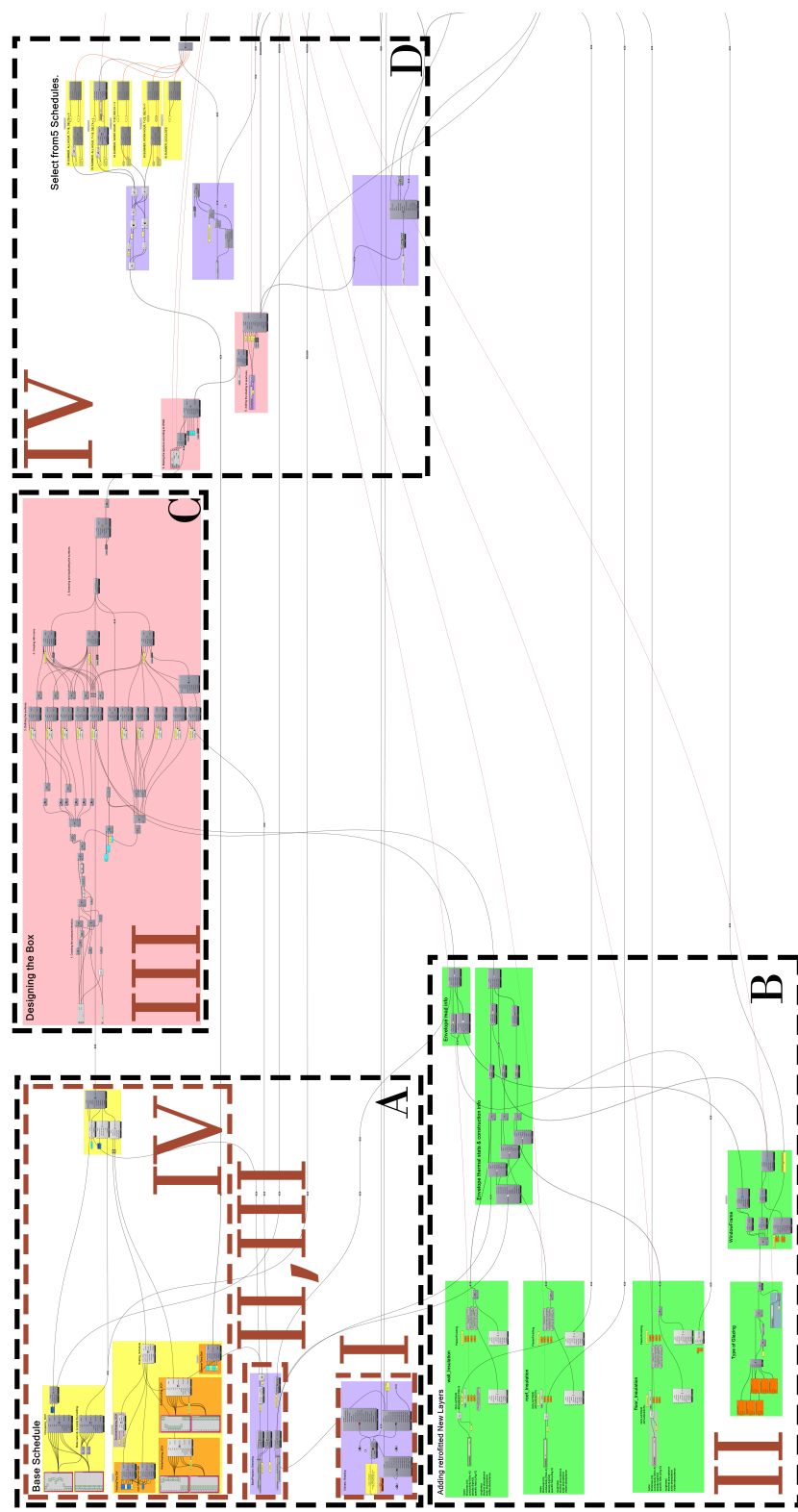


Figure A.3: General GH canvas, part 1/2

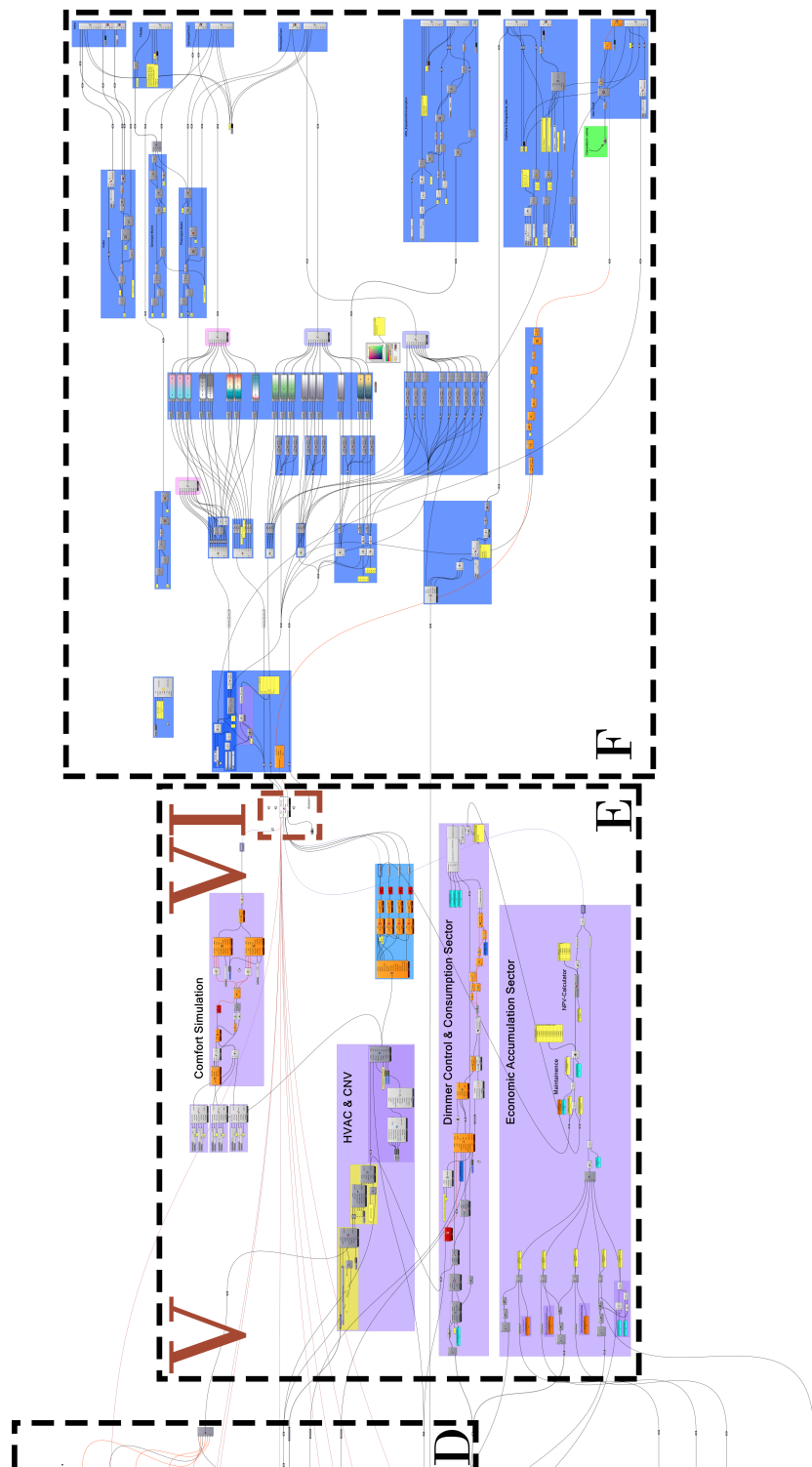


Figure A.4: General GH canvas, part 2/2

Appendix B

Result matrix

We've choose some of our result matrix here. For a quick scan of the outcome from the algorithm. They're also reference of the conclusion in chapters 6 and 7.

For more information, you're welcome to visit:

https://github.com/ArchVittorio/GeneticfAlgorithm_HB_cities

All the result matrix are stored in this repository. It will be helpful for the researchers who want to see all the details.

Result matrix

B.1 Torino

	Indv_Index	Thkns_ExWall(cm)	Thkns_Roof(cm)	Thkns_Floor(cm)	GlassType(0-5)	LouversCount(0-9)	WWR_S(%)	WWR_N(%)	DeltaTemp(C)	PPD(%)	TotEnergyConsump(kWh/year)	TotCost(€)	CoolingConsump(kWh/year)	HeatingConsump(kWh/year)	Nat.Vt.Consump(kWh/year)	FanConsump(kWh/year)	cDA_N(%)	cDA_S(%)	EquipConsump(kWh/year)	
00	13	6	10	0	0	10	22	0.7	74.3	42900	98937	5089	12311	-2048	868	25	24			
01	35	7	28	5	0	74	86	1	59.8	39917	174172	5993	8365	-5612	928	61	72			
02	36	11	27	4	1	34	31	1.3	65	38282	138195	4649	8267	-3636	734	33	53			
03	6	6	14	0	0	74	22	1.2	67.1	46974	116862	8207	12784	-3788	1352	26	72			
04	13	6	13	0	0	10	22	0.8	73.4	42298	100667	5067	11742	-2094	857	26	25			
05	36	21	28	4	1	79	31	1.1	60.2	39419	167519	5757	8144	-4468	887	32	72			
06	36	21	27	4	1	64	31	1.1	61.7	38927	159570	5331	8138	-4285	827	33	68			
07	32	7	28	0	0	79	22	0.6	63.4	45976	132570	8536	11429	-3651	1380	25	74			
08	34	6	23	4	2	70	23	0.4	62.7	39344	145006	5415	8453	-3867	846	22	68			
09	36	6	10	0	1	35	28	-0.4	70.8	43641	108455	5946	12078	-3137	986	29	54			
10	34	6	12	4	0	8	22	-0.3	72.1	40823	110984	4813	10569	-1667	810	25	19			
11	36	19	12	4	1	73	36	1.1	62.5	39735	151717	5580	8654	-4595	870	37	70			
12	13	11	13	4	1	34	31	1.3	69.4	40007	124604	4701	9906	-3635	769	33	53			
13	30	6	16	0	0	71	27	1.2	65.7	46086	120502	8063	12077	-4077	1315	31	71			
14	6	6	14	0	0	71	22	1.2	67.2	46693	116009	8030	12711	-3773	1320	26	71			
15	36	6	16	0	0	32	27	-0.3	68.5	42457	111014	5868	11004	-3221	954	31	53			
16	7	6	13	0	0	36	22	-0.3	70.3	43709	105301	6057	12020	-2999	999	25	56			
17	36	21	27	4	1	61	31	1.1	62	38834	158007	5254	8133	-4256	816	33	67			
18	34	7	25	0	0	70	22	1.3	64	45168	127968	8006	11242	-3863	1288	26	71			
19	36	6	16	4	0	71	28	1.2	66.4	40632	127965	5417	9714	-4103	869	32	71			
																			14789	

Table B.1: Torino.Gen.50

	Indv_Index	Thkns_ExWall(cm)	Thkns_Roof(cm)	Thkns_Floor(cm)	GlassType(0-5)	LouversCount(0-9)	WWR_S(%)	WWR_N(%)	DeltaTemp(C)	PPD(%)	TotEnergyConsump(kWh/year)	TotCost(€)	CoolingConsump(kWh/year)	HeatingConsump(kWh/year)	Nat.Vt.Consump(kWh/year)	FanConsump(kWh/year)	cDA_N(%)	cDA_S(%)	EquipConsump(kWh/year)	
00	13	6	16	0	0	87	8	0.6	65.3	47799	121879	9198	12454	-2528	1505	9	75			
01	39	11	27	4	0	89	35	0.2	59.1	39963	165042	6162	8224	-4561	946	39	75			
02	36	11	29	4	1	34	31	1.3	64.7	38184	139903	4654	8164	-3616	734	33	52			
03	12	5	5	0	0	8	14	0.6	77	44602	94710	5198	13858	-1354	914	16	19			
04	34	7	27	0	0	76	20	-0.3	63.5	45676	131043	8388	11309	-3112	1348	24	73			
05	12	13	7	0	0	75	15	1.4	66.5	46811	116551	8342	12472	-3378	1366	18	72			
06	36	6	16	0	0	32	16	0.6	68.2	42122	110044	5886	10651	-2796	952	19	53			
07	13	5	10	0	0	10	13	-0.3	74.2	42824	96950	5181	12125	-1356	887	15	24			
08	12	5	6	0	0	8	14	0.6	76.4	44151	94967	5180	13434	-1371	905	17	20			
09	36	7	26	5	0	61	23	0.3	62	39107	143706	5421	8213	-3750	842	27	68			
10	38	11	27	4	0	67	20	0.4	61.4	39325	149887	5628	8194	-3670	871	23	70			
11	34	11	17	0	0	84	18	-0.3	64.6	47021	128302	8842	12108	-2982	1439	21	74			
12	38	11	27	4	0	32	20	0.4	65.3	38572	134218	4822	8355	-2926	764	23	54			
13	12	11	27	4	0	87	19	0.3	60.8	40425	156175	6210	8622	-3761	961	22	75			
14	13	11	10	4	0	10	31	-0.3	72.9	41147	113403	4694	11032	-2188	790	35	25			
15	36	6	16	0	0	12	16	-0.4	71.2	41289	106413	5142	10660	-1722	854	19	28			
16	38	11	27	5	0	85	15	0.4	60.2	40184	156975	6244	8346	-3533	963	18	74			
17	39	11	26	4	0	90	31	0.2	59.3	40039	163337	6189	8268	-4440	951	35	75			
18	36	13	6	0	0	12	24	-0.2	72.2	41798	104531	5078	11241	-2250	847	28	29			
19	13	6	16	0	0	6	14	0.6	73.4	42373	102029	5282	11553	-1102	906	16	16			
																			14789	

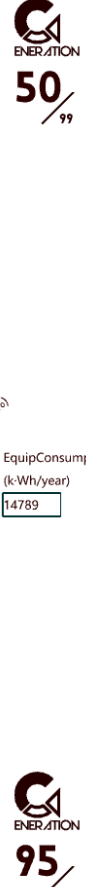


Table B.2: Torino.Gen.96

Result matrix

TORINO, ITA

	Indv_Index	Thkns_ExWall(cm)	Thkns_Roof(cm)	Thkns_Floor(cm)	GlassType(0-5)	LouversCount(0-9)	WWR_S(%)	WWR_N(%)	DeltaTemp(°C)	PPD(%)	TotalEnergyConsump(kWh/year)	TotalCost(€)	CoolingConsump(kWh/year)	HeatingConsump(kWh/year)	Nat.Vt.Consump(kWh/year)	FanConsump(kWh/year)	cDA_N(%)	cDA_S(%)	EquipConsump (kWh/year)
00	36	11	29	4	1	34	31	1.3	64.7	38184	139903	4654	8164	-3616	734	33	52	14789	
01	12	5	5	0	0	8	14	0.6	77	44602	94710	5198	13858	-1354	914	16	19		
02	13	6	16	0	0	87	8	0.6	65.3	47799	121879	9198	12464	-2528	1505	9	75		
03	39	11	27	4	0	89	35	0.2	59.1	39963	165042	6162	8224	-4561	946	39	75		
04	13	5	10	0	0	10	13	-0.3	74.2	42824	96950	5181	12125	-1356	887	15	24		
05	36	6	16	0	0	32	16	0.6	68.2	42122	110044	5886	10651	-2796	952	19	53		
06	12	5	6	0	0	8	14	0.6	76.4	44151	94967	5180	13434	-1371	905	17	20		
07	38	11	27	4	0	67	20	0.4	61.4	39225	149887	5628	8194	-3670	871	23	70		
08	36	7	26	5	0	61	23	0.3	62	39107	143686	5421	8213	-3750	842	27	68		
09	12	13	7	0	0	75	15	1.4	66.5	46811	116551	8342	12472	-3378	1366	18	72		
10	12	11	27	4	0	87	19	0.3	60.8	40425	156175	6210	8622	-3761	961	22	75		
11	13	11	10	4	0	10	31	-0.3	72.9	41147	113403	4694	11032	-2188	790	35	25		
12	34	7	27	0	0	76	20	-0.3	63.5	45676	131043	8388	11309	-3112	1348	24	73		
13	38	11	27	4	0	32	20	0.4	65.3	38572	134218	4822	8355	-2926	764	23	54		
14	36	6	16	0	0	12	16	-0.4	71.2	41289	106413	5142	10660	-1722	854	19	28		
15	34	7	27	0	1	76	20	-0.3	64	45415	131025	8150	11324	-3101	1310	22	71		
16	13	6	16	0	0	12	8	0.6	72.2	41983	101580	5331	11119	-1224	901	9	29		
17	39	11	26	4	0	90	31	0.2	59.3	40039	163337	6189	8268	-4440	951	35	75		
18	36	6	16	0	0	87	16	-0.8	64.7	47463	124784	9091	12262	-2448	1479	19	75		
19	36	13	6	0	0	12	24	-0.2	72.2	41798	104531	5078	11241	-2250	847	28	29		

Table B.3: Torino.Gen.97

TORINO, ITA

	Indv_Index	Thkns_ExWall(cm)	Thkns_Roof(cm)	Thkns_Floor(cm)	GlassType(0-5)	LouversCount(0-9)	WWR_S(%)	WWR_N(%)	DeltaTemp(°C)	PPD(%)	TotalEnergyConsump(kWh/year)	TotalCost(€)	CoolingConsump(kWh/year)	HeatingConsump(kWh/year)	Nat.Vt.Consump(kWh/year)	FanConsump(kWh/year)	cDA_N(%)	cDA_S(%)	EquipConsump (kWh/year)
00	39	11	27	4	0	89	35	0.2	59.1	39963	165042	6162	8224	-4561	946	39	75	14789	
01	12	5	4	0	0	8	14	0.6	64.7	44602	93777	5198	13858	-1354	914	17	21		
02	36	11	29	4	1	34	31	1.3	65.3	47799	121879	9198	12464	-2528	1505	9	75		
03	13	6	16	0	0	87	8	0.6	60.8	40425	156175	6210	8622	-3761	961	22	75		
04	12	11	27	4	0	87	19	0.3	76.4	44151	94967	5180	13434	-1371	905	17	20		
05	12	5	6	0	0	61	23	0.3	62	39107	143686	5421	8213	-3750	842	27	68		
06	36	7	26	5	0	90	31	0.2	59.3	40039	163337	6189	8268	-4440	951	35	75		
07	39	11	26	4	0	76	20	-0.3	64	45415	131025	8150	11324	-3101	1310	22	71		
08	34	7	27	0	1	10	13	-0.3	74.2	42824	96950	5181	12125	-1356	887	15	24		
09	13	5	10	0	0	75	16	1.4	66.6	46809	116513	8325	12487	-3458	1364	19	72		
10	12	13	7	0	0	75	16	1.4	70.9	41290	112363	5308	10464	-1232	886	11	29		
11	36	13	17	0	0	12	9	-0.1	63.5	45676	131043	8388	11309	-3112	1348	24	73		
12	34	7	27	0	0	76	20	-0.3	63.2	39463	139116	5404	8581	-3728	846	27	68		
13	12	5	26	5	0	61	23	0.3	68.2	42122	110044	5886	10651	-2796	952	19	53		
14	36	6	16	0	0	32	16	0.6	72.9	41147	113403	4694	11032	-2188	790	35	25		
15	13	11	10	4	0	10	31	-0.3	65.3	38572	134218	4822	8355	-2926	764	23	54		
16	38	11	27	4	0	32	20	0.4	66.5	46811	116551	8342	12472	-3378	1366	18	72		
17	12	13	7	0	0	75	15	1.4	74.2	42825	96905	5182	12125	-1339	887	15	25		
18	13	5	10	0	0	10	13	-0.4	68.3	42064	111538	5840	10648	-2766	946	18	53		
19	36	8	16	0	0	31	16	0.6											

Table B.4: Torino.Gen.98

Result matrix

B.2 Geneva

	Indv_Index	Thkns_ExWall(cm)	Thkns_Roof(cm)	Thkns_Floor(cm)	GlassType(0-5)	LouversCount(0-9)	WWR_S(%)	WWR_N(%)	DeltaTemp(C)	PPD(%)	TotalEnergyConsump(kWh/year)	TotalCost(€)	CoolingConsump(kWh/year)	HeatingConsump(kWh/year)	Nat.Vt.Consump(kWh/year)	FanConsump(kWh/year)	cDA_N(%)	cDA_S(%)	EquipConsump(kWh/year)
00	40	10	30	4	8	41	19	-0.6		64	35324	137352	2901	7264	-4329	527	4	29	
01	40	10	29	4	0	80	20	-0.5		55.9	37180	153528	4523	7203	-6130	823	24	70	
02	40	10	30	5	0	78	20	-0.5		55.9	37091	153605	4475	7172	-6091	812	23	69	
03	16	17	3	0	0	72	8	-1		62.9	43763	111604	6435	11371	-5435	1326	10	67	
04	19	17	3	0	0	10	12	-1		68.5	38306	95230	3626	9352	-2954	696	15	22	
05	22	13	4	4	0	9	19	-1		68.8	37581	101447	3319	8997	-3161	634	23	20	
06	28	28	5	0	0	72	11	-1		60.9	42970	122821	6392	10639	-5816	1307	13	68	
07	28	21	5	0	0	52	19	-1		62.3	41044	112268	5305	10073	-5824	1035	23	61	
08	26	10	29	5	0	39	20	-0.9		60	35796	132103	3544	6988	-4926	632	24	54	
09	17	28	5	5	0	64	19	-0.4		58	36780	137807	4096	7312	-5707	741	23	65	
10	40	30	5	4	0	75	20	-0.9		56.1	36982	146013	4425	7127	-5823	799	24	68	
11	21	21	5	0	1	25	19	-0.6		65.4	38485	103723	3903	9210	-4613	741	21	42	
12	17	28	5	5	0	72	19	-0.3		57.4	37094	139604	4295	7387	-5932	781	23	68	
13	21	15	5	0	2	25	24	-0.6		67.8	39120	100517	3789	9963	-4746	737	24	38	
14	16	17	4	4	0	73	8	-1		60.3	38333	128531	4560	8296	-4783	845	9	68	
15	28	17	5	0	0	42	8	-1		63	40167	106027	4950	9640	-4439	946	9	56	
16	39	10	30	4	8	41	12	-0.6		64.1	35499	134628	3008	7311	-3963	548	2	29	
17	19	13	4	0	0	24	15	-1		66.9	39271	96645	4041	9821	-4228	778	19	42	
18	16	17	3	5	0	39	8	-0.9		63.9	37362	111043	3782	8246	-3917	703	10	55	
19	28	17	3	0	0	41	8	-1		63.1	40074	103909	4901	9606	-4393	935	10	56	
 50 / 99																			

Table B.5: Geneva.Gen.50

	Indv_Index	Thkns_ExWall(cm)	Thkns_Roof(cm)	Thkns_Floor(cm)	GlassType(0-5)	LouversCount(0-9)	WWR_S(%)	WWR_N(%)	DeltaTemp(C)	PPD(%)	TotalEnergyConsump(kWh/year)	TotalCost(€)	CoolingConsump(kWh/year)	HeatingConsump(kWh/year)	Nat.Vt.Consump(kWh/year)	FanConsump(kWh/year)	cDA_N(%)	cDA_S(%)	EquipConsump(kWh/year)
00	16	16	3	0	0	9	9	-1		69.1	38592	93767	3681	9568	-2512	712	11	20	
01	28	28	5	0	0	72	11	-1		60.9	42970	122850	6392	10639	-5816	1307	13	68	
02	39	39	5	5	0	81	28	-0.6		63.2	34929	141159	2822	6967	-4676	509	12	26	
03	39	37	29	5	0	39	31	-0.5		54.9	36991	177141	4538	7000	-6478	822	33	70	
04	39	17	3	0	0	10	10	-1		67.7	37998	99400	3672	8996	-2785	699	12	21	
05	23	28	5	5	0	60	13	-0.7		58.3	36698	132801	4084	7246	-5144	737	16	64	
06	22	27	5	0	0	42	11	-1		61.6	39590	111907	4866	9170	-4805	921	14	56	
07	20	17	3	0	1	23	8	-0.8		66.2	38663	97814	3985	9286	-3487	760	8	38	
08	20	16	5	0	0	41	11	-1		63.7	40210	103709	4817	9838	-4738	924	13	56	
09	24	28	5	0	0	60	11	-1		61	41553	118496	5780	10000	-5415	1142	13	64	
10	24	17	3	0	0	56	6	-0.5		62.6	41870	107817	5709	10404	-4778	1125	7	63	
11	39	38	5	4	8	60	29.0	-0.5		61.3	35195	148965	3101	6905	-5156	556	11	41	
12	39	38	5	4	8	72	29.0	-0.5		60.2	35421	15428	3290	6910	-5385	590	10	48	
13	18	17	3	0	0	45	11	-1		63.3	40564	103397	5005	9962	-4906	965	13	58	
14	20	27	5	5	0	60	8	-0.5		59.1	37219	130472	4254	7558	-4624	776	10	65	
15	40	28	30	4	0	73	26	-0.5		56.4	36885	167096	4316	7158	-6261	780	30	68	
16	38	37	30	4	0	39	28	-0.6		59.4	35619	158357	3514	6850	-5382	624	33	54	
17	39	27	5	5	0	42	31	-1		59.4	35794	131746	3577	6949	-5471	636	36	56	
18	20	17	3	5	1	23	8	-0.8		66.3	37192	104729	3498	8406	-3263	656	8	38	
19	21	37	29	5	0	81	28	-0.4		55.4	37099	175133	4519	7126	-6524	822	33	70	
 95 / 99																			

Table B.6: Geneva.Gen.96

Result matrix

	Indv_Index	Thkns_ExWall(cm)	Thkns_Roof(cm)	Thkns_Floor(cm)	GlassType(0-5)	LouversCount(0-9)	WWR_S(%)	WWR_N(%)	DeltaTemp(°C)	PPD(%)	TotEnergyConsump(kWh/year)	TotCost(€)	CoolingConsump(kWh/year)	HeatingConsump(kWh/year)	Nat_Vt_Consump(kWh/year)	FanConsump(kWh/year)	cDA_N(%)	cDA_S(%)	EquipConsump (kWh/year)
00	39	37	29	5	0	81	28	-0.6	54.9	36991	177141	4538	7000	-6478	822	33	70	55.2	
01	39	37	29	5	1	81	28	-0.6	63.2	34929	141159	2822	6967	-4676	509	12	26	69.1	
02	39	39	5	5	8	39	31	-0.5	69.1	38592	93767	3681	9568	-2512	712	11	20	60.9	
03	16	16	3	0	0	9	9	-1	60.9	42970	122850	6392	10639	-5816	1307	13	68	67.7	
04	28	28	5	0	0	72	11	-1	67.7	37998	99400	3672	8996	-2785	699	12	21	61.6	
05	39	17	3	0	0	10	10	-1	61.6	39590	111907	4868	9170	-4805	921	14	56	58.3	
06	22	27	5	0	0	42	11	-1	58.3	36698	132801	4084	7246	-5144	737	16	64	66.2	
07	23	28	5	5	0	60	13	-0.7	66.2	38663	97814	3985	9286	-3487	760	8	38	63.7	
08	20	17	3	0	1	23	8	-0.8	63.7	40210	103709	4817	9938	-4738	924	13	56	62.6	
09	20	16	5	0	0	41	11	-1	62.6	41870	107817	5709	10404	-4778	1125	7	63	59.1	
10	24	17	3	0	0	56	6	-0.5	59.1	37219	130472	4254	7558	-4624	776	10	65	60.2	
11	20	27	5	5	0	60	8	-0.5	60.2	35421	154528	3290	6910	-5385	590	10	48	59.4	
12	39	38	5	4	8	72	29.0	-0.5	59.4	35619	158357	3514	6850	-5382	624	33	54	61.3	
13	38	37	30	4	0	39	28	-0.6	61.3	35195	148965	3101	6905	-5156	556	11	41	56.4	
14	39	38	5	4	8	60	29.0	-0.5	56.4	36885	167096	4316	7158	-6261	780	30	68	63.3	
15	40	28	30	4	0	73	26	-0.5	63.3	40564	103397	5005	9962	-4906	965	13	58	68.3	
16	18	17	3	0	0	45	11	-1	68.3	38565	96354	3863	9325	-2239	746	7	22	61	
17	24	17	3	0	0	10	6	-0.5	61	41553	118342	5780	10000	-5415	1142	14	64	55.4	
18	24	28	5	0	0	60	11	-1	55.4	37099	175133	4519	7126	-6524	822	33	70	14789	
19	21	37	29	5	0	81	28	-0.4											

Table B.7: Geneva.Gen.97

	Indv_Index	Thkns_ExWall(cm)	Thkns_Roof(cm)	Thkns_Floor(cm)	GlassType(0-5)	LouversCount(0-9)	WWR_S(%)	WWR_N(%)	DeltaTemp(°C)	PPD(%)	TotEnergyConsump(kWh/year)	TotCost(€)	CoolingConsump(kWh/year)	HeatingConsump(kWh/year)	Nat_Vt_Consump(kWh/year)	FanConsump(kWh/year)	cDA_N(%)	cDA_S(%)	EquipConsump (kWh/year)
00	28	28	5	0	0	72	11	-1	60.9	42970	122850	6392	10639	-5816	1307	13	68	69.1	
01	16	16	3	0	0	9	9	-1	69.1	38592	93767	3681	9568	-2512	712	11	20	63.2	
02	39	39	5	5	8	39	31	-0.5	63.2	34929	141159	2822	6967	-4676	509	12	26	54.8	
03	39	38	29	5	0	81	28	-0.5	54.8	36966	177881	4533	6979	-6508	822	33	70	66.2	
04	20	17	3	0	1	23	8	-0.8	66.2	38663	97814	3985	9286	-3487	760	8	38	61.3	
05	39	38	5	4	8	60	29.0	-0.5	61.3	35195	148965	3101	6905	-5156	556	11	41	63.7	
06	20	16	5	0	0	41	11	-1	63.7	40210	103709	4817	9938	-4738	924	13	56	56.4	
07	40	28	30	4	0	73	26	-0.5	56.4	36885	167096	4316	7158	-6261	780	30	68	67.7	
08	39	17	3	0	0	10	10	-1	67.7	37998	99400	3672	8996	-2785	699	12	21	61.6	
09	22	27	5	0	0	42	11	-1	61.6	39590	111907	4868	9170	-4805	921	14	56	58.1	
10	23	29	5	5	0	60	13	-1	58.1	36671	133484	4107	7194	-4988	739	16	64	58.5	
11	39	37	5	4	0	39	28	-0.6	58.5	35388	136806	3522	6614	-5348	621	32	55	61	
12	24	28	5	0	0	60	11	-1	61	41553	118342	5780	10000	-5415	1142	14	64	59.1	
13	20	27	5	5	0	60	8	-0.5	59.1	37219	130472	4254	7558	-4624	776	10	65	62.3	
14	39	17	3	0	0	59	10	-1	62.3	41901	111041	5743	10389	-5285	1138	12	63	55.9	
15	21	37	29	5	0	81	11	-0.8	55.9	37449	169699	4680	7274	-5333	854	13	70	63.3	
16	18	17	3	0	0	45	11	-1	63.3	40564	103397	5005	9962	-4906	965	13	58	68.3	
17	24	17	3	0	0	10	6	-0.5	68.3	38565	96354	3863	9325	-2239	746	7	22	62.6	
18	24	17	3	0	0	56	6	-0.5	62.6	41870	107817	5709	10404	-4778	1125	7	63	55.4	
19	21	37	29	5	0	81	28	-0.4	55.4	37099	175133	4519	7126	-6524	822	33	70	14789	

Table B.8: Geneva.Gen.98

B.3 Oslo

	Indv_Index	Thkns_ExWall(cm)	Thkns_Roof(cm)	Thkns_Floor(cm)	Glasstype(0-5)	LouversCount(0-9)	WWR_S(%)	WWR_N(%)	DeltaTemp°C	PPD(%)	TotEnergyConsump(kWh/year)	TotCost(€)	CoolingConsump(kWh/year)	HeatingConsump(kWh/year)	Nat.Vt.Consump(kWh/year)	cDA(%)
00	37	40	22	4	2	37	7	0	75.7	41805	155026	2329	14220	-4830	7	
01	37	39	22	4	0	85	6	0.3	73.3	44668	177686	3431	15695	-6959	8	
02	37	39	6	4	0	86	6	0.3	73.3	44740	164354	3453	15738	-6996	8	
03	8	6	5	3	0	5	5	0	83.1	49077	100888	2380	21289	-2089	6	
04	16	8	7	3	0	8	5	0	81.8	47230	104471	2348	19519	-2511	6	
05	24	13	5	3	0	5	6	0	80.2	45372	105396	2308	17748	-2414	8	
06	36	24	6	4	0	86	6	0.6	74.6	45502	153629	3428	16517	-6951	8	
07	36	39	6	5	0	77	6	0.6	73.7	44138	159583	3254	15392	-6656	8	
08	10	26	5	3	0	5	5	0	79.4	44816	111108	2339	17164	-2287	7	
09	14	7	5	3	0	5	5	0	82.2	47821	101441	2355	20090	-2173	6	
10	15	5	5	3	0	5	5	0	82.9	48729	101347	2372	20960	-2129	7	
11	37	39	6	5	0	44	6	0.2	75.1	42264	143244	2570	14383	-5291	8	
12	35	40	5	4	0	38	6	-0.7	75.6	42529	140667	2608	14594	-4690	9	
13	24	25	6	3	0	7	6	0.6	78.4	43655	113762	2277	16100	-2743	8	
14	32	25	5	4	0	46	5	0	76.3	43198	132365	2611	15250	-5205	7	
15	36	39	6	5	0	13	6	0.5	76.6	42133	129844	2288	14593	-3374	9	
16	37	39	6	5	0	6	6	0.2	76.8	42371	127500	2305	14807	-2704	8	
17	36	25	5	4	0	11	6	0.6	77.7	43024	118551	2283	15474	-3202	8	
18	38	24	5	5	0	84	5	0.6	74.7	45375	151610	3404	16420	-6770	7	
19	24	39	6	3	0	7	6	0.6	77.4	42814	123484	2274	15279	-2776	7	

Table B.9: Oslo.Gen.97

	Indv_Index	Thkns_ExWall(cm)	Thkns_Roof(cm)	Thkns_Floor(cm)	Glasstype(0-5)	LouversCount(0-9)	WWR_S(%)	WWR_N(%)	DeltaTemp°C	PPD(%)	TotEnergyConsump(kWh/year)	TotCost(€)	CoolingConsump(kWh/year)	HeatingConsump(kWh/year)	Nat.Vt.Consump(kWh/year)	cDA(%)
00	37	40	6	4	0	86	6	0.3	73.2	44706	165111	3454	15703	-6992	8	
01	8	6	5	3	0	5	5	0	83.1	49077	100888	2380	21289	-2089	6	
02	37	40	22	4	2	37	7	0	75.7	41805	155026	2329	14220	-4830	7	
03	37	39	22	4	0	85	6	0.3	73.3	44668	177686	3431	15695	-6959	8	
04	16	8	7	3	0	8	5	0	81.8	47230	104471	2348	19519	-2511	6	
05	36	39	6	5	0	77	6	0.5	73.7	44138	159583	3254	15392	-6656	8	
06	36	24	6	4	0	86	6	0.6	74.6	45502	153629	3428	16517	-6951	8	
07	24	13	5	3	0	5	6	0	80.2	45372	105396	2308	17748	-2414	8	
08	10	26	5	3	0	5	5	0	79.4	44816	111108	2339	17164	-2287	6	
09	32	25	5	4	0	46	5	0	76.3	43198	132365	2611	15250	-5205	7	
10	24	39	6	3	0	7	6	0.6	77.4	42814	123484	2274	15279	-2776	7	
11	36	25	5	4	0	11	6	0.6	77.7	43024	118551	2283	15474	-3202	8	
12	35	40	5	4	0	38	6	-0.7	75.6	42529	140667	2608	14594	-4690	9	
13	9	7	5	3	0	5	5	0	82.6	48460	101052	2370	20698	-2121	6	
14	24	25	6	3	0	7	6	0.6	78.4	43655	113762	2277	16100	-2743	8	
15	37	39	6	5	0	6	6	0.2	76.8	42371	127500	2305	14807	-2704	8	
16	24	25	6	3	0	10	6	0.6	78.4	43635	114645	2281	16074	-2996	8	
17	36	39	6	5	0	13	6	0.5	76.6	42133	129844	2288	14593	-3374	9	
18	14	7	5	3	0	5	5	0	82.2	47821	101441	2355	20090	-2173	6	
19	24	5	6	3	0	5	6	0.6	82.2	47719	103254	2348	19999	-2296	8	

Table B.10: Oslo.Gen.98

B.4 Kiev

	Indv_Index	Thkns_ExWall(cm)	Thkns_Roof(cm)	Thkns_Floor(cm)	Glasstype(0-5)	LouversCount(0-9)	WWR_S(%)	WWR_N(%)	DeltaTemp°C	PPD(%)	TotEnergyConsump(kWh/year)	TotCost(€)	CoolingConsump(kWh/year)	HeatingConsump(kWh/year)	Nat.Vt.Consump(kWh/year)	cDA(%)
00	39	40	10	4	4	36	18	0.8	73.3	42253	149276	3117	13859	-4685	18	
01	39	39	6	5	4	86	18	0.6	69.8	43749	168342	4192	14089	-6255	18	
02	20	4	4	2	0	8	6	2	81.6	49796	102241	3583	20739	-2219	10	
03	39	40	9	5	0	77	20	0.2	68.4	43794	167246	4434	13855	-6616	35	
04	17	27	9	0	0	86	6	-0.2	71.8	54332	141426	7315	20798	-6722	11	
05	19	27	9	5	0	86	18	0.8	69.3	45112	159638	4695	14846	-6799	32	
06	20	5	9	2	0	6	6	2	79.8	47997	104579	3661	18868	-1855	10	
07	20	5	7	0	0	57.0	7	0.6	75.9	52503	116068	5716	20913	-5923	12	
08	20	5	9	5	0	7	7	2	79.4	47461	107175	3636	18373	-2176	11	
09	32	5	7	0	0	32	9	3	77.5	49625	110782	4569	19442	-4346	16	
10	17	27	9	0	0	61	5	-0.1	72.3	50746	132404	6043	18803	-5563	8	
11	20	31	6	0	0	86	14	0.6	71.7	53954	142207	7096	20676	-7972	26	
12	32	5	9	0	0	32	9	2	76.8	48816	111414	4467	18761	-4817	15	
13	22	5	11	0	0	53	7	0.6	74.8	50922	117134	5510	19605	-5731	12	
14	20	31	7	5	0	61	14	0.6	70.8	43858	146978	4104	14299	-5726	25	
15	20	28	9	5	0	6	18	1.9	76.4	44616	125266	3456	15783	-2790	32	
16	32	26	10	0	0	33	7	2	73.8	46911	126192	4594	16735	-4533	13	
17	20	39	7	5	0	86	8	0.8	68.7	45328	164061	4976	14729	-5794	15	
18	20	5	11	0	0	61	9	0.6	74.5	51974	119541	5858	20225	-6385	16	
19	38	38	9	0	0	32	9	2	73.1	46172	134712	4502	16115	-4694	16	

KIEV, UKR
Latitude: 0050.4
Longitude: 030.45
Elevation: 0168.00



Table B.11: Kiev.Gen.97

	Indv_Index	Thkns_ExWall(cm)	Thkns_Roof(cm)	Thkns_Floor(cm)	Glasstype(0-5)	LouversCount(0-9)	WWR_S(%)	WWR_N(%)	DeltaTemp°C	PPD(%)	TotEnergyConsump(kWh/year)	TotCost(€)	CoolingConsump(kWh/year)	HeatingConsump(kWh/year)	Nat.Vt.Consump(kWh/year)	cDA(%)
00	39	40	9	5	0	77	20	0.2	68.4	43794	167246	4434	13855	-6616	35	
01	17	27	9	0	0	86	6	-0.2	71.8	54332	141426	7315	20798	-6722	11	
02	20	4	4	2	0	8	6	2	81.6	49796	102241	3583	20739	-2219	10	
03	39	40	10	4	4	36	18	0.8	73.3	42253	149276	3117	13859	-4685	18	
04	39	39	6	5	4	86	18	0.6	69.8	43749	168342	4192	14089	-6255	18	
05	20	5	7	0	0	57.0	7	0.6	75.9	52503	116068	5716	20913	-5923	12	
06	20	5	9	5	0	7	7	2	79.4	47461	107175	3636	18373	-2176	11	
07	20	5	9	2	0	6	6	2	79.8	47997	104579	3661	18868	-1855	10	
08	20	31	6	0	0	86	14	0.6	71.7	53954	142207	7096	20676	-7972	26	
09	17	27	9	0	0	61	5	-0.1	72.3	50746	132404	6043	18803	-5563	8	
10	19	27	9	5	0	86	18	0.8	69.3	45112	159638	4695	14846	-6799	32	
11	32	5	7	0	0	32	9	3	77.5	49625	110782	4569	19442	-4346	16	
12	20	5	11	0	0	61	9	0.6	74.5	51974	119541	5858	20225	-6385	16	
13	32	37	10	5	0	33	7	2	72.8	43315	141132	3756	14164	-3822	12	
14	32	5	9	0	0	32	9	2	76.8	48816	111414	4467	18761	-4817	15	
15	20	31	7	5	0	61	14	0.6	70.8	43858	146978	4104	14299	-5726	25	
16	32	26	10	0	0	33	7	2	73.8	46911	126192	4594	16735	-4533	13	
17	38	38	9	0	0	32	9	2	73.1	46172	134712	4502	16115	-4694	16	
18	22	5	11	0	0	53	7	0.6	76.8	45597	123328	3812	16319	-1705	11	
19	20	29	10	5	0	5	7	2								

KIEV, UKR
Latitude: 0050.4
Longitude: 030.45
Elevation: 0168.00



Table B.12: Kiev.Gen.98

Result matrix

B.5 Roma

	Indv_Index	Thkns_ExWall(cm)	Thkns_Roof(cm)	Thkns_Floor(cm)	GlassType(0-5)	LouversCount(0-9)	WWR_S(%)	WWR_N(%)	DeltaTemp(C)	PPD(%)	TotEnergyConsump(kWh/year)	TotCost(€)	CoolingConsump(kWh/year)	HeatingConsump(kWh/year)	Nat.Vt.Consump(kWh/year)	FanConsump(kWh/year)	cDA_N(%)	cDA_S(%)	EquipConsump(kWh/year)
00	8	13	3	4	4	42	46	0.1	53.4	37079	123003	6946	4665	-3213	836	36	51	14789	
01	8	4	3	5	0	88	85	0.5	38.8	38631	152584	9579	3301	-4702	1120	64	78		
02	8	13	3	5	0	86	87	0.5	39	38562	159383	9513	3306	-4721	1112	64	77		
03	7	3	3	0	0	40	8	0.1	45.4	39968	18959	9568	4642	-1133	1127	9	61		
04	7	3	3	2	0	37	19	0.3	56.3	37822	89874	6998	5339	-2125	854	22	59		
05	8	3	3	0	0	83	13	0.6	40.3	43600	101357	12910	4391	-2088	1668	15	77		
06	8	13	3	4	4	73	46	-0.3	46.1	37441	137787	7930	3953	-3388	927	36	68		
07	8	4	3	0	0	51	15	-0.7	42.7	40497	92666	10290	4360	-1187	1215	17	67		
08	8	10	3	0	4	45	13	0.2	49.2	39066	94926	8529	4891	-1745	1015	8	54		
09	8	14	3	4	4	74	13	0.2	47.2	38095	126946	8158	4346	-2371	960	8	66		
10	9	4	3	4	2	41	46	0.1	51.5	37217	115044	7301	4412	-3209	872	43	57		
11	8	6	3	0	0	73	15	-0.7	40.7	42584	100876	12107	4336	-1162	1509	17	75		
12	8	10	3	0	4	42	13	0.2	50.1	38908	94407	8317	4967	-1706	992	8	50		
13	5	13	3	4	0	71	29.0	-1	43.1	38061	128884	8632	3804	-2168	995	32	74		
14	8	4	3	0	0	41	13	0.3	44.9	39759	89779	9494	457	-1674	1117	15	62		
15	8	5	3	0	2	70	18	0.5	42	41446	98872	11085	4379	-2410	1351	16	71		
16	9	4	3	4	4	41	15	-0.7	54.8	37670	104369	7093	5090	-1484	855	10	51		
17	8	4	3	4	4	74	46	0	45.9	37449	131288	7950	3938	-3638	930	36	68		
18	8	13	3	5	4	49	15	-0.3	52.8	37662	114758	7326	4826	-1893	878	10	56		
19	12	16	3	0	0	81	17	0.5	40.3	43279	111605	12673	4346	-2334	1629	19	76		

Table B.13: Roma.Gen.50

	Indv_Index	Thkns_ExWall(cm)	Thkns_Roof(cm)	Thkns_Floor(cm)	GlassType(0-5)	LouversCount(0-9)	WWR_S(%)	WWR_N(%)	DeltaTemp(C)	PPD(%)	TotEnergyConsump(kWh/year)	TotCost(€)	CoolingConsump(kWh/year)	HeatingConsump(kWh/year)	Nat.Vt.Consump(kWh/year)	FanConsump(kWh/year)	cDA_N(%)	cDA_S(%)	EquipConsump(kWh/year)
00	8	3	3	0	0	33	15	-0.9	47.4	39265	87123	8912	4675	-865	1047	17	56	14789	
01	7	3	3	4	4	46	42	0.3	52.6	37060	115233	7020	4567	-3310	842	33	54		
02	7	11	3	4	0	89	90	-0.7	38.5	38787	160684	9746	3273	-3655	1136	65	78		
03	7	3	3	1	0	37	19	1.4	58.6	38511	88817	7005	6005	-2227	869	21	59		
04	7	3	3	0	0	90	17	-0.1	40.1	44216	103653	13431	4383	-1806	1772	19	79		
05	6	3	3	0	0	66	15	-0.2	41.1	41837	95895	11477	4325	-1630	1404	17	72		
06	12	3	3	4	4	61	88	0.2	47.6	37342	141959	7878	3898	-4245	935	58	63		
07	12	3	3	5	0	81	90	0.3	39.6	38373	150513	9328	3325	-4600	1088	65	77		
08	7	3	3	4	3	37	35	0.3	53.9	37293	108235	7029	4786	-2905	847	30	51		
09	7	4	3	0	0	55	11	0	42.3	40968	93466	10665	4400	-1449	1271	13	69		
10	6	11	6	4	0	88	10	-0.7	41.5	39383	132995	9599	4039	-1442	1114	12	78		
11	7	3	3	4	0	60	18	1	46	37896	112293	8182	4124	-2916	958	20	71		
12	12	11	6	4	0	55	21	-0.7	40.4	43335	100761	12714	4360	-1699	1629	17	77		
13	8	3	3	0	0	81	15	-0.1	41.7	38589	127164	9071	3837	-2458	1050	18	77		
14	12	3	4	4	1	86	18	-0.3	44.8	39681	90553	9452	4486	-1770	1111	25	61		
15	14	3	3	0	0	41	22	-0.4	51	38218	105340	7858	4786	-2020	942	7	62		
16	7	3	3	4	2	50	9	0.9	40.3	43290	101472	12678	4353	-2089	1628	20	77		
17	12	3	3	0	0	81	18	0.1	49.3	39235	87475	8645	4926	-1596	1031	8	52		
18	8	3	3	0	2	35	10	0.9	42.1	40786	95050	10548	4346	-2201	1261	25	69		

Table B.14: Roma.Gen.96

Result matrix

	Indv_Index	Thkns_ExWall(cm)	Thkns_Roof(cm)	Thkns_Floor(cm)	GlassType(0-5)	LouverCount(0-9)	WWR_S(%)	WWR_N(%)	DeltaTemp(°C)	PPD(%)	TotEnergyConsump(kWh/year)	TotCost(€)	CoolingConsump(kWh/year)	HeatingConsump(kWh/year)	Nat_Vt_Consump(kWh/year)	FanConsump(kWh/year)	cDA_N(%)	cDA_S(%)	EquipConsump (kWh/year)
00	7	3	3	1	0	37	19	1.4	58.6	38511	88817	7005	6005	-2227	869	21	59	14789	
01	7	3	3	0	0	90	17	-0.1	40.1	44216	103653	13431	4383	-1806	1772	19	79		
02	7	11	3	4	0	89	90	-0.7	38.5	38787	160684	9746	3273	-3655	1136	65	78		
03	8	3	3	0	0	33	15	-0.9	47.4	39265	87123	8912	4675	-865	1047	17	56		
04	7	3	3	4	4	46	42	0.3	52.6	37060	115233	7020	4567	-3310	842	33	54		
05	6	3	3	0	0	66	15	-0.2	41.1	41837	95895	11477	4325	-1630	1404	17	72		
06	7	3	3	4	3	37	35	0.3	53.9	37293	108235	7029	4786	-2905	847	30	51		
07	12	3	3	5	0	81	90	0.3	39.6	38373	150513	9328	3325	-4600	1088	65	77		
08	12	3	3	4	4	62	85	0.2	47.4	37338	141151	7881	3890	-4229	934	57	63		
09	7	4	3	0	0	55	11	0	42.3	40968	93466	10665	4400	-1449	1271	13	69		
10	6	11	6	4	0	88	10	-0.7	41.5	39383	132995	9599	4039	-1442	1114	12	78		
11	7	3	3	4	4	88	18	0.2	44.1	38146	126859	8503	4023	-2847	989	12	71		
12	12	3	3	0	0	81	18	0.1	40.3	43290	101472	12678	4353	-2089	1628	20	77		
13	12	9	6	4	0	55	25	0.2	46.9	37600	120112	7935	4105	-2900	929	28	68		
14	8	3	3	0	0	81	15	-0.1	40.4	43335	100761	12714	4360	-1699	1629	17	77		
15	7	3	3	4	0	60	18	1	46	37896	112293	8182	4124	-2916	958	20	71		
16	12	11	6	4	0	55	88	-0.7	44.9	37667	146311	8391	3664	-3416	981	65	69		
17	13	4	3	0	0	55	22	0	42.1	40786	95050	10548	4346	-2201	1261	25	69		
18	8	3	3	0	2	35	10	0.9	49.3	39235	87475	8645	4926	-1596	1031	8	52		
19	14	3	3	0	0	41	22	-0.4	44.8	39681	90553	9452	4486	-1770	1111	25	61		

Table B.15: Roma.Gen.97

	Indv_Index	Thkns_ExWall(cm)	Thkns_Roof(cm)	Thkns_Floor(cm)	GlassType(0-5)	LouverCount(0-9)	WWR_S(%)	WWR_N(%)	DeltaTemp(°C)	PPD(%)	TotEnergyConsump(kWh/year)	TotCost(€)	CoolingConsump(kWh/year)	HeatingConsump(kWh/year)	Nat_Vt_Consump(kWh/year)	FanConsump(kWh/year)	cDA_N(%)	cDA_S(%)	EquipConsump (kWh/year)
00	8	3	3	0	0	33	15	-0.9	47.4	39265	87123	8912	4675	-865	1047	17	56	14789	
01	7	3	3	4	4	46	42	0.3	52.6	37060	115233	7020	4567	-3310	842	33	54		
02	8	3	3	0	0	90	17	-0.1	40.1	44216	103574	13431	4383	-1806	1772	20	78		
03	7	3	3	1	0	37	19	1.4	38.5	38787	160684	9746	3273	-3655	1136	65	78		
04	7	11	3	4	0	89	90	-0.7	41.1	41837	95895	11477	4325	-1630	1404	17	72		
05	6	3	3	0	0	66	15	-0.2	53.9	37293	108235	7029	4786	-2905	847	30	51		
06	7	3	3	4	3	37	35	0.3	39.6	38373	150513	9328	3325	-4600	1088	65	77		
07	12	3	3	5	0	81	90	0.3	44.1	38146	126859	8503	4023	-2847	989	12	71		
08	7	3	3	4	4	88	18	0.2	44.8	39681	90553	9452	4486	-1770	1111	25	61		
09	14	3	3	0	0	41	22	-0.4	58.5	38531	88807	7027	6000	-2176	872	20	59		
10	7	3	3	1	0	37	18	1.4	40.3	43290	101472	12678	4353	-2089	1628	20	77		
11	12	3	3	0	0	81	18	0.1	40.4	43335	100761	12714	4360	-1699	1629	17	77		
12	8	3	3	0	0	81	15	-0.1	42.1	40786	95050	10548	4346	-2201	1261	25	69		
13	13	4	3	0	0	55	22	0	49.8	37804	113605	7725	4531	-2324	917	8	62		
14	12	3	3	4	4	62	14	0.2	42.3	40968	93466	10665	4400	-1449	1271	13	69		
15	7	4	3	0	0	55	11	0	49.3	39235	87475	8645	4926	-1596	1031	8	52		
16	8	3	3	0	2	35	10	0.9	44.9	37667	146311	8391	3664	-3416	981	65	69		
17	12	11	6	4	0	55	88	-0.7	46.9	37600	120112	7935	4105	-2900	929	28	68		
18	12	9	6	4	0	55	25	0.2	41.5	41191	94363	10932	4303	-2573	1324	20	71		
19	7	3	3	0	0	60	18	0.9											

Table B.16: Roma.Gen.98

B.6 Palermo

	Indv.Index	Thkns_ExWall(cm)	Thkns_Roof(cm)	Thkns_Floor(cm)	GlassType(0-5)	LouversCount(0-9)	WWR_S(%)	WWR_N(%)	DeltaTemprC	PPD(%)	TotEnergyConsump(kWh/year)	TotCost(€)	CoolingConsump(kWh/year)	HeatingConsump(kWh/year)	Nat.Vt.Consump(kWh/year)	cDA(%)
00	12	4	4	0	8	7	16	0.5	-0.1	36.6	37645	85629	10422	1580	774	3
01	12	4	4	0	0	43	14	-0.5	-0.1	24.6	41865	94510	15089	695	2691	27
02	12	4	3	0	0	8	14	-0.5	-0.1	32.5	38491	83666	11597	1150	1688	28
03	34	36	25	5	0	71	70	-0.2	-0.6	15.8	40074	186137	13967	192	2171	82
04	38	39	4	2	9	20	22	-0.2	-0.6	29.1	35512	123524	9337	652	332	6
05	10	24	5	0	0	30	16	0.7	0.6	20.4	39155	104738	12939	381	586	31
06	34	36	23	5	0	71	64	0.6	0.6	16	39889	182187	13783	194	207	81
07	11	6	5	0	0	39	16	-0.2	-0.2	23.4	41081	95208	14483	598	2832	29
08	39	5	26	0	0	39	18	-0.2	-0.2	18.9	40341	116852	14095	305	2494	34
09	35	23	23	5	0	65	16	0.6	0.6	17.9	38996	152402	12923	254	481	30
10	12	36	6	5	0	70	70	-0.2	-0.2	16.1	40023	167598	13913	199	2162	82
11	12	10	5	0	0	43	15	-0.2	-0.2	21.6	41250	99276	14759	469	2846	29
12	34	5	25	2	7	38	24	-0.9	-0.2	27.2	36317	116244	10175	557	3832	16
13	34	38	6	5	0	8	64	0.6	0.6	23.9	36836	142779	10817	375	255	81
14	12	39	6	0	7	7	22	0.6	0.6	31.3	36590	113291	10084	898	487	14
15	5	3	5	0	0	39	16	-0.2	-0.2	26.5	41819	92690	14892	860	3044	31
16	12	4	4	2	7	23	16	-0.9	-0.9	34.4	37330	92343	10454	1257	3548	7
17	32	6	23	5	0	71	64	0.3	0.3	16.5	39901	158613	13780	212	723	81
18	35	23	23	5	0	38	16	-0.9	-0.9	19.7	37661	139180	11679	293	4005	31
19	35	24	23	2	7	65	16	-0.9	-0.9	24.9	37085	135050	10969	475	4599	6

Table B.17: Palermo.Gen.50

	Indv.Index	Thkns_ExWall(cm)	Thkns_Roof(cm)	Thkns_Floor(cm)	GlassType(0-5)	LouversCount(0-9)	WWR_S(%)	WWR_N(%)	DeltaTemprC	PPD(%)	TotEnergyConsump(kWh/year)	TotCost(€)	CoolingConsump(kWh/year)	HeatingConsump(kWh/year)	Nat.Vt.Consump(kWh/year)	cDA(%)
00	38	39	4	2	9	20	22	0.6	-0.6	29.1	35512	123524	9337	652	332	6
01	11	7	5	0	6	19	11	0.5	-0.6	35.2	37282	89276	10282	1380	744	3
02	12	4	3	0	0	8	9	-0.6	-0.6	32.9	38570	83086	11626	1199	2451	17
03	6	5	6	0	1	47	66	0.5	-0.5	23.8	43093	103554	16204	653	820	81
04	39	39	26	4	0	72	86	-0.7	-0.7	15.6	40953	197103	14757	188	5704	84
05	39	39	24	4	0	71	25	-0.9	-0.9	16.6	39918	172909	13812	203	5636	47
06	39	34	5	5	1	43	26	-0.4	-0.4	18.3	37513	138176	11596	235	2196	46
07	39	34	5	5	1	26	26	-0.4	-0.4	20.9	36688	130019	10787	282	1965	45
08	8	11	3	4	0	43	11	0.5	0.5	27.7	39076	110000	12419	844	777	21
09	34	36	26	5	0	72	74	0.6	0.6	15.9	40165	189008	14029	196	173	83
10	5	3	4	5	0	20	27	0.4	0.4	30.6	38081	97872	11423	938	788	51
11	35	5	26	5	0	46	74	-0.4	-0.4	17	38664	152674	12668	217	2596	83
12	38	32	27	5	0	40	28	-0.9	-0.9	18.2	37866	155070	11914	234	4510	52
13	10	11	3	0	0	43	11	0.5	0.5	25.9	42015	98740	15100	806	1188	20
14	5	4	5	0	0	47	17	0.5	0.5	24.5	42232	95463	15396	701	1166	32
15	35	7	23	5	0	20	27	-0.4	-0.4	22.5	36662	121370	10704	343	1945	50
16	38	34	5	5	1	20	17	0.5	0.5	25.2	35992	126789	9996	438	1790	10
17	35	7	30	5	1	20	17	0.5	0.5	23.1	36396	124119	10429	363	555	30
18	38	6	4	2	1	52	21	0.6	0.6	29.3	37814	107378	11287	825	364	38
19	39	39	24	4	0	72	86	-0.9	-0.9	15.6	41425	196039	15127	188	7771	84

Table B.18: Palermo.Gen.96

Result matrix

	Indv.Index	Thkns_ExWall(cm)	Thkns_Roof(cm)	Thkns_Floor(cm)	GlassType(0-5)	LouversCount(0-9)	WWR_S(%)	WWR_N(%)	DeltaTemp(°C)	PPD(%)	ToEnergyConsump(kWh/year)	ToCost(€)	CoolingConsump(kWh/year)	HeatingConsump(kWh/year)	Nat.Vt.Cconsump(kWh/year)	cDA(%)
00	6	5	6	0	1	47	66	0.5								
01	39	39	26	4	0	72	86	-0.7		15.6	40953	197103	14757	188	5704	84
02	12	4	3	0	0	8	9	-0.6		32.9	38570	83086	11626	1199	2451	17
03	38	39	4	2	9	20	22	0.6		29.1	35512	123524	9337	652	332	6
04	11	7	5	0	6	19	11	0.5		35.2	37282	89276	10282	1380	744	3
05	8	11	3	4	0	43	11	0.5		27.7	39076	110000	12419	844	777	21
06	39	34	5	5	1	26	26	-0.4		20.9	366688	130019	10787	282	1965	45
07	35	5	26	5	0	46	74	-0.4		17	38664	152674	12668	217	2596	83
08	39	39	24	4	0	71	25	-0.9		16.6	39918	172909	13812	203	5636	47
09	34	36	26	5	0	72	74	0.6		15.9	40165	189000	14029	196	173	83
10	5	4	5	0	0	47	17	0.5		24.5	42232	95463	15396	701	1166	32
11	5	3	4	5	0	20	27	0.4		30.6	38081	97872	11423	938	788	51
12	39	34	28	5	1	21	26	-0.4		22.4	36544	147760	10606	330	1927	45
13	39	39	24	4	0	72	86	-0.9		15.6	41425	196039	15127	188	7771	84
14	39	39	27	5	0	71	28	-0.9		16.5	39961	176539	13852	200	5731	52
15	35	7	5	5	1	42	17	0.5		24.6	38169	114247	11865	565	633	30
16	10	11	3	0	0	43	11	0.5		25.9	42015	98740	15100	806	1188	20
17	39	34	5	5	1	44	26	-0.4		18.2	37569	138611	11650	233	2226	46
18	5	6	4	5	6	20	29.0	0.4		33	37326	102145	10572	1116	682	26
19	38	6	4	2	1	52	21	0.6		29.3	37814	107378	11287	825	364	38



96
/ 99

Table B.19: Palermo.Gen.97

	Indv.Index	Thkns_ExWall(cm)	Thkns_Roof(cm)	Thkns_Floor(cm)	GlassType(0-5)	LouversCount(0-9)	WWR_S(%)	WWR_N(%)	DeltaTemp(°C)	PPD(%)	ToEnergyConsump(kWh/year)	ToCost(€)	CoolingConsump(kWh/year)	HeatingConsump(kWh/year)	Nat.Vt.Cconsump(kWh/year)	cDA(%)
00	38	39	4	2	9	20	22	0.6		29.1	35512	123524	9337	652	332	6
01	11	7	5	0	6	19	11	0.5		35.2	37282	89276	10282	1380	744	3
02	12	4	3	0	0	8	9	-0.6		32.9	38570	83086	11626	1199	2451	17
03	6	5	6	0	1	47	66	0.5		23.8	43093	103554	16204	653	820	81
04	39	39	26	4	0	72	86	-0.7		15.6	40953	197103	14757	188	5704	84
05	39	34	28	5	1	21	26	-0.4		22.4	36544	147760	10606	330	1927	45
06	39	34	5	5	1	26	26	-0.4		20.9	366688	130019	10787	282	1965	45
07	39	34	5	5	1	44	26	-0.4		18.2	37569	138611	11650	233	2226	46
08	35	5	26	5	0	46	74	-0.4		17	38664	152674	12668	217	2596	83
09	39	39	24	4	0	71	25	-0.9		16.6	39918	172909	13812	203	5636	47
10	39	39	27	4	1	51	25	-0.9		17.5	38315	165173	12343	217	4765	45
11	5	4	5	0	0	47	17	0.5		24.5	42232	95463	15396	701	1166	32
12	10	11	3	0	0	43	11	0.5		25.9	42015	98740	15100	806	1188	20
13	39	39	24	4	0	72	86	-0.9		15.6	41425	196039	15127	188	7771	84
14	34	36	26	5	0	72	74	0.6		15.9	40165	189000	14029	196	173	83
15	38	6	4	2	1	52	21	0.6		29.3	37814	107378	11287	825	364	38
16	39	8	24	4	0	8	10	-0.8		30.2	37107	114075	10648	819	2511	18
17	38	5	4	2	0	52	21	-0.9		26.8	38630	102288	12176	679	4902	40
18	5	6	4	5	6	20	29.0	0.4		33	37326	102145	10572	1116	682	26
19	35	7	5	5	1	42	17	0.5		24.6	38169	114247	11865	565	633	30



97
/ 99

Table B.20: Palermo.Gen.98

Bibliography

- [1] Vitruvius Pollio. *The Ten Books on Architecture*. URL: <https://www.gutenberg.org/ebooks/20239> (cit. on p. 1).
- [2] Eleonora Vignani. «Rhino-Grasshopper EnergyPlus Interfaces». In: (). URL: <https://webthesis.biblio.polito.it/23288/> (cit. on pp. 2, 20).
- [3] European Commission, Directorate-General for Communication, ‘Special Eurobarometer’. Version version v1.00, 2021. URL: http://data.europa.eu/88u/dataset/S2273_95_1_513_ENG (visited on 12/10/2023) (cit. on pp. 2, 3, 7).
- [4] Chiesa Giacomo. *Biomimetica, tra tecnologia e innovazione per l’architettura; Biomimicry, from technology to innovation for architecture*. ITA. Torino, 2008 (cit. on pp. 3, 4, 10).
- [5] European Commission, Directorate-General for Research, Innovation, and K Drabicka. *Climate action in the post-COVID world – Insights from EU-funded projects on how to build forward better*. Ed. by K Drabicka. Publications Office, 2021. doi: doi/10.2777/02755 (cit. on pp. 3, 4).
- [6] *Understanding our planet to benefit humankind*. URL: <https://climate.nasa.gov/> (visited on 12/10/2023) (cit. on p. 3).
- [7] *Thawing Permafrost Could Leach Microbes, Chemicals Into Environment*. URL: <https://climate.nasa.gov/news/3153/thawing-permafrost-could-leach-microbes-chemicals-into-environment/> (visited on 12/10/2023) (cit. on pp. 3, 5).
- [8] *Cambiamenti climatici: una minaccia al benessere delle persone e alla salute del pianeta. Agire ora può mettere al sicuro il nostro futuro*. URL: <https://ipccitalia.cmcc.it/cambiamenti-climatici-una-minaccia-al-benessere-delle-persone-e-all-a-salute-del-pianeta-agire-ora-puo-mettere-al-sicuro-il-nostro-futuro/> (visited on 12/10/2023) (cit. on p. 3).

- [9] *The Paris Agreement*. URL:
<https://unfccc.int/process-and-meetings/the-paris-agreement> (visited on 12/10/2023) (cit. on p. 3).
- [10] *United Nations: The Paris Agreement*. 2015. URL: https://unfccc.int/sites/default/files/english_paris_agreement.pdf (cit. on pp. 3, 4, 6).
- [11] *Carbon monitor project*. URL:
<https://www.iea.org/reports/co2-emissions-in-2022> (visited on 12/10/2023) (cit. on p. 4).
- [12] *CO2 Emissions in 2022*. URL: <https://carbonmonitor.org/> (visited on 12/10/2023) (cit. on pp. 4, 8, 58).
- [13] *Factsheet - Energy Performance of Buildings*. 2021. URL: https://ec.europa.eu/commission/presscorner/detail/en/fs_21_6691 (cit. on p. 4).
- [14] *A Renovation Wave for Europe - greening our buildings, creating jobs, improving lives*. URL:
https://eur-lex.europa.eu/resource.html?uri=cellar:0638aa1d-0f02-11eb-bc07-01aa75ed71a1.0003.02/DOC_1&format=PDF (visited on 12/10/2023) (cit. on pp. 4, 5).
- [15] *Ecosistema urbano: rapporto sulle performance ambientali delle città 2021*. URL: https://www.qualenergia.it/wp-content/uploads/2021/11/EcosistemaUrbano2021_compressed1.pdf (visited on 12/10/2023) (cit. on pp. 4, 5).
- [16] *Horizon 2020 Work Programme 2018-2020*. URL: https://ec.europa.eu/research/participants/data/ref/h2020/wp/2018-2020/main/h2020-wp1820-energy_en.pdf (visited on 12/10/2023) (cit. on pp. 5, 6, 8).
- [17] *DIRECTIVE OF THE EUROPEAN PARLIAMENT AND OF THE COUNCIL on the energy performance of buildings (recast)*. URL:
<https://eur-lex.europa.eu/legal-content/EN/TXT/?uri=celex%3A52021PC0802> (visited on 12/10/2023) (cit. on p. 5).
- [18] *Questions and Answers on the revision of the Energy Performance of Buildings Directive*. URL: https://ec.europa.eu/commission/presscorner/detail/en/QANDA_21_6686 (visited on 12/10/2023) (cit. on p. 5).

- [19] *EPB Center official website*. URL:
<https://epb.center/epb-standards/background/holistic-approach/> (visited on 12/10/2023) (cit. on p. 5).
- [20] *The Architectural Works of Alvar Aalto - a Human Dimension to the Modern Movement*. URL:
<https://whc.unesco.org/en/tentativelists/6509/> (visited on 12/10/2023) (cit. on p. 6).
- [21] Ulrike Passe. «Atmospheres of space: the development of Alvar Aalto's free-flow section as a climate device». In: *arq: Architectural Research Quarterly* 12.3-4 (2008), pp. 295–311. DOI: 10.1017/S135913550800122X (cit. on p. 6).
- [22] Holger Haibach and Kathrin Schneider. «The Politics of Climate Change: Review and Future Challenges». In: 2013. URL:
<https://api.semanticscholar.org/CorpusID:156444743> (cit. on p. 7).
- [23] *Questions and Answers on REPowerEU: Joint European action for more affordable, secure and sustainable energy*. URL: https://ec.europa.eu/commission/presscorner/detail/en/qanda_22_1512 (visited on 12/10/2023) (cit. on p. 7).
- [24] G. Chiesa. *Technological Paradigms and Digital Eras: Data-driven Visions for Building Design*. PoliTO Springer Series. Springer International Publishing, 2019. ISBN: 9783030261993. URL:
<https://books.google.it/books?id=xA1DwAAQBAJ> (cit. on pp. 7, 8, 10, 11).
- [25] Mario Carpo. *The Second Digital Turn Design Beyond Intelligence*. The MIT Press, 2017. ISBN: 9780262534024. URL: <https://mitpress.mit.edu/9780262534024/the-second-digital-turn/> (cit. on pp. 7–10).
- [26] *E-DYCE official website*. URL: <https://edyce.eu/> (visited on 12/10/2023) (cit. on pp. 7, 8).
- [27] Daniel Leiria, Hicham Johra, Anna Marszal-Pomianowska, Michal Zbigniew Pomianowski, and Per Kvols Heiselberg. «Using data from smart energy meters to gain knowledge about households connected to the district heating network: A Danish case». In: *Smart Energy* 3 (2021), p. 100035. ISSN: 2666-9552. DOI:
<https://doi.org/10.1016/j.segy.2021.100035>. URL: <https://www.sciencedirect.com/science/article/pii/S2666955221000356> (cit. on pp. 7, 8).
- [28] *PRELUDGE project official website*. URL: <https://prelude-project.eu/> (visited on 12/10/2023) (cit. on pp. 7, 8).

- [29] Giacomo Chiesa, Andrea Avignone, and Tommaso Carluccio. «A Low-Cost Monitoring Platform and Visual Interface to Analyse Thermal Comfort in Smart Building Applications Using a Citizenndash;Scientist Strategy». In: *Energies* 15.2 (2022). ISSN: 1996-1073. DOI: 10.3390/en15020564. URL: <https://www.mdpi.com/1996-1073/15/2/564> (cit. on pp. 7, 8).
- [30] Giacomo Chiesa, Andrea Avignone, and Tommaso Carluccio. «Explicit-digital design practice and possible areas of implication». In: *TECHNE - Journal of Technology for Architecture and Environment* 13 (2017), pp. 236–242. DOI: <https://doi.org/10.13128/Techne-19738>. URL: <https://www.rivistadistoriadelleducazione.it/index.php/techne/article/download/4643/4643> (cit. on pp. 7, 8).
- [31] David Celanto. «Innovate or Perish. New technologies and architecture's futures». In: *Harvard Design* 27 (2007), pp. 1–9. URL: <https://www.harvarddesignmagazine.org/articles/innovate-or-perish-new-technologies-and-architectures-future/> (cit. on p. 8).
- [32] TEDESCHI ATEDESCHI A. *AAD ALGORITHMS - AIDED DESIGN Parametric Strategies using Grasshopper*. ENG. 2014, p. 496. ISBN: 978-88-95315-30-0 (cit. on pp. 9, 10).
- [33] Ipek Ozkaya and Ömer Akin. «Requirement-driven design: Assistance for information traceability in design computing». In: *Design Studies* 27 (May 2006), pp. 381–398. DOI: 10.1016/j.destud.2005.11.005 (cit. on pp. 10, 11).
- [34] CIRIBINI G. *Dal «performance Design» Alla Strategia Dei Componenti*. ITA. 1969 (cit. on pp. 10, 11).
- [35] CIRIBINI G. *Brevi noti di metodologia della progettazione architettonica*. ITA. Torino: Edizioni Quaderni di Studio, 1968. ISBN: 9780203094235 (cit. on p. 11).
- [36] CERAGIOLI G. et al. CAVAGLIÀ G. *Industrializzazione per programmi : strumenti e procedure per la definizione dei sistemi di edilizia abitativa*. ITA. Piacenza : R.D.B., 1975 (cit. on p. 11).
- [37] Michela Turrin, Peter Von Buelow, and Rudi Stouffs. «Design explorations of performance driven geometry in architectural design using parametric modeling and genetic algorithms». In: *Advanced Engineering Informatics* 25 (Oct. 2011), pp. 656–675. DOI: 10.1016/j.aei.2011.07.009 (cit. on p. 11).
- [38] Robert Woodbury and Andrew Burrow. «Whither design space?» In: *AI EDAM* 20 (May 2006), pp. 63–82. DOI: 10.1017/S0890060406060057 (cit. on p. 11).

- [39] Xing Shi and Wenjie Yang. «Performance-driven architectural design and optimization technique from a perspective of architects». In: *Automation in Construction* 32 (2013), pp. 125–135. ISSN: 0926-5805. DOI: <https://doi.org/10.1016/j.autcon.2013.01.015>. URL: <https://www.sciencedirect.com/science/article/pii/S0926580513000253> (cit. on p. 11).
- [40] Kyle Konis, Alejandro Gamas, and Karen Kensek. «Passive performance and building form: An optimization framework for early-stage design support». In: *Solar Energy* 125 (2016), pp. 161–179. ISSN: 0038-092X. DOI: <https://doi.org/10.1016/j.solener.2015.12.020>. URL: <https://www.sciencedirect.com/science/article/pii/S0038092X15006933> (cit. on p. 11).
- [41] Sigi Goode and David Lacey. «Exploiting organisational vulnerabilities as dark knowledge: conceptual development from organisational fraud cases». In: *Journal of Knowledge Management* 26.6 (Jan. 2022), pp. 1492–1515. ISSN: 1367-3270. DOI: 10.1108/JKM-01-2021-0053. URL: <https://doi.org/10.1108/JKM-01-2021-0053> (cit. on p. 11).
- [42] ARAVIND SESHA DRI. «A FAST ELITIST MULTIOBJECTIVE GENETIC ALGORITHM: NSGA-II». In: (). URL: https://web.njit.edu/~horacio/Math451H/download/Seshadri_NSGA-II.pdf (cit. on pp. 12, 37).
- [43] Jung Song Lee, Lim Cheon Choi, and Soon Cheol Park. «Multi-Objective Genetic Algorithms, NSGA-II and SPEA2, for Document Clustering». In: *Software Engineering, Business Continuity, and Education*. Ed. by Tai-hoon Kim, Hojjat Adeli, Haeng-kon Kim, Heau-jo Kang, Kyung Jung Kim, Akingbehin Kiumi, and Byeong-Ho Kang. Berlin, Heidelberg: Springer Berlin Heidelberg, 2011, pp. 219–227 (cit. on pp. 12, 16, 38).
- [44] K. Deb, A. Pratap, S. Agarwal, and T. Meyarivan. «A fast and elitist multiobjective genetic algorithm: NSGA-II». In: *IEEE Transactions on Evolutionary Computation* 6.2 (2002), pp. 182–197. DOI: 10.1109/4235.996017 (cit. on pp. 12, 36, 38).
- [45] Official website of EnergyPlus. URL: <https://energyplus.net/> (visited on 12/10/2023) (cit. on p. 12).
- [46] EP official. URL: <https://bigladdersoftware.com/epx/docs/8-2/getting-started/energyplus-file-extensions.html#rdd> (visited on 12/10/2023) (cit. on p. 13).

- [47] EVINS R. et al. *EMI report:BESOS – an Expandable Building and EnergySimulation Platform*. Tech. rep. V8P 5C2 - Victoria, 2020. URL: https://emi-ime.ca/wp-content/uploads/2020/03/UVic_Faure_BESOS.pdf (visited on 09/30/2020) (cit. on p. 13).
- [48] *BESOS official website*. URL: <https://besos.uvic.ca/> (visited on 06/30/2023) (cit. on p. 13).
- [49] *jEPlus on BEST*, URL: <https://www.buildingenergysoftwaretools.com/software/jeplus> (visited on 06/30/2023) (cit. on p. 13).
- [50] YI ZHANG. «Use jEPlus as an efficient building design optimisation tool». PhD thesis. Leicester, United Kingdom: De Montfort University, Apr. 2012. URL: <http://www.jeplus.org/wiki/lib/exe/fetch.php?media=docs:072v1.pdf> (cit. on p. 13).
- [51] Giacomo Chiesa (POLITO). *Energy flexible DYnamic building CErtification*. Tech. rep. 2022. URL: https://edyce.eu/wp-content/uploads/2022/03/E-DYCE_D3.2_Free-running-module_28.01.2022_Final.pdf (cit. on p. 14).
- [52] Giacomo Chiesa, Francesca Fasano, and Paolo Grasso. «A New Tool for Building Energy Optimization: First Round of Successful Dynamic Model Simulations». In: *Energies* 14.19 (2021). ISSN: 1996-1073. DOI: 10.3390/en14196429. URL: <https://www.mdpi.com/1996-1073/14/19/6429> (cit. on p. 14).
- [53] *OpenStudio official website*. URL: <https://openstudio.net/> (visited on 06/30/2023) (cit. on pp. 14, 23).
- [54] OpenStudio SDK User Docs. *About Measures*. URL: https://nrel.github.io/OpenStudio-user-documentation/getting_started/about_measures/ (visited on 06/30/2023) (cit. on p. 14).
- [55] OpenStudio SDK User Docs. *OpenStudio Measure Writer's Reference Guide*. URL: https://nrel.github.io/OpenStudio-user-documentation/reference/measure_writing_guide/#:~:text=In%20its%20most%20basic%20form,osm (visited on 06/30/2023) (cit. on p. 14).
- [56] Amir Roth, David Goldwasser, and Andrew Parker. «There's a measure for that!» In: *Energy and Buildings* 117 (2016), pp. 321–331. ISSN: 0378-7788. DOI: <https://doi.org/10.1016/j.enbuild.2015.09.056>. URL: <https://www.sciencedirect.com/science/article/pii/S0378778815302966> (cit. on p. 15).

- [57] OpenStudio SDK User Docs. *Parametric Analysis Tool (PAT) Interface Guide*. URL: https://nrel.github.io/OpenStudio-user-documentation/reference/parametric_analysis_tool_2/#algorithmic-mode (visited on 06/30/2023) (cit. on p. 15).
- [58] WALLACEI. URL: <https://www.food4rhino.com/en/app/wallacei> (visited on 12/10/2023) (cit. on pp. 15, 23).
- [59] WALLACEI. URL: <https://www.wallacei.com/about> (visited on 12/10/2023) (cit. on pp. 15, 16).
- [60] DesignBuilder official website. URL: [https://designbuilder.co.uk/%20\(UK%20version\),%20https://www.designbuilderitalia.it/%20\(Italian%20version\)](https://designbuilder.co.uk/%20(UK%20version),%20https://www.designbuilderitalia.it/%20(Italian%20version)) (visited on 06/30/2023) (cit. on p. 15).
- [61] DesignBuilder UK website. *Parametric Analysis*. URL: https://designbuilder.co.uk/helpv5.3/Content/Parametric_Analysis.htm. (visited on 06/30/2023) (cit. on p. 15).
- [62] DesignBuilder UK website. *Optimisation And Parametric Analysis Settings*. URL: <https://designbuilder.co.uk/helpv5.3/Content/OptimisationAnalysisSettings.htm>. (visited on 06/30/2023) (cit. on p. 15).
- [63] Octopus plug-in manual. URL: [online%20resource%20available%20downloading%20the%20zip%20file%20from%20Food4Rhino%20website%20https://www.food4rhino.com/en/app/octopus%20or%20at%20https://pdfcookie.com/documents/octopus-manual-52e1g5jgw5v8](https://www.food4rhino.com/en/app/octopus%20or%20at%20https://pdfcookie.com/documents/octopus-manual-52e1g5jgw5v8). (visited on 06/30/2023) (cit. on p. 15).
- [64] WALLACEI. URL: <https://www.wallacei.com/research> (visited on 12/10/2023) (cit. on p. 16).
- [65] Abdullah Konak, David W. Coit, and Alice E. Smith. «Multi-objective optimization using genetic algorithms: A tutorial». In: *Reliability Engineering & System Safety* 91.9 (2006). Special Issue - Genetic Algorithms and Reliability, pp. 992–1007. ISSN: 0951-8320. DOI: <https://doi.org/10.1016/j.ress.2005.11.018>. URL: <https://www.sciencedirect.com/science/article/pii/S0951832005002012> (cit. on pp. 16, 38).
- [66] ClimateStudio. URL: <https://www.solemma.com/climatestudio>. (visited on 06/30/2023) (cit. on p. 17).

- [67] *ClimateStudio User Guide*. URL: <https://climatestudiodocs.com/>. (visited on 06/30/2023) (cit. on p. 17).
- [68] Ma Qingsong and Hiroatsu Fukuda. «Parametric Office Building for Daylight and Energy Analysis in the Early Design Stages». In: *Procedia - Social and Behavioral Sciences* 216 (2016). Urban Planning and Architectural Design for Sustainable Development (UPADSD), pp. 818–828. ISSN: 1877-0428. DOI: <https://doi.org/10.1016/j.sbspro.2015.12.079>. URL: <https://www.sciencedirect.com/science/article/pii/S187704281506259X> (cit. on p. 18).
- [69] Ahmed Toutou, Mohamed Fikry, and Waleed Mohamed. «The parametric based optimization framework daylighting and energy performance in residential buildings in hot arid zone». In: *Alexandria Engineering Journal* 57.4 (2018), pp. 3595–3608. ISSN: 1110-0168. DOI: <https://doi.org/10.1016/j.aej.2018.04.006>. URL: <https://www.sciencedirect.com/science/article/pii/S1110016818301534> (cit. on p. 18).
- [70] Y. Fang. «Optimization of Daylighting and Energy Performance Using Parametric Design, Simulation Modeling, and Genetic Algorithms.» In: (2017). URL: <https://escholarship.org/uc/item/2zs2h81m> (cit. on pp. 18, 20).
- [71] Kyle Konis, Alejandro Gamas, and Karen Kensek. «Passive performance and building form: An optimization framework for early-stage design support». In: *Solar Energy* 125 (Feb. 2016), pp. 161–179. DOI: [10.1016/j.solener.2015.12.020](https://doi.org/10.1016/j.solener.2015.12.020) (cit. on pp. 18, 20).
- [72] Yuan Fang and Soolyeon Cho. «Design optimization of building geometry and fenestration for daylighting and energy performance». In: *Solar Energy* 191 (2019), pp. 7–18. ISSN: 0038-092X. DOI: <https://doi.org/10.1016/j.solener.2019.08.039>. URL: <https://www.sciencedirect.com/science/article/pii/S0038092X19308199> (cit. on pp. 18, 20).
- [73] Jianjian Zhang and Lin Ji. «Optimization of Daylighting, Ventilation, and Cooling Load Performance of Apartment in Tropical Ocean Area Based on Parametric Design». In: *Advances in Civil Engineering* 2021 (Aug. 2021), p. 6511290. ISSN: 1687-8086. DOI: [10.1155/2021/6511290](https://doi.org/10.1155/2021/6511290). URL: <https://doi.org/10.1155/2021/6511290> (cit. on pp. 18, 19).

- [74] Anxiao Zhang, Regina Bokel, Andy van den Dobbelenstein, Yanchen Sun, Qiong Huang, and Qi Zhang. «Optimization of thermal and daylight performance of school buildings based on a multi-objective genetic algorithm in the cold climate of China». In: *Energy and Buildings* 139 (2017), pp. 371–384. ISSN: 0378-7788. DOI: <https://doi.org/10.1016/j.enbuild.2017.01.048>. URL: <https://www.sciencedirect.com/science/article/pii/S0378778817301615> (cit. on pp. 18, 19).
- [75] Peiman Pilechiha, Mohammadjavad Mahdavinejad, Farzad Pour Rahimian, Philippa Carnemolla, and Saleh Seyedzadeh. «Multi-objective optimisation framework for designing office windows: quality of view, daylight and energy efficiency». In: *Applied Energy* 261 (2020), p. 114356. ISSN: 0306-2619. DOI: <https://doi.org/10.1016/j.apenergy.2019.114356>. URL: <https://www.sciencedirect.com/science/article/pii/S0306261919320434> (cit. on pp. 18, 19).
- [76] Ali Ahmed Salem Bahdad, Sharifah Fairuz Syed Fadzil, Hilary Omatile Onubi, and Saleh Ahmed BenLasod. «Sensitivity analysis linked to multi-objective optimization for adjustments of light-shelves design parameters in response to visual comfort and thermal energy performance». In: *Journal of Building Engineering* 44 (2021), p. 102996. ISSN: 2352-7102. DOI: <https://doi.org/10.1016/j.jobe.2021.102996>. URL: <https://www.sciencedirect.com/science/article/pii/S2352710221008548> (cit. on p. 19).
- [77] Rendy Perdana Khidmat, Hiroatsu Fukuda, Kustiani, Beta Paramita, Ma Qingsong, and Agus Hariyadi. «Investigation into the daylight performance of expanded-metal shading through parametric design and multi-objective optimisation in Japan». In: *Journal of Building Engineering* 51 (2022), p. 104241. ISSN: 2352-7102. DOI: <https://doi.org/10.1016/j.jobe.2022.104241>. URL: <https://www.sciencedirect.com/science/article/pii/S2352710222002546> (cit. on p. 19).
- [78] Ho-Jeong Kim, Chang-Seok Yang, and Hyeun Jun Moon. «A Study on Multi-Objective Parametric Design Tool for Surround-Type Movable Shading Device». In: *Sustainability* 11.24 (2019). ISSN: 2071-1050. URL: <https://www.mdpi.com/2071-1050/11/24/7096> (cit. on p. 19).
- [79] Parnian Bakmohammadi and Esmatullah Noorzai. «Optimization of the design of the primary school classrooms in terms of energy and daylight performance considering occupants' thermal and visual comfort». ENG. In: *Energy Reports* 6 (2020), pp. 1590–1607. ISSN: 2352-4847. DOI:

- 10.1016/j.egyr.2020.06.008. URL:
<http://hdl.handle.net/10419/244148> (cit. on p. 19).
- [80] Cheng Sun, Qianqian Liu, and Yunsong Han. «Many-Objective Optimization Design of a Public Building for Energy, Daylighting and Cost Performance Improvement». In: *Applied Sciences* 10.7 (2020). ISSN: 2076-3417. DOI: 10.3390/app10072435. URL:
<https://www.mdpi.com/2076-3417/10/7/2435> (cit. on p. 20).
- [81] Mattia Manni, Gabriele Lobaccaro, Nicola Lolli, and Rolf Andre Bohne. «Parametric Design to Maximize Solar Irradiation and Minimize the Embodied GHG Emissions for a ZEB in Nordic and Mediterranean Climate Zones». In: *Energies* 13.18 (2020). ISSN: 1996-1073. DOI: 10.3390/en13184981. URL:
<https://www.mdpi.com/1996-1073/13/18/4981> (cit. on p. 20).
- [82] Mattia Manni and Andrea Nicolini. «Multi-Objective Optimization Models to Design a Responsive Built Environment: A Synthetic Review». In: *Energies* 15.2 (2022). ISSN: 1996-1073. DOI: 10.3390/en15020486. URL:
<https://www.mdpi.com/1996-1073/15/2/486> (cit. on p. 20).
- [83] NAKICENOVIC N.; ALCAMO J.; GRUBLER A.; et al. *Special Report on Emissions Scenarios (SRES)*. Tech. rep. Cambridge, uk, 2000. URL: https://www.ipcc.ch/site/assets/uploads/2018/03/emissions_scenarios-1.pdf (cit. on p. 21).
- [84] Shobhit Chaturvedi, Elangovan Rajasekar, and Sukumar Natarajan. «Multi-objective Building Design Optimization under Operational Uncertainties Using the NSGA II Algorithm». In: *Buildings* 10.5 (2020). ISSN: 2075-5309. DOI: 10.3390/buildings10050088. URL:
<https://www.mdpi.com/2075-5309/10/5/88> (cit. on p. 21).
- [85] Ming-Der Yang, Min-Der Lin, Yu-Hao Lin, and Kang-Ting Tsai. «Multiobjective optimization design of green building envelope material using a non-dominated sorting genetic algorithm». In: *Applied Thermal Engineering* 111 (2017), pp. 1255–1264. ISSN: 1359-4311. DOI:
<https://doi.org/10.1016/j.applthermaleng.2016.01.015>. URL:
<https://www.sciencedirect.com/science/article/pii/S1359431116000703> (cit. on p. 22).
- [86] Yuxing Wang and Chunyu Wei. «Design optimization of office building envelope based on quantum genetic algorithm for energy conservation». In: *Journal of Building Engineering* 35 (2021), p. 102048. ISSN: 2352-7102. DOI:
<https://doi.org/10.1016/j.jobe.2020.102048>. URL: <https://doi.org/10.1016/j.jobe.2020.102048>

- //www.sciencedirect.com/science/article/pii/S2352710220336809 (cit. on p. 22).
- [87] *BigLadder software company official website*. URL: <https://energyplus.net/> (visited on 12/10/2023) (cit. on p. 23).
- [88] *Ladybug*. URL: <https://www.ladybug.tools/ladybug.html> (visited on 12/10/2023) (cit. on p. 23).
- [89] *How to Calculate the Thermal Transmittance (U-Value) in the Envelope of a Building*. URL: <https://www.archdaily.com/898843/how-to-calculate-the-thermal-transmittance-u-value-in-the-envelope-of-a-building> (visited on 12/10/2023) (cit. on p. 24).
- [90] *Lighting design guide*. URL: <https://www.eaton.com.cn/content/dam/eaton/markets/buildings/cooper-1s-brochure-lighting-design-guide.pdf> (visited on 12/10/2023) (cit. on pp. 24, 25).
- [91] J. A. Lynes. «Does the British Zonal System have a future?» In: *Lighting Research & Technology* 11.3 (Sept. 1979), pp. 150–153. ISSN: 0024-3426. DOI: 10.1177/14771535790110030201. URL: <https://doi.org/10.1177/14771535790110030201> (cit. on p. 25).
- [92] *QUANTI LUMEN SONO 100 WATT*. URL: <https://www.lampadadiretta.it/lumen-wattaggio/100-watt-in-lumens> (visited on 12/10/2023) (cit. on p. 26).
- [93] E. Fregonara. *Evaluation Sustainability Design: Life Cycle Thinking and international orientations*. Ricerche di tecnologia dell’architettura. Franco Angeli Edizioni, 2018. ISBN: 9788891765185. URL: <https://books.google.it/books?id=-e9FDwAAQBAJ> (cit. on pp. 26, 27).
- [94] L.Baiardi O.Tronconi. *Valutazione, valorizzazione e sviluppo immobiliare*. 2010 (cit. on p. 27).
- [95] *ISO 15686-5:2017(en) Buildings and constructed assets — Service life planning — Part 5: Life-cycle costing*. URL: <https://www.iso.org/obp/ui/#iso:std:iso:15686:-5:ed-2:v1:en> (visited on 12/10/2023) (cit. on p. 27).
- [96] Task Group 4 et al. *Life Cycle Costs in Construction*. Tech. rep. 2003. URL: <https://onlinebookshop.villareal.fi/docs/LifeCycleCostsinConstruction.pdf> (visited on 09/30/2020) (cit. on p. 27).

- [97] Davis Langdon Management Consulting. *LCC as a contribution to sustainable construction: a commonmethodology*. URL: <https://ec.europa.eu/docsroom/documents/5054/attachments/1/translations/en/renditions/native> (visited on 12/10/2023) (cit. on p. 27).
- [98] *Key ECB interest rates*. URL: https://www.ecb.europa.eu/stats/policy_and_exchange_rates/key_ecb_interest_rates/html/index.en.html (visited on 12/10/2023) (cit. on p. 29).
- [99] *Principle 2: Prioritise comfort for building users*. URL: <https://worldgbc.org/principle-2-prioritise-comfort-for-building-users/> (visited on 06/30/2023) (cit. on p. 29).
- [100] GROSSO M. *Il Raffrescamento passivo degli edifici*, 3rd ed. Maggioli, Santarcangelo di Romagna. ITA. 2011 (cit. on p. 29).
- [101] ASHRAE. «ANSI/ASHRAE Standard 55-2013. Thermal environmental conditions for human occupancy». In: Atlanta - GA, 2013 (cit. on pp. 30, 31).
- [102] Marika Vellei, Manuel Herrera, Daniel Fosas, and Sukumar Natarajan. «The influence of relative humidity on adaptive thermal comfort». In: *Building and Environment* 124 (2017), pp. 171–185. ISSN: 0360-1323. DOI: <https://doi.org/10.1016/j.buildenv.2017.08.005>. URL: <https://www.sciencedirect.com/science/article/pii/S0360132317303505> (cit. on pp. 30, 32, 33).
- [103] F. (Fergus) Nicol. *Adaptive thermal comfort : principles and practice*. ENG. Abingdon ; New York: Routledge, 2012. ISBN: 9780415691598. DOI: <https://doi.org/10.4324/9780203123010> (cit. on pp. 30–33).
- [104] P. O. Fanger. *Thermal comfort: analysis and applications in environmental engineering*. ENG. New York: McGraw-Hill, 1970. ISBN: 0070199159 (cit. on p. 30).
- [105] *ISO-7730 Ergonomics of the thermal environment — Analytical determination and interpretation of thermal comfort using calculation of the PMV and PPD indices and local thermal comfort criteria*. Geneva, Nov. 2005. URL: https://www.buildingreen.net/assets/cms/File/ISO_7730-2005.PDF (cit. on p. 30).

- [106] Richard de Dear, Gail Brager, and Cooper D. «Developing an Adaptive Model of Thermal Comfort and Preference - Final Report on RP-884.» In: *ASHRAE Transactions* 104 (Jan. 1997). URL: <https://escholarship.org/content/qt4qq2p9c6/qt4qq2p9c6.pdf> (cit. on p. 31).
- [107] Richard J. de Dear and Gail S. Brager. «Thermal comfort in naturally ventilated buildings: revisions to ASHRAE Standard 55». In: *Energy and Buildings* 34.6 (2002). Special Issue on Thermal Comfort Standards, pp. 549–561. ISSN: 0378-7788. DOI: [https://doi.org/10.1016/S0378-7788\(02\)00005-1](https://doi.org/10.1016/S0378-7788(02)00005-1). URL: <https://www.sciencedirect.com/science/article/pii/S0378778802000051> (cit. on p. 31).
- [108] M.A. Humphreys, Building Research Establishment, and Building Research Station (Great Britain). *Field Studies of Thermal Comfort Compared and Applied*. Building Research Establishment current paper. Building Research Station, 1975. URL: <https://books.google.it/books?id=9mvtGwAACAAJ> (cit. on p. 31).
- [109] MA Humphreys. «Outdoor temperatures and comfort indoors». In: *Building Research and Practice (J. CIB)* 44.6 (1976), pp. 92–105 (cit. on pp. 32, 34).
- [110] Michael Humphreys, Hom Rijal, and Fergus Nicol. «Examining and developing the adaptive relation between climate and thermal comfort indoors». In: *Proceedings of Conference: Adapting to Change: New Thinking on Comfort, WINDSOR 2010* (Jan. 2010) (cit. on pp. 32, 34).
- [111] *Indoor environmental input parameters for design and assessment of energy performance of buildings addressing indoor air quality, thermal environment, lighting and acoustics*. Brussels, 2007. URL: <https://www.iea.org/policies/7029-en-152512007> (cit. on pp. 31, 33).
- [112] *Energy performance of buildings - Ventilation for buildings - Part 1: Indoor environmental input parameters for design and assessment of energy performance of buildings addressing indoor air quality, thermal environment, lighting and acoustics- Module M1-6*, 2019 (cit. on pp. 31, 33, 79).
- [113] Fergus Nicol. «Adaptive thermal comfort standards in the hot-humid tropics». In: *Energy and Buildings* 36.7 (2004). Building Research and the Sustainability of the Built Environment in the Tropics, pp. 628–637. ISSN: 0378-7788. DOI: <https://doi.org/10.1016/j.enbuild.2004.01.016>. URL: <https://www.sciencedirect.com/science/article/pii/S0378778804000155> (cit. on p. 32).

- [114] R. J. de Dear, K. G. Leow, and A. Ameen. «Thermal comfort in the humid tropics. Part I. Climate chamber experiments on temperature preferences in Singapore». ENG. In: *ASHRAE Transactions* pt 1 (1991), pp. 874–879. ISSN: 0001-2505 (cit. on p. 32).
- [115] Sourabh Katoch, Sumit Singh Chauhan, and Vijay Kumar. «A review on genetic algorithm: past, present, and future». In: *Multimedia Tools and Applications* 80.5 (Feb. 2021), pp. 8091–8126. ISSN: 1573-7721. DOI: 10.1007/s11042-020-10139-6. URL: <https://doi.org/10.1007/s11042-020-10139-6> (cit. on pp. 36–38).
- [116] *IReal-Coded Genetic Algorithms*. URL: <https://engineering.purdue.edu/~sudhoff/ee630/Lecture04.pdf> (visited on 12/10/2023) (cit. on p. 37).
- [117] Kalyanmoy Deb, Karthik Sindhya, and Tatsuya Okabe. «Self-adaptive simulated binary crossover for real-parameter optimization». In: *Annual Conference on Genetic and Evolutionary Computation*. 2007. URL: <https://api.semanticscholar.org/CorpusID:14896895> (cit. on p. 40).
- [118] Daniel Kunkle. «A Summary and Comparison of MOEA Algorithms». In: 2005. URL: <https://api.semanticscholar.org/CorpusID:8356986> (cit. on p. 38).
- [119] *KNAUF ISOLASTRE®ADVANCED*. URL: [https://www.knauf.it/backoffice/userfiles/files/documentiAllegati/189/\[11985\]Isolastre_Brochure%20high%202%203%202022%20web.pdf](https://www.knauf.it/backoffice/userfiles/files/documentiAllegati/189/[11985]Isolastre_Brochure%20high%202%203%202022%20web.pdf) (visited on 12/10/2023) (cit. on p. 43).
- [120] Roberto Lollini, Benedetta Barozzi, Gaetano Fasano, Italo Meroni, and Michele Zinzi. «Optimisation of opaque components of the building envelope. Energy, economic and environmental issues». In: *Building and Environment* (Jan. 2006), pp. 1001–1013 (cit. on p. 43).
- [121] *Italy Electricity Price*. URL: <https://tradingeconomics.com/italy/electricity-price> (visited on 12/10/2023) (cit. on p. 47).
- [122] B. Givoni. *Passive Low Energy Cooling of Buildings*. Architecture Series. Wiley, 1994. ISBN: 9780471284734. URL: <https://books.google.it/books?id=rJsVoRw1geoC> (cit. on pp. 47, 48).
- [123] IEA. *EBC Annex 62 Ventilative Cooling*. ENG. Ed. by Per Heiselberg. 2019 (cit. on p. 47).

- [124] CHIESA G. BELLERI A. «Ventilative Cooling potential tool. User guide - version 1.0». In: *Meteorologische Zeitschrift* (2016). URL: https://www.iea-ebc.org/Data/publications/EBC_SR_Annex62.pdf (cit. on p. 47).
- [125] Annamaria Belleri, Marta Avantaggiato, T Psomas, and P Heiselberg. «Evaluation tool of climate potential for ventilative cooling». ENG. In: *International Journal of Ventilation* 17.3 (2017), pp. 196–208. ISSN: 1473-3315. DOI: 10.1080/14733315.2017.1388627 (cit. on pp. 47, 48).
- [126] *Motore elettrico a catena LIWIN L25 per finestra a sporgere, lucernario - Avorio*. URL: <https://amzn.eu/d/eDTf6Qs> (visited on 12/10/2023) (cit. on p. 49).
- [127] *MatWeb*. URL: <https://www.matweb.com/index.aspx> (visited on 12/10/2023) (cit. on p. 51).
- [128] *HUMAN (by andheum)*. URL: <https://www.food4rhino.com/en/app/human> (visited on 12/10/2023) (cit. on p. 56).
- [129] Jia H. "Weather Converter Program", *Auxiliary EnergyPlus Programs*, Accessed: 2023-06-30. URL: <https://bigladdersoftware.com/epx/docs/8-3/auxiliary-programs/energyplus-weather-file-epw-data-dictionary.html> (cit. on p. 57).
- [130] *epw map website*. Accessed: 2023-06-30. URL: <https://www.ladybug.tools/epwmap/> (cit. on p. 58).
- [131] Hylke E. Beck, Niklaus E. Zimmermann, Tim R. McVicar, Noemi Vergopolan, Alexis Berg, and Eric F. Wood. «Present and future Köppen-Geiger climate classification maps at 1-km resolution». In: *Scientific Data* 5.1 (Oct. 2018), p. 180214. ISSN: 2052-4463. DOI: 10.1038/sdata.2018.214. URL: <https://doi.org/10.1038/sdata.2018.214> (cit. on p. 58).
- [132] Markus Kottek, Jürgen Grieser, Christoph Beck, Bruno Rudolf, and Franz Rubel. «World Map of the Köppen-Geiger climate classification updated». In: *Meteorologische Zeitschrift* 15.3 (July 2006), pp. 259–263. DOI: 10.1127/0941-2948/2006/0130. URL: <http://dx.doi.org/10.1127/0941-2948/2006/0130> (cit. on p. 58).
- [133] M. C. Peel, B. L. Finlayson, and T. A. McMahon. «Updated world map of the Köppen-Geiger climate classification». In: *Hydrology and Earth System Sciences* 11.5 (2007), pp. 1633–1644. DOI: 10.5194/hess-11-1633-2007. URL: <https://hess.copernicus.org/articles/11/1633/2007/> (cit. on p. 58).

- [134] *The Pollination plugin for Grasshopper*. URL:
<https://www.pollination.cloud/grasshopper-plugin> (visited on 12/10/2023) (cit. on p. 61).
- [135] *Honeybee*. URL: <https://www.ladybug.tools/honeybee.html> (visited on 12/10/2023) (cit. on p. 68).
- [136] *What is RADIANCE?* URL:
<https://floyd.lbl.gov/radiance/framew.html> (visited on 12/10/2023) (cit. on p. 75).
- [137] *Optimisation vs. Adaptation: Adaptive Facades*. Accessed: 2023-06-30. URL:
<https://www.unstudio.com/en/page/8645/optimisation-vs.-adaptation-adaptive-facades> (cit. on pp. 81, 91).
- [138] *WALLACEI Learn*. URL: <https://www.wallacei.com/learn> (visited on 12/10/2023) (cit. on p. 81).
- [139] Ranajeet Mohanty, Shakti Suman, and Sarat Das. «Chapter 16. Modeling the Axial Capacity of Bored Piles Using Multi-Objective Feature Selection, Functional Network and Multivariate Adaptive Regression Spline». In: Dec. 2017. DOI: 10.1016/b978-0-12-811318-9.00016-8 (cit. on p. 91).
- [140] Robert Vierlinger. «Multi Objective Design Interface». PhD thesis. Apr. 2013. DOI: 10.13140/RG.2.1.3401.0324 (cit. on p. 91).